UNIVERSITÀ DI PARMA

UNIVERSITA' DEGLI STUDI DI PARMA

DOTTORATO DI RICERCA IN
"Biologia Evoluzionistica ed Ecologia"

CICLO XXXIV

Different cultivation methods of microalgae for biotechnological applications

Coordinatore:
Chiar.mo Prof. Pierluigi Viaroli

Tutore:
Chiar.ma Prof.ssa Simonetta Pancaldi

Dottorando: Michele Maglie

Anni Accademici 2018/2019 – 2020/2021

Il dottorato in Biologia Evoluzionistica ed Ecologia – XXXIV ciclo è in convenzione tra le Università di Ferrara, Firenze e Parma

(sede amministrativa Università di Parma)

Table of Contents

Chapter 1

1. General introduction

In recent decades, environmental issues related to the exploitation and pollution of natural resources, the anthropogenic carbon dioxide (CO_2) emissions, the use and depletion of fossil fuel, together with the constant and inexorable increase in world population, have caused an increase in socio-economic disequilibria (Watson et al. 2018; Mora et al. 2018; Laybourn-Langton et al. 2019; Ganivet 2020). Nevertheless, the increasing attention of the society towards the policies aimed at the development of a circular and green economy have given a strong impulse to the research of sustainable sources to produce energy and food (Gifford and Nilsson 2014; Babutsidze and Chai 2018; United Nation 2020). In this perspective, the biotechnological potential of microalgae has gained considerable importance because of their wide application range: production of biomass for food and feed, synthesis of high-value compounds (e.g. polyunsaturated fatty acids, pigments, polysaccharides) used in cosmetic and pharmaceutical sectors, in renewable green-energy and in phytoremediation systems (Sabia et al. 2015; Valverde et al. 2016; D'Amato et al. 2017; Rizwan et al. 2018). Furthermore**,** microalgae do not compete with food crops, do not require arable land, and can use waste as nutrients for their growth (da Silva Vaz et al. 2016). Moreover, the use of saline algae could help reduce freshwater consumption (Ishika et al. 2017). Microalgae can also act as a natural sink for the reduction of atmospheric CO_2 and some of them can also utilize the CO_2 derived from industrial exhaust gases (Yen et al. 2015).

1.1 Microalgal biodiversity

Microalgae are a wide and heterogeneous group of eukaryotic photosynthetic microorganisms, only a few species are heterotrophic. There are an estimated 100,000 microalgae species, more than 50,000 microalgae species have been identified and out of them 30,000 species have been investigated for potential applications (Connelly 2014; Halder and Azad 2019). Each species presents specific properties making these organisms ubiquitous, in both aquatic and terrestrial ecosystems. Due to their higher photosynthetic efficiencies relative to land plants (they contribute up to 25% of global productivity), to elevated growth rates and metabolic plasticity, and to their great biodiversity, microalgae are adapted to a wide variety of environmental conditions such as fresh, brackish or marine waters, extreme temperatures, acidic or alkaline conditions and even radioactive stress (Mata et al. 2010; Rivasseau et al. 2013; Varshney et al. 2015; Valverde et al. 2016). The taxonomic classification of microalgae is based on some characteristics such as: plastid ultrastructure, photosynthetic pigments pattern, chemical nature

of reserve compounds, wall nature, presence of flagella, cellular and nuclear division modalities (Szymański et al. 2017, Tomaselli 2004). In 1989, Lee was one of the first to propose a classification of these organisms based on the phylogenetic importance of the additional membranes around the chloroplast envelope (Tomaselli 2004; Heimann and Huerlimann 2015; Lee 2018). In fact, according to the endosymbiotic theory (Figure 1), about 1.5 billion years ago, the first photosynthesizing eukaryotic cells appeared as result of a phagocytosis of a cyanobacterium by a eukaryotic ancestor that had already acquired mitochondria through a similar process of phagocytosis that involved an α-proteobacterium. In this process, an ancestral Chlamydia could have helped the cyanobacterium ingress inside the eukaryotic ancestor (Jensen and Leister 2014; Cenci et al. 2017). This primary endosymbiosis led to the emergence of the primary chloroplast; a semiautonomous organelle limited by an envelope of two membranes. Among the phyla characterized by the presence of a primary chloroplast there are Rhodophyta (red algae), Chlorophyta (green algae), Streptophyta (land plants) and Glaucophyta (Tomaselli 2014; Maréchal 2018). However, the major portion of algae presents complex plastids characterized by several envelope membranes (higher than two). These plastids originated from eukaryote-to-eukaryote endosymbiosis (Dorrell and Howe 2012; Füssy and Oborník 2018). Five major groups of eukaryotes are characterized by complex plastids: Haptophyta, Cryptophyta, Ochrophyta, Cercozoa, Myzozoa and Euglenozoa. Euglenozoa and a relevant part of Myzozoa possess three-membrane-bound plastids, while other phyla possess four-membrane-bound plastids, compared to two-membrane-bound plastids of primary algae (Tomaselli 2004; Füssy and Oborník 2018). The primary endosymbiosis of the mitochondrion and chloroplast, as well as the subsequent secondary and tertiary eukaryote-to-eukaryote endosymbiosis, were followed by an internalization of endosymbiont genes into the nucleus of the eukaryotic host (Wollman 2016; Füssy and Oborník 2018). Taking into consideration that the taxonomic organisation can change rapidly due to ongoing studies, recent phylogenetic studies based on molecular analyses have provided new information about the relationships existing among the different algal groups and between individual algal groups and other plant organisms. For example, some studies allowed to confirm the belonging of the green algae and of the higher plants to the same evolutionary line (Viridiplantae) (Pancaldi et al. 2019).

Studied microalgae species: *Tisochrysis lutea* and *Nannochloropsis oculata*

The Haptophyta phylum and *Tisochrysis lutea*

The Haptophyta belong to the Chromista kingdom. Haptophytes are autotrophic, planktonic uninucleate flagellates. 1,159 species are known. They are divided into two classes: the Coccolithophyceae (Prymnesiophyceae) with around 76 genera and the Pavlovophyceae with 4 genera (Edvardsen et al. 2000; Guiry and Guiry 2021). They are mainly marine and unicellular or colonial, although some freshwater species are known. Some species of this phylum are widely used as feed microalgae in aquaculture, i.e. *Isochrysis* aff. *galbana* (*Tisochrysis lutea;* T-ISO) and *Pavlova salina* (Heimann and Huerlimann 2015). The cells are bi-flagellated, the flagella may be slightly different in size and are inserted laterally or in an apical position. However, they do not present the typical characteristics of Heterokonta described above. A typical structure of this division is the haptonema, a third appendage different from the flagella which has anchoring or trophic functions by bending and twisting. The phylum takes its name from this organelle (Eikrem et al. 2017; Cavalier-Smith et al. 2018; Pancaldi et al. 2019). Generally, Haptophyta cells present one or two plastids surrounded by endoplasmic reticulum confluent with the nuclear envelope. Three thylakoid lamellae are present and there is no girdle lamella. Pyrenoids are penetrated by one or a few pairs of thylakoids and generally are located within the plastid or may protrude from it towards the cytoplasm (Barsanti and Gualtieri, 2014; Nicholls 2015). When present, the eye spot consists of a row of spherical globules placed inside the chloroplast, although they can also be in other placements. Chlorophyll *a*, c_1 and c_2 are present. The yellow-brown colour of the chloroplast is due to the presence of accessory pigments such as β-carotene, fucoxanthin and other xanthophylls. The most important reserve product is chrysolaminarin (β-1,3-glucan), also known as leucosin (Barsanti and Gualtieri, 2014). In Coccolithophyceae the cell surface is usually covered with cellulosic or calcified scales (coccoliths). Despite intensive research on coccolithophores, the ecophysiological function of calcification is not yet understood; some theories propose that the production of calcified scales is involved in the removal of Ca^{2+} ions from the cytoplasm (Nicholls 2015; Eikrem et al. 2017). Indeed, according to Müller and co-workers (2015), compared with non-calcifying phytoplankton, coccolithophores can tolerate a greater increase in the concentration of Ca^{2+} ions.

The genus *Tisochrysis* (Haptophyta, Isocheydales) was originally isolated from tropical seawater (Tahiti, French Polynesia) (Bendif et al. 2013). Although *Tisochrysis lutea*

(formerly *Isochrysis aff. galbana* or T-iso) is morphologically identical to *Isochrysis galbana*, comparison of conservative genetic markers showed that there is a genetic distance between the two microalgae equivalent to that commonly found between different genera within the haptophytes. It was therefore classified into a new genus, *Tisochrysis*, and a new species, *T. lutea* (Bendif et al. 2013). This species is characterised by solitary, motile cells, generally between 3 and 7.5 μm in diameter. The cells are covered by layers of organic scales arranged radially on the surface There are two identical flagella, up to 7 μm-long, inserted apically with a short (about 100 nm) haptonema. They have a single, parietal, yellow-brown plastid into which the pyrenoid is immersed and which is traversed by thylakoid membranes (Bendif et al. 2013). Chlorophyll *a*, c_1 and c_2 are present in these algae. Among the carotenoids, diadinochrome, diatoxanthin and fucoxanthin are present in addition to beta-carotene (de Oliveira-Júnior et al. 2020). *T. lutea* is currently used mainly in aquaculture for its high content of protein and fibre, polyunsaturated fatty acids (PUFA), especially docosahexaenoic acid (DHA, C22:6 ω3), and carotenoids such as fucoxanthin (Hu et al. 2018; Bigagli et al. 2018). The presence of several bioactive compounds makes *T. lutea* an interesting source for nutraceutical and pharmaceutical products (Carrier et al. 2018). Among various microalgae strains, *T. lutea* has a higher content of fucoxanthin (more than 50-98% of the pigment by weight, depending on growing conditions) (Mohamadnia et al. 2020). The total lipid content accounts for 20-30% DW and is strongly influenced by the different growth conditions (Hu et al. 2018; Gao et al. 2021). In a recent study Mai et al. (2021) reported that saturated, monounsaturated and polyunsaturated fatty acid accounted for the 28.5%, 17.8% and 45.4% of the total fatty acid, respectively. Furthermore *T. lutea* is recognized as a suitable source of docosahexaenoic acid (DHA; ω-3), that accounts for 12–14% in total fatty acids (Hu et al. 2018).

The Ocrophyta phylum and *Nannochloropsis oculata*

The Ochrophyta belong to the Chromista kingdom, which is believed to have originated by endosymbiosis of a red alga by a heterotrophic eukaryote. This phylum includes about 7,000 species. The ochrophytes are among the organisms Heterokonta: in the mobile forms they possess two different flagella oriented in two opposite directions: the anterior flagellum has tripartite hairs (mastigonemes) and the posterior flagellum is without hairs smooth. This phylum includes many different classes such as Xanthophyceae, Chrysophyceae, diatoms (Bacillariophyceae), Phaeophyceae, Raphidophyceae and Eustigmatophyceae. The characteristic plastid (pheoplast) is bounded by four membranes, the two outermost of which

originate from the rough endoplasmic reticulum and in some cases may be in continuity with the nuclear membrane. Thylakoids are in groups of three along the entire length of the plastid. Often a ring formed by three thylakoids surrounds the plastid periphery. They possess chlorophyll *a*, chlorophylls c_1 and c_2; apart from Aurearenophyceae, Chrysophyceae and Eustigmatophyceae, in which only chlorophyll *a* is present. Xanthophylls and fucoxanthin are also frequently present. One or more pyrenoids are present in all classes of ochrophytes except in the zoospores of Eustigmatophyceae and Raphidophyceae (Barsanti e Gualtieri, 2014; Eliáš et al. 2016; Pancaldi et al. 2019). Eustigmatophyceae differ from most ochrophytes. These unicellular algae are green in colour, have a coccoid shape, and can be single or gathered in colonies, in the latter case there may be a slight morphological differentiation between the organisms forming the colony (Zakariah et al. 2016; Eliáš et al. 2016; Liu et al. 2017). The main reserve polysaccharide is chrysolaminarin (β-1,3-glucan), which is deposited in specific vacuoles in the cytoplasm. The cell wall of these algae is rich in carbohydrates and consists mainly of polyanionic polysaccharides such as alginate and sulphated polysaccharides containing fucose. These polymers predominate over the neutral, crystalline component composed mainly of cellulose (Eliáš et al. 2016; Salmeán et al. 2017).

The genus *Nannochloropsis* (Ochrophyta, Eustigmatophyceae) is widely distributed in oceans all over the world and plays a significant role in the global carbon and mineral cycle (Sukarni et al. 2014). Algae of this genus are often used in aquaculture as feed and have been considered with great interest for biofuel production in recent years (Liu et al. 2017; Zanella and Vianello, 2020). *Nannochloropsis oculata*, identified by Hibberd in 1981, is a small unicellular alga found in both freshwater and seawater. The cells are spherical or slightly ovoid, unflagged and between 2 and 4 μm in size (Borowitzka 2018). The most important photosynthetic pigment in *N. oculata* is chlorophyll *a*, because, unlike most microalgae belonging to the phylum Ocrophyta, chlorophylls *b* and *c* are absent. Among the carotenoids, violaxanthin and vaucheraxanthin are most abundant, zeaxanthin, antheraxanthin and beta-carotene are also present in lower concentrations (Faé Neto et al. 2018). Depending on the different cultivation conditions, the total fatty acid content accounts for 23-30% of DW (Bi and He, 2020). Under stress conditions, however, values of over 40% DW have been observed (Martínez-Maciaset et al. 2021). *N. oculata* is widely used in marine animal nutrition due to its high content of polyunsaturated fatty acids, especially eicosapentaenoic acid (EPA; 20:5n-3) and arachidonic acid (ARA; 20:4n6), important for the growth and development of larval fish, molluscs and crustaceans (Pradhan et al. 2019). Furthermore, due to the presence of palmitic acid (16:0) and

palmitoleic acid (16:1n7), it is also a good option for biodiesel production (Martínez-Macias et al. 2021).

1.2 Photosynthetic apparatus in organisms performing oxygenic photosynthesis

Photosynthesis is the process by which photosynthetic organisms such as plants and algae, as well as some bacteria as cyanobacteria, convert solar energy into chemical energy which is essential in the synthesis of biomolecules necessary for energy storage in the metabolic processes (Junge 2019). Photosynthesis may be split into the 'light' and 'dark' reactions. These reactions occur in two chloroplast compartments. In the thylakoid membranes, light reactions allow the synthesis of ATP and NADPH. In the stroma, the Calvin-Benson cycle utilizes ATP and NADPH to assimilate the atmospheric carbon dioxide for synthesis of carbohydrates (dark reactions) (Taiz et al. 2015; Johnson 2016) The overall reaction catalysed during the photosynthetic process is described as follows:

$$6\ CO_2 + 12\ H_2O + \text{light energy} \rightarrow C_6H_{12}O_6 + 6\ O_2 + 6\ H_2O$$

O_2, ATP and NADPH are produced as the result of water photolysis (Stirbet et al. 2020). In photosynthetic eukaryotes, photosynthesis takes place in the chloroplasts. In plants and green algae, the chloroplast is delimited by a double layer of membranes, mainly composed by phospholipids, a remnant of the primary endosymbiosis. Three or four envelope membranes are present in Chromista chloroplast because of a secondary endosymbiosis event (Larkum 2016). Inside the chloroplasts, the photosynthetic apparatus consists of strongly appressed thylakoid stacks called grana and flat lamellae of the stroma that connect these grana stacks. The lumens of the thylakoids of the stroma and the grana are continuous. This is necessary to ensure the accumulation of the proton motive force between the lumen and the stroma that will drive the photosynthetic production of ATP (Solymosi et al. 2018; Kirchhoff 2019).

The pigments in photosynthetic membranes

In the photosynthetic process, pigments act as an antenna by capturing light energy and channeling it into chlorophyll (Chl) molecules at the reaction center of the photosystem I (PSI) and photosystem II (PSII) photosynthetic units (Mirkovic et al., 2017). In the terrestrial environment, radiation within the 400–700 nm waveband is defined as photosynthetically active radiation (PAR; McCree 1972) with wavelengths outside this range not being used for photosynthesis; pigments are indeed able to adsorb only specific wavelengths (Kume et al 2018). Three main groups of pigments participate in light harvesting for photosynthesis: chlorophylls, carotenoids and phycobilins. Figure 2 reports the chemical structures of the major

photosynthetic pigments. Chlorophylls (Chls) are the green lipid-soluble photosynthetic pigments located in the thylakoid membranes of chloroplasts and are characterized into Chls *a*, *b*, *c*, *d*, *e*, and *f* that are present in a range of photosynthetic organisms such as plants, algae, and cyanobacteria. Chls selectively absorb light in the red and blue regions and therefore emits green colour (Mandal et al. 2020). The chemical structure is a porphyrin ring with magnesium as the prosthetic group. Phytol alcohol is ester-linked to one of the pyrrole groups and methyl alcohol to another (Perera 2019). Chl *a* presents a blue/green colour with maximum absorbance from 660 to 665 nm. It is present in all photosynthetic organisms and is found in both reaction centres (RCs) (PS I - P700 and PS II - P680) and in all light-harvesting complexes (LHCs) and is the first electron acceptor acting as primary donor for RC (Johnson 2016; Mandal et al. 2020). Chl *b* has a green/yellow colour with maximum absorbance from 642 to 652 nm. It is found in higher plants and in a variety of algae as Chlorophyceae. Chl *a* and Chl *b* differ from each other only for the group bound at carbon atom 3: in the former it is a methyl group, while the latter has a formil group (Larkum 2016; Mandal et al. 2020). Chl *c* is found only in algae with secondary plastids as chromophytic algae (also called Chromista) such as Diatoms and Haptophytes. This pigment is divided into Chl c_1 and Chl c_2. Chls *c* differ from Chls *a*, *b* in being Mg-phytoporphyrins rather than Mg-chlorins. It has a blue-green colour, and the spectra are dominated by a huge Soret band absorption (around 450 nm in acetone) and a small absorption close to 630 nm (Büchel 2020). Most algae which possess Chl *c* possess both c_1 and c_2, while a small group, mainly of prymnesiophytes, possess a third type, Chl c_3 (Larkum 2016). Carotenoids are fat-soluble accessory pigments. They vary in colour: β-carotene (orange), lycopene (red), xanthophylls (yellow) and absorb blue light strongly, enabling the chloroplast to trap a larger fraction of the light energy (Perera 2019; Yamori 2020). Depending on the function of the compounds on the microalgal cells, these compounds can be divided as primary carotenoids (i.e., lutein), which absorb light and are strongly linked to the photosynthetic processes or secondary carotenoids (such as astaxanthin and canthaxanthin) that play a major role in cell protective mechanisms (Lafarga et al. 2020). Some carotenoids play a protective role against photodamage at high light intensities by selectively quenching the triplet state of Chl *a* and thus preventing the formation of singlet oxygen, which is a harmful reactive oxygen species (Faraloni and Torzillo, 2017, Lehmuskero et al. 2018). Their fat-solubility derives from long carbon side chains and enables them to partition into the fatty regions of membranes but also makes them susceptible to oxidation. For example, β-Carotene is a vitamin A precursor and is very sensitive to oxidation, especially in the presence of sulphites (Perera 2019). The different carotenes differ little from each other except in chain length, α- and β-

carotenes play a similar role but are often quite specific in their distribution. On the contrary, xanthophylls are a very heterogeneous class of carotenoids. Many of these play a light-harvesting role, such as fucoxanthin, peridinin and vaucherioxanthin, which harvest light in the green region of the spectrum (500-550 nm). But there are other xanthophylls that participate in non-photochemical quenching process in the xanthophyll cycle; this is the case with zeaxanthin and violaxanthin (green algae and land plants) and diatoxanthin and diadinoxanthin in (chromista algae) (Larkum 2016). Due to the commercial importance of these molecules as antioxidants and natural colourants, new methods to increase their natural production are being explored; for example, in several microalgae species, the limitation of N has been considered as one of the main factors influencing the production of carotenoids, as well as that of lipids (Zhang et al. 2017). Phycobilins represent another main group of accessory pigments in photosynthesis; like the chlorophylls, phycobilins are tetrapyrroles. However, the four pyrroles in the phycobilins occur in an open chain, as is the case for phytochrome and not in a closed porphyrin ring, as is the case for the chlorophylls (Nobel 2020). They play an important role in light harvesting in cyanobacteria and a small number of algae classes (Rhodophyceae, Glaucophyceae and Cryptophyceae). Phycobilins harvest light in the 490-650 nm with a relatively small Soret band in the UV; a region of the spectrum where Chls and carotenoids are poorly efficient (Larkum 2016).

The light driven photosynthetic process

The main reactions of the light phase of photosynthesis take place due to the protein complexes embedded in thylakoid membranes, photosystem II (PSII) and photosystem I (PSI), their respective light-harvesting complexes (LHCII and LHCI), cytochrome b_6f (Cyt b_6f), and ATP synthase. Figure 3 shows the photosynthetic electron and proton transfer chain, the oxidation of water occurs on the lumen side, while the NADPH and ATP produced are released into the stroma. These integral membrane complexes are arranged so that proton transition from the stroma to the lumen occurs. The reaction centre of PSII, along with its antenna chlorophylls, is predominantly located in the grana. The reaction centre of PSI, and its associated antenna pigments, are located almost exclusively in the stromatic lamellae. The PSII/PSI ratio can vary with environmental lighting conditions (Taiz and Zeiger 2018; Junge 2019; Stirbet et al. 2020). Electron flow begins by oxidation of water, driven by the Oxygen Evolving Complex (OEC), a protein complex associated with PSII and located on the inner surface of the thylakoid membrane. Two molecules of H_2O are oxidized. Molecular oxygen, four hydrogen ions, and four electrons are produced: electrons are transferred to the reaction centre of the PSII, while

the four H^+ are released into the lumen, resulting in the formation of a proton gradient between the two sides of the thylakoidal membrane (Larkum 2016; Taiz and Zeiger 2018). PSII is a transmembrane protein complex. In the central part called the core is the reaction centre (RCII), with the two homologous proteins D1 and D2 (40kDa), each consisting of five transmembrane helices. These proteins are linked to a pair of chls *a* that absorb light in the red (680 nm) and constitute P680, the main electron donor of the RCII. When excited, these special Chls transfer the electron to an adjacent pheophytin molecule (Pheo), the primary acceptor of RCII (Larkum 2016; Johnson 2016; Taiz and Zeiger 2018; Sheng et al. 2019; Stirbet et al. 2020). The oxidized P680, can return to its fundamental state. An electron is donated by a tyrosine residue of the D1 protein, $TyrZ_{D1}$, which is reduced by an electron from water photolysis. The reduced Pheo transfers the electron to a plastoquinone Q_A. The electron is then moved to the plastoquinone Q_B, which is reduced to the semiquinone form Q_B^-. Reduction to the Q_B^{2-} form is achieved after a further cycle. Q_B^{2-} takes two protons from the stroma, the PQH_2 formed is released within the thylakoid membrane. An oxidized plastoquinone, from the PQ quinone pool, replaces Q_B in PSII. Four photons are required to complete two water molecules oxidation, therefore at each cycle two PQH_2 can be forming and released within the membrane to bind Cyt b_6f. These plastoquinol/plastocyanin reductase complex mediates electron transfer from the PQH_2 to Rieske's Fe-S protein, cytochrome *f* and finally to the plastocyanin (PC), a water-soluble protein located on the lumen side of the membrane. PC diffuses in the lumen to the PSI (Larkum 2016; Taiz and Zeiger 2018; Croce and van Amerongen 2020). The PSI complex is a plastocyanin-ferredoxin oxidoreductase that preferentially absorbs in the red at wavelengths longer than 680 nm. This consists of a reaction center, RCI, a peripheral antenna, LHCI, formed by the Lhca1-4 proteins, and a series of transporters that transfer the electron to the ferredoxin. As in PSII, a pair of specialty chlorophylls, called P700, is the major electron donor in PSI. The energy absorbed by the LHCI allows the excitation of P700 and consequently the transport of an electron from the PC through a series of transporters, such as phylloquinone and three Fe-S proteins. Finally, upon electron transfer to ferredoxin, an $NADP^+$ molecule is reduced to NADPH by ferredoxin-$NADP^+$ reductase (FNR) (Larkum 2016; Johnson 2016; Barber and Ruban 2017; Järviet al. 2018). The ATPase catalyzes ATP synthesis by exploiting the proton gradient energy generated between the two sides of the thylakoid membrane. Protons flow through the CF_0 transmembrane channel from the lumen to the stroma, while ADP and P_i are in the CF_1 catalytic site. As a result of a conformational change in the various subunits of the ATPase, a highly energetic phosphodiester bond is established, and ATP is released (Johnson 2016; Barber and Ruban 2017). In the light-independent reactions phase, the reduction of

carbon dioxide from ATP and NADPH generated in the light phase occurs through a set of reactions that integrate the Calvin-Benson-Bassham cycle (Johnson 2016; Queiroza et al. 2020). The electronic flow of the photosynthetic process is represented by the so-called Z-scheme, which provides the electronic transfer information from both kinetic and thermodynamic points of view (Figure 4). The Z-scheme shows all components involved in the transport chain arranged according to their oxidation-reduction potential (Johnson 2016; Shevela and Lars 2017).

1.3 Biotechnological potential of microalgae: valuable products and commercial development

Microorganisms have been used for decades as sources of antibiotics, vitamins, and enzymes and to produce fermented foods and chemicals. During the 20th century, considerable progress was made in the field of industrial microbiology. Molecular biology helped to discover new potentials of microorganisms and to optimise their productivity. Later, genetic engineering techniques have also allowed the production of non-microbial molecules (Murphy, 2012). Sunlight is the most important input of energy to Earth and photosynthesis is the only biological process channelizes solar energy into the biosphere. Microalgae have high photosynthetic rates and efficiency: under optimal growth conditions the theoretical maximum photosynthetic efficiency for microalgae is approximately 10%, while for C3 and C4 plants is respectively 4.6% and 6% (Barsanti and Gualtieri 2018). In this respect, microalgae have great potential. The variety of species that characterises these microorganisms is the basis of their importance. Simply by using the energy of sunlight and atmospheric CO_2, they are able to rapidly increase their biomass. The biomass can be valorised and used for the sustainable production of food, feed, chemicals, fuel, energy and heat (Chisti 2018, 2020). In fact, microalgae can produce various types of antioxidants, carotenoids, enzymes, lipids, natural dyes, polyunsaturated fatty acids (PUFA) and sterols, all of them with industrial applications (Suganya et al. 2016; Moreno-Garcia et al. 2017). A further use of these microorganisms is in environmental biotechnology. They can be used for biomonitoring of toxic substances, in environmental remediation, in the production of green energy sources, and in CO_2 fixation (Rizwan et al. 2018; Chisti 2020). In this context, the growing inclinations towards natural and eco-friendly products and the demand for green energy sources have spurred the microalgae market growth. In 2018, Europe accounted for 32% of global demand of algae products, becoming the largest consumer in the word. Europe is projected to maintain its dominance during the period 2019-2027. It is also projected to be the fastest-growing market during the forecast period (source:

https://www.credenceresearch.com/report/algae-products-market). In fact, according to the Persistence Market Research Report (2018), worldwide sales of microalgae are estimated to exceed US$ 75 Mn in revenues by 2026-end. At present, microalgae are widely used to produce biofuel. However, fuel-only strategies are not always cost-effective in terms of microalgae cultivation, high-end products with health benefits are gaining more and more consideration. There is growing interest in food and feed grade microalgae due to the demand for plant-based products and consumer awareness of the health benefits of microalgae (Nagarajan et al. 2021).

Biofuel production

The COVID-19 pandemic had a massive impact on energy markets, with both primary energy and carbon emissions falling at their fastest rates since the Second World War, and renewable energy continuing to grow (bp Statistical Review of World Energy 2021). However, in the post-pandemic period, investment in fossil fuels continues to be overwhelming in most countries, including the US and China (Le Quéré et al. 2021). Now more than ever, environmental pollution and the scarcity of energy resources are nowadays extremely important issues limiting the sustainable development of the world economy. Fossil fuels still accounted for 84% of the world's primary energy consumption in 2019 and are estimated to run out between 2069 and 2088 (Stephens et al. 2010; Malhotra 2019; bp Statistical Review of World Energy 2020). Within this framework, there is growing scientific, political and social interest in the production and use of biodiesel as a green and renewable energy source, moreover public appeal promoted governments enforcement of stricter environmental regulations (Chen et al. 2017; Liao and Shi 2018). Biorefinery is defined as the production of biofuels and high-value co-products from biomass, integrating bioprocesses with chemical technologies with a low environmental impact (Suganya et al. 2016). Biofuels can be classified into four main categories according to the feedstock. The 1st generation biofuels come from plant biomass such as corn, sugarcane bagasse, wheat starch, soya bean, rapeseed, canola, jatropha etc. The lignocellulosic biomass and waste animal oils constitute 2nd generation biofuels (Ruan et al. 2019). Despite their known potential to mitigate CO_2 emissions, the demand for large areas, water and nutrients for cultivation and competition with agriculture are some of the major factors limiting the use of these biofuels (Arora et al. 2019). The 3rd generation biofuels try to overcome these issues. They are derived from the biomass of various microorganisms: bacteria, yeasts, fungi and microalgae. Finally, the 4th generation biofuels use genetically modified microorganisms to increase their biofuel potential (Arora et al. 2019; Ganesan et al. 2020). The use of microalgae

to produce biofuels is advantageous compared to other oil crops such as rapeseed, soya and sunflower. In fact, microalgae are the most efficient in terms of both oil yield and high biodiesel productivity (52 000 to 120 000 $kg_{biodiesel}$/ha) and at the same time require no arable lands and in general less area, even 49-132 times less than that required for rapeseed and soy cultivation (Amicarelli et al. 2012; Gambelli et al. 2017). Despite the considerable potential of microalgae, their large-scale application is delayed by technical and economic problems (Arora et al. 2019). The main challenges for biodiesel from microalgae relate to the amount of energy and water required for cultivation and harvesting. The high costs can be reduced combining biofuel production with the extraction of commercially valuable compounds, such as pigments and enzymes (Rizwan et al. 2018; Chia et al. 2018).

Bioactive molecules production for human health and cosmetic

In recent decades, interest in vegetal based bioactive molecules has increased. Bioactive molecules include a wide variety of compounds, commonly assumed through the diet, such as pigments, polyphenols, fatty acids, proteins/enzymes, sterols, vitamins, alkaloids, amino acids, and other compounds not included in these classes. These compounds can modulate numerous biological functions, influencing health positively (Borowitzka 2018b; Basheer et al. 2020). Microalgae are natural sources of these molecules that can be found within the cell biomass or released into the culture medium (Bhagavathy et al. 2011). Significant effects of microalgae bioactive molecules in human health may include anti-inflammatory and antiobesity effects, antiviral antioxidant, antimicrobial and anticancer activities (Chénais 2021). Bioassays of microalgal extracts clearly demonstrate their potential to kill fungi and bacteria and to inhibit growth of viral and cancer cells (Singh et al. 2021). This makes algae and microalgae great candidates for functional food and drugs. However, the small quantities of biomolecules (in terms of μg/g dry weight) made it difficult to produce at large scale (Singh et al. 2021). Nevertheless, the growing phenomenon of antibiotic resistance against pathogenic bacteria drives research to explore new antibacterial compounds derived from different natural environments (Ferrazzano et al. 2020). There are many microalgae that are utilized to produce compounds with antibiotics and antimicrobial activity such as bromophenols, alcohols, tannins, polysaccharide, fatty acids, and terpenoids (Basheer et al. 2020). *Arthrospira* and *Chlorella* are known to produce sulphated polysaccharides with antimicrobial activity (Buono et al. 2014). Carotenoids and phycocyanin are well-known antioxidant molecules and are commonly produced by microalgae and cyanobacteria (Barkia et al. 2019). Among the most common

antioxidants commercially available are β-carotene, widely produced by *Dunaliella salina*, and astaxanthin, which constitutes up to 5% by dry weight of the total biomass of *Haematococcus pluvialis* (Xu et al. 2018; Li et al. 2020). Due to their antioxidant and anti-inflammatory properties, these molecules are involved in preventing and reducing protein degradation, rheumatoid arthritis, cardiovascular diseases, neurodegenerative diseases and cancer (Barkia et al. 2019; Jacob-Lopes et al. 2019; Nabi et al. 2020). Microalgae can have a protein yield of more than 50% in dry weight (Levasseur et al. 2020). Some microalgae proteins have hypolipidemic and hypoglycaemic properties and their ingestion is associated with reduced cholesterol and triglyceride levels (Soto-Sierra et al. 2018). Some of them promote the production of hormones involved in achieving satiety and could be used in foods and in nutraceutical sector to prevent obesity (Patias et al. 2018). Some of the most important microalgal compounds are the long-chain polyunsaturated fatty acids (PUFAs). In this class of molecules are included ω-3 and ω-6 long-chain fatty acids: linolenic, eicosapentaenoic (EPA) and docosahexaenoic (DHA), gamma-linolenic (GLA) and arachidonic (ARA) (Ryckebosch et al. 2014; Basheer et al. 2020). Certain fatty acids are called essential fatty acids due to the inability of humans to synthesise them (Hu et al. 2019). The intake of DHA and EPA provides health benefits by counteracting inflammatory processes and reducing the risk of cardiovascular diseases, helps the development of the nervous system in children and improves brain functions (Bazinet and Layé 2014). Fatty acids are also used in cosmetic formulations to revitalise the skin and prevent ageing (Saini and Keum 2018). Nowadays, the algae industry is estimated to be worth more than USD 6 billion per year, out of which 85% contains products for human utilization (Basheer et al. 2020). The use of microalgae in cosmetics is widespread, especially in the treatment of the skin due to their ability to combat reactive oxygen species (antioxidant activity). Microalgae extracts showed UV photoprotective effects and anti-melanoma effects (Berthon et al. 2017; Corinaldesi et al. 2017).

Human food source

A recent United Nations report estimated that by 2020 the number of people suffering from malnutrition and hunger in the world had risen alarmingly from 650 million to 768 million: about one-tenth of the population. This increase is mainly due to the COVID-19 pandemic and the resulting economic crisis, as well as to the climate crisis which makes food production increasingly difficult for some populations (The state of food security and nutrition in the world 2021; https://www.fao.org/documents/card/en/c/cb4474en). In this context, the need to develop

new sources of foods is growing. Microalgae can be considered a potential food source due to the possibility of large-scale production and high biomass production. They also provide several advantages compared to classical plant and animal food sources, such as requiring a smaller cultivation area and being independent of growing seasons (Colla et al. 2020; Wang et al. 2020) Nowadays, microalgae for human consumption are marketed in various forms, such as tablets, capsules and drinks. They can also be incorporated into various products such as pasta, bread and snacks to give them new and improved nutritional characteristics (Camacho et al. 2019). Microalgae are therefore used as supplements or as foods themselves (Caporgno and Mathys 2018). A limited number of microalgal species are used for human consumption or to produce high-value added foods. This is due to multiple factors. Firstly, production cost of some microalgae biomass is higher than the industry considers reasonable. In addition, technical and economic aspects must be considered, including maintenance, market awareness and regulatory compliance (Jacob-Lopes et al. 2019; Rahman 2020). In this context, understanding the regulatory framework, environmental and ecological law is crucial. While in the United States, Japan and in Brazil the rules are applied to the product, assessing if the final product is safe, the European regulation focuses on the technology that was employed to obtain the product (Jacob-Lopes et al. 2019). Algae are currently listed as Generally Recognized as Safe (GRAS) for human consumption, a status given by the Food and Drug Administration (United States (U.S.) Food and Drug Administration, 2018). However, the GRAS designation only applies to U.S. jurisdiction and only a few microalgae species are included e.g., *Arthrospira platensis, Chlamydomonas reinhardtii, Auxenochlorella protothecoides, Chlorella vulgaris, Dunaliella bardawil,* and *Euglena gracilis* (Torres-Tiji et al. 2020). In the European Union (EU), microalgae and products derived from them are considered "novel foods" if they had no significant history of consumption within the EU prior to 15 May 1997. As microalgae are considered novel foods, they are under Regulation (EU) No. 2015/2283 of the European Parliament and of the Council of 25 November 2015 on novel foods. This regulation became effective on 1 January 2018 and deals with the regulation, production and trade of novel foods in Europe, amending the previous Regulation (EU) No. 1169/2011 of the European Parliament and of the Council and repealing Regulation (EC) No. 258/97 of the European Parliament and of the Council and Regulation (EC) No. 1852/2001 of the Commission (Regulation (EU) 2015/2283 of the European Parliament and of the Council of 25 November 2015 on novel foods). Worldwide, the most used microalgae as food are *Spirulina*, *Chlorella*, *Dunaliella* (Rizwan et al. 2018). In *Spirulina* (*Arthrospira platensis*), the protein content accounts for 45–60% of the dry weight of the total biomass (Pereira et al. 2021). Due to its high nutritional

value, *Spirulina* has been used as a food source in Asia, South America and Africa since ancient times: as far back as 1300 AD, the Aztecs used these microorganisms as food by harvesting them from Lake Texcoco (Barsanti and Gualtieri, 2014). *Spirulina* is widely used also as a source of vitamins A and C, polyunsaturated fatty acids, phenolic compounds and various pigments (Matos et al. 2017; Lafarga et al. 2020). *Dunaliella salina* is used to produce β-carotene, which accounts for about 14% of dry biomass and is employed in the production of vitamin C and food colourants (Blanco et al. 2007; Rizwan et al. 2018). Due to the possibility of growing in hyper-saline media, in prohibitive conditions to the majority contaminating organisms, cultivation of *Dunaliella* may result cost-effective (Zhu et al. 2018; Colusse et al. 2020). *Chlorella* represents a good source of protein, (51-58% of dry weight), carotenoids and several vitamins (Ferreira et al. 2020). The presence of β-glucans stimulates the immune system, fights free radicals and lowers blood cholesterol levels (Abdelhamid et al. 2020). Overall, microalgal proteins may present a lower bioavailability than conventional protein sources, especially those of animal origin. This is due to the possible presence in some microalgae of the cellulosic cell wall, which is indigestible to humans (Wang et al. 2020). The bioavailability of the microalgae proteins can be improved by cracking the cell wall using physical methods such as crushing, grinding and heating (Caporgno and Mathys 2018). Nowadays, an intake of 250 mg to 2 g of EPA and DHA daily is recommended to prevent coronary heart or PUFA-deficient-related aging diseases (Zhang et al. 2018). Traditionally, molluscs and fish have been the primary source of PUFAs in human nutrition. However, these animals are not the primary producers of PUFAs; on the contrary, they bioaccumulate them by directly consuming phytoplankton (microalgae) that primarily produce PUFAs or preying on smaller fish that feed on phytoplankton (Ryckebosh et al. 2014; Tibaldi et al. 2015; Wang et al. 2020). In this framework, microalgae constitute a credible vegetal source for PUFAs production including as a source of ω-3 and ω-6. Moreover, it should be considered that, currently, fish- and animal-derived products are eco-unfriendly source and find less and less consensus among consumers, especially vegetarians or vegans (Wang et al. 2020).

Animal feed and aquaculture

According to the World Population Prospects 2019 of the United Nations (https://population.un.org/wpp/), the world population is expected to increase by 2 billion persons in the next 30 years, reaching 9.7 billion by 2050. To cope with the growing demand for high-quality, protein-rich foods, the production must increase dramatically, potentially

doubling by 2050; this constitutes a potential risk to environmental sustainability (Hunter et al. 2017). Nowadays, 57% of the global protein supply comes from plant sources (mainly terrestrial); the remaining 43% comes from animal sources (Henchion et al. 2017). The provisioning of feed accounts for between 60 and 80% of production costs in the livestock industry (Uyeh et al. 2018). The use of traditional crops such as soya or animal meal such as fishmeal, while economically sustainable, is not environmentally sustainable. Thus, it is crucial found alternative and eco-friendly sources to produce high-quality feeds. Microalgae have been used as a sustainable feed in aquaculture for many years. Most recently, they entered the farm animals feed market with benefits both on the quality and nutritional properties of the meat and on ecological impact. Currently, about 30% of current global microalgae production is sold to the feed industries (Dineshbabu et al. 2019; Levasseur et al. 2020). Similar to their use in human nutrition, the success of microalgae as a feed is based on their nutritional quality: high protein content, pigments (e.g., lutein, astaxanthin, and β-carotene) poly-unsaturated fatty acids, vitamins, and minerals (Yaakob et al. 2014; Nagarajan et al. 2021). The genera *Arthrospira*, *Chlorella*, *Nannochloropsis*, *Tetraselmis*, *Pavlova*, *Isochrysis*, *Chlorella*, *Phaeodactylum*, *Skeletonema*, *Chaetoceros*, *Thalassiosira*, and *Haematococcus* are widely used as animal feed and in aquaculture (Madeira et al. 2017). As a feed component, microalgae provide primary energy through their polysaccharides. The supply of lipids, energy-dense molecules, help to increase the calorific value of the feed (Pina-Pérez et al. 2019; Nagarajan et al. 2021). The use of lipid-rich microalgae in feed makes it possible to obtain foods with high value of PUFAs by means of a bioaccumulation process. Microalgae-based feeds in aquaculture may improve the fatty acid profile of fish; furthermore, microalgae are a viable alternative to fish oil (Carvalho et al. 2020; Levasseur et al. 2020). With respect to the use of microalgae in livestock feed, Vossen and colleagues (2017) reported that feed supplemented of freeze-dried *Schizochytrium* biomass in pigs significantly improved the PUFA content of meat without affecting the sensory quality. Also in lambs, supplemented feeding with lipid rich microalgae reduced the total cholesterol of meat and improved the EPA, DHA, and fatty acids content (Valença et al. 2021). Microalgae, particularly green algae and cyanobacteria are rich in proteins, a key factor in animal feed. Nevertheless, microalgae used in feed are subject to comply stringent criteria of quality, digestibility, absorption and nutrients bioavailability (Amorim et al. 2020). Toxicological assessment for the presence of toxins and heavy metals, microbiological analysis for the presence of bacteria and pathogens, and long-term feeding trials to assess the safety of unidentified components of microalgal origin are also required (Acquah et al. 2020).

Bioremediation

Water scarcity affects more than 40% of the global population and is projected to rise. Over 1.7 billion people are currently living in river basins where water use exceeds recharge. More than 80% of wastewater resulting from human activities is discharged into rivers or sea without any pollution removal (The Sustainable Development Agenda, United Nation 2020). The term wastewater includes all discharges from commercial establishments, households, institutions, industries, hospitals, etc. This definition includes urban runoff and rainwater as well as horticulture, aquaculture and agricultural effluents (Romagnolli 2013; Kumar et al. 2019). Due to its content of macro- and micro-nutrients wastewater provides a low-cost medium for the growth of various microalgae. Nitrate, ammonia, phosphate, urea and trace minerals are the main nutrients found in wastewater. Carbon (C), nitrogen (N) and phosphorus (P) are the three most important nutrients when evaluating a wastewater source for microalgae growth (Salama et al. 2017). For N and P removal, the use of microalgal cultures offers some advantages compared to processes using bacteria, such as a high removal efficiency and lower operation cost because an organic carbon source is not required. Furthermore, the biomass produced can be used for different purposes (e.g., high-value products and biofuel production) (Martínez and Cañizares 2020). In addition to their use in the removal of N and P, microalgae are also employed in the elimination of other important pollutants. In fact, in the last decades, the composition of wastewater greatly changed; new pollutants and emerging contaminants (ECs) have been found. Many of these have persistent nature, negative effects on living organisms and are recalcitrant to traditional purification system. In this framework, search for new microorganisms including algae, fungi and bacteria able to operate efficient purification processes is crucial (Escapa et al. 2015; Matamoros et al. 2015; Rout et al. 2021; Parida et al. 2021). Heavy metals are among these pollutants. Traditionally, their removal from wastewater employs chemical processes that produce huge amounts of sludge with a high concentration of metal to be disposed of as dangerous waste (Azimi et al. 2017). Due to the net negative surface charge, the algal biomass is effective in the adsorptive removal of heavy metal cations (e.g., Cd^{2+}, Pb^{2+}, Ni^{2+}, Zn^{2+}) from industrial wastewater (Chatsungnoen and Chisti 2019; Chisti 2020). The use of microalgae in this field, compared to traditional techniques, may have advantages such as lower costs, high specific surface area compared with other sorbents and, in some cases, the possibility of recovering metals (Raikova et al. 2017; Piccini et al. 2019; Martínez and Cañizares 2020). Moreover, some microalgae species showed an affinity for specific metals: *Chlorella* and *Scenedesmus* showed affinity for many metals such as Cd, Cr,

Cu, Hg, Pb, Zn; good removal rates for Cd, Co, Cr and Ni were found using *Spirulina* (Suresh Kumar et al. 2015). Generally, for wastewater treatment monocultures of microalgae strains are used. However, some studies highlight the advantages of using a consortium of microalgae in several scenarios (Al-Jabri et al. 2021). Typically, there are different contaminants in wastewater, a consortium of different microalgal strains or microalgae and bacteria could be advantageous if the different microorganisms have different target pollutants. In this way the limitation of one strain could be overcome by the others; in fact, each microalgal species may presents different tolerances, bioadsorption or biodegradation rates for each contaminant. (Gonçalves et al. 2017; Sutherland and Ralph 2019). Both native and artificial consortia can be employed in wastewater treatment. Koreivienė et al. (2014) showed that the artificial consortium of *Chlorella* and *Scenedesmus* was highly efficient in the removal of nitrogen and phosphorus from urban wastewater with a removal efficiency ranging between 88.6–96.4 % and 99.7–99.9 %, respectively. Posadas and colleagues (2013) tested a native algae-bacteria consortium on centrate and domestic wastewater. They found superior performance in terms of N and P removal of algal-bacterial biofilms compared to bacterial biofilms (twice higher nutrient removal rates). In addition, the consortium provided more stability and resistance of the biofilm.

1.4 Microalgae cultivation

Microalgae are fast-growing photosynthetic organisms that can convert 9-10% of solar energy into biomass with a theoretical yield of about 77 g/biomass/m^2/day. However, the actual yield is lower than the theoretical yield in both outdoor and indoor culture systems (Khan et al. 2018). Obtained yields are one third to one tenth of the theoretical ones (Williams and Laurens 2010). The cultivation of microalgae does not require arable land, large amounts of fresh water, herbicides and pesticides, and therefore does not compete for agricultural crop resources (Khan et al. 2018, Suparmaniam et al. 2019). Together with the accessibility of nutrients, in particular nitrogen and phosphorus, light, pH and temperature are the main factors influencing the robust growth of microalgae (Suparmaniam et al. 2019). An ideal microalgae culture system has an adequate light source, efficient liquid-gas exchange, user-friendly design, low contamination rates, low production and management costs, and high medium efficiency (Tan et al. 2020). Various cultivation techniques are currently employed to produce microalgae biomass. In terms of facilities, cultivation systems may be classified into two main categories: open culture systems (lakes or ponds) and closed culture systems called photobioreactors (PBR) (Figure 5)

(Yousuf 2020). Based on the types of metabolism, cultures can be classified as autotrophic, heterotrophic and mixotrophic (Vuppaladadiyam et al. 2018).

Open cultivation systems

Open cultivation systems are widely used in microalgae cultivation mainly due to their simplicity and cost-effective design combined with high production capacities (Faried et al. 2017; Ranganathan et al. 2017). Nevertheless, these systems generally require a considerable amount of space and are influenced by environmental conditions fluctuations such as temperature and sunlight, furthermore the production of high-quality microalgae biomass is limited by the high rates of contamination (Suparmaniam et al. 2019). To allow sunlight to reach all layers of the suspension in which the microalgae grow, the depth must be reduced (usually 1-100 cm), moreover a paddlewheel or a pivot rotating agitator provide the circulation of the culture making the distribution of both light and nutrients uniform and preventing the culture from stagnating. Risk of contaminations, high evaporation rates and concomitant diffusion of CO_2 into the atmosphere are other issues in open systems (Singh et al. 2015; Chew et al. 2018). Open ponds are typically built-in raceway or circular configurations. Raceway ponds are characterised by low construction costs: the walls are made of concrete or rammed earth covered by white plastic. One or more paddlewheels provide continuous mixing and recirculation of the culture and baffles guide the flow at bends. These systems are designed to be shallow with an average depth of 30 cm (Faried et al. 2017; Suparmaniam et al. 2019). They can occupy large areas, for example, in Calipatria, CA (USA), a *Spirulina* cultivation plant, that occupies an area of 444, 000 m^2 (Kiran et al. 2014), is present. The most reported algae, include *Spirulina*, *Dunaliella*, *Chlorella* and *Haematococcus,* are cultivated in this type of system (Han et al. 2017). In circular ponds a central pivot rotating agitator mix the culture; this system of recirculation is less efficient than paddle wheels; therefore, the lower efficiency is compensated by the reduction in the size of the ponds (Suparmaniam et al. 2019). Another open system example is the inclined thin-layer cascade system, designed to support a much higher cell density. In this system, the movement of the microalgal culture is provided by gravity: the culture flows from the top to the bottom over a sloped surface; a pump is applied to move the culture from the bottom to the top (Vieira Costa et al. 2019). This system is characterised by a highly turbulent flow and a thin layer of the culture suspension, generally less than 1 cm; this gives a high ratio of exposed surface area to total culture volume, facilitating gas exchange and light capture. Much higher volume yields (up to 40 g L^{-1}) can be achieved than in the other open ponds. The main negative points are the cost of pump use and the high evaporation rate

(Sun et al. 2016; Deruyck et al. 2019). To improve the control of the growing conditions, closed pond systems using greenhouses can be used. These systems allow the control of several environmental parameters and limit the contamination problems associated with open pond systems. The resulting microalgal biomass has a higher quality but also a higher cost (Suparmaniam et al. 2019).

Closed cultivation systems

Closed photobioreactors (PBR) facilitate the cultivation of strains of microalgae for long periods with minimal risk of contamination. For these reasons, enclosed PBRs are widely used to produce biochemical and high-value metabolites. In addition, the regulation and control of many parameters, the reproducibility of cultivation conditions, the need for smaller spaces and the opportunity to use both artificial and natural light are some of the advantages over open systems (Chew et al. 2018; Tan et al. 2018a). However, construction and maintenance costs are higher than for pond systems. Materials such as glass and transparent plastic are generally employed to design of these systems, increasing costs (Suparmaniam et al. 2019). Tubular and flat panel PBRs are the most popular closed culture systems on commercial scale for microalgae cultivation. Tubular PBRs are the most common ones. Construction materials consist of glass or plastic tubes arrayed in horizontal, vertical, fence-like, inclined or helix configurations (Tan et al. 2018a). The culture is mixed by air sparger attached at the bottom of the reactor or a degassing column (Han et al. 2017). Vertical tube PBRs reactor present the simplest design: the bubble column consists of a cylindrical vessel with no internal structure, the movement of the culture is provided by air bubbles. The improved design of this reactor is the airlift reactor, characterised by two interconnected zones inside. In this configuration the air bubbles move the culture more efficiently from the darker inner zone of the tube to the brighter outer zone. Good mixing with low shear stress is achieved (Chew et al. 2018). The horizontal tube system consists of long horizontal tubes which can be arranged in many variations to form walls, helices or panels. This configuration requires a large area but guarantees a high operative surface (Chew et al. 2018). With the help of a pump, the culture circulates from the degassing column, where the gas exchange takes place, to the solar array and back to the degassing column in a continuous operation mode (Faried et al. 2017; Supermaniam et al. 2019). Flat-plate PBRs are another possible design. It has a cuboidal shape and dense microalgae culture pass through grass or plexiglass flat panels. The flat panel system is characterized by high surface area to volume ratio for illumination, flexible design for scale-up process and low amount of oxygen accumulation and high cell densities (> 80 g L^{-1}) (Han et al 2017; Supermaniam et al. 2019).

The culture is moved by a pump, the agitation is provided by mechanical motor or air bubbling through perforated tubes. (Faried et al. 2017). However, this design presents some limitations connected with aeration that causes hydrodynamic stress, formation of biofouling at the surface and biomass adhesion to the walls of the bioreactor (Chew et al. 2018).

Batch, semi-continuous and continuous systems

There are different types of microalgae cultivation, including batch, semi-continuous and continuous methods. Batch cultivation of microalgae is well researched and often used in laboratory-scale studies. It is a closed system in which the volume of the culture remains constant from the beginning to the end of cell growth. As the biomass increases, the available nutrients decrease and are not reintroduced into the system. The biomass grows until it is limited by the lack of nutrients and light caused by self-shading. The metabolites produced remain in the system until the biomass is harvested at the end of the process (Yin et al. 2020). Batch cultures present low risk of contamination, are flexible and simple to operate but lack process efficiency. In a batch system there is downtime for reactor cleaning and start-up between cycles. This results in decreased productivity and increased work, water and chemical usage (Benvenuti et al. 2016; Yadav et al. 2020). Fed-batch mode is a variation on batch culture. Using this system new culture medium or a concentrated nutrient solution is added regularly without removing any biomass. The volume and total biomass of the culture increases with each addition. This results in a longer growth period and a higher final biomass yield (Henley 2019). The semi-continuous or continuous operations are first carried out in batch mode for a fixed term in order to achieve a substantial biomass level, and then in a semi-continuous or continuous mode (Zhu 2015). In semi-continuous culture, biomass is intermittently harvested by supplementing the fresh culture medium (Yin et al. 2020). Semi-continuous cultivation is recommended by researchers as opposed to batch process as it is a more feasible method especially for large scale cultivation. With proper control of the feeding rates of the culture medium, high biomass productivity and stable conditions can be achieved. Furthermore, capacity of treating wastewater (Tan et al. 2018b). This cultivation method is effective in wastewater treatment, CO_2 biofixation and production of secondary metabolites and carbohydrates (Liu et al. 2019; Solís-Salinas et al. 2021). However, in semi-continuous cultivations, the risk of contamination is higher than in batch cultivations, as well as higher economic investments (Yin et al. 2020). In continuous cultures, constant dilution with fresh medium takes place, keeping the volume of culture constant by removing biomass from the system. In this way the density and composition

of the biomass remain stable within narrow limits. Dilution may be continuous or through small, very frequent dilutions. The aim is to reach a steady state (Henley 2019). Growth rates and biomass concentration can be regulated and maintained for the extended period by varying the dilution rate. Continuous cultures offer increased opportunities for system investigation and analysis because the results are more reliable and easily reproducible (Yadav et al. 2020; Chen and Gao 2021). Though continuous systems are the most process efficient, they are difficult to control especially in industrial operations, the long-term growth increases the contamination risk, the higher quality equipment required increases operational costs, finally, the original product strain can be lost over time (Henley 2019; Yin et al. 2020).

Co-cultivation system

A current driving force that inspires the progress in microalgae production is the search for novel cultivation systems to obtain a reduction of the costs and a lower consumption of water and nutrients. Naturally, almost all micro-organisms form mixed consortia sharing multiple relationships with each other: symbiotic, commensalism, mutualism, competition, etc. (Jiang et al. 2019). These microbial interactions are of great importance in nature with respect to the existence of individual microorganisms and in maintaining the ecosystem equilibrium (Das et al. 2021). In this context, several studies have been focused on the co-cultivation of different organisms (Zhu 2015; Ray et al. 2022). Co-culture is a cell cultivation setup where two or more different microorganisms are grown together with some degree of contact between them, a strategy based on the concept of ecological community: no species lives isolated in nature (Smith and Crews 2014; Pacheco and Segrè 2019). Microalgal co-cultivation has a tremendous potential because it can present advantages such as contamination minimisation, increased biomass and lipid yield, improved waste removal and harvesting efficiency, co-production of value-added biosimilar products (Padmaperuma et al. 2018; Yao eta al. 2019; Das et al. 2021; Ray et al. 2022). This cultivation mode can involve different microalgal species or microalgae and other microorganisms such as fungi, bacteria and yest (Zhu et al. 2017). Regardless of the type of microorganisms forming the consortium, in general genetic diversity reduces the vulnerability of ecosystems to disturbances. Therefore, co-cultures are more robust than monocultures (Bradáčová et al. 2019; Tejido-Nuñez et al. 2020). Co-cultures reduce the frequency and severity of viral, bacterial, or fungal infections as well as predation by protozoa in open ponds. Indeed, the severity of contamination can be aggravated by the absence of genetic variability in the culture (Lian et al. 2018; Pleissner et al. 2020). Microalgae-microalgae

co-culture strategy has been observed to incur positive effects on both the biomass and lipid yield along with the change in lipid composition (Zhu et al. 2019; Cheng et al. 2020). One of the advantages of the microalgae-microalgae co-culture strategy is to obtain a relatively denser culture more rapidly than in monocultures. In part this is due to the increased interactions between the microorganisms leading to increased extracellular polymeric substances (EPS) production as a metabolic adaptation strategy to unfavourable conditions, such as competition for nutrients (Ramanan et al. 2016; Ray et al. 2022). The efficiency of microalgae consortia in wastewater treatment has also been demonstrated, heavy metal removal efficiency was also found to be better in consortium (Sharma et al. 2020). In the field of wastewater treatment, good results have been obtained using microalgae-bacteria co-cultures (Khoo et al. 2021). In microalgae cultures, bacteria are often considered as contaminants, especially on a laboratory scale. However, naturally the establishment of microalgae-bacteria consortia is present; the phycosphere, microscale mucus region surrounding the microalgae, is rich in extracellular products feed for bacteria (Ferrer-González et al. 2021). Conversely, heterotrophic bacteria stimulate microalgae growth providing B vitamins as organic cofactors or produce siderophores to bind iron, which could be used by microalgae (Yao et al. 2019). Furthermore, in a co-cultivation system bacteria maintain constant in the culturing medium the dissolved organic carbon (DOC) level (Seymour et al. 2017; Yao et al. 2019; Nef et al. 2019). Microalgae-bacteria co-culture strategy is advantageous by reducing the risk of contamination, the total cost of the operation, and at the same time the recovery of various by-products from the co-culture (Yao et al. 2019; Das et al. 2021). Another useful strategy to reducing process costs is the microalgae-fungi co-cultivation. Many studies are focusing on the harvesting of microalgal cells by the fungal pellets (Veiter et al. 2018). In fact, harvesting of microalgal cells from the large culture may accounts for 50% of the total production cost (Raheem et al. 2018). Some filamentous fungi have self-pelleting capabilities, in co-culture with microalgae this leads to bioflocculation of microalgae without add any external chemical flocculants and reducing the use of methods such as centrifugation. This potentially lowers the energy consumption and cost of the entire cultivation process (Nazari et al. 2020). In addition, in microalgae-fungi co-cultivation strategy an increase in overall lipid productivity has also been demonstrated (Yang et al. 2019; Zorn et al. 2020). In addition to the organisms already considered, oleaginous yeasts are becoming one of the microorganisms that best support microalgae for enhance lipid productivity by utilizing minimal resources, but also as feed for aquaculture, production of biochemicals and wastewater treatment (Arora et al. 2019). In co-cultivation, yeast digest lignocellulosic sugars, which microalgae are unable to metabolize. By converting some of the carbon sources to carbon

dioxide, the yeast will promote the growth of algal biomass. On the other hand, oxygen produced by microalgae will support yeast metabolism and their lipid production. In addition, both algae and yeast share the same ecological niche, which protects them from contamination (Rakesh S and Karthikeyan 2019; Das et al. 2021). Typically, designing synthetic microbial consortia requires many experiments in which various combinations of microorganisms are mixed with positive or negative interactions (Hu et al. 2017). In designing a co-cultivation system, strain selection is the first and one of the main criteria to be addressed (Das et al. 2020). Co-culture partners are selected according to communication profiling (metabolites, peptides, proteins, EPS) or from existing natural associations. Generally, the primary partner is the desired microalgal species selected for biomass and products enhancement (lipids, pigments, metabolites), while the secondary partner is the microorganism that possesses some specific characteristics to provide a successful symbiotic association (Ray et al. 2022). A bottom-up set-up of a co-cultures system consists of selecting one or more products and screening microorganisms capable of producing them (Padmaperuma et al. 2018). In a co-culture, the choice of the culture medium is also important. It must ensure the survival of both organisms even if they present different metabolic necessities. In the case of a mutualistic symbiosis, selecting the optimal growth medium for the primary organism should be sufficient. In a commensal symbiosis, a supplement may be needed to help the secondary partner (Padmaperuma et al. 2018; Rosero-Chasoy et al. 2021). The inoculum ratio for each strain in the consortium is another variable to consider as well as the cultivation time at which the inoculum is added. The growth rate of each strain needs to be considered by avoiding overgrowth of only one of the species (Ray et al. 2022).

Autotrophy, heterotrophy and mixotrophy

Different cultivation conditions influence the growth and productivity of microalgae. Each cultivation method can provide different sources of nutrients and energy and it results in variation of lipid content and biomass productivity (Vuppaladadiyam et al. 2017; Chew et al. 2018). Microalgae usually grow by absorbing light as an energy source and fixing inorganic carbon as CO_2 or utilizing sodium bicarbonate as external source of carbon and derive CO_2 via the action of carbonic anhydrase (autotrophic metabolism) (Mokashi et al. 2016; Baldisserotto et al. 2021). However, some of them are also able to use the organic substrate as an energy and carbon source; this process is known as heterotrophic metabolism. Finally, microalgae can grow mixotrophically, a strategy that combines autotrophy and heterotrophy and allows microalgae

to perform both photosynthesis and respiration of supplied organic carbon (Baldisserotto et al. 2021).

Autotrophy

Autotrophic cultivation is the most common growth system for microalgae and the most economical. Algae use an inorganic carbon source (CO_2) and light as their energy source. The use of sunlight is a good economic advantage especially in large systems. In some areas of the planet, low sunlight availability or high fluctuation throughout the year is a limiting factor in supporting algae growth. In these cases, artificial light can be used (Saha and Murray 2018; Zuccaro et al. 2020). Nowadays the light-emitting diodes (LEDs) constitute an advantageous alternative to the old lighting systems due to its low energy consumption and its light range (e.g., red LED, 624-634 nm; green LED, 515-525 nm; blue LED; 460-465 nm). Variations in wavelengths can be used to enhance the production of specific molecules (Zhong et al. 2018). Autotrophic cultivation is typically used in outdoor cultivation, to increase lipid productivity and to recycle industrial CO_2 (Moreno-Garcia et al. 2017).

Heterotrophy

Compared to autotrophy, heterotrophy does not need light. In this case, both the carbon and energy source are provided as an organic carbon substrate (Zuccaro et al. 2020). The problems related to the availability of sunlight, or the cost of artificial light are eliminated, as well as the require of surface to volume ratio of bioreactors making their design easier (Zhan et al. 2017). Apart from this, the main advantages of heterotrophic cultivation are high growth control and high productivity (Vuppaladadiyam et al. 2018). A constrained number of microalgae strains can be cultivated under these conditions, such as *C. vulgaris, C. protothecoides, Crypthecodinium cohnii,* and *Schizochytrium limacinum* (Moreno-Garcia et al. 2017; Vuppaladadiyam et al. 2018). Substrates used as carbon sources include glycerol, acetate, glucose, sucrose, fructose, mannose, lactose and galactose (Zuccaro et al. 2020). Heterotrophic cultivation is potentially very cost-effective when to replace these carbon sources food waste and agro-industrial by-products are employed, such as whey permeate and molasses (Zhan et at. 2017; Ende and Noke 2019). On the other hand, the presence of organic substrates may constitute a potential risk for microbial contamination of the culture media, in addition, it is not possible to obtain biomass for pigment production with this cultivation method (Lowrey et al. 2016; Zuccato et al. 2020).

Mixotrophy

Mixotrophy is the condition in which organic carbon is supplied in the culture medium together with light, so that microalgae can benefit from the coupling of photosynthetic activity with the assimilation of organic carbon for growth (Zhan et al. 2017; Pang et al. 2019). Mixotrophy has the advantage of both increasing biomass production and stimulating the production of commercially valuable compounds such as pigments and lipids (Penhaul Smith et al. 2020). Mixotrophic metabolism is documented in a number of microalgae, which are even phylogenetically very different, such as *Spirulina platensis*, *Chlamydomonas reinhardtii*, *Scenedesmus acutus*, *Phaeodactylum tricornutum, Neochloris oleoabundans, Thalassiosira pseudonana* and *Chlorella vulgaris* (Giovanardi et al. 2016; Moreno-Garcia et al. 2017; Baldisserotto et al. 2021). The most common sources of organic carbon added to culture media are glucose, fructose, acetate and glycerol (Penhaul Smith et al. 2020; Patel et al. 2020; Baldisserotto et. al. 2021). However, the benefits of this cultivation method could be limited by the high cost of carbon sources, which can account for 50-80% of growth medium (Heredia-Arroyo et al. 2010). This limitation can be overcome by combining the cultivation of microalgae in mixotrophy with the use of by-products of agro-industrial sector and biodiesel production as carbon sources (Giovanardi et al. 2013; Giovanardi et al. 2016; Baldisserotto et al. 2021). For example, the possibility of cultivating *T. pseudonana* mixotrophically using biodiesel-derived crude glycerol as source of carbon was investigated, resulting in an increase in biomass and lipids that could be useful for both energetic and nutraceutical purposes (Baldisserotto et al. 2021). Giovanardi and coworkers (2016) proved the feasibility of using a dairy industry waste as nutrient source for the mixotrophic cultivation of *S. acutus* showing how mixotrophy can be a cost-effective at the same time ecological cultivation method.

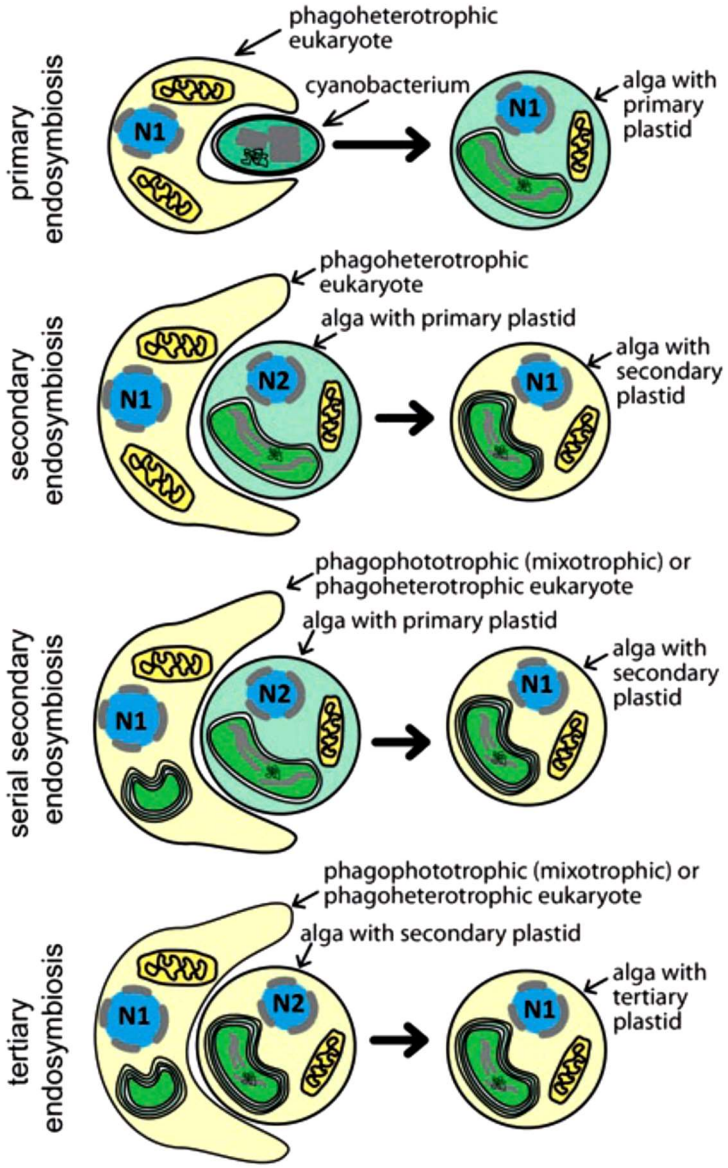

Figure 1 Presentation of the proposed endosymbiont theory for the origin of plastids. A primary endosymbiosis (prokaryote-to-eukaryote) between a unicellular heterotrophic eukaryote and a phototrophic bacterium (cyanobacterium) gave rise to a primary alga. A secondary endosymbiosis (eukaryote-to-eukaryote) occurred when a primary alga was taken up by another eukaryote as an endosymbiont. Higher order endosymbiosis (tertiary, quaternary, etc.) are the result of more complex interactions that leave deeply assembled chimeric organisms. Complex plastids can be distinguished from primary plastids by their ultrastructure: their envelopes consist of multiple membranes, whereas in primary plastids envelopes consist of double membranes (From Füssy and Oborník, 2018)

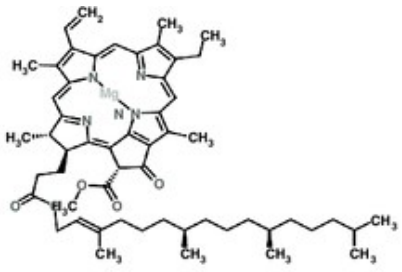

Chlorophyll *a*

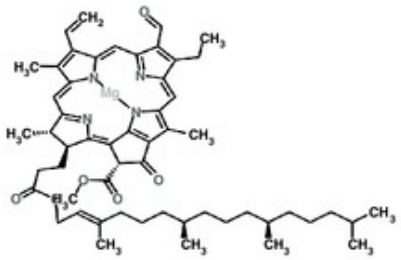

Chlorophyll *b*

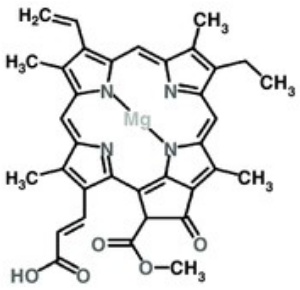

Chlorophyll c_1

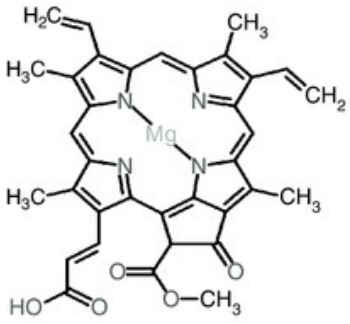

Chlorophyll c_2

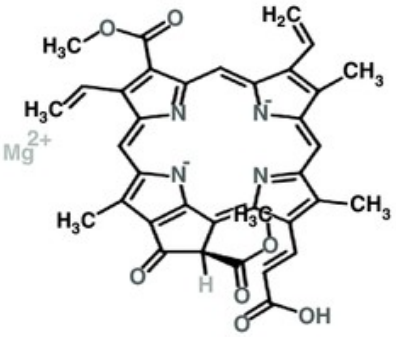

Chlorophyll c_3

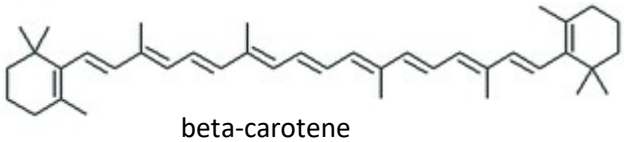

beta-carotene

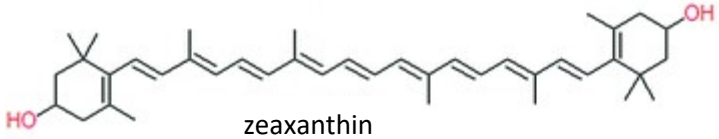

zeaxanthin

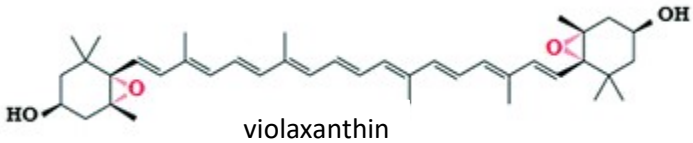

violaxanthin

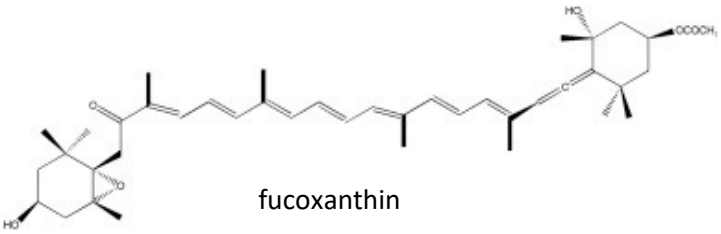

fucoxanthin

Figure 2 Chemical structure of the different chlorophylls (From Pareek et al. 2017) and carotenoids (From Trchounian et al. 2016)

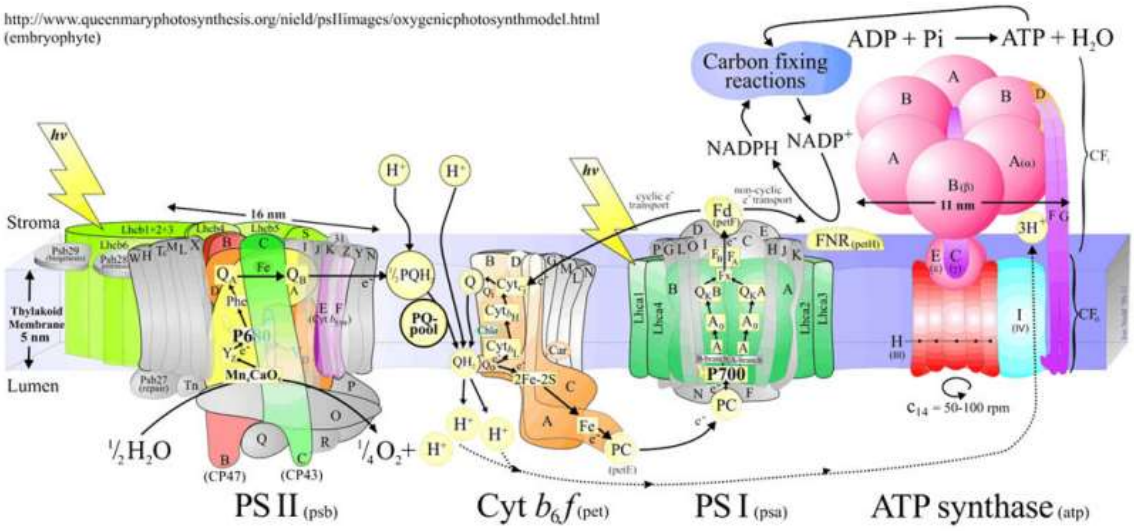

Figure 3 Detailed model of the organisation of the protein complexes involved in electron (e^-) and proton (H^+) transport within the thylakoid membrane of the photosynthetic apparatus in organisms performing oxygenic photosynthesis. PSII = photosystem II; PQ = plastoquinone; PQH = plastoquinol; Cyt b6f = cytochrome b6f complex; PC = plastocyanin; PSI = photosystem I; Fd = ferredoxin; FNR = ferredoxin-$NADP^+$reductase; NADPH = reduced nicotinamide adenine dinucleotide phosphate; ADP = adenosine diphosphate; Pi = inorganic phosphate; ATP = adenosine triphosphate. (Figure downloaded from the official web site: http://www.queenmaryphotosynthesis.org/nield/psllimages/oxygenicphotosynthmodel.html)

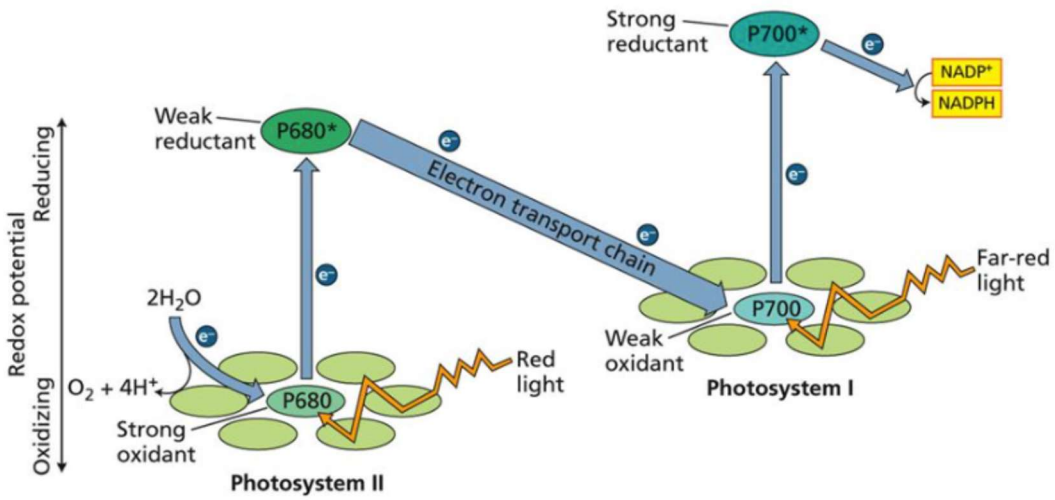

Figure 4 Representation of the Z-scheme of electron transfer during light-reactions in photosynthesis. (Taiz and Zeiger 2018)

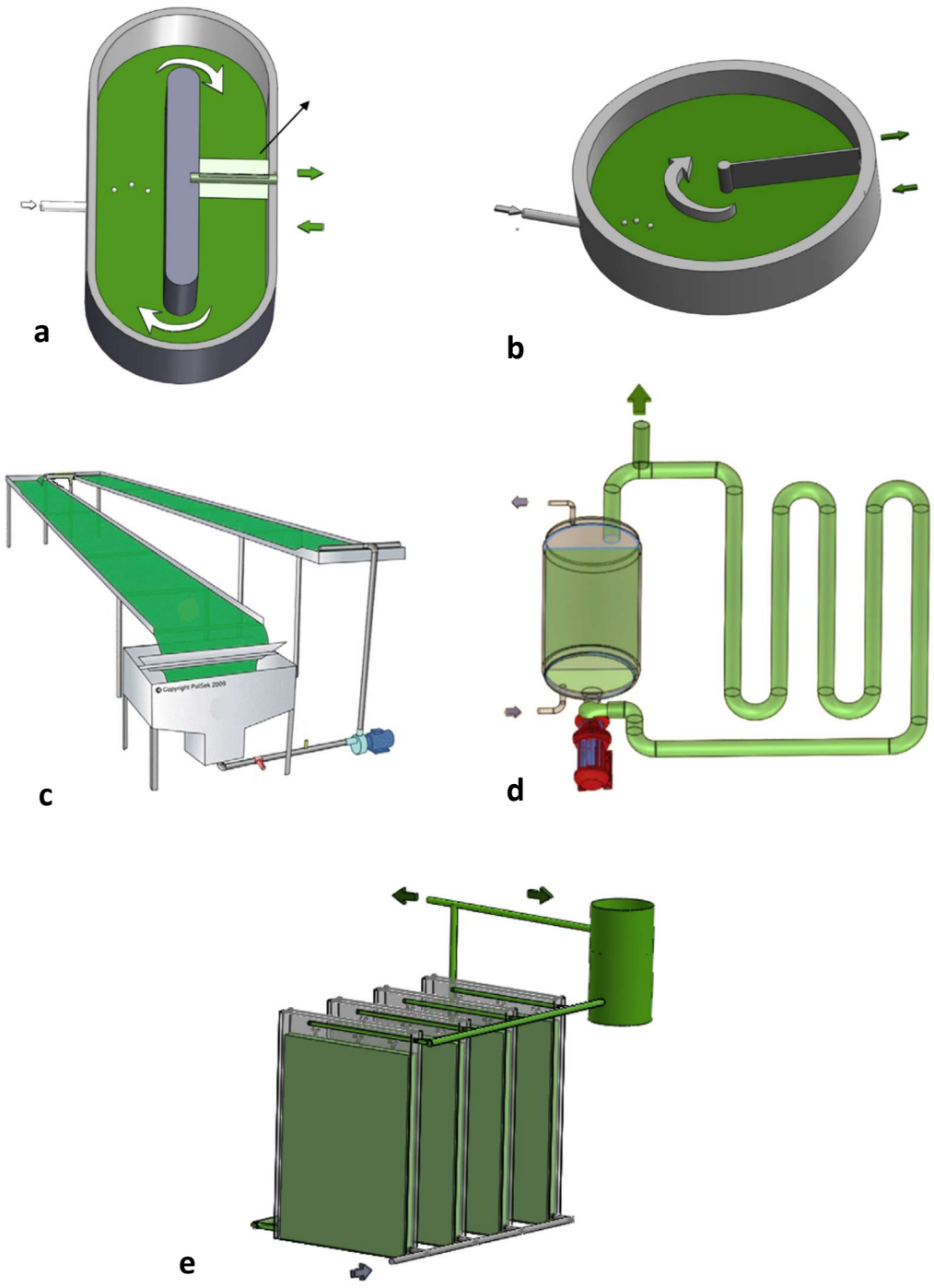

Figure 5 An illustration of examples of open and closed systems. a, Raceway Pond; b, circular pond; c, Tubular photobioreactor with parallel run vertical tubes; d, Flat plate photobioreactor; (e) thin-layer cascade (a, b, d, e - Kiran et al. 2014; c - Grivalský et al.2019)

References

Abdelhamid FM, Elshopakey GE, Aziza AE (2020) Ameliorative effects of dietary *Chlorella vulgaris* and β-glucan against diazinon-induced toxicity in Nile tilapia (*Oreochromis niloticus*). Fish & shellfish immunology, 96, 213-222. https://doi.org/10.1016/j.fsi.2019.12.009

Acquah C, Tibbetts SM, Pan S, Udenigwe C (2020) Chapter 19 - Nutritional quality and bioactive properties of proteins and peptides from microalgae. In: Jacob-Lopes E, Manzoni Maroneze M, Queiroz MI, Queiroz Zepka L (eds) Handbook of Microalgae-Based Processes and Products, Academic Press, Pages 493-531, https://doi.org/10.1016/B978-0-12-818536-0.00019-1

Al-Jabri H, Das P, Khan S, Thaher M, Abdul Quadir M (2021) Treatment of wastewaters by microalgae and the potential applications of the produced biomass. A - review. Water. 13(1):27. https://doi.org/10.3390/w13010027

Amicarelli V., Paiano A., Lobefaro L. (2012) Le microalghe nel settore dei biocombustibili. Sviluppo e sostenibilità. Energia, Ambiente e Innovazione, n. 2-2012

Amorim ML, Soares J, Coimbra JS dos R, Leite M de O, Albino LFT, Martins MA (2020) Microalgae proteins: production, separation, isolation, quantification, and application in food and feed Crit. Rev. Food Sci. Nutr https://doi.org/10.1080/10408398.2020.1768046

Arora N, Patel A, Mehtani J, Pruthi PA, Pruthi V, Poluri KM (2019) Co-culturing of oleaginous microalgae and yeast: paradigm shift towards enhanced lipid productivity. Environ Sci Pollut Res 26, 16952–16973. https://doi.org/10.1007/s11356-019-05138-6

Arora N., Tripathi S., Poluri K.M., Pruthi V. (2019) Advanced Gene Technology and Synthetic Biology Approaches to Custom Design Microalgae for Biodiesel Production. In: Alam M., Wang Z. (eds) Microalgae Biotechnology for Development of Biofuel and Wastewater Treatment. Springer, Singapore. https://doi.org/10.1007/978-981-13-2264-8_8

Azimi A, Azari A, Rezakazemi M, Ansarpour M (2017) Removal of heavy metals from industrial wastewaters: a review. ChemBioEng Reviews, 4: 37-59. https://doi.org/10.1002/cben.201600010

Babutsidze Z, Chai A (2018) Look at me Saving the Planet! The Imitation of Visible Green Behavior and its Impact on the Climate Value-Action Gap. Ecological Economics 146, 290–303. http://dx.doi.org/10.1016/j.ecolecon.2017.10.017

Baldisserotto C, Sabia A, Guerrini A, Demaria S, Maglie M, Ferroni L, Pancaldi S (2021) Mixotrophic cultivation of *Thalassiosira pseudonana* with pure and crude glycerol: Impact on lipid profile, Algal Research, Volume 54, 102194. https://doi.org/10.1016/j.algal.2021.102194

Barber J, Ruban AV (eds.) (2017) Photosynthesis and bioenergetics. World Scientific. https://doi.org/10.1142/10713 |

Barkia I, Saari N, Manning SR (2019) Microalgae for High-Value Products Towards Human Health and Nutrition. Marine Drugs; 17(5):304. https://doi.org/10.3390/md17050304

Barsanti L, Gualtieri P (2014) Algae: anatomy, biochemestry and biotechnology, 2nd edn. CRC Press, Boca Raton

Barsanti L, Gualtieri P (2018) Is exploitation of microalgae economically and energetically sustainable? Algal Research, Volume 31, Pages 107-115. https://doi.org/10.1016/j.algal.2018.02.001

Basheer S, Huo S, Zhu F, Qian J, Xu L, Cui F, Zou B (2020) Microalgae in Human Health and Medicine. In: Alam M, Xu JL, Wang Z (eds) Microalgae Biotechnology for Food, Health and High Value Products. Springer, Singapore. https://doi.org/10.1007/978-981-15-0169-2_5

Bazinet R, Layé S (2014) Polyunsaturated fatty acids and their metabolites in brain function and disease. Nat Rev Neurosci 15, 771–785. https://doi.org/10.1038/nrn3820

Bendif EM, Probert I, Schroeder DC, de Vargas (2013) On the description of *Tisochrysis lutea* gen. nov. sp. nov. and *Isochrysis nuda* sp. nov. in the Isochrysidales, and the transfer of *Dicrateria* to the Prymnesiales (Haptophyta). J Appl Phycol 25, 1763–1776 (2013). https://doi.org/10.1007/s10811-013-0037-0

Benvenuti G, Bosma R, Ji F, Lamers P, Barbosa MJ, Wijffels RH (2016) Batch and semi-continuous microalgal TAG production in lab-scale and outdoor photobioreactors. J Appl Phycol 28, 3167–3177. https://doi.org/10.1007/s10811-016-0897-1

Berthon J-Y, Nachat-Kappes R, Bey M, Cadoret J-P, Renimel I, Filaire E (2017) Marine algae as attractive source to skin care, Free Radical Research, 51:6, 555-567. https://doi.org/10.1080/10715762.2017.1355550

Bhagavathy S, Sumathi P, Jancy Sherene Bell I (2011) Green algae *Chlorococcum humicola*-a new source of bioactive compounds with antimicrobial activity. Asian Pacific Journal of Tropical Biomedicine, Volume 1, Issue 1, Supplement, Pages S1-S7. https://doi.org/10.1016/S2221-1691(11)60111-1

Bi Z, He B (2020) Chapter 13 - Biodiesel from microalgae, Jacob-Lopes E, Manzoni Maroneze M, Queiroz MI, Queiroz Zepka L (eds) Handbook of Microalgae-Based Processes and Products, Academic Press, Pages 329-371, https://doi.org/10.1016/B978-0-12-818536-0.00013-0

Bigagli E, Cinci L, Niccolai A, Biondi N, Rodolfi L, D'Ottavio M, D'Ambrosio M, Lodovici M, Tredici MR, Luceri C (2018) Preliminary data on the dietary safety, tolerability and effects on lipid metabolism of the marine microalga *Tisochrysis lutea*. Algal Research, Volume 34, Pages 244-249. https://doi.org/10.1016/j.algal.2018.08.008

Blanco AM, Moreno J, Del Campo JA, Rivas J, Guerrero MG (2017) Outdoor cultivation of lutein-rich cells of *Muriellopsis* sp. in open ponds. Appl Microbiol Biotechnol 73, 1259–1266. https://doi.org/10.1007/s00253-006-0598-9

Borowitzka MA (2018, b) Chapter 9 - Microalgae in Medicine and Human Health: A Historical Perspective. In: Levine IA, Fleurence J (eds) Microalgae in Health and Disease Prevention, Academic Press, Pages 195-210. https://doi.org/10.1016/B978-0-12-811405-6.00009-8

Borowitzka,MA (2018, a) Chapter 3 - Biology of Microalgae. Levine IA, Fleurence J (eds) Microalgae in Health and Disease Prevention, Academic Press, Pages 23-72. https://doi.org/10.1016/B978-0-12-811405-6.00003-7

Bradáčová K, Florea AS, Bar-Tal A, Minz D, Yermiyahu U, Shawahna R, Kraut-Cohen J, Zolti A, Erel R, Dietel K, Weinmann M, Zimmermann B, Berger N, Ludewig U, Neumann G, Poşta G (2019) Microbial Consortia versus Single-Strain Inoculants: An Advantage in PGPM-Assisted Tomato Production? Agronomy. 9(2):105. https://doi.org/10.3390/agronomy9020105

Büchel C (2020) Light harvesting complexes in chlorophyll c-containing algae. Biochimica et Biophysica Acta (BBA) - Bioenergetics, Volume 1861, Issue 4, 148027. https://doi.org/10.1016/j.bbabio.2019.05.003

Buono S, Langellotti AL, Martello A, Rinna F, Fogliano V (2014) Functional ingredients from microalgae. Food & Function, 5(8), 1669–1685 https://doi.org/10.1039/C4FO00125G

Camacho F, Macedo A, Malcata F (2019) Potential industrial applications and commercialization of microalgae in the functional food and feed industries: A short review. Mar. Drugs, 17, 312. https://doi.org/10.3390/md17060312

Caporgno MP, Mathys A (2018) Trends in microalgae incorporation into innovative food products with potential health benefits. Frontiers in Nutrition, Volume 5. https://doi.org/10.3389/fnut.2018.00058

Caporgno MP, Mathys A (2018) Trends in microalgae incorporation into innovative food products with potential health benefits. Frontiers in nutrition, 5, 58. https://doi.org/10.3389/fnut.2018.00058

Carrier G, Baroukh C, Rouxel C, Duboscq-Bidot L, Schreiber N, Bougaran G (2018) Draft genomes and phenotypic characterization of *Tisochrysis lutea* strains. Toward the production of domesticated strains with high added value. Algal Res., 29 (2018), pp. 1-11. https://doi.org/10.1016/j.algal.2017.10.017

Carvalho M, Montero D, Rosenlund G, Fontanillas R, Ginés R, Izquierdo M (2020) Effective complete replacement of fish oil by combining poultry and microalgae oils in practical diets for gilthead sea bream (*Sparus aurata*) fingerlings. Aquaculture, Volume 529. https://doi.org/10.1016/j.aquaculture.2020.735696

Castenholz RW (2001) General characteristics of the cyanobacteria. In: Garrity G, Boone DR, Castenholz RW (eds) Bergey's Manual of Systematic Bacteriology - Volume One: The Archaea and the Deeply Branching and Phototrophic Bacteria. Eds. ISBN 978-0-387-98771-2

Cavalier-Smith T, Chao EE, Lewis R (2018) Multigene phylogeny and cell evolution of chromist infrakingdom Rhizaria: contrasting cell organisation of sister phyla Cercozoa and Retaria. R. Protoplasma 255(5):1517-1574. https://doi.org/10.1007/s00709-018-1241-1

Cenci U, Bhattacharya D, Weber AP et al (2017) Biotic host-pathogen interactions as major drivers of plastid endosymbiosis. Trends Plant Sci 22(4):316–328. https://doi.org/10.1016/j.tplants.2016.12.007

Cenci U, Nitschke F, Steup M, Minassian BA, Colleoni C, Ball SG (2014) Transition from glycogen to starch metabolism in Archaeplastida. Trends in Plant Science. http://dx.doi.org/10.1016/j.tplants.2013.08.004

Chatsungnoen T, Chisti Y (2019) Chapter 11 - Flocculation and electroflocculation for algal biomass recovery. In: A Pandey, J-S Chang, CR Soccol, D-J Lee, Y Chisti (eds) Biomass, Biofuels, Biochemicals, Biofuels from Algae (Second Edition), Elsevier, Pages 257-286, ISBN 9780444641922. https://doi.org/10.1016/B978-0-444-64192-2.00011-1

Chen S, Gao K (2021) Microalgae Continuous and Semi-continuous Cultures. In: Gao K, Hutchins DA, Beardall J (eds) Research Methods of Environmental Physiology in Aquatic Sciences. Springer, Singapore. https://doi.org/10.1007/978-981-15-5354-7_4

Chénais B (2021) Algae and microalgae and their bioactive molecules for human health. Molecules, 26, 1185. https://doi.org/10.3390/molecules26041185

Cheng P, Cheng JJ, Cobb K, Zhou C, Zhou N, Addy M, Chen P, Yan X, Ruan R (2020) *Tribonema* sp. and *Chlorella zofingiensis* co-culture to treat swine wastewater diluted with fishery wastewater to facilitate harvest. Bioresource Technology, Volume 297, 122516. https://doi.org/10.1016/j.biortech.2019.122516

Chew KW, Chia SR, Show PL, Yap YJ, Ling TC, Chang J-S (2018) Effects of water culture medium, cultivation systems and growth modes for microalgae cultivation: A review. Journal of the Taiwan Institute of Chemical Engineers. Volume 91, Pages 332-344, ISSN 1876-1070. https://doi.org/10.1016/j.jtice.2018.05.039

Chia SR, Chew KW, Show PL, Yap YJ, Ong HC, Ling TC, Chang JS (2018) Analysis of economic and environmental aspects of microalgae biorefinery for biofuels production: A Review. Biotechnol. J.; 13, 1700618. https://doi.org/10.1002/biot.201700618

Chisti Y (2018) Society and Microalgae: Understanding the Past and Present. In: Levine IA, Fleurence J, (eds) Microalgae in Health and Disease Prevention. Academic Press, Pages 11-21, ISBN 9780128114056. https://doi.org/10.1016/B978-0-12-811405-6.00002-5

Chisti Y (2020) Microalgae biotechnology: A brief introduction. In: Jacob-Lopes E, Manzoni Maroneze M, Queiroz MI, Queiroz Zepka L (eds) Handbook of Microalgae-Based Processes and Products. Academic Press, Pages 3-23, ISBN 9780128185360. https://doi.org/10.1016/B978-0-12-818536-0.00001-4

Colla E, Lupatini Menegotto AL, Kalschne DL, da Silva-Buzanello RA, Canan C, Drunkler DA (2020) Chapter 32 - Microalgae: A new and promising source of food. In: Konur O (ed) Handbook of Algal Science, Technology and Medicine, Academic Press, Pages 507-518. https://doi.org/10.1016/B978-0-12-818305-2.00032-2

Colusse GA, Mendes CRB, Duarte MER, de Carvalho JC, Noseda MD (2020) Effects of different culture media on physiological features and laboratory scale production cost of *Dunaliella salina*. Biotechnology Reports, 27, e00508. https://doi.org/10.1016/j.btre.2020.e00508

Connelly R (2014) Second-Generation Biofuel from High-Efficiency Algal-Derived Biocrude. In: Gupta VK et al. (eds) Bioenergy Research: Advances and Applications. Pages 153-170, ISBN 978-0-444-59561-4; https://doi.org/10.1016/B978-0-444-59561-4.00010-3

Corinaldesi C, Barone G, Marcellini F, Dell'Anno A, Danovaro R (2017) Marine microbial-derived molecules and their potential use in cosmeceutical and cosmetic products. Mar. Drugs, 15, 118. https://doi.org/10.3390/md15040118

Croce R, van Amerongen H (2020) Light harvesting in oxygenic photosynthesis: Structural biology meets spectroscopy. Science, 369(6506). https://doi.org/10.1126/science.aay2058

da Silva Vaz B, Botelho Moreira J, de Morais MG, Vieira Costa JA (2016) Microalgae as a new source of bioactive compounds in food supplements. Curr Opin Food Sci 7:73–77. https://doi.org/10.1016/j.cofs.2015.12.006

D'Amato D, Droste N, Allen B, Kettunen M, Lähtinen K, Korhonen J, Leskinen P, Matthies BD, Toppinen A (2017) Green, circular, bio economy: A comparative analysis of sustainability avenues. J Clean Prod 168:716-734. https://doi.org/10.1016/j.jclepro.2017.09.053

Das PK, Rani J, Rawat S, Kumar S (2021) Microalgal co-cultivation for biofuel production and bioremediation: current status and benefits. Bioenerg. Res. https://doi.org/10.1007/s12155-021-10254-8

de Oliveira-Júnior RG, Grougnet R, Bodet PE, Bonnet A, Nicolau E, Jebali A, Rumin J, Picot L (2020) Updated pigment composition of *Tisochrysis lutea* and purification of fucoxanthin using centrifugal partition chromatography coupled to flash chromatography for the chemosensitization of melanoma cells, Algal Research, Volume 51, 102035. https://doi.org/10.1016/j.algal.2020.102035

Deruyck B, Nguyen KHT, Decaestecker E, Muylaert K (2019) Modeling the impact of rotifer contamination on microalgal production in open pond, photobioreactor and thin layer cultivation systems, Algal Research, Volume 38, 101398. https://doi.org/10.1016/j.algal.2018.101398

Dineshbabu G, Goswami G, Kumar R, Sinha A, Das D (2019) Microalgae–nutritious, sustainable aqua- and animal feed source, Journal of Functional Foods, Volume 62, 103545. https://doi.org/10.1016/j.jff.2019.103545

Dorrell RG, Howe CJ (2012) What makes a chloroplast? Reconstructing the establishment of photosynthetic symbioses. J Cell Sci 125:1865–1875. https://doi.org/10.1242/jcs.102285

Eikrem W, Medlin LK, Henderiks J, Rokitta S, Rost B, Probert I, Throndsen J, Edvardsen B (2017) Haptophyta. In: Archibald J. et al. (eds) Springer,Handbook of the Protists. Cham. https://doi.org/10.1007/978-3-319-32669-6_38-2

Eliáš M, Amaral R, Fawley KP, Fawley MW, Němcová Y, Neustupa J, Přibyl P, Santos LMA, Ševčíková T (2016) Eustigmatophyceae. In: Archibald J. et al. (eds) Handbook of the Protists. Springer, Cham. https://doi.org/10.1007/978-3-319-32669-6_39- 1

Ende SSW, Noke A (2019) Heterotrophic microalgae production on food waste and by-products. J Appl Phycol 31, 1565–1571. https://doi.org/10.1007/s10811-018-1697-6

Escapa C, Coimbra RN, Paniagua S, García AI, Otero M (2015) Nutrients and pharmaceuticals removal from wastewater by culture and harvesting of *Chlorella sorokiniana*. Bioresource Technology, Volume 185. https://doi.org/10.1016/j.biortech.2015.03.004

Faé Neto WA, Borges Mendes CR, Abreu PC (2018) Carotenoid production by the marine microalgae *Nannochloropsis oculata* in different low-cost culture media. *Aquac Res*. 2018; 49: 2527– 2535. https://doi.org/10.1111/are.13715

Fakhri S, Abbaszadeh F, Dargahi L, Jorjani M (2018) Astaxanthin: A mechanistic review on its biological activities and health benefits. Pharmacological research, 136, 1-20. https://doi.org/10.1016/j.phrs.2018.08.012

Faraloni C, Torzillo G (2017) Synthesis of antioxidant carotenoids in microalgae in response to physiological stress. Carotenoids. InTechOpen, 143-157. http://dx.doi.org/10.5772/67843

Faried M, Samer M, Abdelsalam E, Yousef RS, Attia YA, Ali AS (2017) Biodiesel production from microalgae: processes, technologies and recent advancements. Renew Sustain Energy Rev; Volume 79; Pages 893–913. https://doi.org/10.1016/j.rser.2017.05.199

Ferrazzano GF, Papa C, Pollio A, Ingenito A, Sangianantoni G, Cantile T (2020) Cyanobacteria and microalgae as sources of functional foods to improve human general and oral health. Molecules, 25, 5164. https://doi.org/10.3390/molecules25215164

Ferreira AS, Ferreira SS, Correia A, Vilanova M, Silva TH, Coimbra MA, Nunes C (2020). Reserve, structural and extracellular polysaccharides of *Chlorella vulgaris*: A holistic approach. Algal Research, 45, 101757. https://doi.org/10.1016/j.algal.2019.101757

Ferrer-González FX, Widner B, Holderman NR, Glushka J, Edison AS, Kujawinski EB, Mora MA (2021) Resource partitioning of phytoplankton metabolites that support bacterial heterotrophy. ISME J 15, 762–773. https://doi.org/10.1038/s41396-020-00811-y

Füssy Z, Oborník M (2018) Complex Endosymbioses I: From Primary to Complex Plastids, Multiple Independent Events. In: Plastids. Methods and Protocols. Ed Maréchal E. Methods in Molecular Biology, vol 1829. Humana Press, New York, NY. https://doi.org/10.1007/978-1-4939-8654-5_2

Gambelli D, Alberti F, Solfanelli F, Vairo D, Zanoli R (2017) Third generation algae biofuels in Italy by 2030: A scenario analysis using Bayesian networks. Energy Policy, Volume 103, Pages 165-178. https://doi.org/10.1016/j.enpol.2017.01.013

Ganesan R, Manigandan S, Melvin SS, Shanmuganathan R, Brindhadevi K, Lan Chi NT, Duc PA, Pugazhendhi A (2020) A review on prospective production of biofuel from microalgae. Biotechnology Reports, Volume 27. https://doi.org/10.1016/j.btre.2020.e00509

Ganivet E. (2020) Growth in human population and consumption both need to be addressed to reach an ecologically sustainable future. Environ Dev Sustain 22, 4979–4998. https://doi.org/10.1007/s10668-019-00446-w

Gao F, Teles I (Cabanelas, ITD), Ferrer-Ledo N, Wijffels RH, Barbosa MJ (2020) Production and high throughput quantification of fucoxanthin and lipids in *Tisochrysis lutea* using single-cell fluorescence, Bioresource Technology, Volume 318, 124104. https://doi.org/10.1016/j.biortech.2020.124104

Gifford R, Nilsson A (2014) Personal and social factors that influence pro-environmental concern and behaviour: A review. International Journal of Psychology, 49, 141–157. https://doi.org/10.1002/ijop.12034

Giovanardi, M, Baldisserotto C, Daglia M, Ferroni L, Sabia A, Pancaldi S (2016) Morpho-physiological aspects of *Scenedesmus acutus* PVUW12 cultivated with a dairy industry waste and after starvation. Plant Biosystems-An International Journal Dealing with all Aspects of Plant Biology, 150(4), 767-775. https://doi.org/10.1080/11263504.2014.991361

Giovanardi, M, Ferroni, L, Baldisserotto C, Tedeschi P, Maietti A, Pantaleoni L, Pancaldi S (2013) Morphophysiological analyses of *Neochloris oleoabundans* (Chlorophyta) grown mixotrophically in a carbon-rich waste product. *Protoplasma* **250,** 161–174. https://doi.org/10.1007/s00709-012-0390-x

Gonçalves AL, Pires JCM, Simões M (2017) A review on the use of microalgal consortia for wastewater treatment. Algal Research, Volume 24, Part B, Pages 403-415. https://doi.org/10.1016/j.algal.2016.11.008

Grivalský T, Ranglová K, da Câmara Manoel JA, Lakatos GE, Lhotský R, Masojídek J (2019) Development of thin-layer cascades for microalgae cultivation: milestones (review). Folia Microbiol 64, 603–614. https://doi.org/10.1007/s12223-019-00739-7

Guiry MD, Guiry GM (2021) *AlgaeBase*. World-wide electronic publication, National University of Ireland, Galway. https://www.algaebase.org

Halder P, Azad AK (2019) Recent trends and challenges of algal biofuel conversion technologies. In: Azad AK and Rasul M (eds) Advanced Biofuels: Applications, Technologies and Environmental Sustainability. Pages 167-179, ISBN 978-0-08-102791-2; https://doi.org/10.1016/B978-0-08-102791-2.00007-6

Han T, Lu H F, Ma S S, Zhang Y H, Liu Z D, Duan N (2017) Progress in microalgae cultivation photobioreactors and applications in wastewater treatment: A review. Int J Agric & Biol Eng; 10(1): 1–29. https://doi.org/10.3965/j.ijabe.20171001.2705

Heimann K, Huerlimann R, (2015) Microalgal Classification: Major Classes and Genera of Commercial Microalgal Species. In: Se-Kwon Kim (eds) Handbook of Marine Microalgae., Academic Press, Pages 25-41, ISBN 9780128007761, https://doi.org/10.1016/B978-0-12-800776-1.00003-0

Henchion M, Hayes M, Mullen AM, Fenelon M, Tiwari B. Future Protein Supply and Demand: Strategies and Factors Influencing a Sustainable Equilibrium. *Foods*. 2017; 6(7):53. https://doi.org/10.3390/foods6070053

Henley WJ (2019) The past, present and future of algal continuous cultures in basic research and commercial applications. Algal Research, Volume 43, 101636, https://doi.org/10.1016/j.algal.2019.101636

Heredia-Arroyo T, Wei W, Hu B (2010) Oil accumulation via heterotrophic/mixotrophic *Chlorella protothecoides*. Appl. Biochem. Biotechnol., 162 (2010), pp. 1978-1995. https://doi.org/10.1007/s12010-010-8974-4

Hibberd DJ (1981) Notes on the taxonomy and nomenclature of the algal classes Eustigmatophyceae and Tribophyceae (synonym Xanthophyceae). Botanical journal of the linnean society, 82(2), 93-119. https://doi.org/10.1111/j.1095-8339.1981.tb00954.x

Hu H, Li J-Y, Pan X-R, Zhang F, Ma L-L, Wang H-J, Zeng RJ (2019) Different DHA or EPA production responses to nutrient stress in the marine microalga *Tisochrysis lutea* and the freshwater microalga *Monodus subterraneus*. Science of The Total Environment, Volume 656, Pages 140-149. https://doi.org/10.1016/j.scitotenv.2018.11.346

Hu H, Ma LL, Shen XF, Li JY, Wang HF, Zeng RJ (2018) Effect of cultivation mode on the production of docosahexaenoic acid by *Tisochrysis lutea*. AMB Express 8:50–61. https://doi.org/10.1186/s13568-018-0580-9

Hu J, Xue Y, Guo H, Gao M, Li J, Zhang S, Tsang YF (2017) Design and composition of synthetic fungal-bacterial microbial consortia that improve lignocellulolytic enzyme activity. Bioresource Technology, Volume 227, Pages 247-255 https://doi.org/10.1016/j.biortech.2016.12.058

Hunter MC, Smith RG, Schipanski ME, Atwood LW, Mortensen DA (2017) Agriculture in 2050: Recalibrating Targets for Sustainable Intensification. *BioScience*, Volume 67, Issue 4, Pages 386–391. https://doi.org/10.1093/biosci/bix010

Ishika T, Moheimani NR, Bahri PA (2017) Sustainable saline microalgae co-cultivation for biofuel production: a critical review. Renew Sust Energ Rev 78:356–368. https://doi.org/10.1016/j.rser.2017.04.110

Jacob-Lopes E, Maroneze MM, Deprá MC, Sartori RB, Dias RR, Zepka LQ (2019) Bioactive food compounds from microalgae: an innovative framework on industrial biorefineries. Current Opinion in Food Science, Volume 25, Pages 1-7. https://doi.org/10.1016/j.cofs.2018.12.003

Järvi S, Rantala M, Aro E-M (2018) Oxygenic photosynthesis—Light reactions within the frame of thylakoid architecture and evolution. In: Barber J, Ruban AV (eds) Photosynthesis and Bioenergetics, p. 243-263. https://doi.org/10.1142/9789813230309_0011

Jensen PE, Leister D (2014) Chloroplast evolution, structure and functions. F1000Prime Rep 6:40. https://doi.org/10.12703/P6-40

Jiang M, Li H, Zhou Y, Zhang J (2019), The interactions of an algae–fungi symbiotic system influence nutrient removal from synthetic wastewater. J. Chem. Technol. Biotechnol., 94: 3993 3999. https://doi.org/10.1002/jctb.6205

Johnson MP (2016) Photosynthesis. Essays Biochem 31; 60 (3): 255 - 273. https://doi.org/10.1042/EBC20160016

Junge W (2019) Oxygenic photosynthesis: History, status and perspective. Quarterly Reviews of Biophysics, 52, E1. https://doi.org/10.1017/S0033583518000112

Khan MI, Shin JH, Kim JD (2018) The promising future of microalgae: current status, challenges, and optimization of a sustainable and renewable industry for biofuels, feed, and other products. Microb Cell Fact, 17, 36. https://doi.org/10.1186/s12934-018-0879-x

Khoo KS, Chia WY, Chew KW, Show PL (2021) Microalgal-bacterial consortia as future prospect in wastewater bioremediation, environmental management and bioenergy production. Indian J. Microbiol., 61, 262–269. https://doi.org/10.1007/s12088-021-00924-8

Kiran B, Kumar R, Deshmukh D (2014) Perspectives of microalgal biofuels as a renewable source of energy. Energy Conversion and Management, Volume 88, Pages 1228-1244. https://doi.org/10.1016/j.enconman.2014.06.022

Kirchhoff H (2019) Chloroplast ultrastructure in plants. New Phytologist, 223(2), 565-574. https://doi.org/10.1111/nph.15730

Koreivienė J, Valčiukas R, Karosienė J, Baltrėnas P (2014) Testing of *Chlorella*/*Scenedesmus* microalgae consortia for remediation of wastewater, CO_2 mitigation and algae biomass feasibility for lipid production. J. Environ. Eng. Landsc. Manag., Volume 22, Pages 105-114. https://doi.org/10.3846/16486897.2013.911182ù

Kumar D, Singh B, Ankit (2019) Phytoremediation of nutrients and valorisation of microalgal biomass: an economic perspective. In: Gupta S, Bux F (eds) Application of Microalgae in Wastewater Treatment. Springer, Cham. https://doi.org/10.1007/978-3-030-13909-4_1

Kumar J, Singh D, Tyagi MB, Kumar A (2019) Chapter 16 - Cyanobacteria: Applications in Biotechnology. In: AK Mishra, DN Tiwari, AN Rai (eds) Cyanobacteria, Academic Press, Pages 327-346. https://doi.org/10.1016/B978-0-12-814667-5.00016-7

Kume A, Akitsu T, Nasahara KN (2018) Why is chlorophyll *b* only used in light-harvesting systems? *J Plant Res* 131, 961–972. https://doi.org/10.1007/s10265-018-1052-7

Lafarga T, Clemente I, Garcia-Vaquero M (2020) 5 - Carotenoids from microalgae. In: Galanakis CM (eds) Carotenoids: Properties, Processing and Applications, Academic Press, 149-187. https://doi.org/10.1016/B978-0-12-817067-0.00005-1

Lafarga T, Fernández-Sevilla JM, González-López C, Acién-Fernández FG (2020) *Spirulina* for the food and functional food industries, Food Research International, Volume 137. https://doi.org/10.1016/j.foodres.2020.109356

Larkum AW (2016) Photosynthesis and light harvesting in algae. In: Borowitzka M, Beardall J, Raven J (eds) The Physiology of Microalgae. Developments in Applied Phycology, vol 6. Springer, Cham. https://doi.org/10.1007/978-3-319-24945-2_3

Laybourn-Langton L, Rankin L, Baxter D (2019) This is a crisis: Facing up to the age of environmental breakdown. IPPR. https://www.ippr.org/research/publications/age-of-environmental-breakdown

Le Quéré C, Peters GP, Friedlingstein P, Andrew RM, Canadell JG, Davis SJ, Jackson RB, Jones MW (2021) Fossil CO_2 emissions in the post-COVID-19 era. *Nat. Clim. Chang.* **11,** 197–199. https://doi.org/10.1038/s41558-021-01001-0

Lee R (2018) Phycology (5th ed.) Cambridge: Cambridge University Press. https://doi.org/10.1017/9781316407219

Lehmuskero A, Chauton MS, Boström T (2018) Light and photosynthetic microalgae: A review of cellular- and molecular-scale optical processes. Progress in Oceanography, Volume 168, Pages 43-56. https://doi.org/10.1016/j.pocean.2018.09.002

Levasseur W, Perré P, Pozzobon V (2020) A review of high value-added molecules production by microalgae in light of the classification, Biotechnology Advances, Volume 41, https://doi.org/10.1016/j.biotechadv.2020.107545

Li X, Wang X, Duan C, Yi S, Gao Z, Xiao C, Agathos SN, Wang G, Li J (2020) Biotechnological production of astaxanthin from the microalga *Haematococcus pluvialis*. Biotechnology Advances, Volume 43, 107602. https://doi.org/10.1016/j.biotechadv.2020.107602

Lian J, Wijffels RH, Smidt H, Sipkema D (2018) The effect of the algal microbiome on industrial production of microalgae. Microbial Biotechnology, 11 (5), 806– 818. https://doi.org/10.1111/1751-7915.13296

Liao X, Shi XR (2018) Public appeal, environmental regulation and green investment: Evidence from China, Energy Policy, Volume 119, Pages 554-562, https://doi.org/10.1016/j.enpol.2018.05.020

Liu J, Song Y, Qiu W (2017) Oleaginous microalgae *Nannochloropsis* as a new model for biofuel production: Review & analysis. Renewable and Sustainable Energy Reviews 72 154–162. https://doi.org/10.1016/j.rser.2016.12.120

Liu S, Elvira P, Wang Y, Wang W (2019) Growth and nutrient utilization of green algae in batch and semi-continuous autotrophic cultivation under high CO_2 concentration. Appl Biochem Biotechnol 188, 836–853. https://doi.org/10.1007/s12010-018-02940-9

Lowrey J, Armenta RE, Brooks MS (2016) Nutrient and media reciclyng in heterotrophic microalgae cultures. Appl. Microbiol. Biotechnol. Vol. 100 Pages 1061-1075. https://doi.org/10.1007/s00253-015-7138-4

Madeira MS, Cardoso C, Lopes PA, Coelho D, Afonso C, Bandarra NM, Prates JAM (2017) Microalgae as feed ingredients for livestock production and meat quality: A review. Livestock Science, Volume 205, Pages 111-121. https://doi.org/10.1016/j.livsci.2017.09.020

Mai TD, Lee-Chang KJ, Jameson ID, Hoang T, Cai NBA, Pham HQ (2021) Fatty Acid Profiles of Selected Microalgae Used as Live Feeds for Shrimp Postlarvae in Vietnam. *Aquaculture Journal*. 2021; 1(1):26-38. https://doi.org/10.3390/aquacj1010004

Malhotra R (2019) Fossil Energy: Introduction. In: Meyers R (eds) Encyclopedia of Sustainability Science and Technology. Springer, New York, NY. https://doi.org/10.1007/978-1-4939-2493-6_920-4

Mandal MK, Chanu NK, Chaurasia N (2020) Chapter 5 - Cyanobacterial pigments and their fluorescence characteristics: applications in research and industry. In: Singh PK, Kumar A, Singh VK, Shrivastava AK (eds) Advances in Cyanobacterial Biology, Academic Press, Pages 55-72. https://doi.org/10.1016/B978-0-12-819311-2.00005-X

Maréchal E (2018) Primary Endosymbiosis: Emergence of the Primary Chloroplast and the Chromatophore, Two Independent Events. In: Plastids. Methods and Protocols. Ed Maréchal E. Methods in Molecular Biology, vol 1829. Humana Press, New York, NY. https://doi.org/10.1007/978-1-4939-8654-5_1

Martínez-Macias MR, Aguilar-Ruiz RJ, Nateras-Ramírez O, Sánchez-Machado DI, López-Cervantes J, Dévora-Isiordia GE, (2021) Influence of different reactor types on *Nannochloropsis oculata* microalgae culture for lipids and fatty acid production. *J Am Oil Chem Soc*. 2021; 98: 993– 1000. https://doi.org/10.1002/aocs.12526

Martínez-Roldán A de J, Cañizares-Villanueva RO (2020) Chapter 7 - Wastewater treatment based in microalgae. In: Jacob-Lopes E, Manzoni Maroneze M, Queiroz MI, Queiroz Zepka L (eds) Handbook of Microalgae-Based Processes and Products. Academic Press, Pages 165-184, ISBN 9780128185360. https://doi.org/10.1016/B978-0-12-818536-0.00007-5

Mata TM, Martins AA, Caetano NS (2010) Microalgae for biodiesel production and other applications: A review. Renewable and Sustainable Energy Reviews 14: 217-232 https://doi.org/10.1016/j.rser.2009.07.020

Matamoros V, Gutiérrez R, Ferrer I, García J, Bayona JM (2015) Capability of microalgae-based wastewater treatment systems to remove emerging organic contaminants: A pilot-scale study. Journal of Hazardous Materials, Volume 288. https://doi.org/10.1016/j.jhazmat.2015.02.002

Matos J, Cardoso C, Bandarra NM, Afonso C. (2017) Microalgae as healthy ingredients for functional food: a review. Food Funct. Aug 1;8(8):2672-2685. https://doi.org/10.1039/C7FO00409E

McCree KJ (1971) The action spectrum, absorptance and quantum yield of photosynthesis in crop plants. Agricultural Meteorology 9: 191-216. https://doi.org/10.1016/0002-1571(71)90022-7

Mirkovic T, Ostroumov EE, Anna JM, Van Grondelle R, Scholes GD (2017) Light absorption and energy transfer in the antenna complexes of photosynthetic organisms. Chemical reviews, 117(2), 249-293. https://doi.org/10.1021/acs.chemrev.6b00002

Mohamadnia S, Tavakoli O, Faramarzi MA, Shamsollahi Z (2020) Production of fucoxanthin by the microalga Tisochrysis lutea: A review of recent developments, Aquaculture, Volume 516, 734637. https://doi.org/10.1016/j.aquaculture.2019.734637

Mokashi K, Shetty V, George SA, Sibi G (2016) Sodium bicarbonate as inorganic carbon source for higher biomass and lipid production integrated carbon capture in *Chlorella vulgaris*. Achievements in the Life Sciences, 10(1), 111-117. https://doi.org/10.1016/j.als.2016.05.011

Mora C, Spirandelli D, Franklin EC et al. (2018) Broad threat to humanity from cumulative climate hazards intensified by greenhouse gas emissions. Nature Clim Change 8, 1062–1071. https://doi.org/10.1038/s41558-018-0315-6

Moreno-Garcia L, Adjalle K, Barnabé S, Raghavan GSV (2017) Microalgae biomass production for a biorefinery system: recent advances and the way towards sustainability. Renew. Sust. Energ. Rev. 76. 493-506. https://doi.org/10.1016/j.rser.2017.03.024

Moustaka-Gouni M, Vardaka E, Michaloudi E, Kormas K, Tryfon E, Mihalatou H, Gkelis S, Lanaras T (2006) Plankton food web structure in a eutrophic polymictic lake with a history of toxic cyanobacterial blooms. Limnol Oceanogr 51:715–727 https://doi.org/10.4319/lo.2006.51.1_part_2.0715

Müller M, Barcelos e Ramos J, Schulz K, Riebesell U, Kaźmierczak J, Gallo F, Mackinder L, Li Y, Nesterenko P, Trull T (2015) Phytoplankton calcification as an effective mechanism to alleviate cellular calcium poisoning. Biogeosciences, 12, 6493–6501. https://doi.org/10.5194/bg-12-6493-2015

Murphy CD (2012) The microbial cell factory.Org. Biomol. Chem., 10, 1949. https://doi.org/10.1039/C2OB06903B

Nabi F, Arain MA, Rajput N, Alagawany M, Soomro J, Umer M, Soomro F, Wang Z, Ye R, Liu J (2020). Health benefits of carotenoids and potential application in poultry industry: A review. Journal of animal physiology and animal nutrition, 104(6), 1809-1818. https://doi.org/10.1111/jpn.13375

Nagarajan D, Varjani S, Lee D-J, Chang J-S (2021) Sustainable aquaculture and animal feed from microalgae – Nutritive value and techno-functional components, Renewable and Sustainable Energy Reviews, Volume 150, 111549. https://doi.org/10.1016/j.rser.2021.111549

Nazari MT, Freitag JF, Cavanhi VAF, Colla LM (2020) Microalgae harvesting by fungal-assisted bioflocculation. Rev Environ Sci Biotechnol 19, 369–388. https://doi.org/10.1007/s11157-020-09528-y

Nef C, Jung S, Mairet F, Kaas R, Grizeau D, Garnier M (2019) How haptophytes microalgae mitigate vitamin B_{12} limitation. Sci Rep 9, 8417. https://doi.org/10.1038/s41598-019-44797-w

Nicholls KH (2015) Chapter 13 - Haptophyte Algae In: Wehr JD, Sheath RG, Kociolek JP (eds) Aquatic Ecology, Freshwater Algae of North America (Second Edition) Academic Press, Pages 587-605, ISBN 9780123858764. https://doi.org/10.1016/B978-0-12-385876-4.00013-X

Nobel PS (2020) 5 - Photochemistry of Photosynthesis. In: Nobel PS (eds) Physicochemical and Environmental Plant Physiology (Fifth Edition), Academic Press, Pages 259-307. https://doi.org/10.1016/B978-0-12-819146-0.00005-5

Pacheco AR, Segrè D (2019) A multidimensional perspective on microbial interactions, FEMS Microbiology Letters, Volume 366, Issue 11. https://doi.org/10.1093/femsle/fnz125

Padmaperuma G, Kapoore RV, Gilmour DJ, Vaidyanathan S (2018) Microbial consortia: a critical look at microalgae co-cultures for enhanced biomanufacturing. Crit Rev Biotechnol. Aug;38(5):690-703. https://doi.org/10.1080/07388551.2017.1390728

Pancaldi S, Baldisserotto C, Ferroni L, Pantaleoni L (2019) Fondamenti di Botanica Generale - Teoria e Pratica. Seconda Edizione. McGraw-Hill Education. ISBN 9788838695360

Pang N, Gu X, Chen S, Kirchhoff H, Lei H, Roje S (2019) Exploiting mixotrophy for improving productivities of biomass and co-products of microalgae. Renewable and Sustainable Energy Reviews, Volume 112, Pages 450-460, https://doi.org/10.1016/j.rser.2019.06.001

Pareek S, Sagar NA, Sharma S, Kumar V, Agarwal T, González-Aguilar GA, Yahia EM (2017) Chlorophylls: Chemistry and Biological Functions. EM Yahia (eds) In: Fruit and Vegetable Phytochemicals. https://doi.org/10.1002/9781119158042.ch14

Parida VK, Saidulu D, Majumder A, Srivastava A, Gupta B, Gupta AK (2021) Emerging contaminants in wastewater: A critical review on occurrence, existing legislations, risk assessment, and sustainable treatment alternatives. Journal of Environmental Chemical Engineering, Volume 9, Issue 5, 105966. https://doi.org/10.1016/j.jece.2021.105966

Patel AK, Choi YY, Sim SJ (2020) Emerging prospects of mixotrophic microalgae: Way forward to sustainable bioprocess for environmental remediation and cost-effective biofuels. Bioresource Technology, Volume 300, 122741. https://doi.org/10.1016/j.biortech.2020.122741

Patias LD, Maroneze MM, Siqueira SF, de Menezes CR, Zepka LQ, Jacob-Lopes E (2018) Chapter 11 - Single-cell protein as a source of biologically active ingredients for the formulation of antiobesity foods. In: Holban AM, Grumezescu AM (eds) Handbook of Food Bioengineering, Alternative and Replacement Foods, Academic Press. Pages 317-353. https://doi.org/10.1016/B978-0-12-811446-9.00011-3

Penhaul Smith JK, Hughes AD, McEvoy L, Day JG (2020) Tailoring of the biochemical profiles of microalgae by employing mixotrophic cultivation. Bioresor. Technol. Rep., 9, p. 100321. https://doi.org/10.1016/j.biteb.2019.100321

Pereira I, Rangel A, Chagas B, de Moura B, Urbano S, Sassi R, Camara F, Castro C (2020) microalgae growth under mixotrophic condition using agro-industrial waste: a review. In: Biotechnological Applications of Biomass pp.1-19, Publisher: IntechOpen. https://doi.org/10.5772/intechopen.93964

Pereira LT, Lisboa CR, Costa JA, da Rosa LM, de Carvalho LF (2021) Evaluation of protein content and antimicrobial activity of biomass from *Spirulina* cultivated with residues from the brewing process. J Chem Technol Biotechnol. https://doi.org/10.1002/jctb.6925

Perera CO, Perera AD (2019) Chapter 13 - Technology of Processing of Horticultural Crops. In: Kutz M (eds) Handbook of farm, dairy and food machinery engineering (3rd Edition), Academic Press, Pages 299-351. https://doi.org/10.1016/B978-0-12-814803-7.00013-0

Persistence Market Research (2018) "Microalgae Market: Global Industry Analysis (2012-2016) & Forecast (2017-2026)"

Piccini M, Raikova S, Allen MJ, Chuck CJ (2019) A synergistic use of microalgae and macroalgae for heavy metal bioremediation and bioenergy production through hydrothermal liquefaction. Sustainable Energy Fuels, 3. https://doi.org/10.1039/C8SE00408K

Pina-Pérez MC, Brück WM, Brück T, Beyrer M (2019) Chapter 4 - Microalgae as healthy ingredients for functional foods. In: CM Galanakis (eds) The role of alternative and innovative food ingredients and products in consumer wellness, Academic Press, Pages 103-137, ISBN 9780128164532, https://doi.org/10.1016/B978-0-12-816453-2.00004-8

Pleissner D, Lindner A, Ambati RR (2020) Techniques to Control Microbial Contaminants in Nonsterile Microalgae Cultivation. Appl Biochem Biotechnol 192, 1376–1385. https://doi.org/10.1007/s12010-020-03414-7

Posadas E, García-Encina P-A, Soltau A, Domínguez A, Díaz I, Muñoz R (2013) Carbon and nutrient removal from centrates and domestic wastewater using algal–bacterial biofilm bioreactors. Bioresource Technology, Volume 139, Pages 50-58. https://doi.org/10.1016/j.biortech.2013.04.008

Pradhan D, Sukla LB, Mishra BB, Devi N (2019) Biosorption for removal of hexavalent chromium using microalgae Scenedesmus sp. *J Clean Prod*. 2019;209:617–29. https://doi.org/10.1016/j.jclepro.2018.10.288

Queiroz MI, Vieira JG, Manzoni Maroneze M (2020) Chapter 2 - Morphophysiological, structural, and metabolic aspects of microalgae. In: Jacob-Lopes E, Manzoni Maroneze M, Queiroz MI, Queiroz Zepka L (eds) Handbook of Microalgae-Based Processes and Products. Academic Press, Pages 25-48. https://doi.org/10.1016/B978-0-12-818536-0.00002-6

Raheem A, Prinsen P, Vuppaladadiyam AK, Zhao M, Luque R (2018) A review on sustainable microalgae based biofuel and bioenergy production: Recent developments. Journal of Cleaner Production, Volume 181, Pages 42-59. https://doi.org/10.1016/j.jclepro.2018.01.125

Rahman KM (2020) Food and High Value products from microalgae: market opportunities and challenges. In: Alam M, Xu JL, Wang Z (eds) Microalgae Biotechnology for Food, Health and High Value Products. Springer, Singapore. https://doi.org/10.1007/978-981-15-0169-2_1 4

Raikova S, Smith-Baedorf H, Bransgrove R, Barlow O, Santomauro F, Wagner JL, Allen MJ, Bryan CG, Sapsford D, Chuck CJ (2016) Assessing hydrothermal liquefaction for the production of bio-oil and enhanced metal recovery from microalgae cultivated on acid mine drainage. Fuel Processing Technology, Volume 142. https://doi.org/10.1016/j.fuproc.2015.10.017

Rakesh S, Karthikeyan S (2019) Co-cultivation of microalgae with oleaginous yeast for economical biofuel production. J Farm Sci, 32(2), 125-130. https://doi.org/10.13140/RG.2.2.10506.41928

Ramanan R, Kim B-H, Cho D-H, Oh H-M, Kim H-S (2016) Algae–bacteria interactions: Evolution, ecology and emerging applications. Biotechnology Advances, Volume 34, Issue 1, Pages 14-29. https://doi.org/10.1016/j.biotechadv.2015.12.003

Ranganathan P, Amal JC, Savithri S, Haridas A (2017) Experimental and modelling of *Arthrospira platensis* cultivation in open raceway ponds. Bioresour Technol; Volume 242; Pages 197–205. https://doi.org/10.1016/j.biortech.2017.03.150

Ray A, Nayak M, Ghosh A (2022) A review on co-culturing of microalgae: A greener strategy towards sustainable biofuels production. Science of The Total Environment, Volume 802, 149765, https://doi.org/10.1016/j.scitotenv.2021.149765

Reyes-Prieto A, Russell S, Figueroa-Martinez F, Jackson C (2018) Chapter Four - Comparative Plastid Genomics of Glaucophytes. In: Chaw S-M,. Jansen RK (eds) Plastid Genome Evolution., Advances in Botanical Research, Academic Press, Volume 85, Pages 95-127. https://doi.org/10.1016/bs.abr.2017.11.012

Rivasseau C, Farhi E, Atteia A, Couté A, Gromova M, de Gouvion Saint Cyr D, Boisson AM, Féret S, Compagnon E, Bligny R (2013) An extremely radioresistant green eukaryote for radionuclide bio-decontamination in the nuclear industry. Energy Environ. Sci., 2013, 6, 1230–1239. https://doi.org/10.1039/C2EE23129H

Rizwan M, Mujtabab G, Memonc S, Leed K, Rashid N (2018) Exploring the potential of microalgae for new biotechnology applications and beyond: A review. Renewable and Sustainable Energy Reviews, Volume 92, Pages 394-404. https://doi.org/10.1016/j.rser.2018.04.034

Romagnolli F (2013) Fitodepurazione: gestione sostenibile delle acque. Dario Flaccovio Editore. ISBN 8857901157, 9788857901152

Rosero-Chasoy G, Rodríguez-Jasso RM, Aguilar CN, Buitrón G, Chairez I, Ruiz HA (2021) Microbial co-culturing strategies for the production high value compounds, a reliable framework towards sustainable biorefinery implementation – an overview. Bioresource Technology, Volume 321, 124458. https://doi.org/10.1016/j.biortech.2020.124458

Rout PR, Zhang TC, Bhunia P, Surampalli RY (2021) Treatment technologies for emerging contaminants in wastewater treatment plants: A review. Science of The Total Environment, Volume 753. https://doi.org/10.1016/j.scitotenv.2020.141990

Ruan R, Zhang Y, Chen P, Liu S, Fan L, Zhou N, Ding K, Peng P, Addy M, Cheng Y, Anderson E, Wang Y, Liu Y, Lei H, Li B (2019) Chapter 1 - Biofuels: Introduction. In: Pandey A, Larroche C, Dussap C-G, Gnansounou E, Khanal SK, Ricke S (eds). Biomass, Biofuels, Biochemicals, Biofuels: Alternative Feedstocks and Conversion Processes for the Production of Liquid and Gaseous Biofuels (Second Edition), Academic Press, Pages 3-43. https://doi.org/10.1016/B978-0-12-816856-1.00001-4

Ryckebosch E, Bruneel C, Termote-Verhalle R, Goiris K, Muylaert K, Foubert I (2014) Nutritional evaluation of microalgae oils rich in omega-3 long chain polyunsaturated fatty acids as an alternative for fish oil. Food Chemistry, Volume 160. https://doi.org/10.1016/j.foodchem.2014.03.087

Sabia A, Baldisserotto C, Biondi S, Marchesini R, Tedeschi P, Maietti A, Giovanardi M, Ferroni L, Pancaldi S (2015) Re-cultivation of *Neochloris oleoabundans* in exhausted autotrophic and mixotrophic media: the potential role of polyamines and free fatty acids. Appl Microbiol Biotechnol 99:10597-609. https://doi.org/10.1007/s00253-015-6908-3

Saha SK, Murray P (2018) Exploitation of microalgae species for nutraceutical purposes: cultivation aspects, Fermentation 4, 46-63. https://doi.org/10.3390/fermentation4020046

Saini RK, Keum Y-S (2018) Omega-3 and omega-6 polyunsaturated fatty acids: Dietary sources, metabolism, and significance — A review. Life Sciences, Volume 203, Pages 255-267. https://doi.org/10.1016/j.lfs.2018.04.049

Salama E-S, Kurade MB, Abou-Shanab RAI, El-Dalatony MM, Yang I-S, Min B, Jeon B-H (2017) Recent progress in microalgal biomass production coupled with wastewater treatment for biofuel generation. Renewable and Sustainable Energy Reviews, Volume 79, Pages 1189-1211, https://doi.org/10.1016/j.rser.2017.05.091

Salmeán AA, Duffieux D, Harholt J, Qin F, Michel G, Czjzek M, Willats WGT, Hervé C (2017) Insoluble (1→3), (1→4)-β-Dglucan is a component of cell walls in brown algae (Phaeophyceae) and is masked by alginates in tissues. Scientific Reports https://doi.org/10.1038/s41598-017-03081-5

Sanfilippo JE; Garczarek L; Partensky F; Kehoe DM (2019) Chromatic acclimation in Cyanobacteria: a diverse and widespread process for optimizing photosynthesis. Annual Review of Microbiology, 73(1), 407–433. https://doi.org/10.1146/annurev-micro-020518-115738

Seymour J, Amin S, Raina JB, Stocker R (2017) Zooming in on the phycosphere: the ecological interface for phytoplankton–bacteria relationships. Nat Microbiol 2, 17065. https://doi.org/10.1038/nmicrobiol.2017.65

Sharma J, Kumar V, Kumar SS, Malyan SK, Mathimani T, Bishnoi NR, Pugazhendhi A (2020) Microalgal consortia for municipal wastewater treatment – Lipid augmentation and fatty acid profiling for biodiesel production. Journal of Photochemistry and Photobiology B: Biology, Volume 202, 111638. https://doi.org/10.1016/j.jphotobiol.2019.111638

Sheng X, Watanabe A, Li A, Kim E, Song C, Murata K, Song D, Minagawa J, Liu Z (2019) Structural insight into light harvesting for photosystem II in green algae. Nat. Plants 5, 1320–1330. https://doi.org/10.1038/s41477-019-0543-4

Shevela D, Lars OB (2017) Evolution of the Z-scheme of photosynthesis: a perspective. Photosynthesis research 133.1 (2017): 5-15. https://doi.org/10.1007/s11120-016-0333-z

Singh P, Gupta SK, Guldhe A, Rawat I, Bux F (2015) Chapter 4 - Microalgae Isolation and Basic Culturing Techniques. In: Kim S-K (eds) Handbook of Marine Microalgae, Academic Press, Pages 43-54, ISBN 9780128007761. https://doi.org/10.1016/B978-0-12-800776-1.00004-2

Singh U, Laxmi, AK Singh, RK Asthana (2021) Chapter 7 - Bioactive molecules from microalgae and constraints in commercialization. In: Sinha R, Häder D-P (eds) Natural Bioactive Compounds, Academic Press, Pages 143-164. https://doi.org/10.1016/B978-0-12-820655-3.00007-0

Smith VH, Crews T (2014) Applying ecological principles of crop cultivation in large-scale algal biomass production. Algal Research, Volume 4, Pages 23-34. https://doi.org/10.1016/j.algal.2013.11.005

Solís-Salinas CE, Patlán-Juárez G, Okoye PU, Guillén-Garcés A, Sebastian PJ, Arias DM (2021) Long-term semi-continuous production of carbohydrate-enriched microalgae biomass cultivated in low-loaded domestic wastewater. Science of The Total Environment, Volume 798, 149227, https://doi.org/10.1016/j.scitotenv.2021.149227

Solymosi K, Lethin J, Aronsson H (2018) Diversity and Plasticity of Plastids in Land Plants. In: Maréchal E (eds) Plastids. Methods in Molecular Biology, vol 1829. Humana Press, New York, NY. https://doi.org/10.1007/978-1-4939-8654-5_4

Soto-Sierra L, Stoykova P, Nikolov ZL (2018) Extraction and fractionation of microalgae-based protein products. Algal Research, Volume 36, Pages 175-192. https://doi.org/10.1016/j.algal.2018.10.023

Stephens E, Ross IL, Mussgnug JH, Wagner LD, Borowitzka MA, Posten C, Kruse O, Hankamer B (2010) Future prospects of microalgal biofuel production systems, Trends in Plant Science, Volume 15, Issue 10, Pages 554-564. https://doi.org/10.1016/j.tplants.2010.06.003

Stirbet A, Lazár D, Guo Y, Govindjee G (2020) Photosynthesis: basics, history and modelling. Annals of Botany, Volume 126, Issue 4, 14 September, Pages 511–537. https://doi.org/10.1093/aob/mcz171

Suganya T, Varman M, Masjuki HH, Renganathan S (2016) Macroalgae and microalgae as a potential source for commercial applications along with biofuels production: a biorefinery approach. Renew Sustain Energy Rev; 55:909–41. https://doi.org/10.1016/j.rser.2015.11.026

Sukarni, Sudjito, Nurkholis, Hamidi, Yanuhar U., Wardana I.N.G. (2014) Potential and properties of marine microalgae *Nannochloropsis oculata* as biomass fuel feedstock. Int J Energy Environ Eng 5:279‑290. https://doi.org/10.1007/s40095-014-0138-9

Sun Z, Liu J, Zhou Z-G (2016) 22 - Algae for biofuels: An emerging feedstock. In: Luque R, Ki Lin CS, Wilson K, Clark J (eds) Handbook of Biofuels Production (Second Edition), Woodhead Publishing, Pages 673-698. https://doi.org/10.1016/B978-0-08-100455-5.00022-9

Suparmaniam U, Lam MK, Uemura Y, Lim JW, Lee KT, Shuit SH (2019) Insights into the microalgae cultivation technology and harvesting process for biofuel production: A review. Renewable and Sustainable Energy Reviews, Volume 115, 109361. https://doi.org/10.1016/j.rser.2019.109361

Suresh Kumar K, Dahms H-U, Won E-J, Lee J-S, Shin K-H (2015) Microalgae – A promising tool for heavy metal remediation. Ecotoxicology and Environmental Safety, Volume 113, Pages 329-352. https://doi.org/10.1016/j.ecoenv.2014.12.019

Sutherland DL, Ralph PJ (2019) Microalgal bioremediation of emerging contaminants - Opportunities and challenges. Water Research, Volume 164, 114921. https://doi.org/10.1016/j.watres.2019.114921

Szymański N, Dąbrowski P, Zabochnicka-Świątek M, Panchal B, Lohse D, Kala HM (2017) Taxonomic classification of algae by the use of chlorophyll a fluorescence. Scientific Review – Engineering and Environmental Sciences, 26 (4), 470–480 http://dx.doi.org/10.22630/PNIKS.2017.26.4.45

Taiz L, Zeiger E, Møller IM, Murphy A (2018) Plant physiology and development. 6th Revised edition. Oxford University Press Inc.

Tan JS, Lee SY, Chew KW, Lam MK, Lim JW, Ho S-H, Show PL (2020) A review on microalgae cultivation and harvesting, and their biomass extraction processing using ionic liquids. Bioengineered, 11:1, 116-129. https://doi.org/10.1080/21655979.2020.1711626

Tan XB - a, Lam MK, Uemura Y, Lim JW, Wong CY, Lee KT (2018) Cultivation of microalgae for biodiesel production: A review on upstream and downstream processing. Chinese Journal of Chemical Engineering, Volume 26, Issue 1, Pages 17-30. https://doi.org/10.1016/j.cjche.2017.08.010

Tan XB - b, Lam MK, Uemura Y, Lim JW, Wong CY, Ramli A, Kiew PL, Lee KT (2018) Semi-continuous cultivation of *Chlorella vulgaris* using chicken compost as nutrients source: growth optimization study and fatty acid composition analysis. Energy Convers. Manag., 164 pp. 363-373, https://doi.org/10.1016/j.enconman.2018.03.020

Tejido-Nuñez Y, Aymerich E, Sancho L, Refardt D (2020) Co-cultivation of microalgae in aquaculture water: Interactions, growth and nutrient removal efficiency at laboratory- and pilot-scale. Algal Research, Volume 49, 101940, https://doi.org/10.1016/j.algal.2020.101940

The state of food security and nutrition in the world 2021. https://www.fao.org/publications/sofi/2021/en/

The Sustainable Development Agenda, United Nation 2020. https://www.un.org/sustainabledevelopment/development-agenda/

Tibaldi E, Chini Zittelli G, Parisi G, Bruno M, Giorgi G, Tulli F, Venturini S, Tredici MR, Poli BM (2015) Growth performance and quality traits of European sea bass (D. labrax) fed diets including increasing levels of freeze-dried *Isochrysis* sp. (T-ISO) biomass as a source of protein and n-3 long chain PUFA in partial substitution of fish derivatives, Aquaculture, Volume 440, Pages 60-68. https://doi.org/10.1016/j.aquaculture.2015.02.002

Titlyanov EA, Titlyanova TV, Li X, Huang H (2017) Marine Plants of Coral Reefs. In: Titlyanov EA, Titlyanova TV, Li X, Huang H (eds) Coral Reef Marine Plants of Hainan Island. Academic Press, Pages 5-39, ISBN 9780128119631. https://doi.org/10.1016/B978-0-12-811963-1.00002-0

Tommaselli L (2008) The microalgal cell. In: Handbook of microalgal culture: Biotechnology and Applied Phycology. Ed Amos Richmond, Pages 3-19, ISBN 0–632–05953–2.

Tomo T, Okumura A, Suzuki T, Okuhara M, Katayama R, Isayama N, Nagao R, Iwai M, Dohmae N, Enami I (2018) Lysyl oxidase-like protein secreted from an acidophilic red alga, *Cyanidium caldarium*. Plant direct 2.102: 1– 10. https://doi.org/10.1002/pld3.84

Torres-Tiji Y, Fields FJ, Mayfield SP (2020) Microalgae as a future food source. Biotechnology Advances, Volume 41. https://doi.org/10.1016/j.biotechadv.2020.107536

Trchounian A, Petrosyan M, Sahakyan N (2016) Plant Cell Redox Homeostasis and Reactive Oxygen Species. Gupta D, Palma J, Corpas F (eds) In: Redox State as a Central Regulator of Plant-Cell Stress Responses. Springer, Cham. https://doi.org/10.1007/978-3-319-44081-1_2

Uyeh DD, Mallipeddi R, Pamulapati T, Park T, Kim J, Woo S, Ha Y (2018) Interactive livestock feed ration optimization using evolutionary algorithms. Computers and Electronics in Agriculture, Volume 155, Pages 1-11. https://doi.org/10.1016/j.compag.2018.08.031

Valença RL, da Silva Sobrinho AG, Borghi TH, Rojas Meza DA, de Andrade N, Guimarães Silva L, Rocha Bezerra L (2021) Performance, carcass traits, physicochemical properties and fatty acids composition of lamb's meat fed diets with marine microalgae meal (*Schizochytrium* sp.). Livestock Science, Volume 243, 104387. https://doi.org/10.1016/j.livsci.2020.104387

Valverde F., Romero-Campero FJ, Leon R., Guerrero MG, Serrano A (2016) New challenges in microalgae biotechnology. European Journal of Protistology. http://dx.doi.org/10.1016/j.ejop.2016.03.002

Varshney P, Mikulic P, Vonshak A, Beardall J, Wangikar P (2015) Extremophilic micro-algae and their potential contribution in biotechnology. Bioresource Technology 184, 363–372 https://doi.org/10.1016/j.biortech.2014.11.040

Veiter L, Rajamanickam V, Herwig C (2018) The filamentous fungal pellet—relationship between morphology and productivity. Appl Microbiol Biot 102, 2997–3006. https://doi.org/10.1007/s00253-018-8818-7

Vieira Costa JA, Bastos Freitas BC, Duarte Santos T, Mitchell BG, Greque Morais M (2019) Chapter 9 – Open pond systems for microalgal culture. In: Pandey A, Chang J-S, Soccol CR, Lee D-J, Chisti Y (eds) Biomass, Biofuels, Biochemicals, Biofuels from Algae (Second Edition), Elsevier, Pages 199-223. https://doi.org/10.1016/B978-0-444-64192-2.00009-3

Vossen, E, Raes K, Van Mullem D, De Smet S (2017) Production of docosahexaenoic acid (DHA) enriched loin and dry cured ham from pigs fed algae: Nutritional and sensory quality. Eur. J. Lipid Sci. Technol., 119: 1600144. https://doi.org/10.1002/ejlt.201600144

Vuppaladadiyam AK, Prinsen P, Raheem A, Luque R, Zhao M (2018), Microalgae cultivation and metabolites production: a comprehensive review. Biofuels, Bioprod. Bioref., 12: 304-324. https://doi.org/10.1002/bbb.1864

Wang A, Yan K, Chu D, Nazer M, Ting Lin N, Samaranayake E, Chang J (2020) Microalgae as a Mainstream Food Ingredient: Demand and Supply Perspective. In: Alam M, Xu JL, Wang Z (eds) Microalgae Biotechnology for Food, Health and High Value Products. Springer, Singapore. https://doi.org/10.1007/978-981-15-0169-2_2

Watson JE, Venter O, Lee J, Jones KR, Robinson JG, Possingham HP et al. (2018). Protect the last of the wild. Nature 563, 27–30.

Williams PJLB, Laurens LM (2010) Microalgae as biodiesel & biomass feedstocks: Review & analysis of the biochemistry, energetics & economics. Energy & environmental science, 3(5), 554-590. https://doi.org/10.1039/B924978H

Wollman FA (2016) An antimicrobial origin of transit peptides accounts for early endo- symbiotic events. Traffic 17(12):1322–1328. https://doi.org/10.1111/tra.12446

Xu Y, Ibrahim IM, Wosu CI, Ben-Amotz A, Harvey PJ (2018) Potential of New Isolates of *Dunaliella Salina* for Natural β-Carotene Production. Biology.; 7(1):14. https://doi.org/10.3390/biology7010014

Yaakob Z, Ali E, Zainal A, Mohamad M, Takriff MS (2014) An overview: Biomolecules from microalgae for animal feed and aquaculture. J of Biol Res-Thessaloniki 21, 6. https://doi.org/10.1186/2241-5793-21-6

Yadav G, Dubey BK, Sen R (2020) A comparative life cycle assessment of microalgae production by CO_2 sequestration from flue gas in outdoor raceway ponds under batch and semi-continuous regime. Journal of Cleaner Production, Volume 258, 120703. https://doi.org/10.1016/j.jclepro.2020.120703

Yamori W (2020) Chapter 12 - Photosynthesis and respiration. In: Kozai T, Niu G, Takagaki M (eds) Plant Factory (Second Edition), Academic Press, Pages 197-206. https://doi.org/10.1016/B978-0-12-816691-8.00012-1

Yang L, Li H, Wang Q (2019) A novel one-step method for oil-rich biomass production and harvesting by co-cultivating microalgae with filamentous fungi in molasses wastewater. Bioresource Technology, Volume 275, Pages 35-43. https://doi.org/10.1016/j.biortech.2018.12.036

Yao S, Lyu S, An Y, Lu J, Gjermansen C, Schramm A (2019) Microalgae–bacteria symbiosis in microalgal growth and biofuel production: a review. J Appl Microbiol, 126: 359-368. https://doi.org/10.1111/jam.14095

Yen H-W, Chen P-W, Chen L-J (2015) The synergistic effects for the co-cultivation of oleaginous yeast-*Rhodotorula glutinis* and microalgae-*Scenedesmus obliquus* on the biomass and total lipids accumulation. Bioresour Technol 184:148–152. https://doi.org/10.1016/j.biortech.2014.09.113

Yin Z, Zhu L, Li S, Hu T, Chu R, Mo F, Hu D, Liu C, Li B (2020) A comprehensive review on cultivation and harvesting of microalgae for biodiesel production: Environmental pollution control and future directions. Bioresource Technology, Volume 301, 122804. https://doi.org/10.1016/j.biortech.2020.122804

Yousuf A (2020) Chapter 1 - Fundamentals of Microalgae Cultivation. In: Abu Yousuf (eds) Microalgae Cultivation for Biofuels Production, Academic Press, Pages 1-9. https://doi.org/10.1016/B978-0-12-817536-1.00001-1

Zakariah NA, Rahman N, Hamzah F, Md Jahi T, Ismail A (2016) *Nannochloropsis oculata* algae as biofuels: a review on two-stage culture. Environmental Science and Sustainable Development: pp. 217-222 https://doi.org/10.1142/9789814723039_0029

Zakryś B, Milanowski R, Karnkowska A (2017) Evolutionary Origin of *Euglena*. In: Schwartzbach S, Shigeoka S (eds) Euglena: Biochemistry, Cell and Molecular Biology. Advances in Experimental Medicine and Biology, vol 979. Springer, Cham. https://doi.org/10.1007/978-3-319-54910-1_1

Zanella L, Vianello F (2020) Microalgae of the genus Nannochloropsis: Chemical composition and functional implications for human nutrition, Journal of Functional Foods, Volume 68, 103919. https://doi.org/10.1016/j.jff.2020.103919

Zhan J, Rong J, Wang Q (2017) Mixotrophic cultivation, a preferable microalgae cultivation mode for biomass/bioenergy production, and bioremediation, advances and prospect. International Journal of Hydrogen Energy, Volume 42, Issue 12, Pages 8505-8517. https://doi.org/10.1016/j.ijhydene.2016.12.021

Zhang P, Li Z, Lu L, Xiao Y, Liu J, Guo J, Fang F (2017) Effects of stepwise nitrogen depletion on carotenoid content, fluorescence parameters and the cellular stoichiometry of *Chlorella vulgaris*. Spectrochimica Acta Part A: Molecular and Biomolecular Spectroscopy, Volume 181, Pages 30-38. https://doi.org/10.1016/j.saa.2017.03.022

Zhang Z, Fulgoni VL III, Kris-Etherton PM, Mitmesser SH (2018) Dietary Intakes of EPA and DHA Omega-3 Fatty Acids among US Childbearing-Age and Pregnant Women: An Analysis of NHANES 2001–2014. Nutrients. 10(4):416. https://doi.org/10.3390/nu10040416

Zhong Y, Jin P, Cheng JJ (2018) A comprehensive comparable study of the physiological properties of four microalgal species under different light wavelength conditions. Planta 248, 489–498. https://doi.org/10.1007/s00425-018-2899-5

Zhu C, Zhai X, Jia J, Wang J, Han D, Li Y, Chi Z (2018) Seawater desalination concentrate for cultivation of *Dunaliella salina* with floating photobioreactor to produce β-carotene. Algal research, 35, 319-324. https://doi.org/10.1016/j.algal.2018.08.035

Zhu L (2015) Microalgal culture strategies for biofuel production: a review. Biofuels, Bioprod. Bioref., 9: 801-814. https://doi.org/10.1002/bbb.1576

Zhu L, Li S, Hu T, Nugroho YK, Yin Z, Hu D, Chu R, Mo F, Liu C, Hiltunen E (2019) Effects of nitrogen source heterogeneity on nutrient removal and biodiesel production of mono- and mix-cultured microalgae. Energy Conversion and Management, Volume 201, 112144. https://doi.org/10.1016/j.enconman.2019.112144

Zhu L, Nugroho YK, Shakeel SR, Li Z, Martinkauppi B, Hiltunen E (2017) Using microalgae to produce liquid transportation biodiesel: What is next? Renewable and Sustainable Energy Reviews, Volume 78, Pages 391-400. https://doi.org/10.1016/j.rser.2017.04.089

Zorn SMFE, Reis CER, Silva MB, Hu B, De Castro HF (2020) Consortium growth of filamentous fungi and microalgae: evaluation of different cultivation strategies to optimize cell harvesting and lipid accumulation. Energies, 13, 3648. https://doi.org/10.3390/en13143648

Zuccaro G, Yousuf A, Pollio A, Steyer J-P (2020) Chapter 2 - Microalgae Cultivation Systems. In: Yousuf A (eds) Microalgae Cultivation for Biofuels Production, Academic Press, Pages 11-29, https://doi.org/10.1016/B978-0-12-817536-1.00002-3

Purposes of the Thesis

The aim of this Thesis entitled "Different cultivation methods of microalgae for biotechnological applications" is to increase knowledge on the morphophysiological and biochemical aspects of certain microalgae that are widely used in the bioenergy, pharmaceutical and nutraceutical sectors. The research focused on the two microalgae which are known for their use in biotechnology *Tisochrysis lutea* and *Nannochloropsis oculata*, in order to improve their growth performance, photosynthetic efficiency and biomass composition.

The Thesis is organized and subdivided in chapters as follows:

Chapter 2 is a study on the feasibility of co-cultivating *T. lutea* and *N. oculata* in a batch system in saline medium. This strategy could aim to obtain distinctive compounds of each alga, such as pigments (chlorophylls and carotenoids) and fatty acids (e.g. DHA and EPA), in a single cultivation process with the concomitant advantage to halve water and nutrient use.

Chapter 3 focuses on the effects of two different illumination conditions on mono- and co-cultures of *T. lutea* and *N. oculata*. The results of control cultures under white light were compared with those of cultures treated with red-enriched light. In addition to studying the effects on cell growth, photosynthetic pigments and lipid content, biochemical analyses were also performed to highlight any adaptations of the two microalgae in the photosynthetic apparatus in response to the different light conditions.

Chapter 4 aims to evaluate the feasibility of cultivating *T. lutea* in rejected brine from the desalination plant of Almería (Spain). A waste-to-value approach was applied to produce microalgal biomass rich in valuable molecules such as lipids and pigments from an industrial by-product, with the added advantage of increased environmental sustainability associated with reduced freshwater consumption.

Chapter 5 concerns a comparative study on cell growth, lipid accumulation, photosynthetic performance and antioxidant activity of *T. lutea* grow under autotrophic and mixotrophic conditions using glycerol as a carbon source. Furthermore, a semi-continuous culture strategy was proposed in other to maximise the possibility of growth of this alga.

During the three years spent for my PhD, publications and presentations to conferences have been produced, as listed below.

Articles on peer reviewed journals:

Maglie M., Baldisserotto C., Guerrini A., Sabia A., Ferroni L., Pancaldi S. (2021) A co-cultivation process of *Nannochloropsis oculata* and *Tisochrysis lutea* induces morpho-physiological and biochemical variations potentially useful for biotechnological purposes. Journal of Applied Phycology https://doi.org/10.1007/s10811-021-02511-2

Baldisserotto C., Sabia A., Guerrini A., Demaria S., **Maglie M.**, Ferroni L., Pancaldi S. (2021) Mixotrophic cultivation of *Thalassiosira pseudonana* with pure and crude glycerol: Impact on lipid profile. Algal Research 54 (2021) 102194; https://doi.org/10.1016/j.algal.2021.102194

Baldisserotto C. Demaria S., Accoto O., Marchesini R., Zanella M., Benetti L., Avolio F., **Maglie M.**, Ferroni L., Pancaldi S. (2020) Removal of nitrogen and phosphorus from thickening effluent of an urban wastewater treatment plant by an isolated green microalga. Plants 2020, 9, 1802; https://doi.org/10.3390/plants9121802

Conference presentations:

Demaria S., Baldisserotto C., **Maglie M.**, Marchesini R., Ferroni L., Benetti L., Zanella M., Pancaldi S. (2021) Microalgae remove nitrogen, phosphorus, and also escherichia coli load from urban wastewater streams. RemTech Europe On-line, 20 - 24 Settembre. (Comunication)

Maglie M., Ibáñez González M.J., Navarro López E., Pancaldi S., Molina-Grima E., Mazzuca-Sobczuk T. (2021) Waste-to-value approach: the production of lipids from the microalga *Tisochrysis lutea* using a reject brine. 116° Congresso della Società Botanica Italiana - VII International Plant Science Conference (IPSC), On-line, 8 -10 Settembre. (Comunication)

Maglie M., Baldisserotto C., Ibáñez González M.J., Mazzuca-Sobczuk T., PancaldiS. (2021) Effects of co-cultivation and red LEDs light on growth and lipids content of *Tisochrysis lutea* and *Nannochloropsis oculata*, Virtual Conference Botany 2021 18-23 Luglio.

Demaria S., Baldisserotto C., **Maglie M.**, Marchesini R., Ferroni L., Benetti L., Zanella M., Pancaldi S. (2021) Isolation of a natural microalgae consortium for the removal of nitrogen and phosphorus from an urban wastewater stream. Riunione scientifica congiunta dei gruppi per la biologia cellulare e molecolare e per le biotecnologie e differenziamento della SBI, On-line, 16-18 Giugno. (Comunication)

Maglie M., Baldisserotto C., Pancaldi S. (2020) Co-cultivation of Tisochrysis lutea and Nannochloropsis oculata: effect of different cultivation media and light spectra. 115° Congresso della Società Botanica Italiana (SBI), online, 9-11 Settembre.

Maglie M., Marzullo A., Maietti A., Baldisserotto C., Pancaldi S. (2020) Semi-continuous autotrophic and mixotrophic cultivation of *Tisochrysis lutea:* antioxidant activity evaluation of methanolic extracts by DPPH assay. Virtual Conference Botany 2020 - 27-31 Luglio.

Maglie M., Baldisserotto C., Guerrini A., Pancaldi S. (2020) Co-cultivation of *Tisochrysis lutea* and *Nannochloropsis oculata*: preliminary tests on cultivation medium and starter inoculum variations. Conference of Young Botanists (CYBO), Genova, 6-7 Febbraio. (Comunication)

Maglie M., De Benedictis M., Barozzi F., Papadia P., De Paolis A., Migoni D., Di Sansebastiano G-P. (2019) In vitro induction of genetic variability of *Dittrichia viscosa* to be improved in soil phytoremediation. RemTech Europe Poster Session 2019 – Ferrara, 18-20 Settembre.

Maglie M., Baldisserotto C., Guerrini A., Pancaldi S. (2019) Optimization of the co-cultivation of *Tisochrysis lutea* and *Nannochloropsis oculata*: preliminary tests. 114° Congresso della Società Botanica Italiana (SBI), Padova, 5-7 Settembre.

Baldisserotto C., Accoto O., Benetti L., Marchesini R., **Maglie M.**, Pancaldi S. (2019) Nitrogen and phosphorous removal by microalgae isolated from sludge surnatants of an urban wastewater treatment plant. 114° Congresso della Società Botanica Italiana (SBI), Padova, 5-7 Settembre.

Maglie M., Baldisserotto C., Guerrini A., Pancaldi S. (2019) Co-cultivation of *Tisochrysis lutea* and *Nannochloropsis oculata* for biotechnological purposes. Riunione scientifica congiunta dei gruppi per la biologia cellulare e molecolare e per le biotecnologie e differenziamento della SBI, Napoli, 12-14 Giugno. (Comunication)

Chapter 2

A co-cultivation process of *Nannochloropsis oculata* and *Tisochrysis lutea* induces morpho-physiological and biochemical variations potentially useful for biotechnological purposes

From the published article:

Maglie M, Baldisserotto C, Guerrini A, Sabia A, Ferroni L, S Pancaldi

Journal of Applied Phycology volume 33, pages2817–2832 **(2021)**

https://doi.org/10.1007/s10811-021-02511-2

1. Introduction

In recent decades, the biotechnological potential of microalgae has gained considerable importance because of their wide application range: production of biomass for food and feed, synthesis of high-value compounds (e.g. polyunsaturated fatty acids, pigments, polysaccharides) for cosmetic and pharmaceutical sectors, employment in renewable green-energy and in phytoremediation systems (Sabia et al. 2015; D'Amato et al. 2017; Rizwan et al. 2018; Alam et al. 2020). The evolutionary and phylogenetic diversity of microalgae results in an interesting variety of their biochemical composition. They are extremely attractive as sources of a wide range of biomolecules, such as vitamins, essential amino acids, polyunsaturated fatty acids (PUFA), minerals, carotenoids, enzymes and fibres (Borowitzka 2013; Matos 2017; Rahman 2020). The production of microalgae may be of interest also because it does not require arable land, does not compete with food crops, and can use waste as nutrients for their growth (da Silva Vaz et al. 2016). Moreover, microalgae can act as a natural sink for the reduction of atmospheric CO_2 and some of them can also utilize the CO_2 derived from industrial exhaust gases (Yen et al. 2015). According to the World Water Development Report 2018 of the United Nations, water use has increased worldwide by about 1% per year since the 1980s, and the global water demand is expected to continue to rise. However, microalgae cultivation is a water intensive process, therefore, the water consumption and loss must be managed efficiently during cultivation (Mayers et al. 2016). The use of saline algae could help to reduce freshwater consumption destined to microalgal cultures as reported in Ishika et al. (2017). A current driving force that inspires the progress in microalgae production is the search for novel cultivation systems to obtain a reduction of the costs and a lower consumption of water and nutrients. In this context several studies have been focused on the co-cultivation of different organisms, a strategy based on the concept of ecological community: no species lives isolated in nature (Smith and Crews 2014; Zhu 2015; Das et al. 2021). In co-cultivation two or more different microorganisms are grown together; in fact, this cultivation mode can involve different microalgal species or microalgae and other microorganisms such as fungi and bacteria (Zhu et al. 2017). With this perspective, the main purpose of this study was to test a co-cultivation strategy in saline medium of *Nannochloropsis oculata* (Ocrophyta) and *Tisochrysis lutea* (Haptophyta), species of microalgae particularly interesting for their composition in pigments and fatty acids (Ryckebosch et al. 2014; Cavalier-Smith et al. 2018; Guiry & Guiry 2021). Natural pigments are used as additives and colorants in aquaculture, and in nutraceutical, pharmaceutical and cosmeceutical industries (Alam et al. 2020); consequently, their demand is increasing over the years. In this context, microalgae are a valuable solution, also considering

that they contain a different pattern of pigments, but also of lipids and other valuable molecules (e.g. polysaccharides), in relation to their phylogenetic position (Barsanti and Gualtieri 2014; Begum et al. 2016). *Nannochloropsis* sp. contains chlorophyll *a*, *β*-carotene and the accessory pigments, violaxanthin, diadinoxanthin and zeaxanthin (Ryckebosch et al. 2014, Sukarni et al. 2014). *T. lutea* is characterized by chlorophyll *a*, *c1* and *c2*, *β*-carotene, diadinochrome, diatoxanthin, and fucoxanthin (Barsanti and Gualtieri 2014; Ryckebosch et al. 2014). In microalgae PUFAs usually account for 25-60% of the total lipids (Richmond 2004). The most common are arachidonic acid (AA; 20:4n6, ω-6), docosahexaenoic (DHA; 22:6n3, ω-3) and eicosapentaenoic acid (EPA; 20:5n3, ω-3) (Pulz and Gross 2004; Mata et al. 2010), which are the most nutritionally significant PUFAs present in marine food and fish oil (Ramesh Kumar et al. 2019; Zhang et al. 2019). In *N. oculata* the lipid content is usually about 30% of the dry weight biomass, but it can increase or decrease as a consequence of growth or stress conditions, e.g. inoculum, irradiance, salinity and nitrogen availability (Su et al. 2011). As regards ω-3 fatty acids, *N. oculata* does not contain DHA, while it accumulates high levels of EPA, about 193 mg g^{-1} of extracted oil (Ryckebosch et al. 2014). *T. lutea* is characterized by a total lipid content of approximately 20% of the dry weight biomass. High levels of DHA are detectable, about 46 mg g^{-1} of extracted oil; conversely, the levels of EPA are low, about 2.8 mg g^{-1} (Ryckebosch et al. 2014). Taken together, *N. oculata* and *T. lutea* could represent a valid alternative to the use of fish oil and fishmeal, both in aquaculture and in human nutrition, because of their complementarity of the biochemical composition, especially in ω-3 PUFAs (Beker 2014, Shah et al. 2018). Moreover, it should be considered that, currently, fish- and animal-derived products find less and less consensus among consumers, especially vegetarians or vegans (Wang et al. 2020). Thus, the aim of this research is focused to ascertain if the co-cultivation of *N. oculata* and *T. lutea* could allow the production of high-value molecules, in particular ω-3 fatty acids, for obtaining in a single cultivation system a microalgal biomass rich in all ω-3 fatty acids typical of fish oil and fishmeal. Furthermore, the co-cultivation represents an added value in the perspective of reducing (in this case, halving) water consumption for algae cultivation.

2. Materials and methods

Algal culture condition and growth

Nannochloropsis oculata (Droop, Hibberd, 1981; strain CCAP 849/1) and *Tisochrysis lutea* (Bendif & Probert 2013; strain CCAP 927/14) were used in this study. Both species belong to Chromista kingdom (Guiry & Guiry 2021). Microalgae were obtained from the Culture Collection of Algae and Protozoa of Scottish Marine Institute (Scotland, United Kingdom;

www.ccap.ac.uk). The two microalgae were co-cultivated, and mono-cultures of each strain were used as controls. Both mono- and co-cultures were inoculated at least in triplicate and grown in 300 mL Erlenmeyer flasks (150 mL of total culture volume). Axenic cultures were grown and maintained in liquid f/2 medium (Guillard and Ryther 1962; Guillard 1975) in artificial seawater ESAW (Berges et al. 2001) in a growth chamber (25 ± 1 °C; 60 $\mu mol_{photons}$ m^{-2} s^{-1} photosynthetically active radiation (PAR); 16:8 h light-dark photoperiod), without shaking, and no external CO_2 was supplied. For mono-cultures, *T. lutea* cells were inoculated at a density of $0.6 \pm 0.1 \times 10^6$ cells mL^{-1}, and *N. oculata* cells at a density of $5 \pm 0.1 \times 10^6$ cells mL^{-1}, corresponding respectively to a dry biomass (DW) of 0.066 ± 0.008 and 0.069 ± 0.006 g L^{-1}. For dry biomass (DW), aliquots of samples were filtered through pre-dried and pre-weighed glass-fibre filters (1.2 μm pore size; Whatman GF/C). Filters with cells were rinsed with 20 mL of distilled water, dried for 72 h at 60°C and weighted until they reached a constant weight (Popovich et al. 2012a). The dry biomass data was used to calculate the biomass yield in cultures (g L^{-1}). For co-cultures, *T. lutea* and *N. oculata* cells were inoculated together at the same densities used in mono-culture. Growth was estimated by measuring the optical density at 750 nm with a Pharmacia Biotech Ultrospec®2000 UV–vis spectrophotometer (1 nm bandwidth; Amersham Biosciences, Piscataway, NJ, USA) and by counting the cells with a Thoma's chamber (HBG, Giessen, Germany) under the light microscope (Zeiss, Axiophot, Jena, DE), sampling 1 mL of culture at days 0, 3, 7, 10, 14, 21. To make the cell counting of *T. lutea* easier, 100 μL of Lugol's iodine were added to 1 mL of culture to stop cell movements. For DW, aliquots of co-cultures were treated as described above for mono-cultures. For a better interpretation of final data, an estimation of DW derived from *T. lutea* and *N. oculata* in co-cultures was obtained using data of biomass yield *vs* cell density of mono-cultures.

Light and fluorescence microscopy

Cell samples were observed at 0, 3, 7, 10, 14 and 21 days, under the same Zeiss microscope cited above, equipped with conventional or fluorescent attachments. The light source for chlorophyll fluorescence examinations was an HBO 100 W pressure mercury vapour lamp (filter set, BP436/10 FT 460, LP470). According to Hillebrand et al. (1999) images were employed to calculate the cell volume using "ImageJ" software (https://imagej.nih.gov/ij/index.html). To highlight the presence of acidic mucopolysaccharides, 40 μL of Alcian Blue (1% in 3% acetic acid) was added to an algal pellet obtained after the centrifugation of 2 mL of culture (Mowry and Scott 1967; Discart et al. 2015). After incubation at room temperature for 30 min, the samples were rinsed twice with culture

medium to remove the stain excess. Cells were then observed under white light with the microscope described above. In order to highlight the intracellular lipid accumulation, cells were stained with Nile Red (Sigma) (9-diethylamina-5Hbenzo [α]phenoxazine-5-one), according to Giovanardi et al. (2013), with some modifications. Aliquots of 10 µL Nile Red (0.5 mg dissolved in 100 mL acetone) were added to 1.9 mL of a cell suspension with 4×10^6 cells for *N. oculata* and 0.5×10^6 cells for *T. lutea*. After incubation at 37°C in darkness for 15 min, cells were observed with excitation at 485 nm (filter set BP485, LP520). All pictures were taken with a Canon Powershot S40 digital camera.

Transmission and scanning electron microscopy

For transmission electron microscopy (TEM), cells were harvested weekly by centrifugation and prepared as reported in Baldisserotto et al. (2012) with minor modifications: the phosphate buffer has been substituted with sodium cacodylate buffer 0.1 M (pH 7.2) for *N. oculata* and sodium cacodylate buffer 0.1 M with sucrose 0.25 M for *T. lutea*. Ultra-thin sections were observed with a Hitachi H800 electron microscope (Electron Microscopy Centre, University of Ferrara). For scanning electron microscopy (SEM), co-cultivated cells were harvested by centrifugation at the 21st day of cultivation. Samples were fixed with 2.5% (v/v) glutaraldehyde in 0.1 M phosphate buffer (pH 7.4), post-fixed overnight with 2% (m/v) OsO_4 in the same fixation buffer and dehydrated in a graded ethanol series. Samples were then mounted on a metal holder, covered with gold with a sputter Edwards S150, and observed with a Zeiss Evo 40 electron microscope at 20 kV (Electron Microscopy Centre, University of Ferrara).

Pigment extraction and analysis

Cells were collected by centrifugation after 0, 3, 10 and 21 days of experiment and treated with 100 % methanol for 10 min at 80 °C (Baldisserotto et al. 2012). Absorption of extracts was measured at 665 nm for chlorophyll *a* (Chl *a*), 632 nm for chlorophyll *c* (Chl *c*) and 470 nm for carotenoids (Cars) (Wellburn 1994; Ritchie 2006) with a Pharmacia Biotech Ultrospec®2000 UV–vis spectrophotometer (1 nm bandwidth; Amersham Biosciences, Piscataway, NJ, USA). Extracts were manipulated under dim light to avoid photo-degradation. Chlorophyll concentration in *T. lutea* was evaluated using the equations of Ritchie (2006). Otherwise, the equations of Wellburn (1994) were employed to determine the chlorophyll concentration in *N. oculata* and the carotenoid concentration in both samples. Cells in the co-culture were separated by a sucrose gradient. The gradient was prepared by layering solutions containing sucrose at different concentrations (20-30-40%) and polyvinylpyrrolidone (PVP; Sigma) 2%, dissolved in f/2 medium in ESAW. 5 mL of the 40% solution was added to the bottom of a 50 mL tube,

followed by 10 mL of the 30% solution and finally 10 mL of the solution with 20% sucrose concentration. An aliquot of co-culture was placed in the 50 mL tube containing the sucrose gradient. After 10 min centrifugation at 5300 g cells of *N. oculata* are separated from those of *T. lutea*. In particular, the cells of *N. oculata* and *T. lutea* stratified at the 20-30% and 30-40% interface, respectively. The two cell fractions were recovered using a Pasteur pipette and washed with f/2 medium in ESAW before analysis.

Chlorophyll fluorescence measurements

At days 0, 3, 7, 10, 14 and 21, fluorescence measurements were performed on cell pellets prepared as described by Ferroni et al. (2011). After 15 min of dark incubation, initial fluorescence F_0 and maximum fluorescence F_M were used to calculate the maximum quantum yield of PSII (F_V/F_M ratio). 15 min was found to be the optimal adaptation time for both microalgae after testing a range between 5- and 40-min dark adaptation time. For analyses, a pulse amplitude modulation fluorometer (PAM; Junior-PAM, Walz) was used with the following setting: measuring light (ML) with intensity and frequency at level 1; 0.6 s saturation pulse at level 6. Before PAM analysis, cells in co-culture were separated through a sucrose gradient as described above. To verify the possible effects of the sucrose gradient procedure on F_V/F_M values, mono-cultivated cells have been tested using the same procedure.

Proteins extraction and quantification

At days 0 and 21, the total proteins were extracted. Aliquots of mono-cultivated and co-cultivated cells (about 100 mL with optical density of 0.5 at 750 nm) were centrifuged at 500 *g* for 10 min and treated according to Ivleva and Golden (2007), with some modifications as described in Baldisserotto et al. (2016). Pellets were resuspended in a small quantity (2 mL) of washing buffer [2 mM Na_2EDTA, 5 mM ε-aminocaproic acid, 5 mM $MgCl_2$, 5 mM dithiothreitol dissolved in 1× PBS buffer; PBS buffer (1 L, stock solution 10×): 80 g NaCl, 2 g KCl,14.4 g $Na_2HPO_4 \cdot 2H_2O$, 2.4 g KH_2PO_4 dissolved in distilled water], transferred into 2 mL tubes and then centrifuged (10 min, 2000 *g*). Subsequently, the pellets were resuspended in the extraction buffer (0.1 M NaOH, 1% sodium dodecyl sulphate, 0.5% β-mercaptoethanol dissolved in water). Samples were frozen three times in liquid N_2 for 2 min each and subsequently heated at 80 °C for other 2 min, then rapidly frozen in liquid N_2 and kept at −20 °C overnight. The subsequent day, the samples were added with glass beads (0.40–0.60 μm diameter; Sartorius, Germany) and vigorously vortexed for 10 min (mixing cycles of 30 s, each followed by 30 s cooling on ice). After centrifugation (1500 *g*,10 min) the supernatants were harvested (extract I). Pellets were re-extracted by resuspending with 0.5 mL of extraction

buffer, vortexing in tubes for 2 min, and finally keeping tubes at 60 °C for 15 min. Samples were then centrifuged (1500 *g*, 10 min) and the supernatant (extract II) was added to the extract I. Finally, the total extract was rapidly frozen in liquid N_2 and stored at −20 °C until quantification. Proteins were quantified following the Lowry's method (1951).

Total lipid content

At the 21st day of cultivation, lipid extraction was performed according to Ryckebosch et al. (2012) with some modifications. Duplicate freeze-dried samples containing 100 mg of biomass were vortexed for 30 s at room temperature in 6 mL chloroform:methanol (1:1, v:v) and 0.4 mL of distilled water. The solvent mixture (2 mL) and water (0.4 mL) were then added and the tube was mixed again with a vortex and subsequently centrifuged. The aqueous layer was removed, and the solvent layer was transferred into a clear tube. The pellet was re-extracted with 4 mL of chloroform:methanol (1:1, v:v). The combined solvent layers were passed through a layer of anhydrous Na_2SO_4 using Whatman No. 1 filter paper in a funnel. After removal of the solvent by rotary evaporation at 40 °C, the lipid content was determined gravimetrically.

Lipid fractionation and fatty acid profile

Lipid fractionation in neutral lipids, glycolipids and phospholipids was performed using a silica Sep–Pak (SP) of 700 mg (Waters) according to Popovich et al. (2012b) with some modifications. Adsorbent conditioning was performed with 10 mL of chloroform, and samples were loaded by 1 mL of chloroform/oil solution containing 15 mg of oil in 100 mL of chloroform. Elution of neutral lipids from the adsorbent bed was performed with 15 mL of chloroform, glycolipids were recovered by elution with 10 mL of acetone/methanol (9:1, v:v) and phospholipids by elution with 10 mL of methanol. Each fraction was collected into a conical vial and evaporated to dryness under nitrogen. The efficiency of SP was verified by thin layer chromatography (Silicagel G 60 70–230 mesh, Merck, Darmstadt, Germany). Concentrated solutions of each fraction of lipids were applied to the bottom of the plates and the plates were processed with chloroform:methanol (2:1, v:v). After solvent evaporation, plates were sprayed with phosphomolybdic acid and heated at 120–130 °C. Fatty acid profiles were determined by methyl ester derivation and gas chromatographic (GC) analysis, with a Varian GC-3800 gas chromatograph, equipped VF-5ms column with stationary phase bound poly-5% phenyl-95% dimethyl-siloxanes (internal diameter, 0.25 mm, length, 30 m, film thickness, 0.25 μm) and a Varian MS-4000 mass spectrometer with ionization for electronic

impact and ion trap, equipped with a NIST library. Fatty acid methyl esters (FAMEs) have been identified comparing their retention time and the mass spectrum with that of a mixture of 37 pure compounds (Supelco, Sigma-Aldrich).

Statistical analysis

Data were processed and analysed using Excel (Microsoft Office 2016). When necessary, statistical tests such as Student t-test, one-way ANOVA and two-way ANOVA were performed using Origin® 2018 analysis software, followed by Tukey post-hoc test ($p < 0.05$).

3. Results

Growth kinetics

Growth kinetics of *N. oculata* and *T. lutea* in mono- and in co-cultivation are reported in Fig. 1. In both systems of cultivation, *N. oculata* cells remained in the logarithmic phase of growth up to the 10th day, then the cells entered the stationary phase. However, the mono-cultures showed a higher cell density, and the final cell density was about $26 \pm 1.5 \times 10^6$ cell mL^{-1} in co-culture and $35 \pm 5.2 \times 10^6$ cell mL^{-1} in mono-culture. In contrast, both mono- and co-cultures of *T. lutea* showed a rapid growth during the first 3 days. Subsequently, while the growth of the mono-cultures continued slowly until the end of the experiment, the growth of the co-cultivated cells entered the stationary phase already on the third day. Final cell density was about $1 \pm 0.3 \times 10^6$ cell mL^{-1} in co-cultures and $6 \pm 0.6 \times 10^6$ cell mL^{-1} in mono-cultures. As shown in Fig 1, both microalgae species had a lower growth in co-cultivation than in mono-cultivation. Furthermore, at the end of the experiment, biomass, evaluated for all cultures, yielded 0.95 and 0.93 g L^{-1} for mono-cultivated *T. lutea* and *N. oculata*, respectively, and 0.99 g L^{-1} for co-cultures (ANOVA, $p > 0.05$). For co-cultures, it was estimated that *T. lutea*, which was about only 3% of total cells, yielded about 0.165 g L^{-1} (17% of total biomass), while *N. oculata* 0.821 g L^{-1} (83% of total biomass).

Cell morphology

Figure 2 shows light and fluorescence microscope observations of mono- and co-cultivated *N. oculata* and *T. lutea* cells. Observed under the light microscope, both mono- and co-cultivated cells of *N. oculata* had a spheroid shape, with a variable diameter between 2 and 3 μm, corresponding to a cell volume between 10 and 14 μm^3. Mono- and co-cultivated cells differed in the accumulation of translucent globules: in mono-cultivation, they were visible already at the 7th day and increased during the experiment (Fig. 2b and c); in co-cultivation, some

translucent globules were observed only in the final stages of growth, 18-21 days (Fig. 2q). The lipid-specific fluorochrome Nile Red was used to investigate the nature of these translucent globules (Fig. 3). The *N. oculata* cells grown in mono-culture showed an increase in fluorescent lipid droplets during the period of cultivation, reaching the most intense reaction at the end of the experiment, when the globules were in number of 3-4 per-cell and occupied a large part of the cell volume (Fig. 3c). In contrast, cells grown in co-culture accumulated lipids only at the end of the experiment (Fig. 3i). *T. lutea* cells, typically golden brown in colour, had a shape from spherical to ovate or oblong, with two apical flagella. In some cells the loss or rupture of one or both flagella were observed in the in the late stages of cultivation. The volume of the microalga in co-cultures was smaller than in mono-cultures, 80 and 190 μm^3, respectively (mean values at 21st day). The cup shaped plastid laid peripherally in the cell. From the 7th day, vacuoles of variable size appeared in both mono- (Fig. 2h and i) and co-cultivated *T. lutea* cells (Fig. 2p and q). Moreover, from the first days of cultivation, translucent globules were visible, and their number increased over time in both mono- and co-cultivated cells; since the beginning of the experiment, 2-3 lipid globules were present in most of the cells (Fig. 3d and g). In the 10-14 days interval, the number and volume of globules increased (Fig 3e and h) and, at the final stages of cultivation, 4-5 lipid droplets occurred in the cells and were larger than during the previous days (Fig. 3f and i).

SEM and TEM observations

TEM observations are shown in Figure 4. In the early stages of mono-cultivation (3-10 days), the *N. oculata* chloroplast occupied more than half of the cell volume. Large mitochondria indicated an intense cellular activity during the early stages of cultivation. Small globules, probably corresponding to lipid droplets, were visible (Fig. 4a). After 10 days of cultivation, the chloroplast still occupied a significant portion of the total cell volume, but the thylakoids were less numerous and locally appressed. Several large lipid globules were always present (Fig. 4b). At the 21st day, the thylakoids were fewer and more appressed than in previous days; moreover, the stroma appeared darker. On the other hand, the lipid globules increased in size and number, consistent with Nile Red analysis (Fig. 4c). No morphological differences in the co-cultivated cells were noted in the early phases of cultivation (Fig. 4d). After 10 days of co-cultivation, the thylakoids looked appressed (Fig. 4e) and even more after 21 days; nevertheless, well-structured mitochondria were visible (Fig. 4f). Lipid globules only occurred at the last stages of cultivation, confirming the observations in epifluorescence with Nile Red (Fig. 4f). In mono-cultivated *T. lutea* cells, the cup-shaped plastid and pyrenoid were visible (Fig. 4i).

Already from the 3rd day of cultivation, some lipid globules were visible in mono-cultivated cells (Fig. 4g). After 10 and 21 days from the inoculation, the cells showed the first signs of vacuolisation, and the lipids droplets appeared darker than at the early stages (Fig. 4h, i). Moreover, from the 10th day a great secretion activity was visible and characterized by the presence of many vesicles releasing their contents outside the cells (Fig. 5a). During the early phases of co-cultivation, *T. lutea* cells showed no substantial differences compared to those mono-cultivated (Fig. 4l). On the other hand, from the 10th day, all organelles and membranes were altered (Fig. 4m, n). The extrusion of vesicles was also found in co-cultures and Alcian Blue staining highlighted on the surface of *T. lutea* cells the presence of acid mucopolysaccharides which were probably responsible for the cell aggregation phenomena observed in co-cultures (Fig. 5b, insert): *N. oculata* cells adhered to the surface of *T. lutea* cells (Fig. 5b).

Pigment content

The time-course of pigment content is shown in Fig. 6. In order to compare the pigment content in mono- and co-cultivated cells, *N. oculata* and *T. lutea* from co-cultures were separated in a sucrose gradient. An increase in Chl *a* (Fig. 6a) and total carotenoids (Fig. 6b) occurred when *N. oculata* cells were co-cultivated. This increase was observed at the 3rd and 10th day of cultivation. In co-cultivated cells Chl *a* content was 63% higher than that in mono-cultivated algae at the 3rd day ($p < 0.05$; Student t-test) and 119% higher at the 10th day ($p < 0.05$; Student t-test). The same trend characterized the carotenoids concentration: 75% higher in co-cultivated *N. oculata* cells after 3 days ($p < 0.05$; Student t-test) and 105% after 10 days ($p < 0.05$; Student t-test). In contrast, after 21 days, carotenoids were significantly less concentrated in co-cultivated cells than in the mono-cultivated ones ($p < 0.05$; Student t-test), while Chl *a* content was similar in mono- and co-cultivated *N. oculata* cells. Likewise, *T. lutea* co-cultivated cells showed a higher concentration of pigments, which underwent a progressive increase during cultivation and especially in the last phases (Fig. 6c, d and e). At the 21st day, the co-cultured cells contained 173% higher content of Chl *a*, 63% higher content of Chl *c* and 129% higher amount of total carotenoids than in mono-cultivated *T. lutea* ($p < 0.05$; Student t-test).

PSII maximum quantum yield measure

The effects of the co-cultivation process on photosynthetic efficiency were evaluated by PAM fluorimetry. In order to compare the PSII maximum quantum yield, measured as F_V/F_M ratio, in mono- and co-cultivated cells, *N. oculata* and *T. lutea* from co-cultures were separated in a sucrose gradient. Mono-cultivated cells have been tested using the same procedure to verify the

possible effects of the sucrose gradient procedure on F_V/F_M values. *T. lutea* cells showed no significant differences ($p = 0.1$; Student t-test) in F_v/F_M values between gradient-treated and no-treated cells. On the contrary, *N. oculata* cells showed a significant decrease of 13% ($p < 0.05$; Student t-test) in F_v/F_M values after the treatment with sucrose gradient. This difference was considered and used to correct the values recorded from gradient-treated co-cultivated cells. In microalgae, F_v/F_M values of about 0.6 indicate an efficient use of light in the photosynthetic processes (White et al. 2013; Sirin and Sillanpää 2015; Bhola et al. 2016). F_V/F_M was overall higher in mono-cultivated than in the co-cultivated cells (Fig. 7); this difference was always significant ($p < 0.05$; Student t-test), except for *N. oculata* cells at 7th day, when there was no significant difference between mono- and co-culture. *N. oculata* co-cultivated cells showed low F_V/F_M values, until they reached an average value of 0.359 ± 0.016 after 21 days of cultivation. However, F_V/F_M also decreased in mono-cultures, reaching the average value of 0.431 ± 0.030 at the end of experiment (Fig. 7a). In *T. lutea* mono-cultivated cells, the ratio remained almost stable above 0.600 throughout the experiment, with a decrease to 0.540 only after 21 days (Fig. 7b). Co-cultivated *T. lutea* showed F_V/F_M values lower than 0.600 already from the 7th day. The ratio decreased to less than 0.450 in the last stages of cultivation (14-21 days).

Protein content

As reported in Figure 8, both microalgal species, either in mono-cultivation or co-cultivation, showed a significant reduction in their protein content from the day of the inoculation to the 21st day ($p < 0.05$; Student t-test): in *N. oculata* it decreased from 22.15 to 3.62 µg proteins 10^{-6} cells (-83%); in *T. lutea* from 174.18 to 24.76 µg proteins 10^{-6} cells (-85 %); in co-cultivated cells from 55.65 to 4.59 µg proteins 10^{-6} cells (-91 %).

Lipid fraction

The lipid amount is very important in order to select oleaginous microalgae species. All analyses of lipid fraction were performed at the 21st day of cultivation, when Nile Red staining and TEM observations showed the maximum presence of lipid droplets inside all cells. Fig. 9 shows the total lipid content (% DW) in *N. oculata* and *T. lutea* mono- and co-cultures: differences between the tested samples were not significant ($p > 0.2$; one-way ANOVA). However, the fractions of neutral lipids, glycolipids and phospholipids showed significant differences only in the content of neutral lipids ($p < 0.05$; one-way ANOVA) (Fig. 10). In particular, the percentage content of neutral lipids differed between mono-cultivated *T. lutea* and *N. oculata* (55% and 69% respectively; $p<0.05$; one-way ANOVA followed by Tukey's

post-hoc test) and between *T. lutea* and the co-cultivated microalgae, in which the neutral lipids were about 67% of total lipids ($p<0.05$; one-way ANOVA followed by Tukey's post-hoc test).

Fatty acid profile

The fatty acid profile of the neutral lipid fraction was characterized by gas-chromatography coupled to mass spectrometry (GC-MS; Table 1). In mono-cultivated *N. oculata*, palmitoleic (C16:1) and palmitic (C16:0) acids were the major components (respectively 31.41% and 24.32%), followed by oleic acid (C18:1n9c; 13.68%). The characteristic ω-3 of this species, i.e. EPA (C20:5n3), accounted for 11.1% and the probable presence of eicosatrienoic acid (ETE – C20:3n3) accounted for 2.38%. Furthermore, two ω-6 PUFAs, linoleic (C18:2n6) and arachidonic (C20:4n6) acids, were also present, with 5.55% and 1.34%, respectively. Differently, in mono-cultivated *T. lutea*, the most abundant fatty acid was oleic acid (C18:1n9; 25.46%), followed by the ω-3 SDA (C18:4n3) and DHA (C22:6n3), 20.23% and 17.59%, respectively. The ω-3 EPA was extremely low (0.43%) (Table 1).

The fatty acid profile of co-cultivated cells was quite similar to that of *N. oculata* mono-cultivated samples; this was attributable to the low number of *T. lutea* in co-cultures at the 21st day, i.e. only 3% of total cells (estimated to be approximately 17% of total DW). For example, palmitoleic and palmitic acids, i.e. the major components in mono-cultivated *N. oculata*, were only slightly reduced in co-cultures. Differently, oleic acid, 25.46% in *T. lutea* and 13.68% in *N. oculata*, was reduced to about 15%. Finally, SDA, present only in *T. lutea*, accounted for about 1.6% (Table 1). Moreover, the co-cultures showed a not significant lower fatty acid percentages than the mono-cultivated *N. oculata* (about 21% *vs* 24%) (Fig. 9). Interestingly, the contribution of *T. lutea* to the ω-3 profile in the co-cultivated samples was visible owing to the detection of the characteristic DHA and SDA, absent in *N. oculata* (Ryckebosch et al. 2014), and to the increase, even if small, in EPA percentage. An estimation of fatty acid profile productivity in the neutral lipid fraction of samples was also calculated (data not shown). Results are consistent with those expressed as percentage of total fatty acids (Table 1). In both cases, it emerges that total ω-3 PUFAs are accumulated the most in *T. lutea* mono-cultures (38.46% of total fatty acids or 6.442 g/100g_{DW} algal biomass), while the lower content was observed for *N. oculata* (13.48% of total fatty acids or 2.225 g/100g_{DW} algal biomass). Interestingly, in co-cultures, characterized by a 97% of *N. oculata* of total cells (about 83% of total biomass), ω-3 content was improved, due to the even less presence of *T. lutea* cells in the biomass. In co-cultures total ω-3 PUFAs accounted for 17.1% of total fatty acids or 2.438

$g/100g_{DW}$ algal biomass, i.e. about 10% and 26% more than in mono-cultivated *N. oculata*, if considering results as total percentage or as yield, respectively.

4. Discussion

We studied the capability of *T. lutea* and *N. oculata* to grow in a co-cultivation batch system in saline medium. This strategy may aim to obtain distinctive compounds of each algae, like pigments (chlorophylls and carotenoids), as well as fatty acids (e.g. DHA and EPA), using a single process of cultivation, with the concomitant advantage to halve water and nutrient use. Typical goals of co-culture are, in fact, overyielding (higher productivity of the desired product(s) than mono-cultures), greater stability under perturbations, and/or more efficient use of inputs (e.g. nutrients or water). Under the experimental conditions used in this study, both microalgae grew better in mono-culture than in co-cultivation, as reported in some other studies on microalgae-microalgae co-cultivation systems (Tejido-Nuñez et al. 2020; Rashid et al. 2019) Recently, Tejido-Nuñez and collaborators (2020) reported that *Chlorella vulgaris* and *Tetradesmus obliquus*, when co-cultivated in sterile and non-sterile water both derived from an aquaponic system, grew less than in mono-cultures. In our research, although the initial dry biomass used to inoculate was the same for each species, the lower growth, observed in co-culture, might have been depended upon the inoculum ratio used for the two microalgae: at the beginning of the experiment the ratio between the two algae was about 1:8 (0.6×10^6 cells mL^{-1} of *T. lutea* and 5×10^6 cells mL^{-1} of *N. oculata*). Indeed, the initial cell density affects the growth and metabolism of microalgae, both in mono- and in co-cultures. As an example, Lu et al. (2012) reported different growth rates and lipid profile in mono-cultures of *C. sorokiniana* depending on inoculum size, from 10×10^4 to 1×10^7 cells mL^{-1}. Similarly, the co-cultivation of *Ettlia* sp. with *Chlorella* sp. starting from different proportions of both algae gave different results in terms of productivity and was related to even very different percentages of the inoculated algae in the cultures at the end of experiment (Rashid et al. 2019). Independent from final cell density, it is noteworthy that mono- and co-cultivated *N. oculata* entered the stationary phase from the 10^{th} day, sharing same kinetics. Differently, both mono- and co-cultivated *T. lutea* concluded the logarithmic phase on the 3^{rd} day, consistent with other studies in mono-cultivations, which reported the end of the exponential growth between the 3^{rd} and 6^{th} day (Garnier et al. 2014; Rasdi and Qin 2015; del Pilar Sánchez-Saavedra et al. 2016). In our experiment, while mono-cultivated *T. lutea* continued to grow slowly after the 3^{rd} day and reached the stationary phase around the end of the experiment, the number of co-cultivated *T. lutea* cells decreased, pointing to negative competition with *N. oculata*. As above mentioned,

growth of algae in co-cultivation is not obvious and the issue deserves dedicated studies to guarantee good biomass production. The limited growth of co-cultured *T. lutea* is consistent with decrease in size, alterations of thylakoids and the other cellular structures observed by TEM analyses. Moreover, especially for co-cultivated *T. lutea*, a stress condition was confirmed by the lower mobility observed under the light microscope. At the best of our knowledge, nowadays no literature data report alterations of size in *T. lutea* due to stresses, but analogous results are described in several other microalgae with flagella and without a robust cell wall (Goiris et al. 2015; Borowitzka 2018; Wang and Lan 2018). In this research, we propose that the presence in co-culture of abundant small *N. oculata* cells with a hard wall can have triggered reduction in cell size of the Haptophyta, as an effect linked to a sort of shear or hydrodinamic stress. In addition, already at early stages of co-cultivation *T. lutea* produced acidic eso-mucopolysaccharides, as shown by Alcian Blue staining and SEM analysis. Extrusion of such polysaccharidic compounds by microalgae often represents a defensive mechanism against stress conditions, also due to the presence of other microorganisms (Wotton 2004). Furthermore, the production of these defensive molecules by *T. lutea* may in part support the lower growth of *N. oculata* in co-cultures compared to mono-cultures. The extrusion activity of *T. lutea* was also observed in mono-cultivated cells, but only in advanced stages of cultivation (about after 18 days from the inoculation; not shown), when microalgae entered the stationary phase. An early and progressive decline of PSII maximum quantum yield was observed in co-cultivated cells, which showed F_V/F_M values below 0.6, lower than in the mono-cultured controls. The low F_V/F_M values is in line with the lower growth observed in co-culture and indicates a stress condition of the microorganisms; in fact, the analysis of the PSII maximum quantum yield by PAM fluorimetry allows an estimate of the photosynthetic efficiency and can be used as a parameter to evidence the physiological stress in microalgae (Cosgrove and Borowitzka 2010; Ramanna et al. 2014; Dao and Beardall 2016). In microalgae, F_V/F_M values higher than 0.6 indicate good conditions of growth and an efficient use of light for photosynthesis, a condition met in mono-cultures (White et al. 2013; Sirin and Sillanpää 2015; Bhola et al. 2016). Lower F_V/F_M values were generally reported under nutrient deficiency or very dense cultures or light-stressed cultures (Beardall et al. 2001 a, b; Baldisserotto et al. 2014; Benvenuti et al. 2015). In our experiment conducted under non-photo-inhibiting light and leading to not very dense cultures, the lower F_V/F_M values in co-cultivation could not depend on these two latter factors. While a nutrient deficiency could have occurred, this cause of stress seems not supported by the photosynthetic pigment content. In particular, up to 10 days of cultivation, the strong accumulation of chlorophylls/cell, hosted in more appressed thylakoids,

did not justify a nutrient limitation, especially nitrogen (da Silva Ferreira and Sant'Anna 2017). Conversely, the accumulation of chlorophylls could be an attempt to compensate for the decreased photosynthetic efficiency of PSII. The reason why the co-cultivation of *N. oculata* and *T. lutea* decreased F_V/F_M in both algae is still unknown, but strongly suggests that the co-cultivation is a source of stress for both.

On the other hand, the accumulation of pigments can have relevant impact on the biotechnological exploitation of the co-cultivation itself. Not only carotenoids, but also chlorophylls have a wide market: carotenoids are mainly used due to their antioxidant properties (García et al. 2017; Mourelle et al. 2017; Sayo et al. 2013), while chlorophylls are employed as food colorant, as cosmetic ingredient e.g. in toothpaste or in deodorant, and also for human health for their anticancer and antioxidant activities (Timberlake and Henry 1986; Abad 1994; da Silva Ferreira and Sant'Anna 2017; Vesenick et al. 2012). At the end of cultivation, the lipid accumulation inside cells was the higher, as highlighted by morphological observations. Total lipids (24, 31 and 21% of algal DW, respectively for monocultures of *N. oculata* and *T. lutea*, and for the co-cultures) did not differ significantly between mono- and co-cultivated algae ($p > 0.2$; one-way ANOVA). The results for mono-cultures were substantially in line with those available in the literature for the same algae (Su et al. 2011; Gao et al. 2020). Interestingly, the lower, even if not significant, value obtained for the co-cultures reflected the different proportion of algae in the whole population, where *N. oculata* was dominant over *T. lutea*. The obvious influence of different proportion of algae in the co-cultures on lipid content was already observed also in other microalgae-microalgae co-cultivation experiments, e.g. *Ettlia* with *Chlorella* (Rashid et al. 2019). From the analysis of neutral lipids, glycolipids and phospholipids, neutral lipids were higher in samples of the co-culture and of the mono-cultivated *N. oculata* (67% and 69% of total lipids, respectively). For *N. oculata* cells, our results are in contrast to those by Ryckebosch et al. (2014), who reported that standard cultures of the alga contained about 40% of neutral lipids. Hovewer, our data are in agreement with other papers using the alga under stress conditions (Obeid et al. 2018). In our experiments the stress conditions could be the age of culture in mono-cultivation and both the age of the culture and other stresses, like hydrodynamic stress or interaction with mucopolysaccharides released by *T. lutea*. Differently, in mono-cultivated *T. lutea,* the neutral lipids accounted for about 55% of total lipids, quite similar to that found by Ryckebosch et al. (2014) for the same alga (about 60%).

In co-culture, *N. oculata* cells were dominant and *T. lutea* represented only the 3% of the total cells (about 17% of total biomass) at the end of experiment. In fact, the fatty acid profile of co-

cultivated cells was similar to that of mono-cultivated *N. oculata*. In accordance, Rashid et al. (2019) described an analogous effect on fatty acids profile during their research on co-cultivated microalgae *Ettlia* and *Chlorella,* both under standard autotrophic condition and under mixotrophy. Despite the low number of *T. lutea* cells, in co-culture ω-3 DHA and SDA were detectable; probably, the larger cell size of *T. lutea* compared to *N. oculata* influenced this result. The obtainment of a mixture of ω-3 fatty acids combining EPA as the main one (1.74 $g/100g_{DW}$), plus SDA and DHA, even if as minor components (0.223 and 0.139 $g/100g_{DW}$, respectively), represents a promising starting point to produce a "green" alternative to fish oil for food/feed. Currently, fish oil is one of the main sources of long-chain ω-3 fatty acids for human nutritional supplement use and for animal feed (Misund et al. 2017; Chua et al. 2020; Matsui et al. 2020). However, the increasing demand for this material raises issues related to sustainability; in fact, fish oil is a limited resource derived from wild fish (Shepherd and Bachis 2014). Currently, the mixture of ω-3 PUFAs obtained from our co-cultivated *N. oculata* and *T. lutea* opens a novel understanding on the co-cultivation of two microalgae phylogenetically very distant, thus with a great diversity in their morpho-physiology, also in terms of molecules they produce. Furthermore, the two microalgae share marine media for their cultivation, making it possible to employ seawater, instead of freshwater, for the cultivation. This, combined with the halving of water consumption, makes more sustainable the whole process. The knowledge acquired in this work can drive future research, for example by modulating environmental parameters (e.g. light quality, temperature) that can help emphasize biomass and lipid production in a new kind of co-cultivation.

fThe aim of the present work was to test the feasibility to co-cultivate *N. oculata* and *T. lutea*, two marine microalgae that, due to their phylogenetic position, produce different and complementary molecules, with the added advantage of a higher environmental sustainability linked to a less consumption of freshwater. The method has still some limitations, but it is noteworthy that the algal biomass from co-cultivation was enriched both in natural pigments and in a promising blend of ω-3 PUFAs, the latter being exploitable as a plant alternative to fish oil. The opportunity to set up a single cultivation, instead of two, can imply a reduction of production costs in terms of culturing facilities, energy and nutrients consumption, and water demand. Through the improvement of some cultivation parameters, the co-cultivation of *N. oculata* and *T. lutea* could become a promising method to produce valuable natural fatty acids and pigments in a single cultivation process, potentially using seawater.

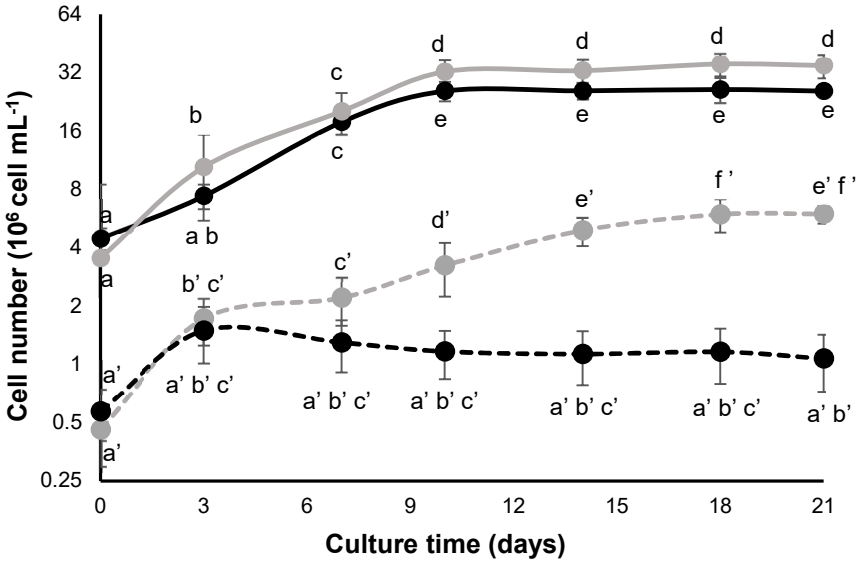

Figure 1 Growth kinetics of *N. oculata* (solid lines**)** and *T. lutea* (dashed lines) in co-culture (black) and mono-culture (grey). Data are plotted on a logarithmic scale. Values are means ± SD. Different letters indicate statistically significant differences ($p < 0.05$, two-way ANOVA)

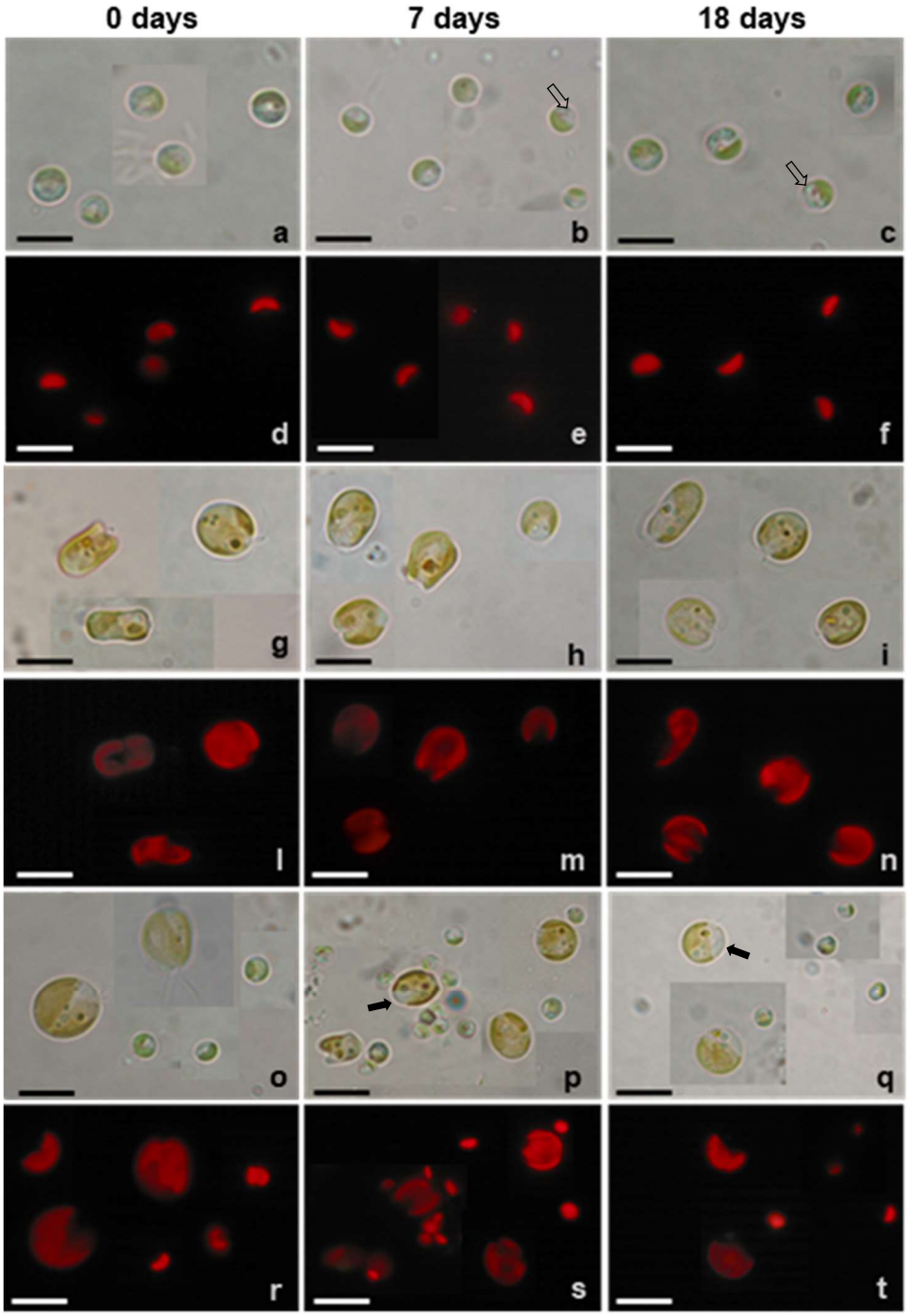

Figure 2 Light and epifluorescence microscope observations of mono- and co-cultivated cells of *N. oculata* and *T. lutea* at different stage of cultivation. *N. oculata* (a-f); *T. lutea* (g-n); co-cultivated cells (o-t). Most figures consist of a collage of photos exemplifying the observations made. Empty arrows indicate translucent globules; filled arrows indicate vacuoles. Scale bars = 6µm

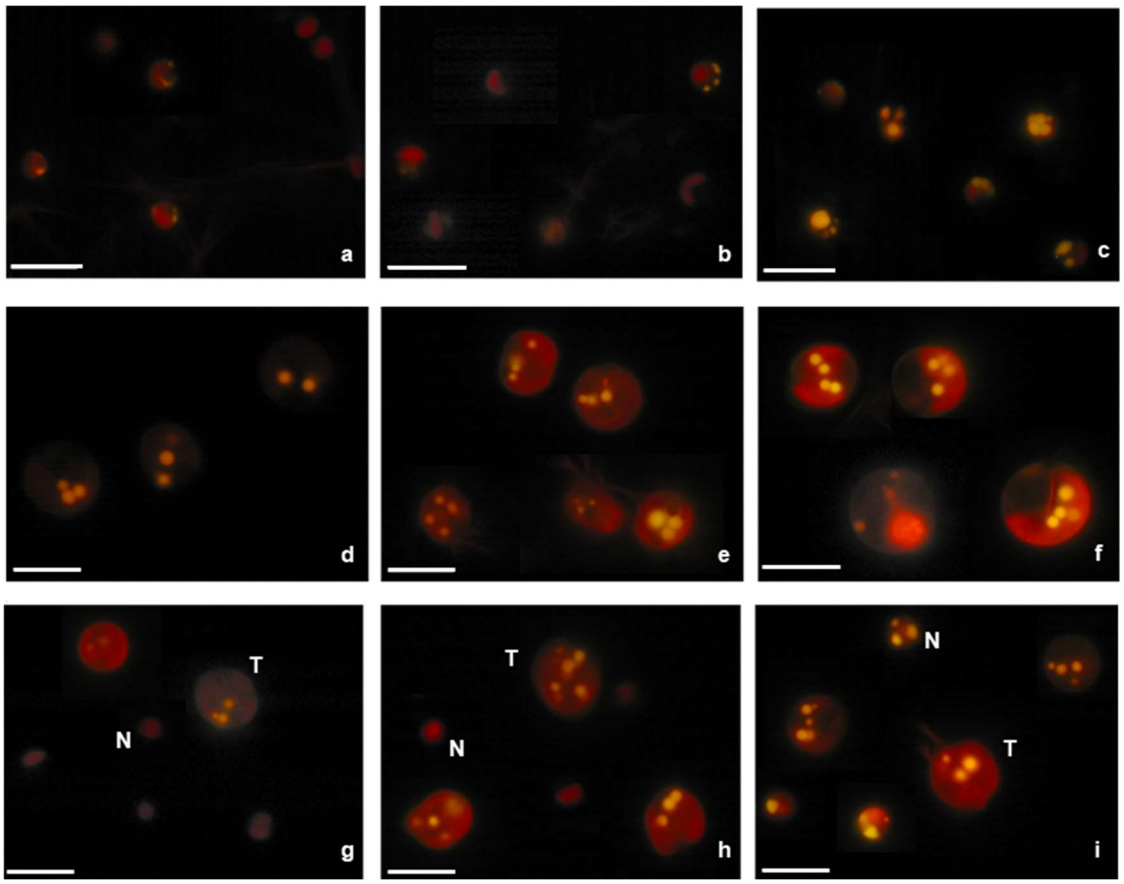

Figure 3 Epifluorescence photomicrographs of Nile Red stained cells of mono-cultivated and co-cultivated *N. oculata* and *T. lutea* at different stage of cultivation: 7 (a *N. oculata*; d *T. lutea*; g co-cultivated cells), 14 (b *N. oculata*; e *T. lutea*; h co-cultivated cells) and 21 days (c *N. oculata*; f *T. lutea*; i co-cultivated cells) day. T *T. lutea* cells, N *N. oculata* cells. In co-cultivated *N. oculata* cells the reaction is negative in the early stages of experimentation (g, h). Scale bars = 6 µm

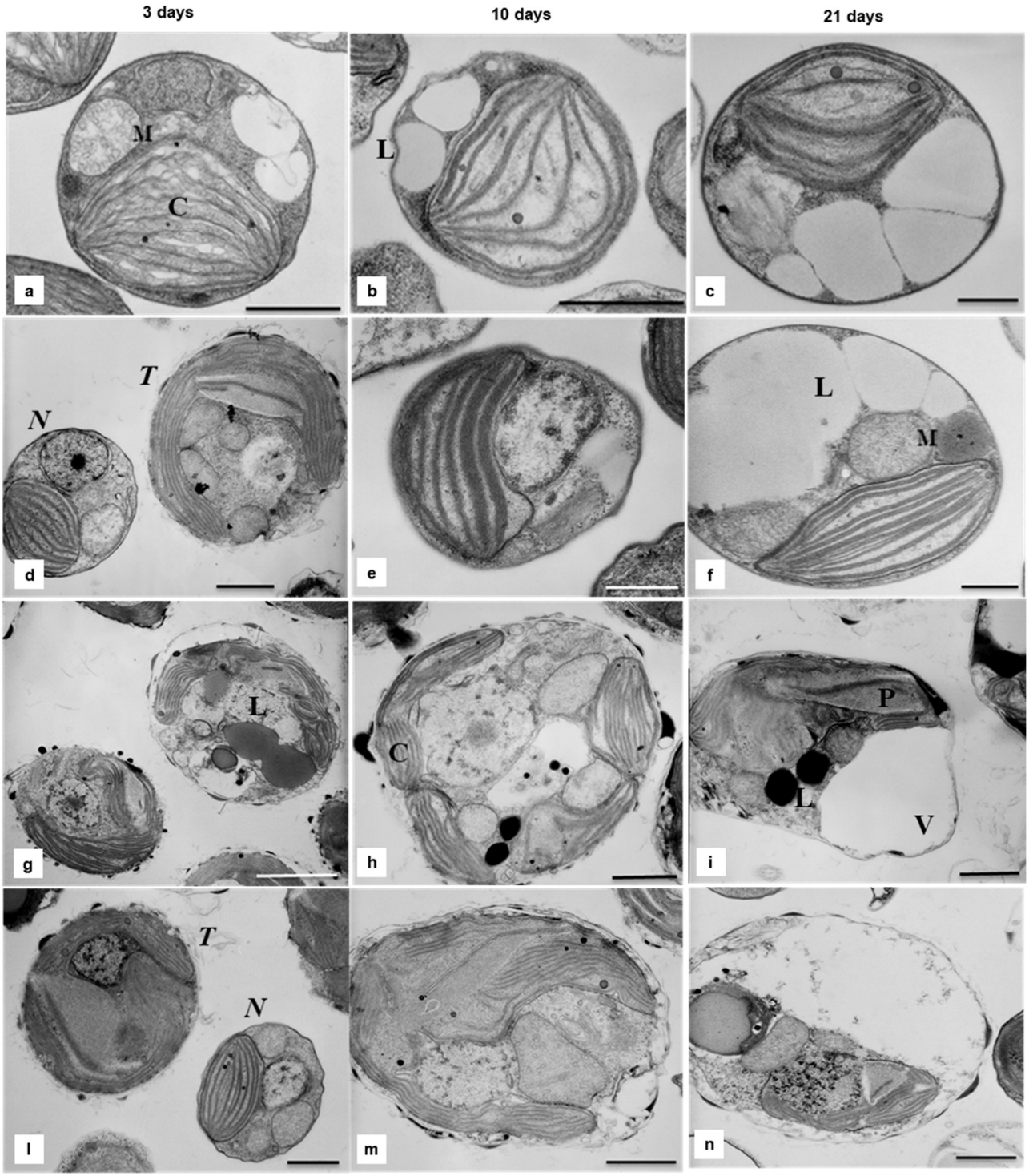

Figure 4 Transmission electron micrographs of mono-cultivated and co-cultivated cells of *N. oculata* and *T. lutea* at different stage of cultivation. Mono-cultivated (a-c) and co-cultivated (d-f) *N. oculata* cells; mono-cultivated (g-i) and co-cultivated (l-n) *T. lutea* cells. N *N. oculata* cells; T *T. lutea* cells; C chloroplast; L lipid globules; M mitochondrion; P pyrenoid; V vacuole. Scale bars: a, b, d, l, h, i, m and n = 1 µm; c, e and f = 0.5 µm; g = 2 µm

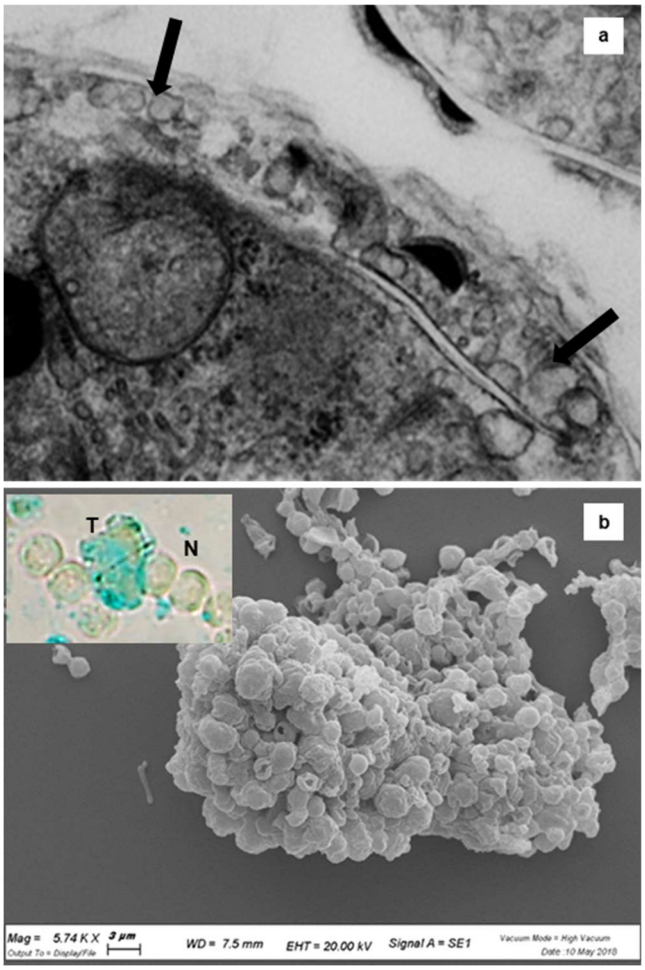

Figure 5 Production and extrusion of acidic mucopolysaccharides in *T. lutea* cells. *T. lutea* cell secretory vesicles (arrows) at 10 days of cultivation (a). Scanning electron micrographs of *N. oculata* and *T. lutea* cells at the 21st day of co-cultivation (b); insert shows light microscopy observation of co-cultivated cells at the 21st day after Alcian Blue staining: N *N. oculata* T *T. lutea*

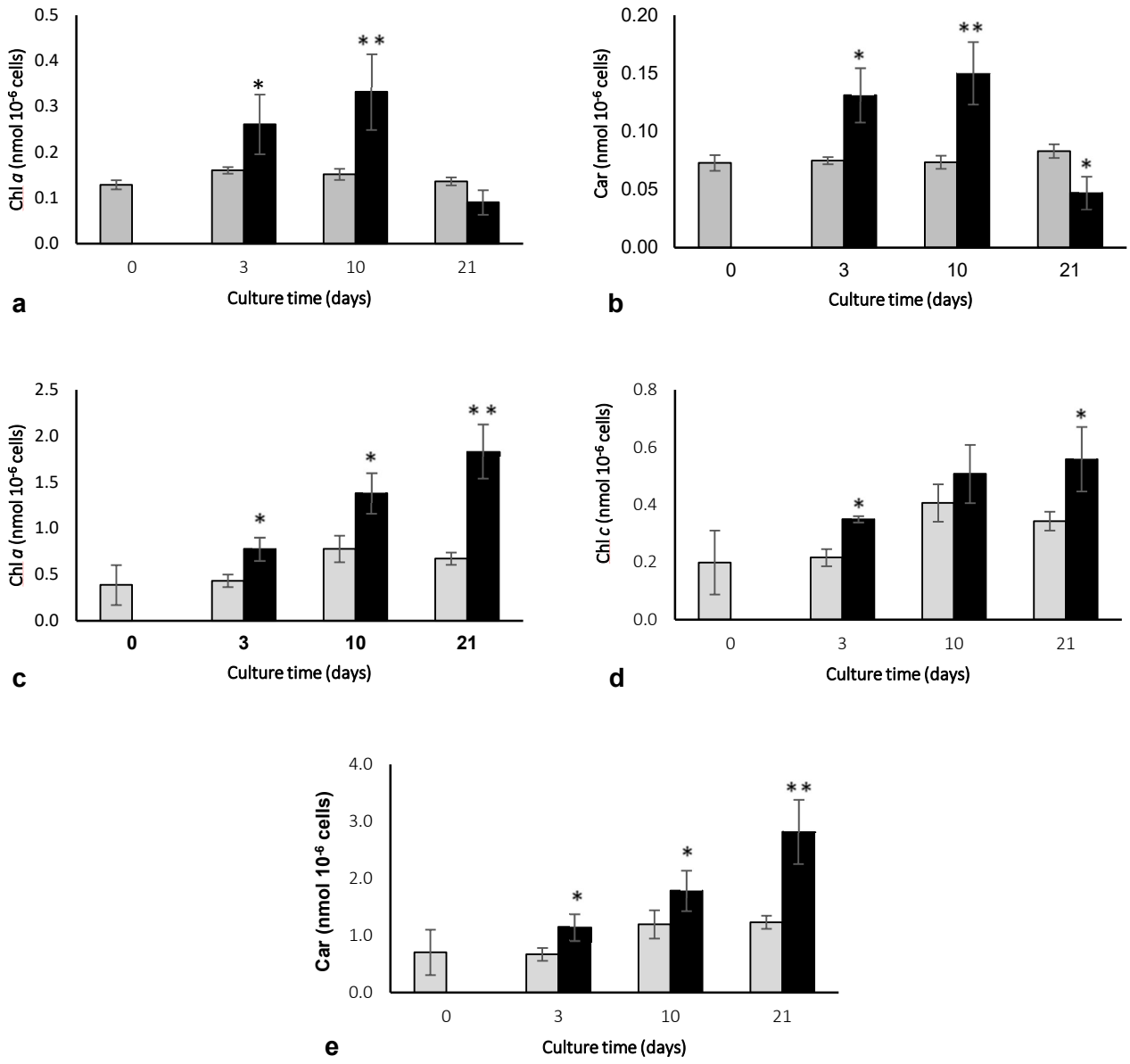

Figure 6 Time-course variations of pigment content (nmol 10^{-6} cells) in *N. oculata* and *T. lutea* cells in mono-culture (grey) and co-culture (black). *N. oculata*: Chl *a* (a) and total carotenoids (b) content; *T. lutea*: Chl *a* (c), Chl *c* (d) and total carotenoids (e) content. Values are means ± SD. Asterisks identify significant differences between samples: * $p < 0.05$; ** $p < 0.01$ (Student t-test)

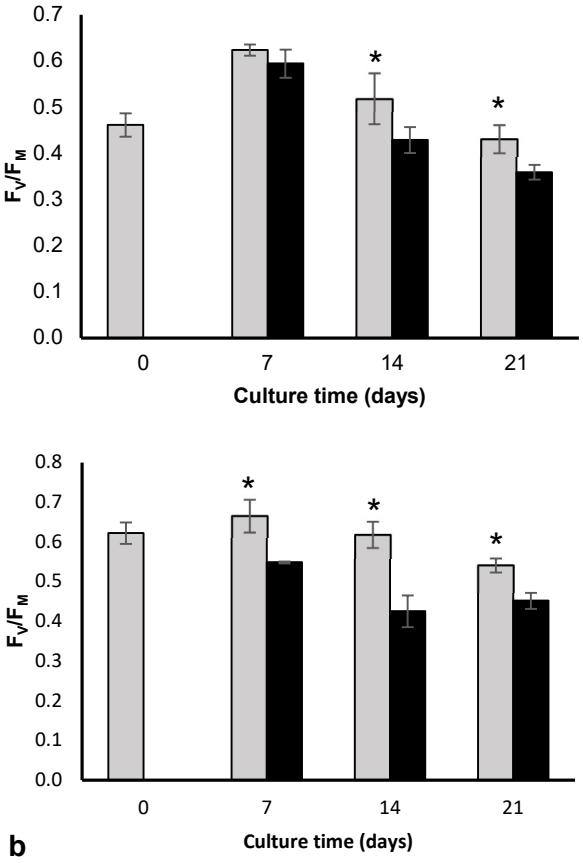

Figure 7 Time-course variations of F_V/F_M ratio in *N. oculata* (a) and *T. lutea* (b) cells in mono-culture (grey) and co-culture (black). Values are means ± SD. Asterisks identify significant differences between samples: * $p < 0.05$ (Student t-test)

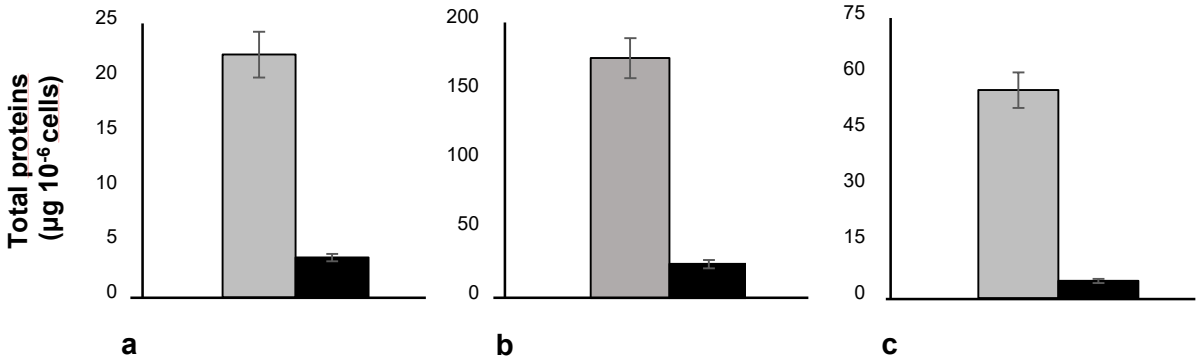

Figure 8 Concentration of total proteins (µg 10^{-6} cells) at day 0 (grey) and after 21 days (black) of cultivation in mono-cultivated *N. oculata* (a) and *T. lutea* (b) cells, and in co-cultivated samples (c). Values are means ± SD

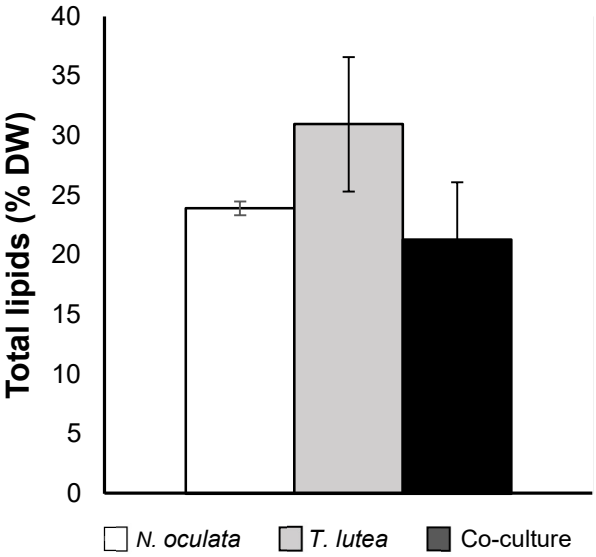

Figure 9 Total lipid content (% DW) in mono-cultivated *N. oculata* and *T. lutea*, and in co-cultures at the 21st day of cultivation. Values are means ± SD

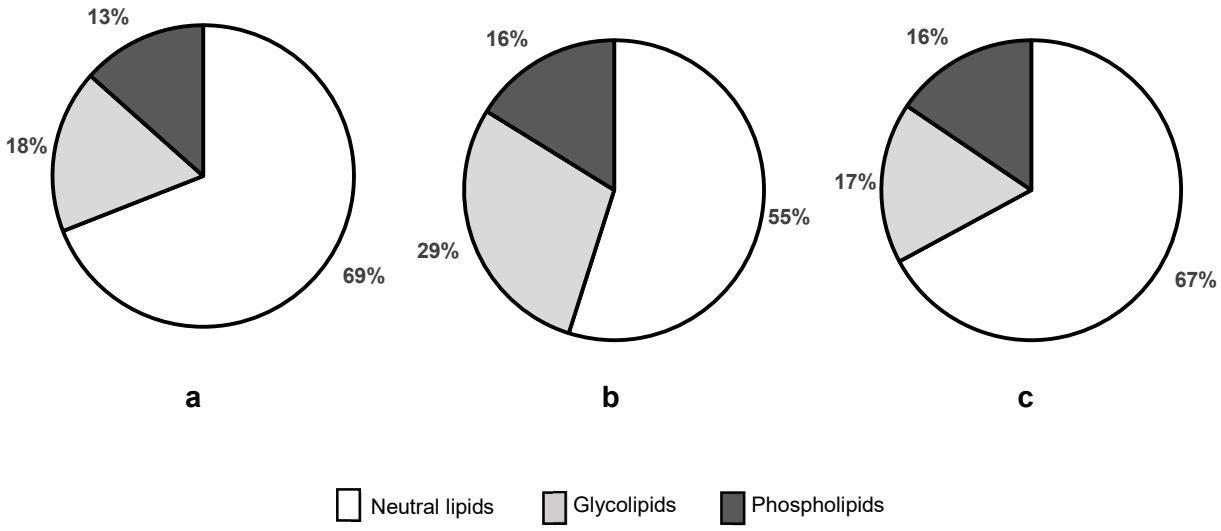

Figure 10 Relative proportions of lipid fractions (percentage of total lipids, %) in mono-cultivated *N. oculata* (a) and *T. lutea* (b), and in co-cultivated cells (c)

Table 1 Fatty acid profile (percentage of total fatty acids) in the neutral lipid fraction of *T. lutea* and *N. oculata* mono-cultures and in co-cultures. Values are means ± SD.

Fatty acids	*N. oculata*		*T. lutea*		Co-culture	
	mean	**SD**	**Mean**	**SD**	**Mean**	**SD**
C12:0	0.22	0.01	0.12	0.03	0.26	0.02
C14:0	5.31	0.52	10.46	1.5	5.07	0.86
C15:0	0.79	0.09	0.93	0.11	0.72	0.07
C16:2	0.29	0.05	0.13	0.01	0.34	0.11
C16:1	31.41	1.72	4.13	0.28	27.26	0.95
C16:1 t	0.56	0.01	–	–	0.43	0.06
C16:0	24.32	0.63	10.71	1.63	19.97	2.32
C17:2	–	–	–	–	0.2	0.01
C17:1	–	–	0.58	0.32	0.23	0.18
C17:0	–	–	0.6	0.3	0.92	0.35
C18:4n3	–	–	20.23	0.53	1.57	0.54
C18:2n6c	5.55	0.11	4.61	0.05	6.35	0.95
C18:1n9c	13.68	0.44	25.46	0.73	14.99	0.27
C18:1n9t	1.36	0.03	2.14	1.94	1.71	0.62
C18:0	1.7	0.09	0.5	0.21	2.05	0.62
C20:4n6	1.37	0.21	–	–	2.25	1.06
C20:5n3	11.1	2.3	0.43	0.24	12.19	0.22
C20:3n6	2.38	0.25	0.21	0.06	2.36	0.12
C20:0	–	–	0.35	0.16	0.23	0.13
C22:6n3	–	–	17.59	4.26	0.98	0.56

References

Adarme-Vega TC, Lim DKY, Timmins M, Vernen F, Li Y, Schenk PM (2012) Microalgal biofactories: a promising approach towards sustainable omega-3 fatty acid production. Microb Cell Fact 11, 96. https://doi.org/10.1186/1475-2859-11-96

Abad R (1994) Therapeutic and cosmetic composition for treatment of skin. Patent US005538740A.

Alam MdA, Xu J-L, Wang Z (2020) Microalgae biotechnology for food, health and high value products Springer Nature, Singapore. https://doi.org/10.1007/978-981-15-0169-2

Baldisserotto C, Ferroni L, Giovanardi M, Boccaletti L, Pantaleoni L, Pancaldi S (2012) Salinity promotes growth of freshwater *Neochloris oleoabundans* UTEX 1185 (Sphaeropleales, Chlorophyta): morphophysiological aspects. Phycologia 51:700–710. https://doi.org/10.2216/11-099.1

Baldisserotto C, Giovanardi M, Ferroni L, Pancaldi S (2014) Growth, morphology and photosynthetic responses of *Neochloris oleoabundans* during cultivation in a mixotrophic brackish medium and subsequent starvation. Acta Physiol Plant 36:461–472. https://doi.org/10.1007/s11738-013-1426-3

Baldisserotto C, Popovich C, Giovanardi M, Sabia A, Ferroni L, Constenla D, Leonardi P, Pancaldi S (2016) Photosynthetic aspects and lipid profiles in the mixotrophic alga *Neochloris oleoabundans* as useful parameters for biodiesel production. Algal Res 16:255-265. https://doi.org/10.1016/j.algal.2016.03.022

Barsanti L, Gualtieri P (2014) Algae: anatomy, biochemestry and biotechnology 2nd edn. CRC Press

Beardall J, Berman T, Heraud P, Kadiri MO, Light BR, Patterson G, Roberts S, Sulzberger B, Sahan E, Uehlinger U, Wood B (2001 a) A comparison of methods for detection of phosphate limitation in microalgae. Aquat Sci 63(1):107-121. https://doi.org/10.1007/Pl00001342

Beardall J, Young E, Roberts S (2001 b) Approaches for determining phytoplankton nutrient limitation. Aquat Sci 63:44–69. https://doi.org/10.1007/PL00001344

Becker W (2004) Microalgae in human and animal nutrition. In: Handbook of microalgal culture: biotechnology and applied phycology. Richmond A (ed) Blackwell Science Ltd, Oxford, pp 312–351

Begum H, Yusoff HM, Banerjee S, Khatoon H, Shariff M (2016) Availability and utilization of pigments from microalgae. Crit Rev Food Sci Nutrit 56:2209-2222. https://doi.org/10.1080/10408398.2013.764841

Bendif EM, Probert I, Schroeder DC, de Vargas C (2013) On the description of *Tisochrysis lutea* gen. nov. sp. nov. and *Isochrysis nuda* sp. nov. in the Isochrysidales, and the transfer of *Dicrateria* to the Prymnesiales (Haptophyta). J Appl Phycol, 25:1763-1776. https://doi.org/10.1007/s10811-013-0037-0

Benvenuti G, Bosma R, Cuaresma M, Janssen M, Barbosa MJ, Wijffels RH (2015) Selecting microalgae with high lipid productivity and photosynthetic activity under nitrogen starvation. J Appl Phycol, 27:1425–1431. https://doi.org/10.1007/s10811-014-0470-8

Berges, JA, Franklin DJ, Harrison PJ (2001) Evolution of an artificial seawater medium: improvements in enriched seawater, artificial water over the last two decades. J Phycol 37:1138-1145. https://doi.org/10.1046/j.1529-8817.2001.01052.x

Bhola VK, Swalaha FM, Nasr M, Kumari S, Bux F (2016) Physiological responses of carbon-sequestering microalgae to elevated carbon regimes. Eur J Phycol 51:401–412.

Borowitzka MA (2013) High-value products from microalgae - their development and commercialisation. J Appl Phycol 25:743–756

Borowitzka MA (2018) The 'stress' concept in microalgal biology—homeostasis, acclimation and adaptation. J APPL Phycol 30:2815–2825. https://doi.org/10.1007/s10811-018-1399-0

Cavalier-Smith T, Chao EE, Lewis R (2018) Multigene phylogeny and cell evolution of chromist infrakingdom Rhizaria: contrasting cell organisation of sister phyla Cercozoa and Retaria. Protoplasma 255:1517–1574. https://doi.org/10.1007/s00709-018-1241-1

Chauton M S, Reitan KI, Norsker NH, Tveterås R, Kleivdal HTA (2015) A techno-economic analysis of industrial production of marine microalgae as a source of EPA and DHA-rich raw material for aquafeed: Research challenges and possibilities. Aquaculture 436:95-103. https://doi.org/10.1016/j.aquaculture.2014.10.038

Chazalon F, Rabouille S, Hartmann P, Sciandra A, Bernard O (2014) A Dynamical Model to study the Response of Microalgae to Pulse Amplitude Modulated Fluorometry. IFAC Proceedings Volumes 47:7152-7157. https://doi.org/10.3182/20140824-6-ZA-1003.02162

Chua ET, Dal'Molin C, Thomas-Hall S, Netzel ME, Netzel G, Schenk PM (2020) Cold and dark treatments induce omega-3 fatty acid and carotenoid production in *Nannochloropsis oceanica*. Algal Res 51: 102059. https://doi.org/10.1016/j.algal.2020.102059

Cosgrove J, Borowitzka MA (2010) Chlorophyll fluorescence terminology: an introduction. In: Chlorophyll a fluorescence in aquatic sciences: methods and applications. Suggett DJ, Prášil O, Borowitzka MA (eds). Springer, pp 1–17

Da Costa F, Le Grand F, Quéré C, Bougaran G, Cadoret JP, Robert R, Soudant P (2017) Effects of growth phase and nitrogen limitation on biochemical composition of two strains of *Tisochrysis lutea.* Algal Res 27:177–189. https://doi.org/10.1016/j.algal.2017.09.003

da Silva Ferreira V, Sant'Anna C (2017) Impact of culture conditions on the chlorophyll content of microalgae for biotechnological applications. World J Microbiol Biotechnol. 33(1):20. https://doi.org/10.1007/s11274-016-2181-6

da Silva Vaz B, Botelho Moreira J, de Morais MG, Vieira Costa JA (2016) Microalgae as a new source of bioactive compounds in food supplements. Curr Opin Food Sci 7:73-77. https://doi.org/10.1016/j.cofs.2015.12.006

D'Amato D, Droste N, Allen B, Kettunen M, Lähtinen K, Korhonen J, Leskinen P, Matthies BD, Toppinen A (2017) Green, circular, bio economy: A comparative analysis of sustainability avenues. J Clean Prod 168:716-734. https://doi.org/10.1016/j.jclepro.2017.09.053

Dao LH, Beardall J (2016) Effects of lead on growth, photosynthetic characteristics and production of reactive oxygen species of two freshwater green algae. Chemosphere 147:420–429. https://doi.org/10.1016/j.chemosphere.2015.12.117

Das PK, Rani J, Rawat S, Kumar S (2021) Microalgal Co-cultivation for Biofuel Production and Bioremediation: Current Status and Benefits. Bioenerg. Res. https://doi.org/10.1007/s12155-021-10254-8

del Pilar Sánchez-Saavedra M, Maeda-Martínez AN, Acosta-Galindo S (2016) Effect of different light spectra on the growth and biochemical composition of *Tisochrysis lutea.* J Appl Phycol 28:839–847. https://doi.org/10.1007/s10811-015-0656-8

Discart V, Bilad MR, Vankelecom IF, (2015) Critical evaluation of the determination methods for transparent exopolymer particles, agents of membrane fouling. Critical Reviews in Environmental Science and Technology 45(2): 167-192.

Ferroni L, Baldisserotto C, Giovanardi M, Pantaleoni L, Morosinotto T, Pancaldi S (2011) Revised assignment of room-temperature chlorophyll fluorescence emission bands in single living cells of *Chlamydomonas reinhardtii.* J Bioenerg Biomembr 43:163–173. https://doi.org/10.1007/s10863-011-9343-x

Gao F, Teles I (Cabanelas, ITD), Ferrer-Ledo N, Wijffels RH, Barbosa MJ (2020) Production and high throughput quantification of fucoxanthin and lipids in *Tisochrysis lutea* using single-cell fluorescence. Bioresour Technoly 318: 124104. https://doi.org/10.1016/j.biortech.2020.124104

García JL., de Vicente M, Galán B (2017) Microalgae, old sustainable food and fashion nutraceuticals. Microb Biotechnol 10 (5): 1017–1024

Garnier M, Carrier G, Rogniaux H, Nicolau E, Bougaran G, Saint-Jean B, Cadoret JP (2014) Comparative proteomics reveals proteins impacted by nitrogen deprivation in wild-type and high lipid-accumulating mutant strains of *Tisochrysis lutea.* Journal of Proteomics 105:107–120. https://doi.org/10.1016/j.jprot.2014.02.022

George B, Pancha I, Desai C, Chokshi K, Paliwal C, Ghosh T, Mishra S (2014) Effects of different media composition, light intensity and photoperiod on morphology and physiology of freshwater microalgae Ankistrodesmus falcatus - a potential strain for bio-fuel production. Bioresour Technol 171:367–374. https://doi.org/10.1016/j.biortech.2014.08.086

Giovanardi M, Ferroni L, Baldisserotto C, Tedeschi P, Maietti A, Pantaleoni L, Pancaldi S (2013) Morphophysiological analyses of *Neochloris oleoabundans* (Chlorophyta) grown mixotrophically in a carbon-rich waste product. Protoplasma 250:161–174

Goiris K, Van Colen W, Wilches I, León-Tamariz F, De Cooman L, Muylaert K (2015) Impact of nutrient stress on antioxidant production in three species of microalgae. Algal Res 7:51-57

Gonçalves AL, Pires JCM, Simões M (2016) Biotechnological potential of *Synechocystis salina* co-cultures with selected microalgae and cyanobacteria: Nutrients removal, biomass and lipid production. Bioresour Technol 200:279–286. https://doi.org/10.1016/j.biortech.2015.10.023

Guillard RRL (1975) Culture of Phytoplankton for Feeding Marine Invertebrates. In: Smith WL, Chanley MH (eds) Culture of Marine Invertebrate Animals. Springer, Boston, MA. https://doi.org/10.1007/978-1-4615-8714-9_3

Guillard RRL, Ryther JH (1962) Studies of marine planktonic diatoms. I. *Cyclotella nana* Hustedt and *Detonula confervacea* (Cleve). Can J Microbiol 8:229-239. https://doi.org/10.1139/m62-029

Guiry, MD, Guiry, GM (2021) AlgaeBase. World-wide electronic publication, National University of Ireland, Galway. https://www.algaebase.org; searched on 30 April 2021

He Q, Yang H, Wua L, Hua C (2015) Effect of light intensity on physiological changes, carbon allocation and neutral lipid accumulation in oleaginous microalgae. Bioresour Technol 191:219–228

Hibberd DJ (1981) Notes on the taxonomy and nomenclature of the algal classes Eustigmatophyceae and Tribophyceae (synonym Xanthophyceae). Botanical Journal of the Linnean Society 82:93–119. https://doi.org/10.1111/j.1095-8339.1981.tb00954.x

Hillebrand H, Dürselen C-D, Kirschtel D, Pollingher U, Zohary T (1999) Biovolume calculation for pelagic and benthic microalgae. J. Phycol. 35: 403–424

Ishika T, Bahri PA, Laird DW, Moheimani NR (2018) The effect of gradual increase in salinity on the biomass productivity and biochemical composition of several marine, halotolerant, and halophilic microalgae. J Appl Phycol 30:1453–1464. https://doi.org/10.1007/s10811-017-1377-y

Ishika T, Moheimania NR, Bahri PA (2017) Sustainable saline microalgae co-cultivation for biofuel production: A critical review. Renewable and Sustainable Energy Reviews 78:356–368. https://doi.org/10.1016/j.rser.2017.04.110

Ivleva NB, Golden SS (2007) Protein extraction, fractionation, and purification from Cyanobacteria. In: Circadian Rhythms. Rosato E (ed) Methods in Molecular Biology™, vol 362. Humana Press

Krul ES, Lemke SL, Mukherjea R, Taylor ML, Goldstein DA, Sub H, et al. (2012) Effects of duration of treatment and dosage of eicosapentaenoic acid and stearidonic acid on red blood cell eicosapentaenoic acid content. Prostaglandins, Leukotrienes and Essential Fatty Acids 86:51–59. https://doi.org/10.1016/j.plefa.2011.10.005

Lowry OH, Rosebrough NJ, Faee AL, Randall RJ (1951) Protein measurement with the Folin phenol reagent. J Biol Chem 193:265-275

Lu S, Wang J, Niu Y, Yang J, Zhou J, et al. (2012) Metabolic profiling reveals growth related FAME productivity and quality of *Chlorella sorokiniana* with different inoculum sizes. Biotechnol Bioeng 109: 1651–1662.

Mata TM, Martins AA, Caetano NS (2010) Microalgae for biodiesel production and other applications: A review. Renewable and Sustainable Energy Reviews 14:217-232. https://doi.org/10.1016/j.rser.2009.07.020

Matos AP (2017) The Impact of Microalgae in Food Science and Technology. Journal of the American Oil Chemists' Society 94:1333–1350. https://doi.org/10.1007/s11746-017-3050-7

Matsui H, Intoy MMB, Waqalevu V, Ishikawa M, Kotani T (2020). Suitability of *Tisochrysis lutea* at different growth phases as an enrichment diet for *Brachionus plicatilis* sp. complex rotifers. J Appl Phycol 32:3933–3947. https://doi.org/10.1007/s10811-020-02216-y

Mayers JJ, Ekman Nilsson A, Svensson E, Albers E (2016) Integrating microalgal production with industrial outputs - reducing process inputs and quantifying the benefits. Industrial Biotechnology 12:219-234. https://doi.org/10.1089/ind.2016.0006

Minhas AK, Hodgson P, Barrow CJ, Adholeya A (2016) A Review on the Assessment of Stress Conditions for Simultaneous Production of Microalgal Lipids and Carotenoids. Front Microbiol https://doi.org/10.3389/fmicb.2016.00546

Misund B, Oglend A, Mezzalira Pincinato RB (2017) The rise of fish oil: From feed to human nutritional supplement. Aquaculture Economics & Management. http://dx.doi.org/10.1080/13657305.2017.1284942

Mourelle ML, Gómez CP, Legido JL (2017) The Potential Use of Marine Microalgae and Cyanobacteria in Cosmetics and Thalassotherapy. Cosmetics. https://doi.org/10.3390/cosmetics4040046

Mowry RW, Scott JE (1967) Observations on the basophilia of amyloids. Histochemie, 10(1): 8-32.

Mujtaba G, Rizwan M, Lee K (2017) Removal of nutrients and COD from wastewater using symbiotic co-culture of bacterium *Pseudomonas putida* and immobilized microalga *Chlorella vulgaris*. Journal of Industrial and Engineering Chemistry 49:145–151. https://doi.org/10.1016/j.jiec.2017.01.021

Novoveská L, Franks DT, Wulfers TA, Henley WJ (2016) Stabilizing continuous mixed cultures of microalgae. Algal Res 13:126–133. https://doi.org/10.1016/j.algal.2015.11.021

Obeid S, Beaufils N, Camyd S, Takache H, Ismail A, Pontaliera P-Y (2018) Supercritical carbon dioxide extraction and fractionation of lipids from freeze-dried microalgae *Nannochloropsis oculata* and *Chlorella vulgaris*. Algal Res 34:49-56. https://doi.org/10.1016/j.algal.2018.07.003

Ördög V, Stirk WA, Bálint P, van Staden J, Lovász C (2012) Changes in lipid, protein and pigment concentrations in nitrogen-stressed *Chlorella minutissima* cultures. J App Phycol 24:907-914. https://doi.org/10.1007/s10811-011-9711-2

Popovich CA (a), Damiani C, Constenla D, Leonardi PI (2012) Lipid quality of the diatoms *Skeletonema costatum* and *Navicula gregaria* from the South Atlantic Coast (Argentina): evaluation of its suitability as biodiesel feedstock. J Appl Phycol 24:1–10. https://doi.org/10.1007/s10811-010-9639-y

Popovich CA (b), Damiani C, Constenla D, Martínez AM, Freije H, Giovanardi M, Pancaldi S, Leonardi PI (2012) Neochloris oleoabundans grown in enriched natural seawater for biodiesel feedstock: evaluation of its growth and biochemical composition. Bioresour Technol 114:287-293. https://doi.org/10.1016/j.biortech.2012.02.121

Pulz O, Gross W (2004) Valuable products from biotechnology of microalgae. Appl Microbiol Biotechnol 65:635–48

Qi W, Mei S, Yuan Y, Li X, Tang T, Zhao Q, Wu M, Wei W, Sun Y (2018) Enhancing fermentation wastewater treatment by co-culture of microalgae with volatile fatty acid- and alcohol-degrading bacteria. Algal Res 31:31-39. https://doi.org/10.1016/j.algal.2018.01.012

Ramanna L, Guldhe A, Rawat I, Bux F (2014) The optimization of biomass and lipid yields of *Chlorella sorokiniana* when using wastewater supplemented with different nitrogen sources. Bioresour Technol 168:127–135. https://doi.org/10.1016/j.biortech.2014.03.064

Ramesh Kumar B, Deviram G, Mathimani T, Duc PA, Pugazhendhi A (2019) Microalgae as rich source of polyunsaturated fatty acids. Biocatalysis and Agricultural Biotechnology 17:583–588584. https://doi.org/10.1016/j.bcab.2019.01.017

Rasdi NW, Qin JG (2015) Effect of N:P ratio on growth and chemical composition of *Nannochloropsis oculata* and *Tisochrysis lutea.* J Appl Phycol 27:2221–2230 https://doi.org/10.1007/s10811-014-0495-z

Rashid N, Ryu AJ, Jeong KJ, Lee B, Chang Y-K (2019) Co-cultivation of two freshwater microalgae species to improve biomass productivity and biodiesel production. Energy Convers Manag 196: 640–648. https://doi.org/10.1016/j.enconman.2019.05.106

Richmond A (2004) Handbook of microalgal culture: biotechnology and applied phycology. Blackwell Publishing Ltd, Oxford

Ritchie RJ (2006) Consistent sets of spectrophotometric chlorophyll equations for acetone, methanol and ethanol solvents. Photosynth Res 89:27–41. https://doi.org/10.1007/s11120-006-9065-9

Rizwan M, Mujtabab G, Memonc S, Leed K, Rashid N (2018) Exploring the potential of microalgae for new biotechnology applications and beyond: A review. Renewable and Sustainable Energy Reviews 92:394-404. https://doi.org/10.1016/j.rser.2018.04.034

Rodolfi L, Zittelli C, Bassi G, Padovani N, Biondi G, Tredici MR (2009) Microalgae for oil: strain selection, induction of lipid synthesis and outdoor mass cultivation in a low-cost photobioreactor. Biotechnol Bioeng 102:100–112. https://doi.org/10.1002/bit.22033

Ryckebosch E, Bruneel C, Termote-Verhalle R, Goiris K, Muylaert K, Foubert I (2014) Nutritional evaluation of microalgae oils rich in omega-3 long chain polyunsaturated fatty acids as an alternative for fish oil. Food Chem 160:393–400. https://doi.org/10.1016/j.foodchem.2014.03.087

Ryckebosch E, Muylaert K, Foubert I (2012) Optimization of an Analytical Procedure for Extraction of Lipids from Microalgae. Journal of the American Oil Chemists' Society 89:189–198. https://doi.org/10.1007/s11746-011-1903-z

Sabia A, Baldisserotto C, Biondi S, Marchesini R, Tedeschi P, Maietti A, Giovanardi M, Ferroni L, Pancaldi S (2015) Re-cultivation of *Neochloris oleoabundans* in exhausted autotrophic and mixotrophic media: the potential role of polyamines and free fatty acids. Appl Microbiol Biotechnol 99:10597-609. https://doi.org/10.1007/s00253-015-6908-3

Sayo T, Sugiyama Y, Inoue S (2013) Lutein: a nonprovitamin A, activates the retinoic acid receptor to induce HAS3-dependent hyaluronan synthesis in keratinocytes. Biosci Biotechnol Biochem 77 (6): 1282–1286.

Shah MR, Lutzu GA, Alam A, Sarker P, Chowdhury K, Parsaeimehr A, Liang Y, Daroch M (2018) Microalgae in aquafeeds for a sustainable aquaculture industry. J Appl Phycol 30:197–213. https://doi.org/10.1007/s10811-017-1234-z

Shepherd J, Bachis E (2014) Changing supply and demand for fish oil. Aquaculture Economics & Management 18(4):395–416. https://doi.org/10.1080/13657305.2014.959212

Sirin S, Sillanpää M (2015) Cultivating and harvesting of marine alga *Nannochloropsis oculata* in local municipal wastewater for biodiesel. Bioresource Technology 191:79–87. https://doi.org/10.1016/j.biortech.2015.04.094

Skretting (2014) Sustainability Report 2014. Retrieved from http://www.skretting.no

Smith VH, Crews T (2014) Applying ecological principles of crop cultivation in large-scale algal biomass production. Algal Res 4:23–34. https://doi.org/10.1016/j.algal.2013.11.005

Su C, Chien LJ, Gome, J et al. (2011) Factors affecting lipid accumulation by *Nannochloropsis oculata* in a two-stage cultivation process. J Appl Phycol 23:903-908. https://doi.org/10.1007/s10811-010-9609-4

Sukarni, Sudjito, Hamidi N, Yanuhar U, Wardana ING (2014) Potential and properties of marine microalgae *Nannochloropsis oculata* as biomass fuel feedstock. Int J Energy Environ Eng 5:279–290. https://doi.org/10.1007/s40095-014-0138-9

Tejido-Nuñeza Y, Aymerich E, Sancho L, Refardt D (2020) Co-cultivation of microalgae in aquaculture water: Interactions, growth and nutrient removal efficiency at laboratory- and pilot-scale. Algal Res 49:101940

Timberlake CF, Henry BS (1986) Plant pigments as natural food colours. Endeavour 10: 31–36.

Vesenick DC, Paula NA, Niwa AM, Mantovani MS (2012) Evalu ation of the effects of chlorophyllin on apoptosis induction, inhibition of cellular proliferation and mRNA expression of CASP8, CASP9, APC and b-catenin. Curr Res J Biol Sci 4:315–322

Wang C, Lan CQ (2018) Effects of shear stress on microalgae – A review. Biotechnology Advances 36:986–1002

Wang A, Yan K, Chu D, Nazer M, Lin NT, Samaranayake E, Chang J (2020) Microalgae as a mainstream food ingredient: demand and supply perspective. In: Microalgae biotechnology for food, health and high value products. Alam MdA, Xu J-L, Wang Z (eds) Springer Nature, Singapore. https://doi.org/10.1007/978-981-15-0169-2

Wei L, Huang X (2017) Long-duration effect of multi-factor stresses on the cellular biochemistry, oil-yielding performance and morphology of *Nannochloropsis oculata.* PLoS ONE. https://doi.org/10.1371/journal.pone.0174646

Wellburn AR (1994) The Spectral Determination of Chlorophylls *a* and *b*, as well as Total Carotenoids, Using Various Solvents with Spectrophotometers of Different Resolution. J Plant Physiol 144:307-313. https://doi.org/10.1016/S0176-1617(11)81192-2

White S, Anandraj A, Trois C (2013) The effect of landfill leachate on hydrogen production in *Chlamydomonas reinhardtii* as monitored by PAM fluorometry. Int J Hydrog Energy 38:14214–14222. https://doi.org/10.1016/j.ijhydene.2013.08.115

Wotton RS (2004) The ubiquity and many roles of exopolymers (EPS) in aquatic systems. Sci Mar 68:13–21.

Yen H-W, Chen P-W, Chen L-J (2015) The synergistic effects for the co-cultivation of oleaginous yeast-*Rhodotorula glutinis* and microalgae-*Scenedesmus obliquus* on the biomass and total lipids accumulation. Bioresour Technol 184:148–52. https://doi.org/10.1016/j.biortech.2014.09.113

Zhang T-T, Xu J, Wang Y-M, Xue C-H (2019) Health benefits of dietary marine DHA/EPA-enriched glycerophospholipids. Progress in Lipid Research 75:1009972. https://doi.org/10.1016/j.plipres.2019.100997

Zhu L (2015) Microalgal culture strategies for biofuel production: a review. Biofuels Bioprod Bioref 9:801–814 https://doi.org/10.1002/bbb.1576

Zhu L, Nugroho YK, Shakeel SR, Li Z, Martinkauppi B, Hiltunen E (2017) Using microalgae to produce liquid transportation biodiesel: What is next? Renewable and Sustainable Energy Reviews 78:391–400. https://doi.org/10.1016/j.rser.2017.04.089

Chapter 3

Mono- and co-cultivation of *Tisochrysis lutea* and *Nannochloropsis oculata* under white and red-enriched light

1. Introduction

In this chapter, the possibility of co-cultivating two different species of microalgae, *Tisochrysis lutea* (Haptophyta) and *Nannochloropsis oculata* (Ochrophyta), in order to obtain biotechnologically and commercially useful compounds was tested under two different lighting conditions. Based on the results obtained by Maglie et al. (2021), further tests were conducted; mono- and co-cultures were grown in different synthetic media and exposed to light sources of different wavelengths, also changing the concentration of the initial inoculum (data not shown). Based on these tests, *T. lutea* and *N. oculata*, both mono- and co-cultured, were grown in SWES medium, exposed to a total light intensity of 100 $\mu mol_{photons}\ m^{-2}\ s^{-1}$ and using a starting inoculum of $1x10^6$ cells mL^{-1}, as these growing conditions were the best for both species. Cultures were exposed to white light and white light enriched in the red wavelength. After trials with different light sources, red LEDs with a wavelength peak at 660 nm and white LEDs with a colour temperature of 4000K were used. Light is one of the environmental factors that most influences the growth and productivity of microalgae, both through its intensity and its quality (Wong et al. 2016; Maltsev et al. 2021). Furthermore, microalgae are influenced by the duration and frequency of lighting (Oostlander et al 2020). In this study the effects of the light composition on *T. lutea* and *N. oculata* in mono- and co-culture were evaluated. In fact, the wavelength of light is an essential parameter for the growth of microalgae and the quality of the light spectrum influences the metabolism of the algae (Raquida et. al 2019). Indeed, the pigments in the photosynthetic complexes absorb photons from different portions of the light spectrum. Different groups of microalgae have different pigment patterns, so that different microorganisms use different wavelengths of light more or less efficiently (Maltsev et al. 2021). Changes in wavelength lead to changes in cellular metabolism, resulting in variations in biomass production and the accumulation of compounds of biotechnological and commercial interest such as lipids and carotenoids (Kwan et al. 2021). Nowadays, the technology of LEDs offers numerous advantages over fluorescent lamps. For example, LEDs allow the use of monochromatic light or a specific spectral composition (Schulze et al. 2014; Al-amshawee and Yunus 2019). This study highlighted that in both, white and red light, it was found that, in the co-cultivation, the growth of *N. oculata* was enhanced at the expense of *T. lutea,* which, on the contrary, grew better in mono-cultures. In terms of photosynthetic efficiency, all red-light cultures showed values of F_V/F_M lower than those of the white-light cultures, which maintained constant values close to the optimal value of 0.6 or slightly lower towards the end of the experiment, except in the co-cultures, which showed values below 0.6 under both light conditions. In order to understand the physiological and biochemical effects of exposure to

different light sources on the photosynthetic apparatus of the two microalgae, studies were carried out on the organisation of the thylakoid membrane proteins. The SDS-PAGE technique followed by Western blot was used for these studies. As it was not possible to separate the two microalgae properly in co-cultivation, these studies were only performed on the mono-cultivated organisms. These analyses showed that in *N. oculata* red light leads to an increase in the PS I content, while it does not seem to particularly influence the PS II content compared to white light controls. For *T. lutea*, red light led to an increase in the content of cytochrome b_6-*f* complex and ATP synthetase. There was no significant difference in PS I content, while PS II content decreased slightly in cultures exposed to red light compared to white light controls. At the University of Almeria, gas-chromatographic analyses were performed to evaluate the lipid profile of mono- and co-cultures in white and red light. Red light increased the percentage of total fatty acids per dry weight (%DW) in *N. oculata* and co-cultures, while there was no significant difference in *T. lutea.* The co-cultures showed a lipid profile very similar to that of the *N. oculata* mono-cultures, with a predominance, under red light, of saturated and monounsaturated fatty acids of possible interest in the field of biorefinery. Furthermore, the red light stimulated the production of DHA in *T. lutea* by almost twice.

2. Materials and methods

Algal culture condition and growth

Tisochrysis lutea (Bendif et al. 2013; strain CCAP 927/14) and *Nannochloropsis oculata* (Hibberd 1981; strain CCAP 849/1) were obtained from the Culture Collection of Algae and Protozoa of Scottish Marine Institute (Scotland, UK; www.ccap.ac.uk). Mono- and co-cultures of the two microalgae strains were inoculated at least in triplicate and grown in 300-mL Erlenmeyer flasks (150 mL of total culture volume). Axenic cultures were maintained in liquid SWES medium (Sea Water Erddekokt Salze medium; www.epsag.uni-goettingen.de) in a growth chamber (25 ± 1 °C), 16:8 h light-dark photoperiod, 100 $\mu mol_{photons}\ m^{-2}s^{-1}$ photosynthetically active radiation (PAR), without shaking, and no additional CO_2 supply according to Maglie and coworkers (2021) and were used as algae inocula. For the experiments, both mono- and co-cultures were grown for 18 days in SWES medium with the same parameters cited above under two different lighting conditions: white light and red-enriched light. Cultures were pre-acclimated to red light conditions for 7 days before the inoculation day. Longer acclimation periods negatively affected photosynthetic efficiency. In both lighting conditions, cultures were exposed to 100 $\mu mol_{photons}\ m^{-2}s^{-1}$ total PAR. Red-enriched light (following also "red light") was obtained using 60 $\mu mol_{photons}\ m^{-2}s^{-1}$ of red LEDs (peak at 660 nm; OSLON®

Square LEDs) and 40 $\mu mol_{photons}\ m^{-2}s^{-1}$ of white LEDs (colour temperature 4000 K; OSLON® Square LEDs), the same used during white light experiments. For mono-cultures, both *T. lutea* and *N. oculata* cells were inoculated at a density of $1 \pm 0.1 \times 10^6$ cells mL^{-1}. For co-cultures, *T. lutea* and *N. oculata* cells were inoculated together at the same densities used in mono-culture; thus, the co-cultures presented a total cell density of $2 \pm 0.1 \times 10^6$ cells mL^{-1}. All cultures were set up at least in three replicas. Growth was estimated by measuring the optical density at 750 nm and by counting the cells with a Thoma's chamber (HBG, Germany) sampling 1 mL of culture at days 0, 3, 7, 10, 14, 18. To make the cell counting of *T. lutea* easier, 100 µL of Lugol's iodine was added to 1 mL of culture to stop cell movement (Maglie et al. 2021).

Light and fluorescence microscopy

Cell samples were observed at 0, 3, 7, 10, 14 and 18 days of cultivation, under a Zeiss Axiophot microscope equipped with conventional or fluorescent attachments. The light source for chlorophyll fluorescence examinations was an HBO 100 W pressure mercury vapour lamp (filter set, BP436/10 FT 460, LP470). To highlight the intracellular lipid accumulation, cells were stained with Nile Red (9- diethylamina-5Hbenzo[α]phenoxazine-5-one, NR; Sigma-Aldrich, Gallarate, Milano, Italy) according to Giovanardi et al. (2013), with some modifications. Aliquots of 10 µL NR (0.5 mg dissolved in 100 mL acetone) were added to 1.9 mL of a cell suspension with 0.5×10^6 cells for *T. lutea* and 4×10^6 cells for *N. oculata*. After incubation at 37 °C in darkness for 15 min, cells were observed with excitation at 485 nm (filter set BP485, LP520). All pictures were taken with a digital camera for fluorescence applications, VisiCAM PR0 20C.

Transmission electron microscopy

For transmission electron microscopy (TEM), cells were harvested weekly by centrifugation and prepared as reported in Baldisserotto et al. (2020) with minor modifications according to Maglie et al. (2021): the phosphate buffer was substituted with 0.1 M sodium cacodylate buffer (pH 7.2) for *N. oculata* and 0.1 M sodium cacodylate buffer with 0.25 M sucrose for *T. lutea* and co-cultures. Ultra-thin sections were observed with a Zeiss EM910 transmission electron microscope (Electron Microscopy Centre, University of Ferrara).

Pigment extraction and analysis

Cells were collected by centrifugation after 7, 10 and 18 days of experiment. The pigment concentration values at day 0 refer to the cultures used for the inoculum. Cells were treated with 100% methanol for 10 min at 80 °C (Baldisserotto et al. 2012). Absorption of extracts was

measured at 665 nm for chlorophyll *a* (Chl *a*), 632 nm for chlorophyll *c* (Chl *c*) and 470 nm for carotenoids (Cars) (Wellburn 1994; Ritchie 2006). Extracts were manipulated under dim light to avoid photo-degradation. Chlorophyll *a* and *c* concentration in *T. lutea* was evaluated using the equations reported in Ritchie (2006) (total Chls data are reported). Otherwise, the equations proposed by Wellburn (1994) were employed to determine the chlorophyll *a* concentration in *N. oculata* and the carotenoid concentration in both samples. Pigment content in co-cultures was evaluated on the mixtures of cells using the same methods described above and using equations of Ritchie (2006) for chlorophylls.

Chlorophyll fluorescence measurements

At days 0, 3, 7, 10, 14 and 18, fluorescence measurements were performed on cell pellets prepared as described by Ferroni et al. (2011). After 15 min of dark incubation, initial fluorescence F_0 and maximum fluorescence F_M were used to calculate the maximum quantum yield of PSII (F_V/F_M ratio). Fifteen minutes were found to be the optimal adaptation time for both microalgae after testing a range between 5 and 40 min dark adaptation time. For analyses, a pulse amplitude modulation fluorometer (PAM; Junior-PAM, Walz, Germany) was used with the following setting: measuring light (ML) with intensity and frequency at level 1; 0.6 s saturation pulse at level 6. Fluorescence measurements in co-cultures were performed on the mixtures of cells using the same methods described above.

Thylakoid isolation

Thylakoid membranes of microalgal samples were isolated according to Järvi et al. (2011) with modification as in Giovanardi et al (2017). Thylakoid isolation was performed only on mono-cultures to evaluate possible variations resulting from the different lighting conditions. For extraction, 900 mL of algal culture at 18 days of cultivation were harvested by centrifugation at 540 g for 10 min at 4 °C. Pellets were transferred to an ice-cold mortar (-20 °C) containing sand quartz (particle size: 40-100 mesh). The extraction was performed grinding cells with liquid N_2, then the lysate was resuspended in a grinding buffer (330 mM sorbitol, 50 mM Tricine-NaOH pH 7.5, 2 mM Na_2EDTA, 1 mM $MgCl_2$, 5 mM ascorbate, 0.05% bovine serum albumin BSA, 10 mM NaF) and transferred to 15 mL tubes by filtering with miracloth. Samples were centrifuged at 125 g for 5 min at 4 °C to remove sand quartz and cell debris. Pellets were discarded and the supernatant re-centrifuged at 125 g for 5 min at 4 °C. Thylakoids present in the supernatant were collected by centrifugation at 500 g for 5 min at 4 °C. Pellets containing thylakoids were carefully resuspended with a small brush in small volume (1-4 mL) of shock buffer (5 mM sorbitol, 50 mM Tricine-NaOH pH 7.5, 2 mM Na2EDTA, 5 mM $MgCl_2$, 10 mM

NaF), transferred into 2 mL Eppendorf tubes and centrifuged at 500 g for 10 min at 4 °C. After that, the supernatant was removed and around 100 µL of storage buffer (100 mM sorbitol, 50 mM Tricine1-NaOH pH 7.5, 2 mM Na_2EDTA, 5 mM $MgCl_2$, 10 mM NaF) were added to the pellets. Thylakoid samples were rapidly frozen and stored in liquid nitrogen until further analyses. For quantification of pigments, thylakoids were solubilized in 90% (v/v) acetone buffered with HEPES-KOH (pH 7.8) and analyzed using the spectrophotometer described above. Chlorophylls and carotenoid content were determined according to Wellburn (1994) and Ritchie (2006). All the procedures were performed on ice and under dim light.

Denaturing gel electrophoresis

Thylakoid proteins were separated by SDS-PAGE according to Laemmli (1970) and Giovanardi et al. (2018) on a 15% acrylamide resolving gel containing 6 M urea. Each thylakoid sample was loaded on the gel on a chlorophyll basis (2 µg of Chl). After electrophoresis, proteins were blotted onto a nitrocellulose membrane (Schleicher and Schuell, Dessel, Germany). Before immunodetection, membranes were blocked with 0.5% BSA in TBS buffer (Tris-HCl 10 mM pH 7.4 and NaCl 1.5 M). Proteins were visualized by Ponceau staining and, after a brief de-staining step with distillated water, membrane was photographed. Western blot was performed using protein-specific antibodies obtained from Agrisera (www.agrisera.com): ATP-β subunit of ATPase, PsaA subunit of PSI, CP43 and D1 subunits of PSII, Cyt *f* subunit of Cyt b_6f. Goat anti-rabbit secondary antibody (Agrisera) was used for protein detection. Protein band intensity was quantified with Image J freeware (National Institutes of Health, Bethesda, MD, USA).

Fatty acid determination by gas chromatography

The fatty acid analysis was performed at the Department of Chemical Engineering, University of Almería (Spain), in the laboratories directed by Prof. EM Grima and thanks to the precious collaboration of Professors TM Sobczuk, MJI González and EN López. Fatty acids were methylated by the method described transesterification by Lepage and Roy (1984). A gas chromatograph Hewlett Packard model 5890 Series II (Hewlett Packard Company, Avondale, PA) was used. Twenty mg of biomass were weighted into a glass tube and 1 mL of hexane was added to the sample. Then 1 ml of methylation mixture (methanol / acetyl chloride in the ratio 20:1) was added. Ten µL of standard solution were added to the sample using a Hamilton syringe; the standard solution consisted of 25 mg of heptadecanoic acid (17:0) in 1 mL of toluene. The tubes were placed in the ultrasound for 5 min. The transesterification reaction took place at 100 ºC for 1 h; a metal block thermostat, model Multiplace, provided by Selecta (JP

Selecta SA, Barcelona) was used. The tubes were shaken every 10 min. When the reaction was over, the tubes were cooled, and 1 mL of distilled water and 0.5 mL of hexane were added to the sample to obtain two phases. For the biomass, the phase separation was performed by centrifugation at 450 g for 3 min. The hexane phase was introduced into a vial of 2 mL capacity, hermetically sealed with a cap. The vials were placed in the autosampler of the gas chromatograph. The qualitative analysis of fatty acids was accomplished by standard mixture n-3 PUFAs, Catalog No. 47085-U (Supelco Analytical).

Statistical analysis

Data were processed and analysed using Microsoft® Excel® (version 2111). When necessary, statistical tests such as Student *t*-test, one-, two- or three-way ANOVA were performed using Origin® 2021 analysis software, followed by Tukey post-hoc test ($p < 0.05$).

3. Results

Growth kinetics

Figure 1a shows the growth of *T. lutea* mono-cultivated and co-cultivated with *N. oculata* exposed to white and red-enriched light. In mono-cultures, the cell density was similar under both light conditions up to 10 days of cultivation, when values of 4.02 ± 0.27 x10^6 cells mL^{-1} and 4.46 ± 0.38 x10^6 cells mL^{-1} for white and red-light cultures, respectively, were observed. After the 10th day, the white-light cultures showed a higher density than the red-light ones; at the end of the experiment, a cell density of 13.87 ± 1.35 x10^6 cells mL^{-1} was reported compared to 9.96 ± 0.505 x10^6 cells mL^{-1} in the red-light experiment ($p < 0.05$; three-way ANOVA followed by Tukey's post-hoc test). In co-cultivation with *N. oculata*, growth of *T. lutea* was limited in both white and red-light conditions. Under red light, the growth in co-culture was comparable to that in mono-culture up to 7 days. In contrast, in co-culture in white light, the cell density was significantly lower at 7 days than in mono-culture under the same light conditions. At the end of the experiment the cell density in co-cultivated cultures was about 2 ± 0.01 x10^6 cells mL^{-1} in red light and 1.78 ± 0.28 x10^6 cells mL^{-1} in white light ($p > 0.05$; three-way ANOVA followed by Tukey's post-hoc test). Figure 1b shows the growth of *N. oculata* in both mono- and co-cultures under both lighting conditions. The cell density of the mono-cultures was similar until 10 days of cultivation under both lighting conditions. On day 14, the white light cultures were more concentrated than those in red light ($p < 0.05$; three-way ANOVA followed by Tukey's post-hoc test). However, at the end of the experiment the red-light cultures had a higher cell density than those in white light ($p < 0.05$; three-way ANOVA

followed by Tukey's post-hoc test). In white light cultures, the growth of *N. oculata* was stimulated by co-cultivation with *T. lutea*. From day 7 to day 14, the cell density of *N. oculata* was significantly higher than that of the red-light co-culture and of the mono-culture in both light conditions ($p < 0.05$; three-way ANOVA followed by Tukey's post-hoc test). At 14 days the cell density in white-light co-culture was 46.8 ± 1.2 x10^6 cells mL^{-1}, compared to 29.64 ± 1.63, 25.93 ± 0.33, 32.9 ± 5.8 (x10^6 cells mL^{-1}),) respectively in red-light co-culture, red-light mono-culture and white-light mono-culture. Therefore, the co-cultivation process had positive effects on the growth of *N. oculata*, especially in white light. On the contrary, it strongly limited the growth of *T. lutea* under both tested light conditions.

Cell morphology

Figure 2 shows light and fluorescence microscope observations of mono- and co-cultivated *T. lutea* and *N. oculata* cells at 7 and 14 days of cultivation under both lighting conditions, white and red-enriched light. In white light, *T. lutea* mono-cultivated cells showed the typical morphology, and cell dimensions remained similar throughout the experiment (Fig. 2a, b, e, f). In fact, independent of the growth time, cells had the typical golden brown colour and an ovate or oblong shape. One cup-shaped yellow-brownish chloroplast occupied most of the cell volume and emitted red fluorescence due to the presence of chlorophylls (Fig. 2b, f). Translucent globules of probable lipidic nature were visible in some cells at 14 days of cultivation (Fig. 2e). During red-enriched light growth, *T. lutea* cells presented a normal shape in the early stages of growth (7 days) (Fig. 2c). As the experiment continued (14 days), some cells assumed irregular or spherical shapes (Fig. 2g). Translucent globules were present already at 7 days, increasing as growth continued (Fig. 2d, h). The lipid-specific fluorochrome Nile Red (NR) was used to confirm the lipidic nature of these translucent globules (Figure 3). In the early stages of cultivation, regardless of the type of light used, there were no substantial differences in the amount and size of lipid globules present in the cells of *T. lutea* (Fig. 3a, b). At 14 days the number and size of lipid globules increased in both light conditions (from 2 to 4 in some cells). Generally, cells grown in red light (Fig. 3d) showed an increase in number of the fluorescent lipid droplets and, in some cases, the globules were larger than those in cells grown in white light (Fig. 3c). In both illumination conditions, *T. lutea* cells co-cultured with *N. oculata* did not show distinctive morphological changes compared with mono-cultured cells (Fig. 2q-x). At advanced stages of culture, cell mobility was limited and sometimes absent. In both white and red light, lipid globules highlighted with NR were already present at 7 days (Fig. 3i, j). After 14 days of co-culture, an increase in the fluorescence of lipid droplets was observed

(Fig. 3k, l); moreover, cells exposed to red light showed in some cases globules of considerable size compared to the total size of the cells (Fig. 3l). Both in white and red-enriched lighting, *N. oculata* mono-cultivated cells showed the characteristic spheroid shape, with a variable diameter between 2 and 3 μm; no differences in cell morphology were appreciable (Fig. 2i, k, m, o). In both lighting conditions, the chloroplast was visible and occupied a large part of the cell, as shown by the epifluorescence microscope images (Fig. 2j, l, n, p). Translucent globules, attributable to the presence of lipids within the cells, were clearly visible only in the advanced stages of the culture (Fig. 2m, o). In the early stages of cultivation, staining with NR showed the presence of lipid globules only in microalgae grown in red light, although the emitted fluorescence was low (Fig. 3f). At 14 days, also in cells grown under white light, the first lipid globules became visible (Fig. 3g); in cultures grown under red light, all cells showed one or two lipid droplets with intense fluorescence and considerable size (Fig. 3h). When *N. 86culate* was co-cultured with *T. lutea*, cell morphology did not differ from that of mono-cultures, in both white and red light (Fig. 2 q-x). However, it should be remarked that staining of cells with NR revealed the presence of lipid globules already after one week of co-cultivation not only in red light but also in white light cultures, unlike what was observed in mono-cultures (Fig. 2i, j). After 14 days of co-cultivation with *T. lutea*, both *N. oculata* cells exposed to white light (Fig. 3k) and those exposed to red light (Fig. 3l) contained one or two lipid droplets with intense fluorescence. In some cases, the lipid globules also reached large sizes.

Subcellular TEM observations

TEM observations of mono- and co-cultures in white and red light after 14 days of cultivation are shown in Figure 4, 5 and 6. The mono-cultured *T lutea* cells in white light were characterized by a normal morphology (Fig. 4a, b). The typical organic scales outside the cell were clearly visible. The parietal cup-shaped plastids contained a large pyrenoid crossed by a thylakoid lamella in longitudinal section. The thylakoid membranes did not show any alterations. Large mitochondria were also visible. In red light cells, a large part of the cytosol was occupied by two or more lipid globules, consistent with that observed by NR staining (Fig. 4c). The chloroplast with pyrenoid was still clearly visible. The thylakoids were more appressed than in white light and large mitochondria were present (Fig. 4d). In *N. oculata* mono-cultures under white light, the chloroplast occupied a large part of the cell volume with thylakoidal membranes clearly visible and large portions of stroma (Fig. 5a, b). One or two lipid droplets were visible and sometimes had considerable size. Large mitochondria were also present. In red light, mono-cultivated cells of *N. oculata* presented chloroplasts with thylakoid membranes damaged or

with a distorted structure. In some cases, the stroma was not clearly visible (Fig. 5c). However, as already observed by NR staining under fluorescence microscopy, many large lipid droplets were present and, in some cases, they occupied a large part of the cell volume (Fig. 5d). As already observed for the mono-cultures, also the co-cultured cells of both *T. lutea* and *N. oculata* presented lipid droplets more frequently in red light (Fig. 6 d-f) than in white light (Fig. 6 a-c). In *T. lutea*, globules with a darker coloration, which could result either from a different qualitative composition of fatty acids, were observed (Fig. 6e). *N. oculata* cells contained large lipid globules, occupying a large part of the cell volume (Fig. 6f). In general, *T. lutea* cells co-cultured under both white and red light showed an altered morphology, with irregularly shaped cells (Fig. 6b, d, e) and, in some cases, large areas of cytosol characterized by vacuolation. Despite the visible changes in the cytoplasm, numerous mitochondria were present, indicating an active metabolism (Fig. 6b, d). As observed for mono-cultivated *T. lutea* cells under red light, in co-cultivated cells the thylakoidal membranes appeared appressed in both lighting conditions (Fig. 6 c, e). In the case of *N. oculata* cells, there were no remarkable changes compared to what was observed in the mono-cultures under the respective lighting conditions (Fig. 6 a, c, d, f).

Photosynthetic pigment content

The time-course of pigment content is shown in Figure 7. The pigment concentration values of day 0 are referred to the cultures used for the inoculum. Red-light cultures were pre-adapted during 7 days before the inoculation day to this lighting condition. Day 0 values are only shown in the histograms for mono-cultures. At time 0 day, the difference in pigment content between white- and red-light cultures is due to the red-light pre-adaptation period the cultures were subjected during the 7 days before the inoculation. In *T. lutea* cells mono-cultivated in white light, the concentration of total chlorophylls tended to increase in the first 10 days of cultivation and then decreased to values comparable to the initial ones at the end of the experiment (at 18 days). During cultivation in red-enriched light, a decrease in chlorophylls concentration was observed during the first week of cultivation. Afterwards, the concentration remained constant and there were no significant differences ($p > 0.05$; two-way ANOVA followed by Tukey's post-hoc test) compared to the cultures grown in white light (Fig. 7a). A same trend was found in the concentrations of carotenoids (Fig. 7b). In mono-cultures of *N. oculata* in white light, the final chlorophyll concentration (at 18 days) was 30% higher than the initial concentration ($p < 0.05$; two-way ANOVA followed by Tukey's post-hoc test) (Fig. 7c). In red light the highest chlorophyll concentration was reached at 10 days of cultivation and there were no significant

differences ($p > 0.05$; two-way ANOVA followed by Tukey's post-hoc test) compared to cells in white light, whereas, at the end of the experiment, the chlorophyll concentration in *N. oculata* grown in red light was 41% lower than those in white light ($p < 0.05$; two-way ANOVA followed by Tukey's post-hoc test) (Fig. 7c). Although carotenoids were slightly more concentrated in the white-light cultures, the difference with the red-light cultures was not significant ($p > 0.05$; two-way ANOVA followed by Tukey's post-hoc test) (Fig. 7d). In *N. oculata* there was a significant increase in both chlorophyll and carotenoid concentrations in the cultures at the 7th day of white light cultivation; however, these values are not credible due to the high standard deviations (Fig. 7c, d). In contrast to the findings highlighted in the two mono-cultured microalgae, the co-cultured cells showed a progressive decrease in both chlorophyll and carotenoid concentrations. This trend was found in both white and red-enriched light co-cultures as reported in Figures 7e and f.

PSII maximum quantum yield measure

The effects of the different lighting conditions in mono- and co-cultivation process on the photosynthetic efficiency were evaluated by PAM fluorimetry (Figure 8). In microalgae, F_V/F_M values between 0.6 and 0.8 indicate an efficient use of light in the photosynthetic processes (Bhola et al. 2016; Patil et al. 2020). In *T. lutea* cultures, the best F_V/F_M values (>0.6) were obtained under white light, with values between 0.69 and 0.68 throughout the cultivation process. In contrast, cultures exposed to red light showed significantly lower F_V/F_M values than those in white light ($p < 0.05$; two-way ANOVA followed by Tukey's post-hoc test). After an initial fluctuation of the values in the early culture phases, from day 10 the values remained slightly lower than 0.6, in detail between 0.54 and 0.56 (Fig. 8a). Under both lighting conditions, *N. oculata* cells showed values close to or slightly below 0.6. Although the values were lower in red light than in white light, the differences were not always significant (Fig. 8b). Values obtained during the co-cultivation in white light were slightly below 0.6 (0.59-0.52). However, there was a general decrease in photosynthetic efficiency in the final stages of the experiment. In red light co-cultivated cells, photosynthetic efficiency was negatively affected; F_V/F_M values were considerably lower than 0.6 throughout the cultivation period, with the lowest values at 3 and 18 days (0.44 and 0.45, respectively) (Fig 8c).

Thylakoid protein complexes

Thylakoidal membranes were isolated from both *T. lutea* and *N. oculata* cells mono-cultivated under white and red light. Thylakoid proteins were separated by SDS-PAGE and subsequently blotted on a nitrocellulose membrane. Ponceau stain was performed to highlight the proteins on

the membranes (Fig. 9). The key proteins belonging to major thylakoid complexes PsaA of PSI, ATP-β of ATPase, CP43 and D1 of PSII, Cyt *f* of Cyt b_6f complex, were detected by immunoblot analyses as shown in Figure 10a. The signal obtained from CP43 and Cyt *f* in *N. oculata* samples was insufficient to be properly photographed and analysed. Proteins band intensity was quantified and shown in Figures 10b (*T. lutea*) and c (*N. oculata*). Evidently enhanced signals of ATP- β and Cyt *f* were found in *T. lutea* samples cultivated under red light ($p < 0.05$; Student t-test). On the contrary, CP43 and D1 showed lower signals than the white light samples ($p < 0.05$; Student t-test); in particular, CP43 gave a 78% lower signal. No differences were found between white and red-light samples for PsaA signals (Fig. 10b). On the other hand, in *N. oculata* the PsaA signals were significantly enhanced in red light samples compared to white light samples (73% higher) ($p < 0.05$; Student t-test). No significant differences were observed for ATP- β and D1 (Fig. 10c).

Fatty acid profile

The lipids extraction and analysis by gas chromatography were performed on samples of mono- and co-cultures in both light conditions tested. All analyses of the lipid fraction were performed at the 18th day of cultivation, when the cultures were sufficiently concentrated, and the cells had already accumulated lipid droplets as suggested by microscopic observations (Fig. 3-6). Figure 11 shows the fatty acid content (% DW) in *T. lutea*, *N. oculata* and co-cultures under both white- and red-enriched light. *T. lutea* cultures showed no significant differences ($p > 0.05$; Student t-test) between white- and red-enriched light treatment: fatty acids were 10.74% and 13.06% of total DW, respectively. In contrast, in both *N. oculata* and co-cultures, red light significantly enhanced the fatty acid content ($p < 0.05$; Student t-test). *N. oculata* cultures under red light had 27.67% more fatty acids than those under white light (11.49% and 9% of total DW, respectively). This result was more remarkable in the co-cultures: fatty acids increased by 128.30% in the red-light cultures compared to the white light cultures (from 8.27% to 18.88% of the total DW). Furthermore, under red light in co-cultures the fatty acid content resulted higher than that of mono-cultures ($p < 0.05$; Student t-test). Although comparing the cultures in white and in red light there were no significant differences ($p > 0.05$; Student t-test) between relative proportions of saturated, mono- and polyunsaturated fatty acids, Figure 12 shows that in *N. oculata* and co-cultures under red light the 76% and the 80% of the lipids were saturated and monounsaturated, potentially interesting in the biodiesel field (in white light saturated and monounsaturated fatty acids were respectively the 64% and the 62%). The fatty acid profile was characterized by GC-MS and are showed in Table 1. In *T. lutea* stearidonic acid (SDA;

18:4n3) was the major component in both lighting conditions (30.51% in cultures under white light and 21.73% in those under red light). In the white light cultures, the amount of SDA was 28.63% higher than that found in the red-light cultures ($p < 0.05$; Student t-test). Likewise, palmitoleic acid (16:1n7) and α-linolenic acid (ALA; 18:3n3) were present in higher amounts in the white light cultures than in the red-light cultures, respectively 44.30% and 47.22% more ($p < 0.05$; Student t-test). On the contrary red light significantly stimulated the accumulation of oleic acid (18:1n9) and of the omega-3 docosahexaenoic acid (DHA; 22:6n3) ($p < 0.05$; Student t-test). Oleic acid increased from 9.55% in white light cultures to 15.94% in red light ones, whereas DHA from 6.44% to 11.09%; an increase of 66.91% and of 72.20%, respectively. Palmitic acid (16:0) also resulted quite increased in red light cultures but the difference was not significant because of the elevated standard deviation in red light samples ($p > 0.05$; Student t-test). Palmitoleic acid (16:1n7) was the prevailing fatty acid in *N. oculata* cultures, both in white and red light (31.11% and 34.20%, respectively). As already observed in *T. lutea*, the growth of *N. oculata* in red light stimulated the accumulation of oleic acid (18:1n9): 4.06% in white light cultures and 7.71% in red light ones, an almost twofold increase ($p < 0.05$; Student t-test). Palmitic acid (16:0) also increased by 22.44% in cells grown in red light, from 23.31% in white light to 28.54% in red light ($p < 0.05$; Student t-test). However, in red light the accumulation of the omega-3 eicosapentaenoic acid (EPA; 20:5n3) was 38.26% lower than in white light cultures. EPA decreased from 24.78% in the white light cultures to 15.30% in the red-light ones. The fatty acid profile of co-cultivated cells was more similar to that of *N. oculata* mono-cultivated samples in both lighting conditions. This was consistent with the low number of *T. lutea* cells in co-cultures at the 18th day. In fact, *T. lutea* constituted only the 3.89% of the total cells present in co-cultures in white light and the 4.49% in red light co-cultures. As in mono-cultures of *N. oculata*, in white light co-cultures the prevailing fatty acid was palmitoleic acid (16:1n7), 26.23% of the total. In red light co-cultures, palmitic acid (16:0) and palmitoleic acid (16:1n7) were the major components, 30.21% and 29.41% respectively. Both palmitic and palmitoleic acid were significantly higher (+34.33% and +12.12%) in red light co-cultures than in white co-cultures ($p < 0.05$; Student t-test). As observed in *N. oculata* also in co-cultures oleic acid (18:1n9) doubled in cells under red light, raising from 5.01% to 10.38% ($p < 0.05$; Student t-test). On the contrary, EPA levels in the co-cultures were higher in the white light samples (+22.69%) than in the red light ones, in which EPA was about half of that observed in white light (10.05%) ($p < 0.05$; Student t-test). Despite the scarce presence of cells, the contribution of *T. lutea* to the fatty acids profile in the co-cultivated samples was visible, owing to the detection of the characteristic omega-3 SDA, absent in *N. oculata*, in both white and red

light co-culture. On the contrary, DHA was slightly detectable only in red light co-cultures. This can be partially explained by the increased levels of DHA observed in *T. lutea* mono-cultures in red light compared to those in white light.

4. Discussion

Based on previous studies (Maglie et al. 2021), in the present work the capability of *T. lutea* and of *N. oculata* to grow in a co-cultivation batch system in saline SWES medium was evaluated. In addition, the response of cell cultures to two different lighting conditions - white light and red-enriched light - was assessed. Co-cultivation strategy may aim to obtain distinctive compounds of each alga, like pigments (chlorophylls and carotenoids) as well as fatty acids (e.g., DHA and EPA), using a single cultivation process, with the concomitant advantage to halve water and nutrient use (Zhu et al. 2019; Cheng et al. 2020; Ray et al. 2022). Furthermore, it is known that the use of different light spectra during the growth of microalgae influences both the biomass production, the pigments content and the lipid yield along with the change in lipid and pigments pattern composition (Amaro et al. 2020; Gao et al. 2021).

Under both lighting conditions used in this study, *T. lutea* growth was strongly limited by co-cultivation with *N. oculata* as previously observed in other experiments reported in Maglie et al. (2021) and in some other studies on microalgae-microalgae co-cultivation systems (Rashid et al. 2019; Tejido-Nuñeza et al. 2020). Rashid and colleagues (2019) showed that during the co-cultivation process of *Chlorella* and *Ettlia,* the total biomass of the co-culture was higher than that of the respective mono-cultures. However, regardless of the initial inoculum ratio used, the final *Ettlia* population in co-cultures was always limited by the presence of *Chlorella* due to its high growth rate. Differently from *T. lutea*, under both lighting conditions, the growth of *N. oculata* was not inhibited by co-cultivation and showed better growth in co-culture than in mono-culture when the microalgae were exposed to white light. This result contrasted with what observed in a previous study, in which both microalgal species in co-culture grew less than in mono-cultures (Maglie et al. 2021). This may be due to the different inoculum ratio used in this study (1:1) compared to the previous one (1:8; 0.6 and 5×10^6 cells mL^{-1}, respectively for *T. lutea* and *N. oculata*). Indeed, the inoculum size influences the growth of microalgal even in mono-cultures (Pham et al. 2018). This factor is crucial in co-cultures. For example, Cheng and coworkers (2020) reported that the inoculum ratio in the co-cultures of *Tribonema* sp. and *Chlorella zofingiensis* in wastewater influenced both the microalgae growth and the removal efficiency of pollutants, achieving the best results when the ratio of the two microalgae was 1:1. Lighting conditions are another important factor for microalgae growth (Nwoba et al. 2019;

Amaro et al. 2020). Although in red light the growth trend of *N. oculata* was not exactly comparable to that in white light, no negative effects were observed. On the contrary, at the end of the experiment, in both mono- and co-cultures, the cell density was comparable to that of the white light co-cultures and higher than in the white light mono-cultures. Similar evidence is reported in Yuan et al. (2020). Indeed, *N. oculata* showed similar biomass concentrations and productivity at all wavelengths tested (white, blue, red and green light), with minor differences only in growth rate, which was higher in blue light and lower in green light. On the contrary, a low growth of *T. lutea* under red light was observed, consistent with other studies (del Pilar Sánchez-Saavedra et al. 2016; Gao et al. 2021). Gao and colleagues (2021) tested the growth of *T. lutea* under red, blue, green light and a mix of these wavelengths, highlighting how cultures grew less under red light than in other wavelengths. Whereas the best results were found in blue light and when all wavelengths were mixed. *T. lutea* growth under red light was limited compared to white and blue light also in the studies of del Pilar Sánchez-Saavedra et al. (2016). The reason may be that *T. lutea* can accumulate up to 80 $mg \cdot g^{-1}$ fucoxanthin in dry biomass, while most species range from 1 to 10 $mg \cdot g^{-1}$ of dry biomass (Mohamadnia et al. 2020; Wang et al. 2021). Since fucoxanthin can absorb blue and green light, the limitated growth under red light could be due to a lack of this wavelength. Indeed, the light harvesting complex fucoxanthin-chlorophyll *a*/*c*-protein (FCP) plays an important role in capturing photons and transferring them to the photosynthetic reaction center (Wang et al. 2019; Gao et al. 2021). On the other hand, a study on *I. galbana*, a microalga similar to *T. lutea*, showed that there were no significant differences in the growth of the cultures under red, blue and white light (Ra et al. 2018). Differently, a mixture of blue and red light resulted the best growth (Ra et al. 2018).

The limited growth of co-cultured *T. lutea* under both white and red light was consistent with alterations in the cellular structures observed by TEM analyses, such as the vacuolation in large areas of the cytosol. Moreover, a stress condition was confirmed by the lower mobility observed under the light microscope. The presence in co-culture of abundant small *N. oculata* cells with a hard wall can have triggered a sort of shear or hydrodynamic stress in *T. lutea* cells (Maglie et al. 2021).

An early and progressive decline of PSII maximum quantum yield was observed in co-cultivated cells under both lighting conditions and in *T. lutea* mono-cultivated cells under red light. F_V/F_M values were below 0.6. The low F_V/F_M values were consistent with the low growth of *T. lutea*, observed in both lighting conditions in co-cultivation and in red-light mono-cultures. Low values of the F_V/F_M ratio indicate a stress condition of the microorganisms. In

fact, the analysis of the PSII maximum quantum yield allows an estimate of the photosynthetic efficiency and can be used as a parameter to highlight the physiological stress in microalgae (Cosgrove and Borowitzka 2010; Bhola et al. 2016; Patil et al. 2020). These data were consistent with what previously observed in Maglie et al. (2021) and were supported by TEM observations of more appressed thylakoid membranes of *T. lutea* cells in red light (mono- and co-cultivated) and in co-cultivation under white light. The inefficiency of *T. lutea* and similar Isochrysidales algae in exploiting red wavelengths may be partly responsible for what has been observed in present study and was highlighted also in other studies (Li and Liu 2020; Gao et al. 2021). However, results on F_V/F_M values in co-cultures contrasted with the growth observed in *N. oculata*, which was not affected by the co-culture process. Low F_V/F_M values were generally reported under nutrient deficiency or very dense cultures or light-stressed cultures (Beardall et al. 2001a, b; Baldisserotto et al. 2014; Benvenuti et al. 2015). This experiment led to not very dense cultures, thus it can be proposed that inhibiting effect of red light on *T. lutea* and a nutrient deficiency in co-cultures could have occurred. This hypothesis can be supported by the progressive decrease of pigments content observed in the co-culturing process, under both lighting conditions, compared to that observed in the mono-cultures. In fact, nutrient limitation, and in particular nitrogen starvation, is known to suppress chlorophylls synthesis in microalgae (da Silva Ferreira and Sant'Anna 2017). Furthermore, the effect of nutrient deficiency varies according to the type of pigment, the type of nutrient missing and the organism (Gauthier et al. 2020). For example, in *T. lutea*, nitrogen starvation is known to cause a decline in both chlorophylls and fucoxanthin accumulation (Gao et al. 2020) and the reduction in *Isochsysis galbana* pigmentation under nitrogen limitation was alsowas reported (Falkowski et al. 1989). In *N. oculata* nutrient availability has a noticeable impact on the concentration of photosynthetic pigments (Faé Neto et al. 2018). For example, nitrogen depletion induces higher xanthophyll yield, whereas phosphorus depletion leads to a higher β-carotene concentration, and phosphorus deprivation affects Chl *a* accumulation, while violaxanthin content is not influenced (Forján et al. 2007; Van Vooren et al. 2012; Matsui et al. 2020). Oxygenic photosynthetic organisms convert light energy into electron flow in the reaction centre (RC) of photosystems (PS). Electron transfer is shared between two PSs (PSII and PSI) via the cytochrome b_6f complex and maintaining the excitation balance between PSII and PSI is extremely important to ensure efficient photosynthesis and avoid photo-damage (Tikkanen et al. 2012; Mirkovic et al. 2017; Ueno et al. 2019). The red light used in this experiment with a peak at 660 nm preferentially stimulates PSII. Due to continuous excitation, the maximum yield of PSII decreased in red light cultures and the excitation balance between PSII and PSI was

compromised. Possible strategies used by photosynthesising organisms to control stress on the photosynthetic system include control of relative excitation of PSII and PSI, regulation of the speed of electron transfer via the cyt b_6f complex and tuning the amount of active PSII reaction centres (Tikkanen et al. 2012; Yamamoto and Shikanai 2019). The analysis of thylakoidal proteins by SDS-Page and immunoblotting showed that *T. lutea* and *N. oculata* adopt two different strategies to deal with this problem. In both cases the stoichiometry between PSI and PSII changes favouring PSI. In *T. lutea*, the PsaA of PSI does not change between white and red light but a decrease in PSII-related proteins CP43 and D1 was observed. This suggests that in *T. lutea* the number of PSII was reduced in red light compared to white light. This strategy allows limiting the electron transfer to PSI, thus preventing excessive damage (Tikkanen and Aro 2014). In addition, the increase observed in Cyt *f* subunit of Cyt b_6f could suggests the activation of cyclic electron transport (CET) around PSI. Consequently, CET generates ΔpH without net accumulation of NADPH. ΔpH formed by CET contributes to additional ATP production (Yamamoto and Shikanai 2019). This explains the increase in ATP-β subunit of ATPase observed in *T. lutea.* Furthermore, lumen acidification activates a mechanism called photosynthetic control consisting in a slower plastoquinol oxidation at the Cyt b_6f complex. This prevents excess electron flow toward PSI (Shimakawa and Miyake 2018; Yamamoto and Shikanai 2019). On the other hand, in *N. oculata* under red light an increase in the PSI protein PsaA was observed, while there was no variation between white light and red-light samples for D1, assuming that there was no change in the quantities of PSII. Therefore, differently from *T. lutea, N. ocualta* modified the stoichiometry between PSI and PSII enhancing the number of PSI that to control the flow of electrons from the PSII.

As highlighted by microscopy observations, in the late phase of cultivation, the greatest accumulation of lipids in the cells was noted. Under white light, mono-cultures of *T. oculata* showed a total fatty acids (TFA) content (% DW) lower than that observed in the previous study (Maglie et al. 2021). The results for mono-cultures were also lower than those available in the literature for the same algae (Su et al. 2011; Rashid and Qin 2015; Hu et al. 2018; Gao et al. 2020). For example, Hu et al. (2018) reported values of about 25% (DW) after 16 days of cultivation. In *T. lutea* no significant differences were found in total fatty acid content and in the degree of fatty acids saturation between white and red lights, as also shown by Gao and colleagues (2021). Similar results about saturation degree were obtained by del Pilar Sánchez-Saavedra et al. (2016). These studies highlighted that the level of saturation in *T. lutea* is independent of light spectra.

On the contrary red light enhanced lipid content in co-cultures and in *N. oculata.* In *N. oculata,* the enhanced lipid accumulation under red light was also reported by Schulze et al. (2016), who compared the effect of red *vs* blue and white lights. Red light stimulated the lipid accumulation also in other species of *Nannochloropsis*. For example, in *N. gaditana*, total fatty acids content was 11.35% in white light, and 21.12% in red light (Kim et al. 2014). On the contrary, Yuan et al. (2020) reported the greatest accumulation of lipids when *N. oculata* was cultured under blue light. In the present work, the proportions of saturated and unsaturated fatty acids were analysed and, interestingly, the co-cultures showed a profile very similar to that of *N. oculata*, both under white and red light. This was consistent with what already observed in co-cultures of *T. lutea* and *N. oculata* in a previous study (Maglie et al. 2021) and with the predominance of *N. oculata* cells in co-culture. Indeed, *T. lutea* represented just the 3.89% and 4.49% of the cells in the co-culture, under white and red light, respectively. The influence of different proportion of algae in the co-cultures on lipid content was already observed also in other microalgae-microalgae co-cultivation experiments, e.g., *Ettlia* together with *Chlorella* (Rashid et al. 2019). Overall, red light caused a qualitative change in the fatty acid profile, although there were no significant changes in total fatty acid content and in the degree of saturation between white and red light in *T. lutea* samples. Similar results were observed in *N. oculata* and consequently in co-cultures samples. Indeed, both in *N. oculata* and co-cultures, in addition to the increase in lipids, exposure to wavelengths in the red region altered the composition of fatty acid with a predominance of saturated and monounsaturated fatty acids (such as 16:0 and 18:1n9) of possible interest in the field of biorefinery (Baldey et al. 2021). In fact, a higher quantity of saturated fatty acids is preferable, because biodiesel having more polyunsaturated fatty acids emits more oxides of nitrogen and exhibits lower thermal efficiency (Gopinath et al. 2010; Redel-Macías et al. 2012; Baldey et al. 2021). On the other hand, considering the low temperature fluidity and oxidative stability monounsaturated fatty resulted important in the composition of biodiesel (Cao et al. 2014; Baldey et al. 2021). In particular, the C16:0 component, which improves biodiesel quality, was higher in both *N. oculata* and co-cultures samples under red light. Similar effect of red light was observed also in *N. oceanica* (Kim et al. 2014). The changes observed in DHA (*T. lutea*) and in EPA (*N. oculata* and co-cultures) contents, between white and red-light cultures, are noteworthy. Indeed, DHA and EPA are known for several highly beneficial effects on human health, such as preventing atherosclerosis and cardiovascular diseases (Zhang et al. 2018; Tocher et al. 2019). After all *T. lutea* is known to accumulate high levels of DHA (Mayer et al. 2021). In the present study, the DHA levels increased in cultures exposed to red light, being nearly doubled (from 6.44% TFA under white

light, to 11.09% TFA under red light). del Pilar Sánchez-Saavedra and coworkers (2016) reported that, during the exponential growth phase under red light, *T. lutea* synthesizes high DHA levels, but also in the stationary phase and under green light. On the contrary, the blue light increased the DHA content in both growth phases. Gao et al. (2021) reported the same positive influence of blue light on the accumulation of DHA, even if no significant differences in terms of DHA content were found between cells exposed to red and other wavelengths, such as green and mixed blue or green and red light. As regards EPA, *Nannochloropsis* species represents an important natural source of this omega-3 fatty acid (Chua et al. 2020; Sá et al. 2020). A general decrease in polyunsaturated fatty acids was observed in mono-cultivated *N. oculata* and in co-cultures exposed to red light. In particular, EPA decreased from 24.78 % to 15.30 % in mono-cultures of *N. oculata* and from 22.69 % to 10.05% in co-culture. This result was in contrast with Ma et al. (2018) that in *Nannochloropsis* sp. observed an increase in EPA levels under red light.

Overall, the use of red light for the cultivation of *T. lutea* increases the production of DHA. Unfortunately, in co-culture the contribution of *T. lutea* to the lipid profile is minimal due to its low growth compared to that of *N. oculata* in both lighting conditions. Although the fatty acid profile obtained from co-cultivation process did not contain all the omega-3 and omega-6 fatty acids that are useful for nutraceutical purposes, the results obtained represent a promising starting point for the production of a plant and "green" alternative DHA for food/feed respect fish oil. Indeed, fish oil is one of the main sources of long-chain ω-3 fatty acids used for the production of animal feed and of nutritional supplements for human consumption (Misund et al. 2017; Matsui et al. 2020). On the other hand, the increase of saturated fatty acids as C16:0 in *N. oculata* and co-cultures, in red light, is attractive from the point of view of the exploitation of microalgae in the field of bioenergy. Indeed, *Nannochloropsis* already represents a suitable microalga for the production of biofuel (Liu et al. 2017; López-Rosales et al. 2019). Thus, a better knowledge about its exploitation in the green energy field is advantageous because of the continuously increasing demand for alternative energy sources linked to the rising world population, the diminishing fossil fuel reserves and the increasingly restrictive environmental legislations (Abd Rahman et al. 2020; He et al. 2020).

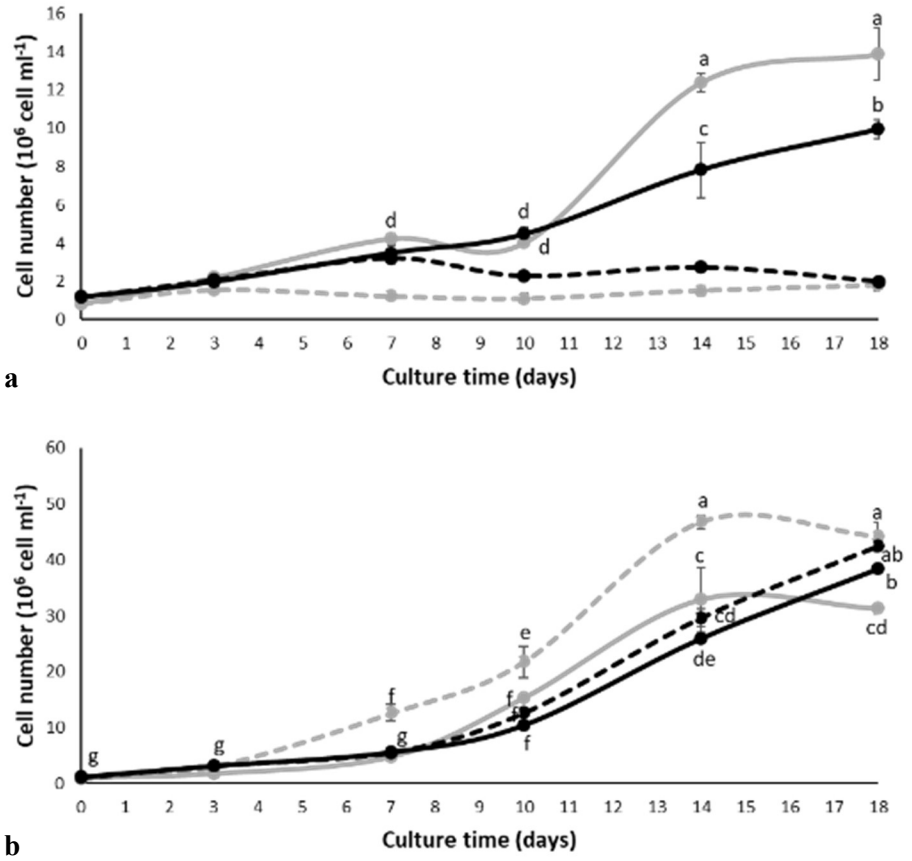

Figure 1 Growth kinetics of *T. lutea* (**a**) and *N. oculata* (**b**) under white (grey) and red-enriched light (black) in mono-cultures (solid lines) and in co-culture (dashed lines). Values are means ± SD (n = 4). Different letters indicate statistically significant differences ($p < 0.05$, three-way ANOVA). To improve the readability of the picture, the graphical representation of the statistical analyses performed has been simplified. For comprehensive information on the statistical analysis, please refer to Table 1 and 2 in the appendix to this chapter.

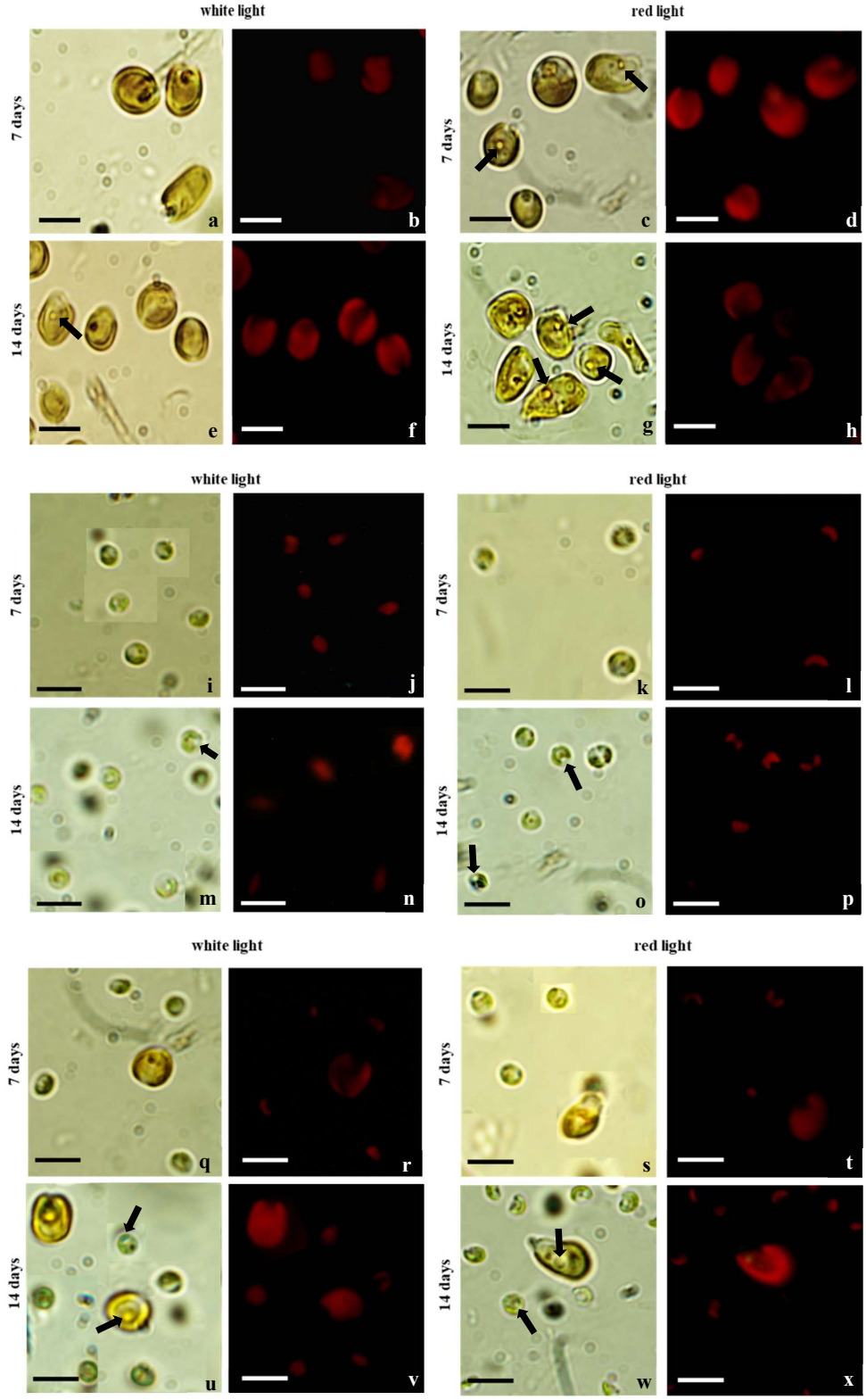

Figure 2 Light and epifluorescence microscope observations of mono- and co-cultivated cells of *T. lutea* and *N. oculata* at different stage of cultivation (7 and 14 days) and in different culturing light conditions (white and red-enriched light). *T. lutea* (a–h); *N. oculata* (i–p); co-cultivated cells (q–x). Most figures consist of a collage of photos exemplifying the observations made. Black arrows indicate translucent globules. Scale bars = 5 µm

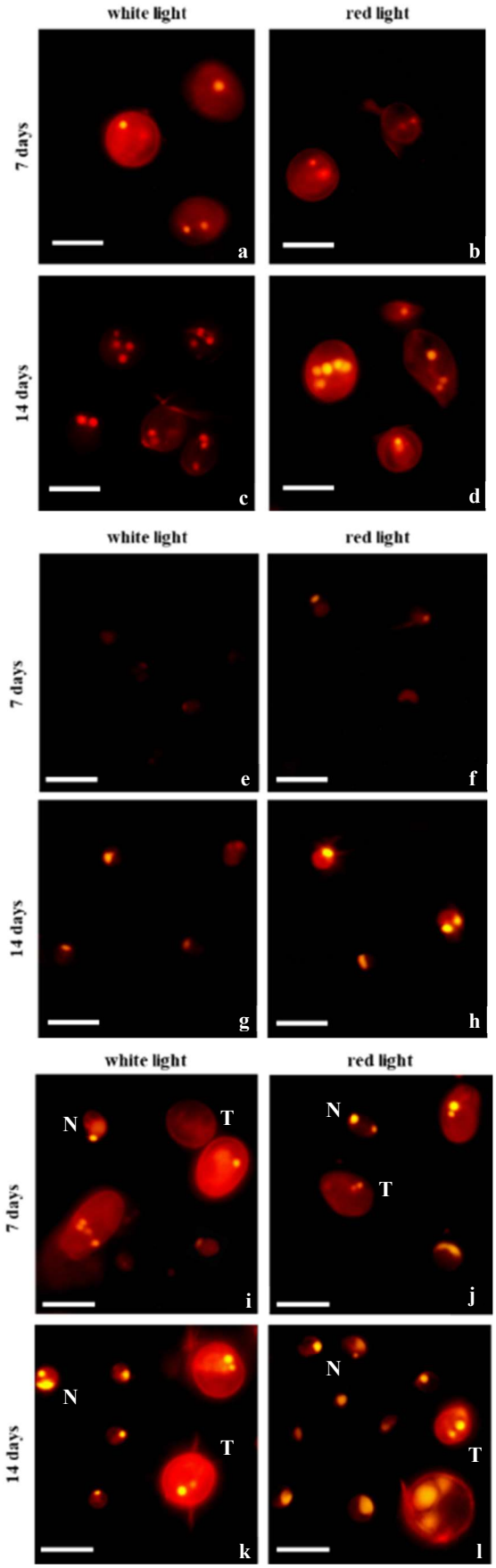

Figure 3 Epifluorescence photomicrographs of Nile Red stained cells of mono-cultivated and co-cultivated *T. lutea* and *N. oculata* at different stage of cultivation (7 and 14 days) and in different culturing light conditions (white and red-enriched light). *T. lutea* (a–d); *N. oculata* (e–h); co-cultivated cells (i–l). Most figures consist of a collage of photos exemplifying the observations made. **T** *T. lutea* cells, **N** *N. oculata* cells. In *mono*-cultivated *N. oculata* cells the reaction is negative in the early stages of experimentation (e). Scale bars = *5* μm

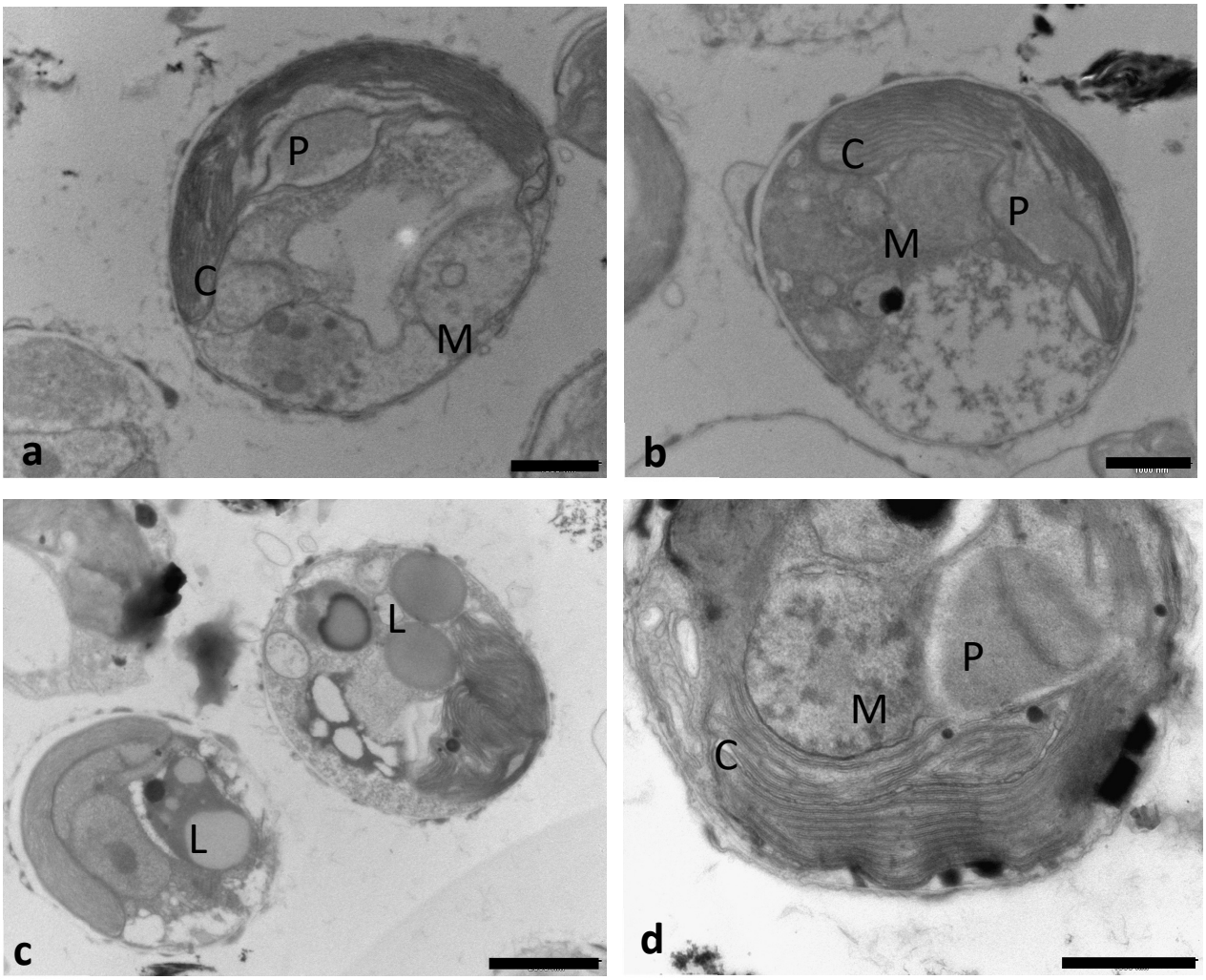

Figure 4 Transmission electron micrographs of mono-cultivated cells of *T. lutea* at 14 days of cultivation under white (a, b) and red-enriched light (c, d). C chloroplast; L lipid globules; M mitochondrion; P pyrenoid. Scale bars (μm): a, b, d = 1; c = 7

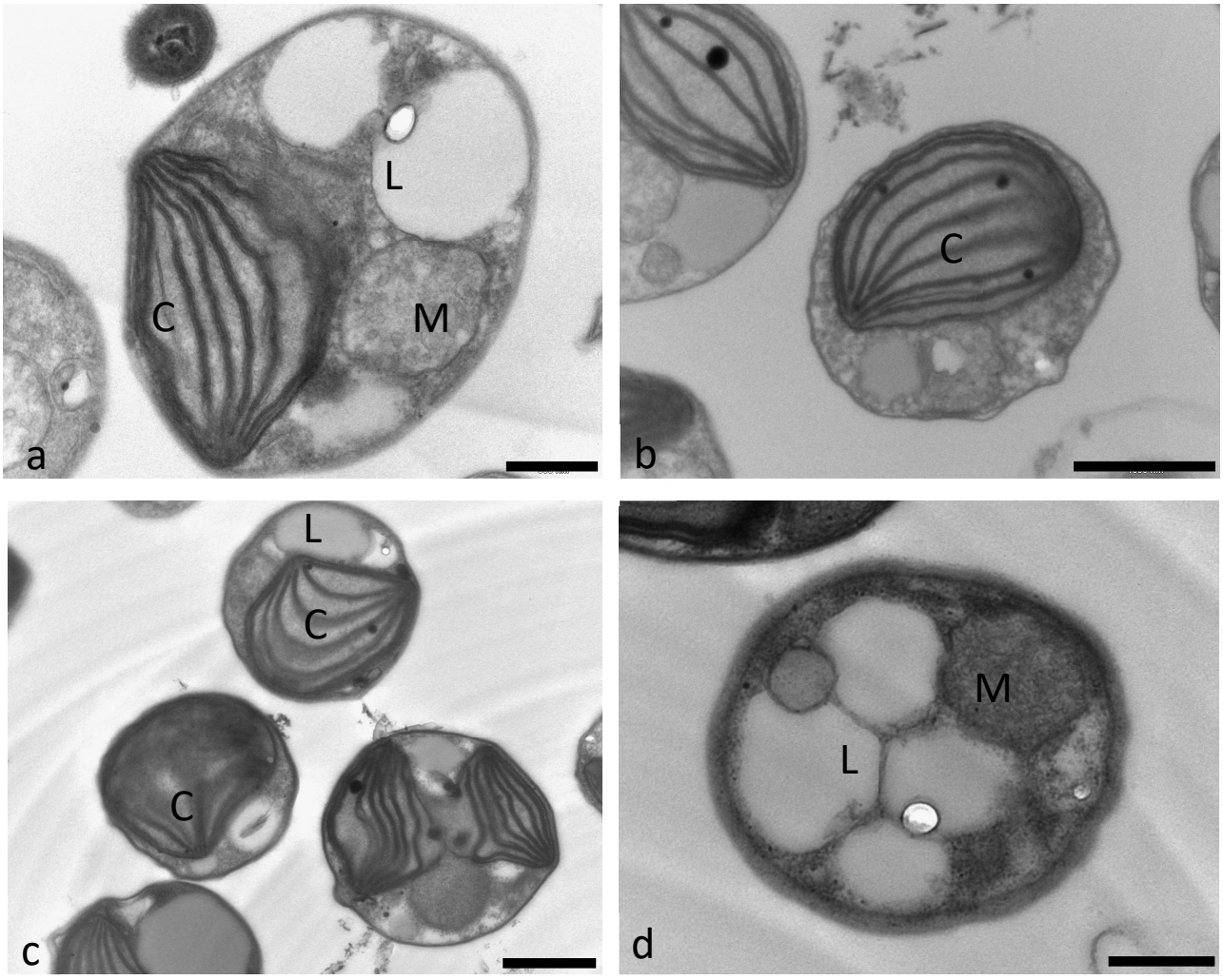

Figure 5 Transmission electron micrographs of mono-cultivated cells of *N. oculata* at 14 days of cultivation under white (a, b) and red-enriched light (c, d). C chloroplast; L lipid globules; M mitochondrion. Scale bars (μm): a, d = 0.5; b, c = 1

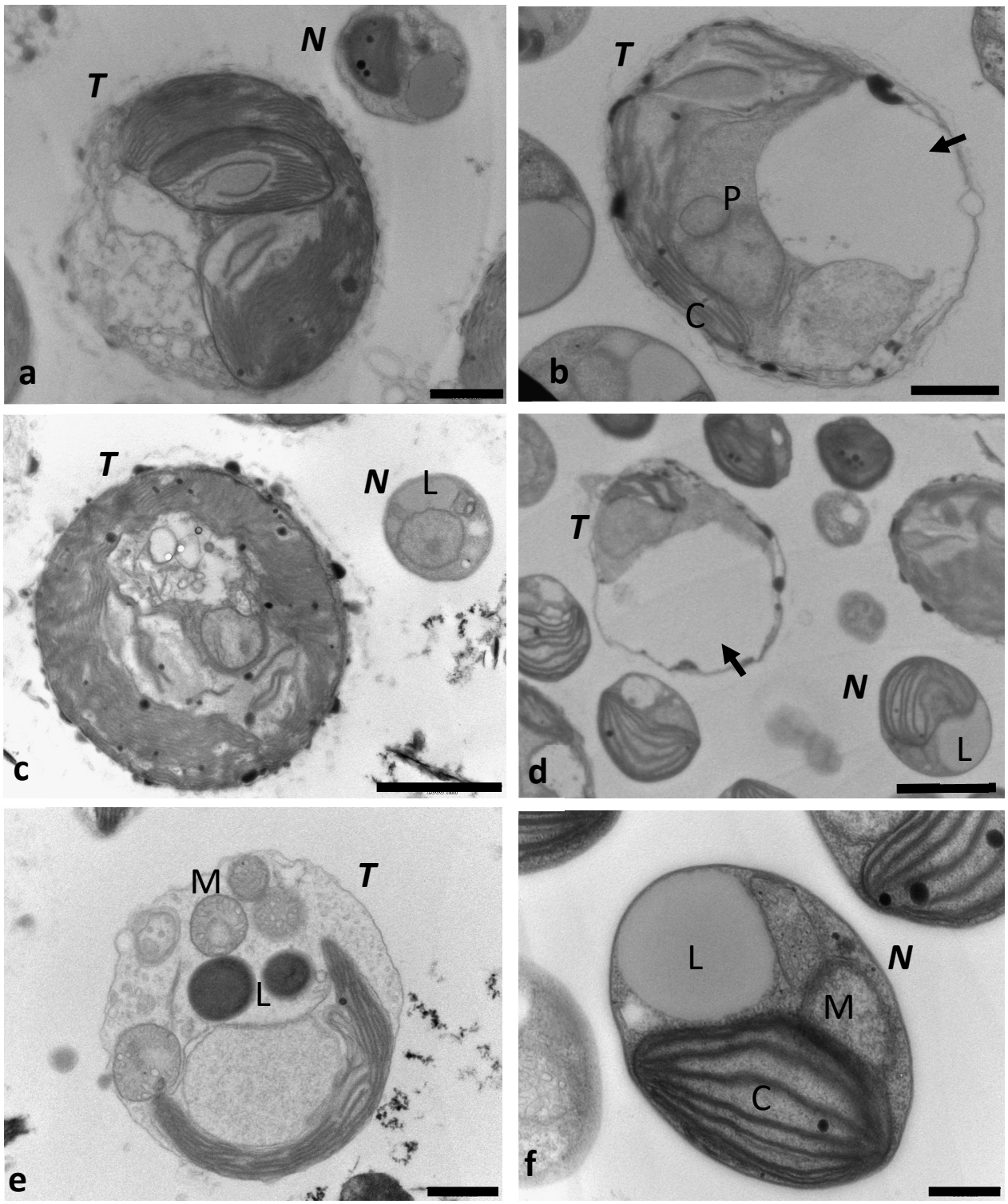

Figure 6 Transmission electron micrographs of co-cultivated cells of *T. lutea (T)* and *N. oculata (N)* at 14 days of cultivation under white (a, b, c) and red-enriched light (d, e, f). C chloroplast; L lipid globules; M mitochondrion. Arrows: empty areas in the cytosol. Scale bars (μm): a, b, e = 1; c, d = 2; f = 0.5

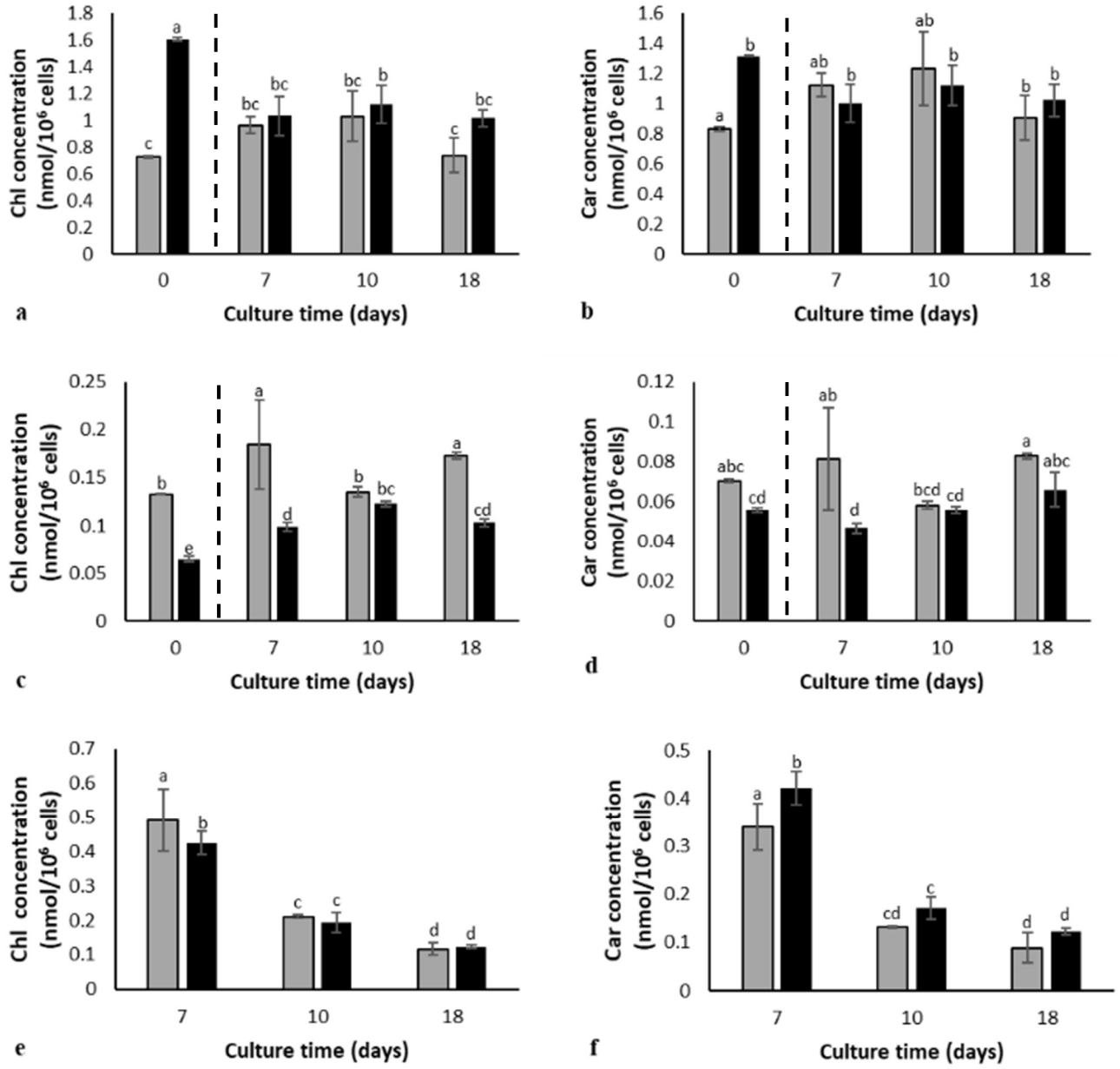

Figure 7 Time-course variations of pigment content (nmol 10^{-6} cells) in *T. lutea* and *N. oculata* cells in mono-culture and in co-cultivated cells under white (grey) and red light (black). *T. lutea*: Chl (a) and carotenoids (b) content; *N. oculata*: Chl (c) and carotenoids (d) content; co-cultivated cells: Chl (e) and carotenoids (f) content. In a-d the dushed lines separe pigment concentration values of day 0 that are referred to the cultures used for the inoculum. They are therefore only shown in the histograms for mono-cultures. Values are means ± SD (n = 3). Different letters indicate statistically significant differences ($p < 0.05$, two-way ANOVA)

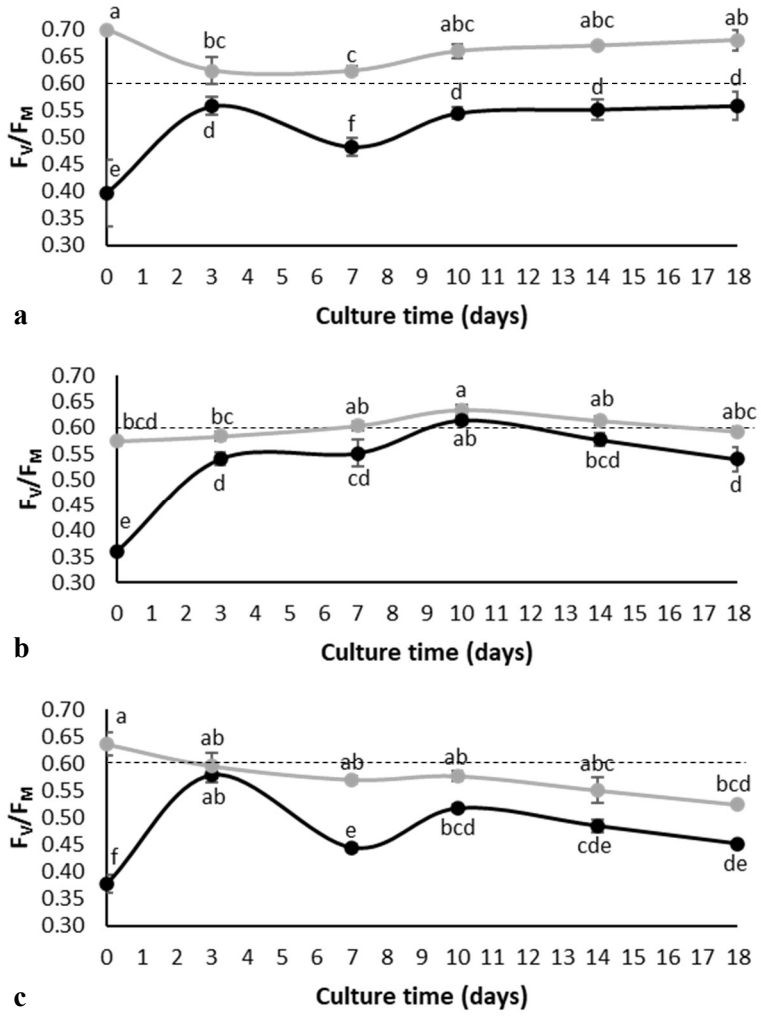

Figure 8 Time-course variations of F_V/F_M ratio in *T. lutea* and *N. oculata* cells mono-cultivated (a and b respectively) and co-cultivated cells (c) under white (grey) and red light (black). Dashed lines indicate the optimal 0.6 value of F_V/F_M. Values are means ± SD (n = 4). Different letters indicate statistically significant differences ($p < 0.05$, two-way ANOVA)

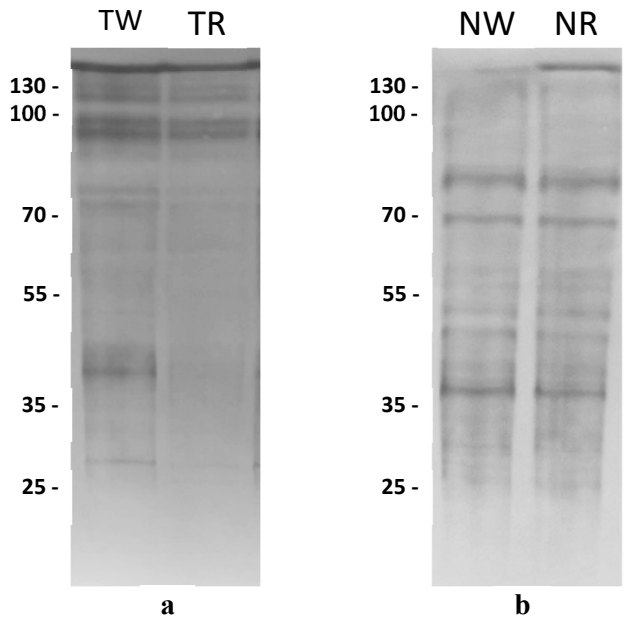

Figure 9 Thylakoid proteins were separated by SDS-PAGE and subsequently blotted on a nitrocellulose membrane. Ponceau stained membranes are shown. Thylakoid proteins of *T. luea* (a) grown under white (TW) and red light (TR), and of *N. oculate* (b) grown under white (NW) and red light (NR). Molecular weight (kDa) marker is reported on the left and corresponds to a Thermo Scientific™ PageRuler™ Plus Prestained Protein Ladders (#26619). Representative membranes are shown

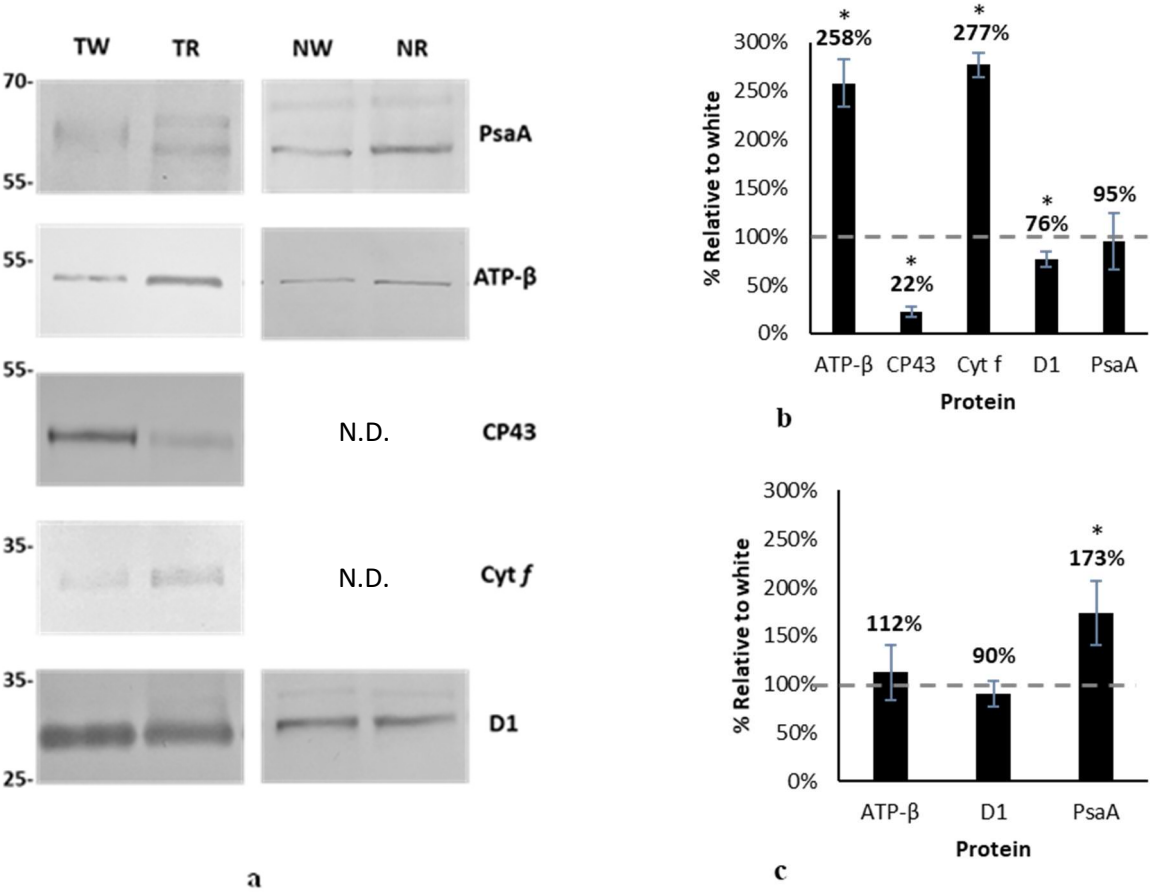

Figure 10 (a) Immunodetection of subunits representative for the main thylakoid protein complexes in *T. lutea* and *N. oculate* grown under white (TW and NW) and red light (TR and NR). Thylakoid proteins were separated by SDS-PAGE and blotted on a nitrocellulose membrane for immunodetection of PsaA subunit of PSI, ATP-β subunit of ATPase, CP43 subunit of PSII, Cyt *f* subunit of Cyt b_6f (only in *T. lutea*), D1 subunit of PSII. On gels were loaded 1 of Chl for ATP-β, D1, CP43 and 2 µg for PsaA, Cyt *f*. Molecular weight (kDa) marker is reported on the left and corresponds to a Thermo Scientific™ PageRuler™ Plus Prestained Protein Ladders (#26619). Representative membranes are shown. N.D. Not detected. (b, c) Protein band intensity was quantified with Image J freeware. Values are reported as relative % in figures b (*T. lutea*) and c (*N. oculata*). The values obtained from the white light samples were used as a reference (100% - dashed grey lines) to calculate the relative percentages referring to the values obtained from the red light samples (black bars). $^{*}p < 0.05$ (Student t-test)

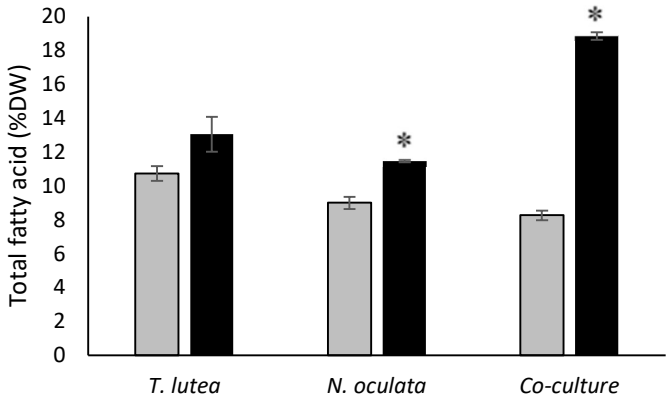

Figure 11 Fatty acid content (% DW) in mono-cultivated *T. lutea* and *N. oculata*, and in co-cultures at the 18th day of cultivation under white (grey) and red-enriched light (black). Values are means ± SD (n = 2). Asterisks identify significant differences between samples grown under different lighting. $^{*}p < 0.05$ (Student t-test)

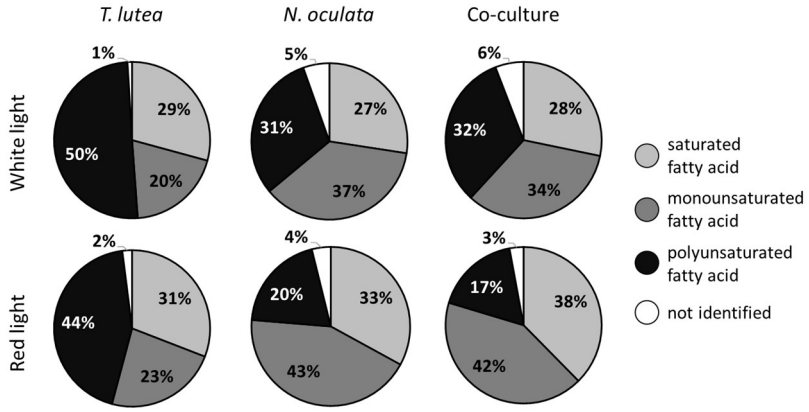

Figure 12 Relative proportions of fatty acids fractions (percentage of total fatty acids, %) in *T. lutea* and *N. oculata* mono-cultivated and in co-cultivated cells.

Table 1 Fatty acid profile (percentage of total fatty acids) in mono-cultivated *T. lutea* and *N. oculata* and in co-cultures at the 18th day of cultivation under white and red-enriched light. Values are means ± SD (n = 2)

Fatty acids	*T. lutea* white light		*T. lutea* red light		*N. oculata* white light		*N. ocualta* red light		Co-culture white light		Co-culture red light	
	Mean	SD	Mean	SD	Mean	SD	Mean	SD	Mean	SD	Mean	SD
14:0	19.61	0.05	19.14	0.54	4.53	0.04	5.08	0.01	6.04	0.03	5.39	0.01
16:0	9.92	0.28	12.96	1.93	23.31	0.49	28.54	0.56	22.49	0.44	30.21	0.17
16:1n7	6.08	0.05	4.13	0.00	31.11	0.26	34.20	0.28	26.23	0.10	29.41	0.10
16:2n4	1.90	0.52	1.48	0.24	0.67	0.02	0.25	0.29	0.88	0.09	0.44	0.01
18:1n9	9.55	0.35	15.94	0.48	4.06	0.11	7.71	0.07	5.49	0.10	10.38	0.05
18:1n7	1.22	0.08	0.90	0.02	0.25	0.31	0.24	0.28	0.83	0.01	0.44	0.01
18:2n6	2.73	0.02	2.29	0.20	4.42	0.16	3.98	0.05	4.23	0.07	3.81	0.00
18:3n3 (ALA)	7.85	0.07	5.44	0.68	--	--	--	--	0.55	0.01	0.58	0.02
18:4n3 (SDA)	30.51	0.42	21.73	2.58	--	--	--	--	2.55	0.11	2.27	0.01
20:1n9	3.34	0.02	3.11	0.02	--	--	--	--	--	--	0.42	0.04
20:4n6	--	--	--	--	4.55	0.00	3.82	0.09	5.01	0.03	2.79	0.03
20:5n3 (EPA)	--	--	0.46	0.60	24.78	0.08	15.30	0.00	22.69	0.62	10.05	0.15
22:6n3 (DHA)	6.44	0.10	11.09	0.89	--	--	--	--	--	--	1.44	0.00
other	0.85	0.01	1.34	0.06	2.32	0.32	0.90	0.46	3.04	0.60	2.36	0.14

Appendix

Table 1 Three-way ANOVA followed by Tukey post-hoc test results referred to the growth data of *T. lutea* under white and red light in mono-cultures and in co-culture at different culture time (Fig. 1). Means that do not share a letter are significantly different ($p < 0.05$).

Culture time (days)	Lighting conditions	Cultivation Mode	Mean	Groups								
18	White	Mono-cultivation	13.87	a								
14	White	Mono-cultivation	12.40	a								
18	Red	Mono-cultivation	9.95		b							
14	Red	Mono-cultivation	7.83			c						
10	Red	Mono-cultivation	4.46				d					
7	White	Mono-cultivation	4.25				d	e				
10	White	Mono-cultivation	4.02				d	e	f			
7	Red	Mono-cultivation	3.48				d	e	f	g		
7	Red	Co-Cultivation	3.21				d	e	f	g	h	
14	Red	Co-Cultivation	2.74				d	e	f	g	h	i
10	Red	Co-Cultivation	2.28					e	f	g	h	i
3	White	Mono-cultivation	2.21					e	f	g	h	i
3	Red	Cocultivation	2.07						f	g	h	i
18	Red	Cocultivation	2.00						f	g	h	i
3	Red	Mono-cultivation	1.98						f	g	h	i
18	White	Co-Cultivation	1.78						f	g	h	i
3	White	Co-Cultivation	1.54							g	h	i
14	White	Co-Cultivation	1.51							g	h	i
7	White	Co-Cultivation	1.22								h	i
0	Red	Co-Cultivation	1.19									i
0	Red	Mono-cultivation	1.17									i
10	White	Co-Cultivation	1.11								h	i
0	White	Mono-cultivation	0.85									i
0	White	Co-Cultivation	0.83									i

Table 2 Three-way ANOVA followed by Tukey post-hoc test results referred to the growth data of *N. oculata* under white and red light in mono-cultures and in co-culture at different culture time (Fig. 2). Means that do not share a letter are significantly different ($p < 0.05$).

Culture time (days)	Lighting conditions	Cultivation Mode	Mean	Groups						
14	White	Co-Cultivation	46.80	a						
18	White	Co-Cultivation	44.18	a						
18	Red	Co-Cultivation	42.50	a	b					
18	Red	Mono-cultivation	38.40		b					
14	White	Mono-cultivation	32.90			c				
18	White	Mono-cultivation	31.25			c	d			
14	Red	Co-Cultivation	29.64			c	d			
14	Red	Mono-cultivation	25.93				d	e		
10	White	Co-Cultivation	21.78					e		
10	White	Mono-cultivation	15.30						f	
10	Red	Co-Cultivation	12.64						f	
7	White	Co-Cultivation	12.60						f	
10	Red	Mono-cultivation	10.40						f	
7	Red	Co-Cultivation	5.57							g
7	Red	Mono-cultivation	5.52							g
7	White	Mono-cultivation	4.75							g
3	Red	Co-Cultivation	3.15							g
3	White	Co-Cultivation	3.10							g
3	Red	Mono-cultivation	3.07							g
3	White	Mono-cultivation	1.72							g
0	Red	Mono-cultivation	1.13							g
0	Red	Co-Cultivation	1.01							g
0	White	Mono-cultivation	0.95							g
0	White	Co-Cultivation	0.93							g

References

Abd Rahman N, Ramli A, Jumbri K, Uemura Y (2020) Biodiesel Production from *N. oculata* Microalgae Lipid in the Presence of Bi_2O_3/ZrO_2 Catalysts. Waste Biomass Valor 11, 553–564. https://doi.org/10.1007/s12649-019-00619-8

Al-amshawee S, Yunus MYBM (2019) Influence of light emitting diode (LED) on microalgae. Journal of Chemical Engineering and Industrial Biotechnology, 5(2), 9-16. https://doi.org/10.15282/jceib.v5i2.3771

Amaro HM, Pagels F, Azevedo IC, Azevedo J, Pinto IS, Malcata FX, Guedes AC (2020) Light-emitting diodes—a plus on microalgae biomass and high-value metabolite production. J Appl Phycol 32, 3605–3618. https://doi.org/10.1007/s10811-020-02212-2

Baldev E, Ali DM, Pugazhendhi A, Thajuddin N (2021). Wastewater as an economical and ecofriendly green medium for microalgal biofuel production. Fuel, 294, 120484. https://doi.org/10.1016/j.fuel.2021.120484

Baldisserotto C, Demaria S, Accoto O, Marchesini R, Zanella M, Benetti L, Avolio F, Maglie M, Ferroni L, Pancaldi S (2020) Removal of nitrogen and phosphorus from thickening effluent of an urban wastewater treatment plant by an isolated green microalga. Plants, 9, 1802. https://doi.org/10.3390/plants9121802

Baldisserotto C, Ferroni L, Giovanardi M, Boccaletti L, Pantaleoni L, Pancaldi S (2012) Salinity promotes growth of freshwater *Neochloris oleoabundans* UTEX 1185 (Sphaeropleales, Chlorophyta): morphophysiological aspects. Phycologia 51:700–710. https://doi.org/10.2216/11-099.1

Baldisserotto C, Giovanardi M, Ferroni L, Pancaldi S (2014) Growth, morphology and photosynthetic responses of *Neochloris oleoabundans* during cultivation in a mixotrophic brackish medium and subsequent starvation. Acta Physiol Plant 36:461–472. https://doi.org/10.1007/s11738-013-1426-3

Beardall J, Berman T, Heraud P, Kadiri MO, Light BR, Patterson G, Roberts S, Sulzberger B, Sahan E, Uehlinger U, Wood B (2001a) A comparison of methods for detection of phosphate limitation in microalgae. Aquat Sci 63:107–121. https://doi.org/1015-1621/01/010107-15

Beardall J, Young E, Roberts S (2001b) Approaches for determining phytoplankton nutrient limitation. Aquat Sci 63:44–69. https://doi.org/1015-1621/01/010044-26

Bendif EM, Probert I, Schroeder DC, de Vargas C (2013) On the description of *Tisochrysis lutea* gen. nov. sp. nov. and *Isochrysis nuda* sp. nov. in the Isochrysidales, and the transfer of *Dicrateria* to the Prymnesiales (Haptophyta). J Appl Phycol 25**,** 1763–1776. https://doi.org/10.1007/s10811-013-0037-0

Benvenuti G, Bosma R, Cuaresma M, Janssen M, Barbosa MJ, Wijffels RH (2015) Selecting microalgae with high lipid productivity and photosynthetic activity under nitrogen starvation. J Appl Phycol 27:1425–1431. https://doi.org/10.1007/s10811-014-0470-8

Bhola VK, Swalaha FM, Nasr M, Kumari S, Bux F (2016) Physiological responses of carbon-sequestering microalgae to elevated carbon regimes. Eur J Phycol 51:401–412. https://doi.org/10.1080/09670262.2016.1193902

Cao Y, Liu W, Xu X, Zhang H, Wang J, Xian M (2014) Production of free monounsaturated fatty acids by metabolically engineered Escherichia coli. Biotechnol Biofuels. Apr 10;7:59. doi: 10.1186/1754-6834-7-59. PMID: 24716602; PMCID: PMC4021618. https://dx.doi.org/10.1186%2F1754-6834-7-59

Cheng P, Cheng JJ, Cobb K, Zhou C, Zhou N, Addy M, Chen P, Yan X, Ruan R (2020) *Tribonema* sp. and *Chlorella zofingiensis* co-culture to treat swine wastewater diluted with fishery wastewater to facilitate harvest. Bioresource Technology, Volume 297, 122516. https://doi.org/10.1016/j.biortech.2019.122516

Chua ET, Dal'Molin C, Thomas-Hall S, Netzel ME, Netzel G, Schenk PM (2020) Cold and dark treatments induce omega-3 fatty acid and carotenoid production in *Nannochloropsis oceanica*. Algal Research, Volume 51, 102059. https://doi.org/10.1016/j.algal.2020.102059

Cosgrove J, Borowitzka MA (2010) Chlorophyll fluorescence terminology: an introduction. In: Suggett DJ, Prášil O, Borowitzka MA (eds) Chlorophyll *a* fluorescence in aquatic sciences: methods and applications. Springer, Dordrecht, pp 1–17. https://doi.org/10.1007/978-90-481-9268-7_1

da Silva Ferreira V, Sant'Anna C (2017) Impact of culture conditions on the chlorophyll content of microalgae for biotechnological applications. World J Microbiol Biotechnol 33:20. https://doi.org/10.1007/s11274-016-2181-6

del Pilar Sánchez-Saavedra M, Maeda-Martínez AN, Acosta-Galindo S (2016) Effect of different light spectra on the growth and biochemical composition of *Tisochrysis lutea* . J Appl Phycol 28**,** 839–847 https://doi.org/10.1007/s10811-015-0656-8

Faé Neto WA, Borges Mendes CR, Abreu PC (2018) Carotenoid production by the marine microalgae *Nannochloropsis oculata* in different low-cost culture media. Aquac Res. 49: 2527– 2535. https://doi.org/10.1111/are.13715

Falkowski PG, Sukenik A, Herzig R (1989) Nitrogen limitation in *Isochrysis galbana* (Haptophyceae). ii. relative abundance of chloroplast proteins. J. Phycol. 10.1111/j.1529-8817.1989.tb00252.x

Ferroni L, Baldisserotto C, Giovanardi M, Pantaleoni L, Morosinotto T, Pancaldi S (2011) Revised assignment of room-temperature chlorophyll fluorescence emission bands in single living cells of *Chlamydomonas reinhardtii*. J Bioenerg Biomembr 43:163–173. https://doi.org/10.1007/s10863-011-9343-x

Forján E, Garbayo I, Casal C, Vílchez C, Forján Lozano E, Garbayo Nores I, Vílchez C (2007) Enhancement of carotenoid production in *Nannochloropsis* by phosphate and sulphur limitation. Communicating Current Research and Educational Topics and Trends in Applied Microbiology, 1, 356–364. http://rabida.uhu.es/dspace/handle/10272/45

Gao F, Teles I (Cabanelas, ITD), Ferrer-Ledo N, Wijffels RH, Barbosa MJ (2020) Production and high throughput quantification of fucoxanthin and lipids in *Tisochrysis lutea* using single-cell fluorescence, Bioresource Technology, Volume 318, 124104. https://doi.org/10.1016/j.biortech.2020.124104

Gao F, Woolschot S, Cabanelas ITD, Wijffels RH, Barbosa MJ (2021) Light spectra as triggers for sorting improved strains of *Tisochrysis lutea*, Bioresource Technology, Volume 321, 124434. https://doi.org/10.1016/j.biortech.2020.124434

Gauthier MR, Senhorinho GNA, Scott JA (2020) Microalgae under environmental stress as a source of antioxidants, Algal Research, Volume 52, 102104. https://doi.org/10.1016/j.algal.2020.102104

Giovanardi M, Ferroni L, Baldisserotto C, Tedeschi P, Maietti A, Pantaleoni L, Pancaldi S (2013) Morphophysiological analyses of *Neochloris oleoabundans* (Chlorophyta) grown mixotrophically in a carbon-rich waste product. Protoplasma 250:161–174. https://doi.org/10.1007/s00709-012-0390-x

Giovanardi M, Pantaleoni L, Ferroni L, Pagliano C, Albanese P, Baldisserotto C, Pancaldi S (2018) In pea stipules a functional photosynthetic electron flow occurs despite a reduced dynamicity of LHCII association with photosystems. Biochimica et Biophysica Acta (BBA) - Bioenergetics, Volume 1859, Issue 10, Pages 1025-1038. https://doi.org/10.1016/j.bbabio.2018.05.013

Giovanardi M, Poggioli M, Ferroni L, Lespinasse M, Baldisserotto C, Aro E-M, Pancaldi S (2017) Higher packing of thylakoid complexes ensures a preserved Photosystem II activity in mixotrophic *Neochloris oleoabundans*. Algal Research, Volume 25, Pages 322-332. https://doi.org/10.1016/j.algal.2017.05.020

Gopinath A, Puhan S, Nagarajan G (2010) Effect of unsaturated fatty acid esters of biodiesel fuels on combustion, performance and emission characteristics of a DI diesel engine. International Journal of Energy & Environment, (3)

He Y, Zhang B, Guo S, Guo Z, Chen B, Wang M (2020) Sustainable biodiesel production from the green microalgae Nannochloropsis: Novel integrated processes from cultivation to enzyme-assisted extraction and ethanolysis of lipids. Energy Conversion and Management,Volume 209, 112618. https://doi.org/10.1016/j.enconman.2020.112618

Hibberd DJ (1981) Notes on the taxonomy and nomenclature of the algal classes Eustigmatophyceae and Tribophyceae (synonym Xanthophyceae). Botanical journal of the linnean society 82.2: 93-119. https://doi.org/10.1111/j.1095-8339.1981.tb00954.x

Hu H, Ma L-L, Shen X-F, Li J-Y, Wang H-F, Zeng RJ (2018) Effect of cultivation mode on the production of docosahexaenoic acid by *Tisochrysis lutea.* AMB Expr., 8 (1). https://doi.org/10.1186/s13568-018-0580-9

Järvi S, Suorsa M, Paakkarinen V, Aro E-M (2011) Optimized native gel systems for separation of thylakoid protein complexes: novel super- and mega-complexes. Biochem J 15 October 2011; 439 (2): 207–214. https://doi.org/10.1042/BJ20102155

Kim CW, Sung M-G, Nam K, Moon M, Kwon J-H, Yang J-W (2014) Effect of monochromatic illumination on lipid accumulation of *Nannochloropsis gaditana* under continuous cultivation. Bioresource Technology, Volume 159, Pages 30-35, ISSN 0960-8524, https://doi.org/10.1016/j.biortech.2014.02.024

Kwan PP, Banerjee S, Shariff M, Yusoff FM (2021) Influence of light on biomass and lipid production in microalgae cultivation. Aquaculture Research. 2021; 52: 1337– 1347. https://doi.org/10.1111/are.15023

Laemmli U (1970) Cleavage of structural proteins during the assembly of the head of Bacteriophage T4. Nature 227, 680–685. https://doi.org/10.1038/227680a0

Lepage G, Roy CC (1984) Improved recovery of fatty acid through direct transesterification without prior extraction or purification. Journal of Lipid Research, Volume 25, Issue 12, Pages 1391-1396. https://doi.org/10.1016/S0022-2275(20)34457-6

Li Y, Liu J (2020) Analysis of light absorption and photosynthetic activity by *Isochrysis galbana* under different light qualities. *Aquac Res*. 51: 2893– 2902. https://doi.org/10.1111/are.14628

Liu J, Song Y, Qiu W (2017) Oleaginous microalgae *Nannochloropsis* as a new model for biofuel production: review & analysis. Renewable and Sustainable Energy Reviews, 72, 154-162. https://doi.org/10.1016/j.rser.2016.12.120

López-Rosales AR, Ancona-Canché K, Chavarria-Hernandez JC, Barahona-Pérez F, Toledano-Thompson T, Garduño-Solórzano G, López-Adrian S, Canto-Canché B, Polanco-Lugo E, Valdez-Ojeda R (2019) Fatty Acids, Hydrocarbons and Terpenes of *Nannochloropsis* and *Nannochloris* Isolates with Potential for Biofuel Production. Energies.; 12(1):130. https://doi.org/10.3390/en12010130

Ma R, Thomas-Hall SR, Chua ET, Eltanahy E, Netzel ME, Netzel G, Lu Y, Schenk PM (2018) LED power efficiency of biomass, fatty acid, and carotenoid production in *Nannochloropsis* microalgae. Bioresource Technology, Volume 252, Pages 118-126. https://doi.org/10.1016/j.biortech.2017.12.096

Maglie M, Baldisserotto C, Guerrini A, Sabia A, Ferroni L, Pancaldi S (2021) A co-cultivation process of *Nannochloropsis oculata* and *Tisochrysis lutea* induces morpho-physiological and biochemical variations potentially useful for biotechnological purposes. J Appl Phycol 33**,** 2817–2832. https://doi.org/10.1007/s10811-021-02511-2

Maltsev Y, Maltseva K, Kulikovskiy M, Maltseva S (2021) Influence of Light Conditions on Microalgae Growth and Content of Lipids, Carotenoids, and Fatty Acid Composition. *Biology*.; 10(10):1060. https://doi.org/10.3390/biology10101060

Matsui H, Intoy MMB, Waqalevu V, Ishikawa M, Kotani T (2020) Suitability of *Tisochrysis lutea* at different growth phases as an enrichment diet for *Brachionus plicatilis* sp. complex rotifers. J Appl Phycol 32:3933–3947. https://doi.org/10.1007/s10811-020-02216-y

Matsui H, Shiozaki K, Okumura Y, Ishikawa M, Waqalevu V, Hayasaka O, Honda A, Kotani T (2020) Effects of phosphorous deficiency of a microalga *Nannochloropsis oculata* on its fatty acid profiles and intracellular structure and the effectiveness in rotifer nutrition, Algal Research, Volume 49, 101905. https://doi.org/10.1016/j.algal.2020.101905

Mayer C, Richard L, Côme M, Ulmann L, Nazih H, Chénais B, Ouguerram K, Mimouni V (2021) The Marine Microalga, *Tisochrysis lutea*, Protects against Metabolic Disorders Associated with Metabolic Syndrome and Obesity. *Nutrients*. 13(2):430. https://doi.org/10.3390/nu13020430

Mirkovic T, Ostroumov EE, Anna JM, van Grondelle R, Govindjee, Scholes GD (2017) Light absorption and energy transfer in the antenna complexes of photosynthetic organisms. Chem Rev 117:249–293. https://doi.org/10.1021/acs.chemrev.6b00002

Misund B, Oglend A, Mezzalira Pincinato RB (2017) The rise of fish oil: from feed to human nutritional supplement. Aquac Econ Manag 21:185–210. https://doi.org/10.1080/13657305.2017.1284942

Nwoba EG, Parlevliet DA, Laird DW, Alameh K, Moheimani NR (2019) Light management technologies for increasing algal photobioreactor efficiency. Algal Research, Volume 39, 101433, https://doi.org/10.1016/j.algal.2019.101433

Oostlander PC, Van Houcke J, Wijffels RH, Barbosa MJ (2020) Optimization of *Rhodomonas* sp. under continuous cultivation for industrial applications in aquaculture. Algal Res., 47, 101889. https://doi.org/10.1016/j.algal.2020.101889

Patil S, Arvind ML, Gunjan P (2020) An efficient algae cell wall disruption methodology for recovery of intact chloroplasts from microalgae. Journal of Applied Biology & Biotechnology Vol 8.03: 23-28. http://doi.org/10.7324/JABB.2020.80305

Pham KT, Nguyen TC, Luong TH, Dang PH, Vu DC, Do TN, Phi TCM, Nguyen DB (2018) Influence of inoculum size, CO2 concentration and LEDs on the growth of green microalgae *Haematococcus pluvialis* Flotow. Vietnam Journal of Science, Technology and Engineering, v. 60, n. 4, p. 59-65. https://doi.org/10.31276/VJSTE.60(4).59-65

Ra CH, Sirisuk P, Jung JH, Jeong G-T, Kim S-K (2018) Effects of light-emitting diode (LED) with a mixture of wavelengths on the growth and lipid content of microalgae. Bioprocess Biosyst Eng 41, 457–465. https://doi.org/10.1007/s00449-017-1880-1

Raqiba H, Sibi G (2019) Light emitting diode (LED) illumination for enhanced growth and cellular composition in three microalgae. Adv. Microb. Res., 3, 007. http://dx.doi.org/10.24966/AMR-694X/100007

Rasdi NW, Qin JG (2015) Effect of N:P ratio on growth and chemical composition of *Nannochloropsis oculata* and *Tisochrysis lutea*. J Appl Phycol 27:2221–2230. https://doi.org/10.1007/s10811-014-0495-z

Ray A, Nayak M, Ghosh A (2022) A review on co-culturing of microalgae: A greener strategy towards sustainable biofuels production. Science of The Total Environment, Volume 802, 149765, https://doi.org/10.1016/j.scitotenv.2021.149765

Redel-Macías MD, Pinzi S, Ruz MF, Cubero-Atienza AJ, Dorado MP (2012) Biodiesel from saturated and monounsaturated fatty acid methyl esters and their influence over noise and air pollution. Fuel, Volume 97, Pages 751-756. https://doi.org/10.1016/j.fuel.2012.01.070

Ritchie RJ (2006) Consistent sets of spectrophotometric chlorophyll equations for acetone, methanol and ethanol solvents. Photosynth Res 89:27–41. https://doi.org/10.1007/s11120-006-9065-9

Sá M, Ferrer-Ledo N, Wijffels R, Crespo JG, Barbosa M, Galinha CF (2020) Monitoring of eicosapentaenoic acid (EPA) production in the microalgae *Nannochloropsis oceanica*. Algal Research, Volume 45, 101766. https://doi.org/10.1016/j.algal.2019.101766

Schulze PS, Barreira LA, Pereira HG, Perales JA, Varela JC (2014) Light emitting diodes (LEDs) applied to microalgal production. *Trends in biotechnology*, *32*(8), 422-430. https://doi.org/10.1016/j.tibtech.2014.06.001

Schulze PSC, Pereira HGC, Santos TFC, Schueler L, Guerra R, Barreira LA, Perales JA, Varela JCS (2016) Effect of light quality supplied by light emitting diodes (LEDs) on growth and biochemical profiles of *Nannochloropsis oculata* and *Tetraselmis chuii*. Algal Res., 16 (2016), pp. 387-398. https://doi.org/10.1016/j.algal.2016.03.034

Shimakawa G, Miyake C (2018) Oxidation of P700 ensures robust photosynthesis. Frontiers in plant science, 9, 1617. https://doi.org/10.3389/fpls.2018.01617

Su C, Chien LJ, Gome J et al (2011) Factors affecting lipid accumulation by *Nannochloropsis oculata* in a two-stage cultivation process. J Appl Phycol 23:903–908. https://doi.org/10.1007/s10811-010-9609-4

Tejido-Nuñeza Y, Aymerich E, Sancho L, Refardt D (2020) Co-cultivation of microalgae in aquaculture water: interactions, growth and nutrient removal efficiency at laboratory- and pilot-scale. Algal Res 49:101940. https://doi.org/10.1016/j.algal.2020.101940

Tikkanen M, Aro E-M (2014) Integrative regulatory network of plant thylakoid energy transduction. Trends in Plant Science, Volume 19, Issue 1, Pages 10-17. https://doi.org/10.1016/j.tplants.2013.09.003

Tikkanen M, Grieco M, Nurmi M, Rantala M, Suorsa M, Aro E-M (2012) Regulation of the photosynthetic apparatus under fluctuating growth light. Phil. Trans. R. Soc. B3673486–3493. http://doi.org/10.1098/rstb.2012.0067

Tocher DR, Betancor MB, Sprague M, Olsen RE, Napier JA (2019) Omega-3 Long-Chain Polyunsaturated Fatty Acids, EPA and DHA: Bridging the Gap between Supply and Demand. *Nutrients*. 11(1):89. https://doi.org/10.3390/nu11010089

Ueno Y, Aikawa S, Kondo A, Akimoto S (2019) Adaptation of light-harvesting functions of unicellular green algae to different light qualities. Photosynth Res 139, 145–154 https://doi.org/10.1007/s11120-018-0523-y

Van Vooren G, Le Grand F, Legrand J, Cuiné S, Peltier G, Pruvost J (2012) Investigation of fatty acids accumulation in *Nannochloropsis oculata* for biodiesel application. Bioresource Technology, 124, 421–432. https://doi.org/10.1016/j.biortech.2012.08.009

Wellburn AR (1994) The spectral determination of chlorophylls *a* and *b*, as well as total carotenoids, using various solvents with spectrophotometers of different resolution. J Plant Physiol 144:307–313. https://doi.org/10.1016/S0176-1617(11)81192-2

Wong YK, Ho YH, Lai YT, Tsang PM, Chow KP, Yau YH, Choi MC, Ho RSC (2016) Effects of light intensity, illumination cycles on microalgae *Haematococcus pluvialis* for production of astaxanthin. J. Mar. Biol. Aquacult., 2, 1–6.

Yamamoto H, Shikanai T (2019) PGR5-Dependent cyclic electron flow Protects Photosystem I under fluctuating light at donor and acceptor sides. Plant Physiology, Volume 179, Issue 2, February, Pages 588–600, https://doi.org/10.1104/pp.18.01343

Yuan H, Zhang X, Jiang Z, Wang X, Wang Y, Cao L, Zhang X (2020) Effect of light spectra on microalgal biofilm: cell growth, photosynthetic property, and main organic composition. Renewable Energy, Volume 157, Pages 83-89. https://doi.org/10.1016/j.renene.2020.04.109

Zhang Z, Fulgoni VL III, Kris-Etherton PM, Mitmesser SH (2018) Dietary Intakes of EPA and DHA Omega-3 Fatty Acids among US Childbearing-Age and Pregnant Women: An Analysis of NHANES 2001–2014. *Nutrients*.; 10(4):416. https://doi.org/10.3390/nu10040416

Zhu L, Li S, Hu T, Nugroho YK, Yin Z, Hu D, Chu R, Mo F, Liu C, Hiltunen E (2019) Effects of nitrogen source heterogeneity on nutrient removal and biodiesel production of mono- and mix-cultured microalgae. Energy Conversion and Management, Volume 201, 112144. https://doi.org/10.1016/j.enconman.2019.112144

Chapter 4

Waste-to-value approach: the production of lipids from the microalga *Tisochrysis lutea* using a reject brine

1. Introduction

World population growth together with global climate changes are leading to a continuous demand for water and to the impoverishment of the reserves, exacerbating the problem of water scarcity in many regions of the world (Damania et al., 2017; Jones et al. 2019). To meet the demand for water and overcome the problem of its scarcity, the use of desalination plants is increasing. In fact, when fresh water becomes scarce, its cost tends to rise, making desalination progressively more cost-effective (Pistocchi et al. 2020b). However, the desalination process involves environmental impacts related to energy consumption, land use, seawater intake and impacts related to the disposal and discharge of brine (Fernández-Torquemada et al. 2019; Jones et al. 2019). Brine represents the main by-product of water desalination process, is characterized by extreme salinity (1.6–2 times higher than the seawater salinity), and is treated as a waste, needing effective solutions for its disposal (Hanley 2018; Fernández-Torquemada et al. 2019; Panagopoulos et al. 2019; Sola et al. 2020). Nowadays, the production of brine is increasing worldwide: for example, Jones and coworkers (2019) estimated that desalination plants produce about 1.5 m^3 of brine per m^3 of desalinated water. In about 20% of cases, the brine is generated far from the coast, resulting in technical challenges for its disposal. In the remaining 80% of cases the brine is generally disposed in the seas and oceans. Overall, brine disposal represents both an economic and an environmental challenge. Indeed, brine may include trace concentrations of contaminants; moreover, its disposal from multiple plants operating close to each other for prolonged periods could negatively affect the sea environment (Jones et al. 2019; Aljohani et al. 2021). The quantity and quality of desalination brine and its chemical composition depend on feed water quality, water recovery rate, pretreatment, as well as on the substances added during the desalination process and on the release of contaminants from the desalination equipment (Panagopouloset al. 2019; Pistocchi et al. 2020b). Some of the substances contained in the brine can be recovered. In fact, concentrated brine could also facilitate the recovery of valuable minerals from seawater (e.g., sodium chloride, calcium carbonate, magnesium oxide, bromine, rubidium, uranium, lithium, sodium hydroxide, chlorine and acids and bases) (Cipolletta et al. 2021). Some authors support this approach to make desalination more cost-effective (e.g., Quist-Jensen et al. 2016; Loganathan et al. 2017). However, this approach is not always economically and environmentally advantageous, and in some contexts results more convenient to invest upstream, for example, in decarboxylation of the desalination process using renewable energies (Bogdanov et al. 2019; Hansen et al. 2019). The major environmental problems due to the discharge of brine into the sea may concern the high salinity of this by-product that can produce physical/chemical alterations to the seawater

around brine discharge outlets (Jones et al. 2019; Pistocchi et al. 2020a). Due to its higher density than that of seawater, brine settles on the seabed unless mixed with ocean water. Hypersalinity can damage or be lethal to marine organisms because it interferes with osmotic processes (Rodríguez-Rojas et al. 2020). In addition, its damaging effects can be increased by synergistic effects in combination with other stress factors, such as temperature, metal pollution and pH variations (Clark et al. 2018). Brine disposal has a particular impact on primary producers such as seagrass meadows and benthic communities (Pistocchi et al. 2020b). The impacts associated with brine are highly species- and ecosystem-specific; to date, studies are often at local scale, and it is difficult to extrapolate data on global impacts resulting from brine discharges (Clark et al. 2018; Rodríguez-Rojas et al. 2020). A partial mitigation of the harmful effects due to brine disposal on marine organisms can be achieved through different design and engineering approaches, for example using diffusers system that can increase the mixing of brine within the seawater column and prevent accumulation on the seabed (Missimer and Maliva 2018). On the other hands, some Authors propose a "waste-to-value" approach in managing brine using microalgae (Sánchez et al. 2015; Matos et al. 2017; Shirazi et al. 2018). Some studies are focusing on the potentialities of the biological desalination process, a method based on the absorption of salts by different salt-tolerant living organisms (Gan et al. 2016; Sahle-Demessie et al. 2019; Wei et al. 2020). However, brine can represent a source of nitrogen, phosphorus, and micronutrients for microalgae cultivation (Matos et al. 2017; Shirazi et al. 2018). Microalgae are well known to grow in a variety of wastewaters and industrial wastes (Giovanardi et al. 2013, 2016; Baldisserotto et al. 2020, 2021), coupling the biomass production with that of various high-value-added compounds, such as natural pigments and fatty acids, that are used in the pharmaceutical, cosmetics, food industries and in the green energy sector (Baldisserotto et al. 2020; Maglie et al. 2021; Torres et al. 2021). Furthermore, microalgae show high adaptability to a range of environmental variations, including high salinity (Ishika et al. 2018; Shetty et al. 2019; Yang et al. 2021). In this context, salinity is known as possible stress source for some microalgae species, e.g., limiting their growth (Ishika et al. 2018; Shetty et al. 2019; Mohamadnia et al. 2021). At the same time an increase of the salinity in the culture medium is often coupled with higher lipid content as the result of activation of specific metabolic reactions and overexpression or suppression of gene expression (Sun et al. 2018; Atikij et al. 2019; Yang et al. 2021). For example, Atikij and coworkers (2019) showed how, in *Chlamydomonas reinhardtii,* NaCl stress dramatically increased saturated fatty acids accounting for 70.2% of the total fatty acids, while KCl stress led to a slight increase in saturated fatty acids (47.05% of the fatty acid). NaCl-induced stress was found to up-regulate genes

involved in fatty acids biosynthesis. In *Dunaliella salina,* one of the most halotolerant and studied algae, β-ketoacyl-coenzyme A synthase is a salt-inducible enzyme that, together with fatty acid desaturases, seems to play a role in the adaptation of intracellular membranes to salinity, influencing the fatty acid elongation process (Nedbalová et al. 2016). However, the adaptive processes to high salinities and the effect of this source of stress on fatty acids production is not always clear or well-studied for all microalgal species (Nedbalová et al. 2016; Yang et al. 2021). In this study, we tested the growth and the lipid production of *Tisochrysis lutea* cultured in brine discharged by the Almería (Spain) desalination plant. Cultures in SWES medium prepared using artificial seawater (ESAW - 40‰) were used as controls. The Almería desalination plant employs reverse osmosis process to produce 50000 m^3/day of water characterized by an output salinity < 0.4‰ (input salinity: 38.5‰). The brine used in this study presents a salinity of 80‰, more than twice the normal salinity of seawater and synthetic medium used as control. Brine derived from the Almerìa plant is discharged at 430 m from the coast through an outfall. *T. lutea* is a marine microalga of the Haptophyta phylum (Bendif et al. 2013). The production of commercially valuable carotenoids such as fucoxanthin and important ω-3 fatty acid such as docosahexaenoic acid (DHA) makes *T. lutea* a microalga of biotechnological interest (Maglie et al. 2020; Mohamadnia et al. 2021; Premaratne et al. 2021). In marine microalgae the salinity tolerance range usually varies from 35‰ to 50‰ (Ishika et al. 2018). After a period of adaptation to different dilutions of brine with different salinity levels, a solution of brine and distilled water with a salinity of 65‰ was selected for the growth of *T. lutea*. The cultivation in 65‰ salinity-brine still presented some limitations, but it is noteworthy that the algal biomass obtained showed increased accumulation of neutral lipids and a promising blend of PUFAs, with the added advantage of a higher environmental sustainability linked to a less consumption of freshwater and valorisation and reuse of brine.

2. Materials and methods

Experimental design

In this experiment a dilution of reject brine (following also just “brine”) from Almería (Spain) desalination plant was employed to cultivate *Tisochrysis lutea*, strain CCAP 927/14, cells. In order to establish the maximal brine concentration for cultivating the microalgae, an initial screening was conducted in a 12 wells cell-culture plate using 2 mL of culture volume. Cells were inoculated in triplicate at a density of $1 \pm 0.1 \times 10^6$ cells mL^{-1} and cultured for 7 days under 60 $\mu mol_{photons}$ $m^{-2}s^{-1}$ PAR, in brine diluted with sterile deionized water at 50%, 60%, 70% and 80% resulting in a salinity of about 40‰, 50‰, 55‰ and 65‰, respectively. Cells cultivated

at a salinity of 65‰ were selected, scaled up and used as inocula in the experiments. Using cells adapted to the salinity of 65‰, cultivation trials were conducted in 90% dilution and undiluted brine, but without acceptable results (data not shown).

The first experimental phase was performed at the University of Ferrara. The growth of the microalgae was evaluated in batch mode. Brine diluted to 80% was used to evaluate the capacity of *T. lutea* to withstand to higher salinity than that of SWES medium used for maintenance and growth of standard cultures. *T. lutea* cells were inoculated at a density of $1 \pm 0.1 \times 10^6$ cells mL^{-1} and grown under 100 $\mu mol_{photons}\ m^{-2}s^{-1}$ PAR for 14 days, in 300-mL Erlenmeyer flasks (150 mL of total culture volume), using 80% diluted brine with a final salinity of 65‰. Cultures in SWES medium (salinity 40‰) were used as control. A cultivation test was also performed in SWES with a salinity of 65‰. However, the amount of precipitation formed during medium preparation was not compatible with the cultivation of *T. lutea* cells (data not shown). The cell density and maximum quantum yield of PSII (F_V/F_M ratio) were evaluated. In addition, microscopy observations in both light/fluorescence microscopy and transmission electron microscopy (TEM) were performed. Furthermore, the presence of lipid droplets was investigated via Nile Red *in vivo* staining. Once the possibility of cultivating *T. lutea* in diluted brine was confirmed and the presence of lipids in cells grown at high salinity was detected, the next phase of experimentation was carried out.

The second phase of experiment was performed at the Department of Chemical Engineering, University of Almería (Spain), in the laboratories directed by Prof. E Molina-Grima and thanks to the precious collaboration of Prof. T Mazzuca-Sobczuk. *T. lutea* cells were inoculated at a density of $1 \pm 0.1 \times 10^6$ cells mL^{-1} using 80% diluted brine (salinity of 65‰) and SWES medium (salinity 40‰) as control. Cultures grew under 100 $\mu mol_{photons}\ m^{-2}s^{-1}$ PAR in 2.5 L bubble column photobioreactors (2 L of total culture volume) with no CO_2 insufflation except that normally present in the flushed air used to mix the culture (CO_2: about 0.4%; flux: 1 L min^{-1}). Cells were grown in batch mode until the 8^{th} day, when the cultures reached a cell density sufficient for the start of the semi-continuous phase of the experiment. From the 8^{th} until the 18^{th} day, microalgae were cultivated in semi continuous mode: 10% of the culture was daily removed and replaced with new culture medium or diluted brine. The biomass daily collected was used for analysis. In fact, during the stationary phase of growth, the photosynthetic pigments content and the accumulation of neutral lipids, were evaluated. Furthermore, the total fatty acid profile was determined. The results of these analyses are obtained from the average

of daily measurements during the semi-continuous phase of the experimentation (8-18 days) and the cells were in a stable condition.

Algal strain and culture condition

Tisochrysis lutea (Bendif et al. 2013; strain CCAP 927/14) were obtained from the Culture Collection of Algae and Protozoa of Scottish Marine Institute (Scotland, UK; www.ccap.ac.uk). Axenic cultures were maintained in liquid SWES medium (Sea Water Erddekokt Salze medium; www.epsag.uni-goettingen.de) in a growth chamber (25 ± 1 °C), 16:8 h light-dark photoperiod, 100 $\mu mol_{photons}\ m^{-2}s^{-1}$ photosynthetically active radiation (PAR), without additional CO_2 supply according to Maglie and coworkers (2021) and were used as algae inocula for the initial screening and control cultures.

Growth estimation

For both control and brine-treated cultures, the inoculum was performed using dense cultures diluted until a cell density of $1 \pm 0.1 \times 10^6$ cells mL^{-1}. Growth was estimated by measuring the optical density at 750 nm and by counting the cells with a Thoma's chamber (HBG, Germany) sampling 1 mL of culture. To make the cell counting easier, 100 µL of Lugol's iodine was added to 1 mL of culture to stop cell movement (Maglie et al. 2021).

Characteristics of rejected brine

Rejected brine was gently provided by the Almería (Spain) desalination plant (04120 El Bobar, Almería, Spain. 36.817067957612146, -2.424135015341435). Quantitative determination of chemical elements was performed through inductively coupled plasma-mass spectrometry (ICP-MS) using a Thermo Electron Corporation X series spectrometer (Thermo Fisher Scientific). The analysis was performed at the Department of Physics and Earth Science of the University of Ferrara in the laboratories directed by Prof. M Coltorti and thanks to the precious collaboration of Dr. R Tassinari. The samples of brine were also analyzed for nitrogen and phosphorus content at the Department of Environmental and Prevention Sciences (University of Ferrara) - Applied Botany Section in laboratories coordinated by Prof. R Gerdol and thanks to the precious collaboration of Dr R Marchesini. In detail, $N\text{-}NH_4$ was analyzed by the salicylate method, $N\text{-}NO_3$ by the cadmium reduction method, $P\text{-}PO_4$ and total P by the molybdenum blue method, using a continuous flow analyzer (FlowSys, Systea, Roma, Italy). The characteristics of rejected brine are summarized in Table 1.

Batch experiment

Light and fluorescence microscopy

Cell samples were observed under a Zeiss Axiophot microscope equipped with conventional or fluorescent attachments. The light source for chlorophyll fluorescence examinations was an HBO 100 W pressure mercury vapour lamp (filter set, BP436/10 FT 460, LP470). To highlight the intracellular lipid accumulation, cells were stained with Nile Red, NR (9-diethylamina-5Hbenzo[α]phenoxazine-5-one; Sigma-Aldrich, Gallarate, Milano, Italy) according to Giovanardi et al. (2013), with some modifications. Aliquots of 10 μL NR (0.5 mg dissolved in 100 mL acetone) were added to 1.9 mL of a cell suspension with 0.5×10^6 cells. After incubation at 37 °C in darkness for 15 min, cells were observed with 485 nm excitation wavelength (filter set BP485, LP520). All pictures were taken with a VisiCAM PR0 20C digital camera managed by a pc thanks to the WaveImage software.

Transmission electron microscopy

For transmission electron microscopy (TEM), cells were harvested by centrifugation and prepared as reported in Baldisserotto et al. (2020) with minor modifications according to Maglie et al. (2021): the phosphate buffer was substituted with 0.1 M sodium cacodylate buffer (pH 7.2) and 0.25 M sucrose. Ultra-thin sections were observed with a Zeiss EM910 transmission electron microscope (Electron Microscopy Centre, University of Ferrara).

Chlorophyll fluorescence measurements

Fluorescence measurements were performed on cell pellets prepared as described by Ferroni et al. (2011). After 15 min of dark incubation, initial fluorescence F_0 and maximum fluorescence F_M were used to calculate the maximum quantum yield of PSII (F_V/F_M ratio). Fifteen minutes were found to be the optimal adaptation time after testing a range between 5 and 40 min of dark adaptation time. For analyses, a pulse amplitude modulation fluorometer (PAM; Junior-PAM, Walz, Germany) was used with the following setting: measuring light (ML) with intensity and frequency at level 1; 0.6 s saturation pulse at level 6.

Semi-continuous experiment

Photosynthetic pigment extraction and analysis

During the stationary phase of growth (days 8-18), cells were collected each day to evaluate the photosynthetic pigments content. The results obtained were averaged together. Cells were

treated with 100% methanol for 10 min at 80 °C (Baldisserotto et al. 2012). Absorption of extracts was measured at 665 nm for chlorophyll *a* (Chl *a*), 632 nm for chlorophyll *c* (Chl *c*) and 470 nm for carotenoids (Cars) (Wellburn 1994; Ritchie 2006). Extracts were manipulated under dim light to avoid photo-degradation. Chlorophyll *a* and *c* concentration was evaluated using the equations of Ritchie (2006). Otherwise, the equations of Wellburn (1994) were employed to determine the carotenoid concentration.

Fluorometric analysis: neutral lipid content evaluation using Nile Red

During the stationary phase of growth (days 8-18), cells were collected each day to evaluate the intracellular neutral lipid content by measuring fluorescence after staining with Nile Red. The results obtained were averaged together. According to Gao et al. (2020) with minor modifications, the cultures were diluted to OD_{750} = 0.2 using fresh medium or diluted brine. Cells were stained with NR (final concentration 2 μg mL^{-1}) in dark and agitation for 10 min at 37 °C. An amount of 100 μL of the stained cell suspension was pipetted at least in triplicate in a black 96-well plate. The NR fluorescence was measured from the top using a FLUOstar OPTIMA FL - Microplate Reader by BMG LABTECH at an excitation wavelength of 488 nm with emission wavelength of 575 nm. The autofluorescence was measured using the same procedure on *T. lutea* cells without NR staining and was used as blank. Milk diluted in fresh medium (1μL/mL) stained with NR represented the positive control.

Fatty acid determination by gas chromatography

During the stationary state (days 8-18), cells were collected each day to perform fatty acids analysis. The results obtained were averaged together. Fatty acids were methylated by the method described for transesterification by Lepage and Roy (1984). A gas chromatograph Hewlett Packard model 5890 Series II (Hewlett Packard Company, Avondale, PA) was used. 20 mg of biomass were weighted into a glass tube and 1 mL of hexane was added to the sample. Then 1 mL of methylation mixture (methanol / acetyl chloride in the ratio 20:1) was added. 10 μL of standard solution were added to the sample using a Hamilton syringe; the standard solution consisted of 25 mg of heptadecanoic acid (17:0) in 1 mL of toluene. The tubes were placed in the ultrasound for 5 min. The transesterification reaction took place at 100 ºC for 1 h, in a metal block thermostat, model Multiplace, provided by Selecta (JP Selecta SA, Barcelona). The tubes were shaken every 10 min. When the reaction was over, the tubes were cooled, and 1 mL of distilled water and 0.5 mL of hexane were added to the sample to obtain two phases. For the biomass, the phase separation was performed by centrifugation at 450 g for 3 min. The

hexane phase was introduced into a vial of 2 mL capacity, hermetically sealed with a cap. The vials were placed in the autosampler of the gas chromatograph. The qualitative analysis of fatty acids was accomplished by standard mixture n-3 PUFAs, Catalog No. 47085-U (Supelco Analytical).

Statistical analysis

Data were processed and analysed using Microsoft® Excel® (version 2111). When necessary, statistical tests such as Student *t*-test, one-, two-way ANOVA were performed using Origin® 2021 analysis software, followed by Tukey post-hoc test ($p < 0.05$). Experiments were conducted at least in triplicate.

3. Results

Preliminary test

Figure 1 reports the cell density of *T. lutea* after 7 days of cultivation in different dilutions of rejected brine. The initial screening was performed to establish the maximal brine concentration at which microalgae were able to grow. *T lutea* showed good growth capacity in all salinity levels tested. The highest cell density was obtained in brine diluted to 70% (salinity 55‰) followed by dilution to 80% (salinity 65‰), 9.54 ± 0.84 and 8.87 ± 0.76 × 10^6 cells mL^{-1}, respectively. As the difference was not significant ($p>0.05$; one-way ANOVA followed by post-hoc Tukey test), cells grown at the higher salinity (65‰) were selected to set up cultures of 25 mL and then 50 mL and 150 mL.

Batch experiment

Growth kinetics

Figure 2 shows the growth of *T. lutea* during the 14 days batch experiment in 80% dilute brine (65‰ salinity) and in SWES medium as control (40‰ salinity). In the early phases of cultivation (0-7 days), cell density in brine was always significantly higher than in the control ($p < 0.05$; two-way ANOVA followed by post-hoc Tukey test). From day 3, the cultures in brine entered a stationary phase, which was maintained until day 14 at the end of the experiment. The control cultures in SWES medium reached only a cell density similar to that of the brine-treated cultures on day 10, when there was no significant difference between treated and control, 3.08 ± 0.24 and 2.90 ± 0.18 × 10^6 cells mL^{-1} respectively ($p > 0.05$; two-way ANOVA followed by post-hoc Tukey test). However, at the end of the experiment, cultures in SWES medium resulted 42.72% more dense than those in brine (6.25 ± 0.42 and 4.41 ±

0.20×10^6 cells mL^{-1}, respectively – $p < 0.05$; two-way ANOVA followed by post-hoc Tukey test).

PSII maximum quantum yield measure

The effects of the different salinity on the photosynthetic efficiency were evaluated by PAM fluorimetry as showed in Figure 3. From the 3rd day of cultivation onwards, the cultures grown in diluted brine showed a progressive decrease in F_V/F_M values. In fact, already from the 7th day until the end of the experiment, values significantly lower than 0.6 were observed ($p < 0.05$; two-way ANOVA followed by post-hoc Tukey test). In microalgae, F_V/F_M values between 0.6 and 0.8 are typically observed in non-stressed cultures and indicate an efficient use of light for the photosynthetic processes (Bhola et al. 2016; Patil et al. 2020). On the other hands, control cultures in SWES medium at 40‰ of salinity showed values of F_V/F_M always above 0.6 up to 7 days and only slightly lower in the later stages of the experiment at 10 and 14 days of cultivation (0.58 at both experimental times).

Cell morphology

Figure 4 shows the microscope observations of *T. lutea* cells in the stationary phase during the batch cultures in diluted brine and SWES medium. In the control cultures (Fig.4a), cells showed the typical ovate or oblong shape and a golden-brown colour due to the presence of the cup-shaped chloroplast that occupied most of the cell volume and emitted red fluorescence due to the presence of chlorophylls (Fig. 4b). Overall, cells were in good condition and the mobility resulted not compromised. In diluted brine, so at a higher salinity than that of the controls, cells lost their typical oblong shape and changed to a more spherical shape (Fig. 4d). In some cases, some portions of the cell appeared less coloured due to the presence of vacuolation. Although not clearly visible in conventional light observations, the cup shape of the chloroplast could be seen during fluorescence observations. The emitted fluorescence was less intense than that of the controls (Fig. 4e). In both control and treated samples, globules of probable lipid nature were present within the cells. In order to confirm their nature, Nile Red stained cells were observed. In both SWES medium and brine, the cells contained lipid droplets. 2-3 droplets per cell were present inside control cells (Fig. 4d), while the number of globules slightly increased in treated algae. For example, up to 4-5 globules were present in some brine-cultivated cells. Furthermore, these globules appeared larger in size and emitted a stronger fluorescence than in control samples (Fig. 4f).

Subcellular TEM observations

TEM observations of *T. lutea* cells at the stationary phase in SWES medium and diluted brine are shown in Figure 5. A typical morphology characterized *T lutea* cells grown in SWES medium (Fig. 5a, b). The cell membrane presented the typical organic scales on the outer surface. The parietal cup-shaped plastids presented a standard morphology, characterized by the presence of a pyrenoid of considerable size crossed by a thylakoid lamella. The thylakoid membranes were clearly visible in groups of three and characterised by a regular morphology (Fig. 5c). On the other hands, cells grown in brine at 65‰ salinity that of showed an altered morphology and in some cells the plasma membrane appeared detached from the rest of the cell (Fig. 5d, e). The chloroplast had an altered shape in most cells: in some cases, it appeared flattened or irregularly shaped, but with the pyrenoid clearly visible. Large vacuoles were present in some cells (Fig. 5e). Noteworthy was the presence of 1 or more large, dark-coloured lipid globules in most of the cells (Fig. 5d, e). Compared with controls, the thylakoid membranes resulted altered (Fig. 5f). In both controls and treated cells it was possible to observe mitochondria characterised by a regular morphology, indicating good metabolic activity also in cells grown at high salt concentration (Fig. 5a, d).

Semi-continuous experiment

Growth kinetics and photosynthetic pigment content

Figure 6 shows the growth of *T. lutea* during the semi-continuous experiment in 2.5 L photobioreactors, in both SWES medium and diluted brine. Control and treated cultures were grown in batch mode until day 8, when the cultures reached sufficient cell density to begin the semi-continuous phase of the experiment. Control and treated cultures grew similarly up to 5 days of cultivation ($p > 0.05$; two-way ANOVA followed by post-hoc Tukey test), then the control cultures started to show increased cell density until day 8 when cell density was $6.11 \pm 0.28 \times 10^6$ cells mL^{-1} in the controls and $5.28 \pm 0.32 \times 10^6$ cells mL^{-1} in treatments ($p < 0.05$; two-way ANOVA followed by post-hoc Tukey test). During the semi-continuous phase of the experiment, 10% of the culture was daily removed and replaced with new culture medium or diluted brine. Compared to the control cultures, treated samples maintained a significantly lower cell density until the end of the experiment at 18 days ($p < 0.05$; two-way ANOVA followed by post-hoc Tukey test). During this phase, the brine cultures had an average cell density of $4.91 \pm 0.54 \times 10^6$ cells mL^{-1}, while those in SWES had an average cell density of $6.70 \pm 0.52 \times 10^6$ cells mL^{-1}. Therefore, at 65‰ of salinity *T. lutea* cultures were about 27%

less dense than the controls at 40 ‰. During the semi-continuous cultivation phases, the content of photosynthetic pigments was evaluated (Figure 7). Treated algae and controls showed no significant difference in chlorophyll *a* content ($p > 0.05$; Student t-test). On the contrary an increment in chlorophyll *c* content was observed in the samples grown in diluted brine (65‰ of salinity) ($p < 0.05$; Student t-test). However, the content of total chlorophylls was not significantly different (data not shown). The cells grown at higher salinity also showed a higher carotenoid content than the controls ($p < 0.05$; Student t-test).

Relative neutral lipid content evaluation by Nile Red assay

During the semi-continuous cultivation phase the relative content of neutral lipids inside the cells was evaluated by measuring the fluorescence emitted after Nile Red staining. Figure 8 shows the fluorescence values emitted by cells cultured in diluted brine at the salinity of 65‰ compared with the control cells cultured in SWES medium at a salinity of 40‰. The high salinity promoted the accumulation of neutral lipids in the cells. Indeed, cells in brine showed a fluorescence 45.6% higher than that recorded inside cells in SWES medium.

Fatty acid determination by gas chromatography

The lipids extraction and analysis by gas chromatography were performed on the biomass daily harvested during the semi-continuous phase of the experiment. Figure 9 shows the total fatty acid content (% DW) in *T. lutea* cultivated in SWES medium and 80% diluted brine (salinity of 40 and 65% respectively). No significant differences were highlighted between control and brine-cultivated algae, being fatty acids 12.11% and 10.24% of total DW, respectively ($p > 0.05$; Student t-test). When the relative proportions of saturated, mono- and polyunsaturated fatty acids were compared, no significant differences emerged between the control cultures and those cultivated at higher salinity ($p > 0.05$; Student t-test) (Figure 10). Saturated fatty acid accounted for the largest fraction, around 41% of the total in both SWES and brine cultures, followed by polyunsaturated fatty acids, which accounted for 35.94% and 31.63% of the total, respectively. Finally, monounsaturated fatty acids represented 22.27% (control samples) and 27.24% (treated samples) of the total fatty acids. Although there were no significant differences in total fatty acid content, the lipid profile showed that the proportions of specific fatty acids changed between control and treated samples. Table 2 reported the fatty acid profile characterized by GC-MS. In brine cultures the ω-3 stearidonic acid (SDA; 18:4n3) and the ω-9 oleic acid (18:1n9) were the most present, accounting for the 19.42% and 16.06%, respectively, while myristic acid (C14:0) accounted for the14.47%. In control cultures the most represented

fatty acid was myristic acid (14:0) followed by SDA, 17.53% and 14.40% respectively; the oleic acid was the 7.86%. Palmitic acid (16:0) was more represented in brine culture than in SWES ones, 13.54% and 9.72%, respectively. The ω-3 α-linolenic acid (ALA; 18:3n3) represented the 12.88% of the total fatty acid in the control cultures, but only the 7.16% in the cultures grown in brine. Finally, the important ω-3 docosahexaenoic acid **(**DHA; 22:6n3) accounted for about 12% in both SWES and brine cultures.

4. Discussion

In a waste-to-value approach, in this chapter it has been evaluated the feasibility of obtaining microalgal biomass and high-value products, such as carotenoids and fatty acids, from the cultivation of *T. lutea* in a diluted brine derived from the desalination plant in the city of Almeria, Spain. It is well known that the cultivation of microalgae under salinity stress can trigger physiological processes that lead to an increased accumulation of fatty acids or changes in the type of lipids and the relative amounts of specific fatty acids (Atikij et al. 2019; Yang et al. 2021; Cañavate and Fernández-Díaz 2021a). However, this is usually accompanied by a decrease in growth and biomass production (Ishika et al. 2018). In batch experiments, in the first phase of cultivation (0-7 days), the cultures grown at 65‰ of salinity resulted more concentrated than the controls; however, in the final phases of the experiment, the cultures in SWES medium at 40‰ salinity resulted almost twice denser. Even when growing semi-continuously in photobioreactors, cells in brine grew less than those in SWES. Thus, in batch cultivation experiment the salinity of 65‰ was limiting for the growth of *T. lutea* compared with controls at 40‰. Growth limitation due to salinity stress was consistent with scientific literature for *T. lutea* and other marine microalgal species adapted to this source of stress (Ishika et al. 2017; Ishika et al. 2018; Shetty et al. 2019; Mohamadnia et al. 2021). Ishika and coworkers (2017) studied, in semi-continuous cultivation, the effects of increasing salinity (in a range from 35 to 75‰) on two groups of algae: two halotolerant and four marine microalgae including *T. lutea.* The highest salinity limit for *Tisochrysis* was 75‰, but at this salinity the lowest productivity in terms of biomass was achieved. Biomass production was highest at a salinity of 45‰ and then decreased as the salinity increased. On the other hands, in Mohamadnia et al. (2021), the growth of *T. lutea* was found optimal at the salinity of 35‰, while the other salinity concentration had not significant effect on the cell growth (tested salinity rage 25-45‰). In our experiment in batch, in parallel to the limited growth, the state of stress due to salinity was also apparent by monitoring the variation in the quantum yield of (F_V/F_M) of the PS II. The analysis of the PSII maximum quantum yield by PAM fluorimetry allows an estimate of the

photosynthetic efficiency and can be used as a rapid parameter to evidence the physiological stress in microalgae (Cosgrove and Borowitzka 2010; Bhola et al. 2016; Patil et al. 2020). In fact, although in batch experiment the brine cultures entered an early stationary state (3rd day of cultivation), the F_V/F_M values gradually decreased and remained below the value of 0.6. On the contrary, controls cultures showed values above or slightly below 0.6. This is considered a limit value above which the use of light in the photosynthetic process is optimal (Patil et al. 2020). Ramanna et al. (1999) reported that salinity stress can generate very low F_V/F_M values. This was consistent with the results of this experiment and was confirmed in two recent studies of Ishika and collegues (2017; 2018): in *T. lutea,* as well as in *C. carterae* and *C. muelleri,* the values of F_V/F_M decreased when the microalgae grew in non-optimal salinity conditions. Furthermore, the values of F_V/F_M have been found to be strongly correlated with biomass productivity. A lower photosynthetic efficiency under non-optimal salinity conditions is documented in many microalgae. For example, F_V/F_M values decreased with increasing concentration of NaCl also in *C. vulgaris*. This increase in salinity was also limiting for the growth (Yadav et al. 2021). The stress condition in the brine cultures was also confirmed by microscopic observations. At salinity of 65‰, in addition to a reduction in mobility, cells presented an altered morphology, with a spheroidal shape instead of the typical oblong or ovate shape as in the controls. Changes in the morphology of the microalgae caused by variations in salinity, both higher and lower than the optimum, are a response to osmotic stresses to which the cells are subjected (Pugkaew et al. 2019; Papry et al. 2021). For example, in *Chlamydomonas*, high salt concentration leads to a slowing down of cell division, a reduction in cell size and an absence of motility and triggers the formation of palmelloid forms (Shetty et al. 2019). On the other hands, at sub-optimal salinity levels (30‰), severe growth inhibition, changes in cell morphology and reduced photosynthetic rate were observed in *T. suecica* (Pugkaew et al. 2019). In the present experiment, changes in the ultrastructure of *T. lutea* cells cultured in brine (65‰ of salinity) were also visible by TEM images. In fact, a general disorganization in the cellular structure, an accumulation of several lipid droplets and collapsed chloroplasts with damaged thylakoidal membranes were evident. Thylakoid alterations were also consistent with the decreased F_V/F_M values found in *T. lutea* grown in brine. Subcellular alterations, accompanied by a low photosynthetic yield and a reduced growth, were also observed in other species of microalgae exposed at a sub-optimal salinity, e.g. *Scenedesmus* sp. (Arora et al. 2019; Al-Enazi 2020), *Trebouxia* sp. (Hinojosa-Vidal et al. 2018) and *Nannochloropsis* sp. (Liu et al. 2019). However, the changes in *T. lutea* cells grown in brine at 65‰ of salinity were accompanied by an increase in the number and size of lipid droplets in

the cytosol. This was confirmed by both fluorescence microscopy after NR staining and TEM observations. In fact, microalgal cells accumulate lipids as high-energy carbon stores during nutrient deficiency or environmental stress such as high levels of salinity (Shi et al. 2020). Furthermore, additional amounts of carotenoids are produced to mitigate oxidative damage caused by stressful conditions (Shi et al. 2020). In order to assess how brine salinity affected the accumulation of lipids and pigments content in *T. lutea*, tests were performed on cells grown 10 days semi-continuously in photobioreactors containing 2L of culture. This cultivation method made it possible to collect the biomass needed for the analysis and at the same time to keep the cultures in a semi-stationary state for longer than was possible with a batch experiment. A comparison of the relative content of neutral lipids in algae grown in SWES and brine was performed by staining with Nile Red and analysing the emitted fluorescence. This method provides a faster and more economical evaluation than gravimetric and gas chromatographic methods; it can be also performed *in vivo* and provide an estimate in real time (Gao et al. 2020; Miranda et al. 2020). Based on the fluorescence emitted by the samples after staining with NR, the content of neutral lipids in *T. lutea* grown in brine at a salinity of 65‰ was on average 45.6% higher than in the controls (40‰ salinity). However, when total fatty acid content (%DW) was analysed by GC-MS, there were no significant differences between treatments grown at 65‰ salinity and controls at 40‰. This was in slight contrast to some studies that report increased fatty acid content in microalgae exposed to salt stress. For example, Almutairi et al. (2020) reported an increase in total lipid content under salt stress in *T. lutea*; the increase was particularly significant at intermediate salinities (e.g., 0.6 and 0.8 M), but higher salinity (e.g., 1.0 M) comported a decrease in lipid content and limitations in growth and biomass production. The increase in total fatty acid content with the increase in salinity was also found in other microalgae species. For example, in the microalga *Scenedesmus* sp., increasing the NaCl concentration in the culture medium resulted in an increase in total lipid content from 18.98% in control cultures to 33.13% in treated cultures grown at 400 mM NaCl, a 1.8-fold increase (Pancha et al. 2015). Yang et al. (2021) tested the effects of different salt contents in the culture medium (0.5%, 1.0%, 2.0% and 3.0%, mass percent NaCl) on the lipid content of *Chlorella pyrenoidosa* and, with increasing salt content, the lipid content of the microalgae showed an increasing trend. However, the effects of salinity are not limited to increasing or decreasing the lipid content in the microalgae, but also change their quality (Cañavate and Fernández-Díaz 2021b). In the present study on *T. lutea* cultivated in rejected brine, the GS-MS analysis showed no significant changes between controls and treatments in the relative proportions of saturated, monounsaturated and polyunsaturated fatty acids, nevertheless the

lipid profile showed that the proportions of certain fatty acids changed between control and treated samples. The difference in lipid profile of the cultures grown under different salinity conditions could partly explain the lack of difference in the ratios of the different levels of fatty acid saturation. As for saturated fatty acids, the high levels of 14:0 in the SWES cultures were compensated by the high level of 16:0 observed in the brine cultures, while the levels of 18:0 resulted the same in both. Some studies suggest that high salt stress is responsible for increased levels of 16:0 in some halophilic microalgae such as *D. salina* and *A. subtropica* (Azachi et al. 2002; BenMoussa-Dahmen et al. 2016). However, in some marine microalgae the 16:0 content does not seem to be influenced by salinity, e.g., in *Tetraselmis suecica* and *I. galbana* (Pugkaew et al. 2019; Cañavate et al. 2020). The same interspecific variability observed for palmitic acid (16:0) in response to salinity is also observed for the stearic acid (18:0) and myristic acid (14:0). For example, an increase in salinity corresponded to an increase in myristic acid in *Nannochloropsis* sp. and *A. subtropica* (Pal et al. 2011; BenMoussa-Dahmen et al. 2016), while no effect was observed in *I. galbana* in a salinity range between 5 and 50 psu (Cañavate et al. 2020). Although the difference in monounsaturated fatty acid content between the control and 65‰ cultures was not significant, some increase was observed in the brine cultures. The content of monounsaturated fatty acids was 27% in the treated cultures and 22% in the control cultures. This difference can be attributed to the high elaidic acid (18:1n9) levels in brine cultures. On the other hand, there was no difference in the accumulation of 16:1n7 and 18:1n7 between cultures in SWES and brine. This can potentially be explained by the evidence that frequently salt stress induces a change or 16:1n-7 or 18:1n-9 because the desaturase involved in the synthesis of 16:1n7 can change the preference for its substrate between 16-C or 18-C fatty acids in response to stress sources (An et al. 2013). In addition, delta-9 desaturation occurs in a faster time frame under salt stress than other desaturations (Cañavate and Fernández-Díaz 2021b). As for the 18-C polyunsaturated acids, a trend towards an increase in the proportion of 18:2n6 and 18:3n3 due to salt stress has been documented in literature (BenMoussa-Dahmen et al. 2016; Almutairi et al. 2020; Cañavate and Fernández-Díaz 2021b). This was also found in *T. lutea* in a study by Almutairi and co-workers (2020). However, this evidence contrasts with the results obtained when *T. lutea* was cultivated in brine at 65‰ salinity. In fact, the percentage values of 18:2n6 and 18:3n3 were lower in the brine cultures than in the control cultures at 40‰ salinity. On the other hand, a dramatic increase in SDA (18:4n3) was observed in brine cultured cells. The long-chain polyunsaturated fatty acids appear to be little affected by changes in salinity (Pugkaew et al. 2019; Cañavate et al. 2020). Consistently, the SWES and brine cultures had approximately the same 20:5n3 and 22:6n3

(DHA) content. Interestingly, salt stress caused a positive effect on pigment accumulation. In fact, carotenoids production could be influenced by abiotic environmental stress. Under salt stress, carotenoids accumulate and protect cells as antioxidants to increase microalgae survival (Ren et al. 2021). The content of total carotenoids in *T. lutea* grown in brine at the salinity of 65‰ was on average 21.25% higher than in the controls (40‰ of salinity). This result seemed to contradict a recent study by Ishika and colleagues (2017), in which it was observed that the maximum content of total carotenoids in *T. lutea* was reached at a salinity of 45‰ and then decreased in algae exposed to higher salinities. The lowest levels were observed at the limiting salinity of 75‰. On the other hand, there are numerous studies reporting an increase in carotenoid content in various species of microalgae associated with an increase in specific range of increased salinity. For example, an increase in total carotenoid content was observed in *Chlamydomonas* sp. that was ameliorated by a gradual increase in sea salt concentration. In particular, lutein and other carotenoids gradually increased when the sea salt concentration increased from 0 to 3%, while they decreased at higher salinity levels (Xie et al. 2019). In *H. pluvialis*, the treatment with 0.2 g L^{-1} NaCl resulted in a 42% increase in astaxanthin content compared to the control group (Ding et al. 2019). Sedjati and coworkers (2019) observed that in *D. salina*, chlorophyll production decreased with increasing salinity, led cells to produce carotenoids (carotenogenesis), which help chlorophyll capture of photons while protecting it. Although no decrease in chlorophyll content was observed in the cultures grown in brine in this study, salinity affected photosynthetic efficiency and thus growth of the cultures. The increase in carotenoids can therefore be explained as an adaptation of the cells to protect themselves from the oxidative stress caused by exposure to the high salinity. Furthermore, salinity stress induces the formation of reactive oxygen species (ROS) in cells (Zhao et al. 2019; Ren et al. 2021). Indeed, ROS is a stress indicator in response to abiotic stress in microalgae and can affect cell growth, photosynthetic process and metabolite synthesis. ROS can lead to lipid peroxidation, membrane degradation, DNA and protein damage (Arif et al. 2020). To cope with oxidative damage caused by excess ROS, microalgae have evolved two major mechanisms: antioxidant enzymes (such as superoxide dismutase and catalase) and molecules with antioxidant activity (such as carotenoids) (Zhao et al. 2019). Overall, the aim of the present work was to test the feasibility of cultivating *T. lutea* in rejected brine from a desalination plant. A waste-to-value approach was followed to produce microalgal biomass rich in valuable molecules such as lipids and pigments using an industrial by-product. Cultivation of *T. lutea* in rejected brine has still some limitations. However, the obtained algal biomass showed increased accumulation of neutral lipids compared to cultivation in synthetic SWES medium. Given the

crisis of fossil fuel reserves and the growing interest in alternative and renewable energy sources, this finding could add to the knowledge of biofuel production from microalgal biomass. Indeed, neutral lipids are precursors for biodiesel production (Gilmour 2019). Furthermore, the increased concentration of carotenoids as the result of cultivation in brine is of commercial interest since the global market for carotenoids was estimated at $1.24 billion in 2016 and has grown in recent years (Ambati et al. 2019). Indeed, carotenoids have practical applications in many areas of the food, feed, cosmetics and nutraceutical industries and there is a growing demand for natural products that can drive the market for carotenoids of microalgal origin (Novoveská et al. 2019). Finally, cultivation of *T. lutea* in rejected brine has the added advantage of increased environmental sustainability associated with reduced freshwater consumption and the valorisation and reuse of a by-product of the desalination process. Looking to the future, we could use a two-step cultivation process to increase biomass production at lower salinities and then promote lipid and carotenoid production by increasing the salinity of the culture medium by increasing the percentage of brine in the culture medium.

Table 1 Characteristics of rejected brine from Almeria Desalination Plant. Salinity (‰), pH, chemical elements, N (NO_3 and NH_4) P (PO_4) (ppm).

Salinity	**80‰**
pH	7.2

Element	ppm	Element	ppm
N (NO_3)	7.576	**Zn**	0.521
N (NH_4)	0.435	**Ga**	N.D.
P (PO_4)	0.170	**As**	0.014
Li	0.582	**Se**	0.002
Be	N.D.	**Rb**	0.209
B	5.797	**Sr**	14.022
P	0.348	**Mo**	3.113E-03
Sc	0.008	**Cd**	N.D.
Ti	0.256	**Ba**	0.082
V	0.002	**Tl**	N.D.
Cr	0.001	**Pb**	3.776E-04
Mn	0.013	**Bi**	N.D.
Fe	0.410	**U**	1.173E-03
Co	N.D.	**Ni**	0.031
Cu	0.034		

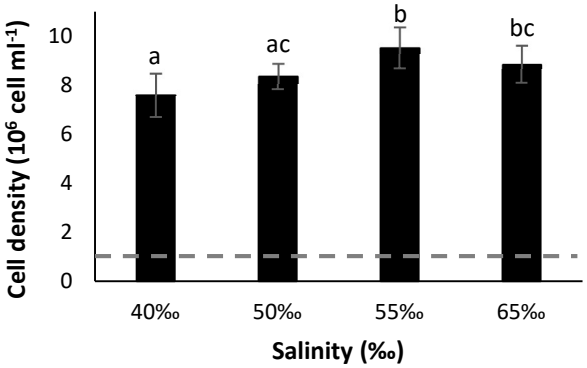

Figure 1 Cell density of *T. lutea* after 7 days of cultivation in different salinity concentrations obtained by different brine dilutions (in order from left to right 50-60-70-80%). Dashed line indicated the cell density of the starter inoculum at day 0. Values are means ± SD. Different letters indicate statistically significant difference ($p<0.05$ one-way ANOVA**)**

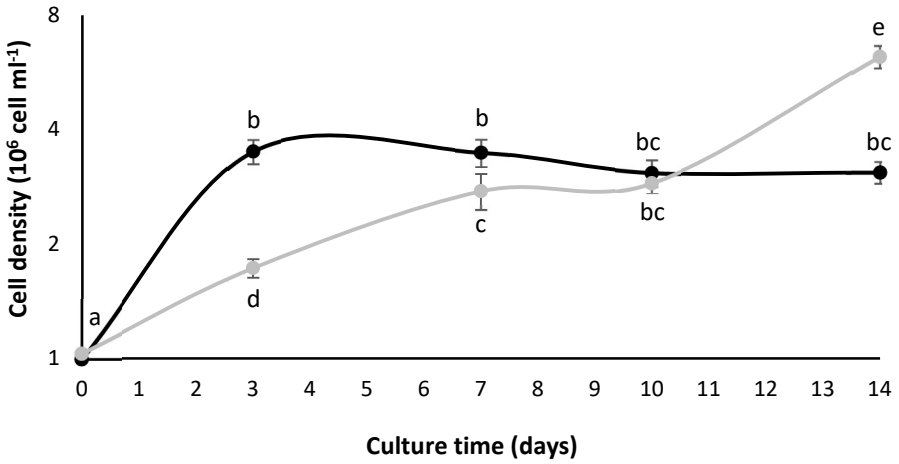

Figure 2 Growth kinetics of *T. lutea* batch cultures in 80% diluted brine (blaalck - 65‰) and SWES medium (grey - 40‰). Data are plotted on a logarithmic scale. Values are means ± SD (n = 4). Different letters indicate statistically significant differences ($p < 0.05$, two-way ANOVA)

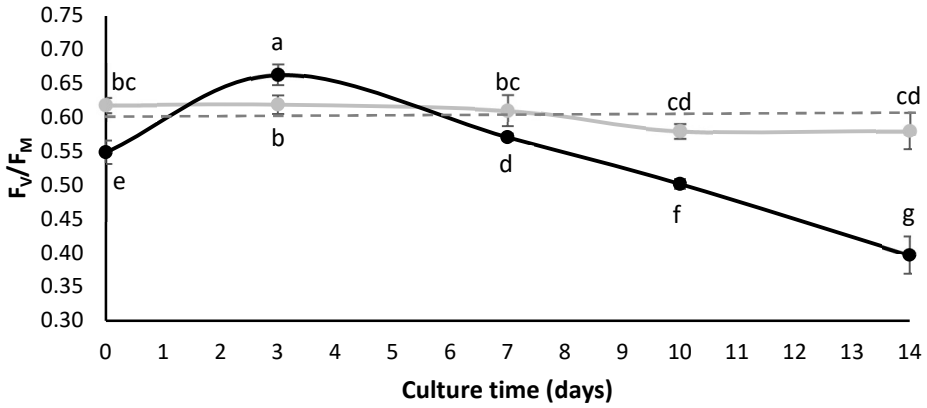

Figure 3 Time-course variations of F_V/F_M ratio in *T. lutea* batch cultures in 80% diluted brine (black - 65‰) and SWES medium (grey - 40‰). Dashed lines indicate the optimal 0.6 value of F_V/F_M. Values are means ± SD. Different letters indicate statistically significant differences ($p < 0.05$, two-way ANOVA)

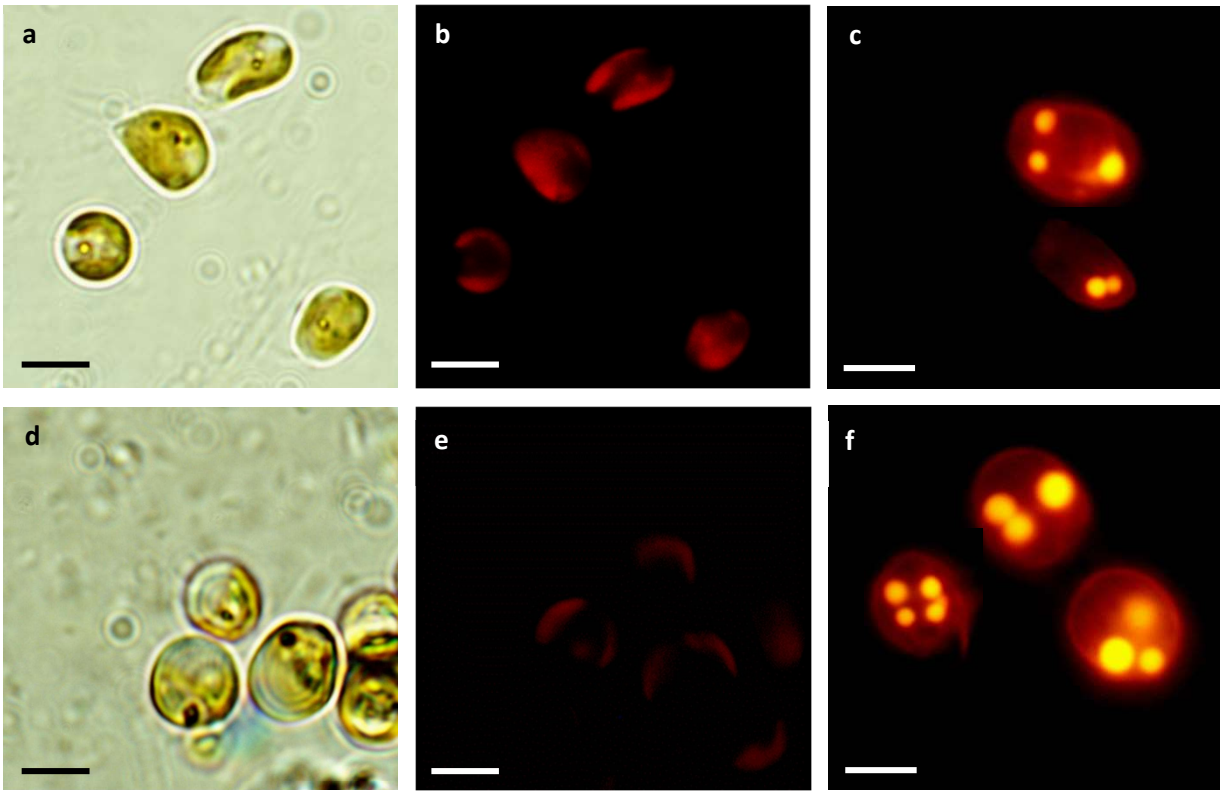

Figure 4 Microscope observations of *T. lutea* cells at stationary state of batch cultivation in SWES medium (a, b, c) and 80% diluted brine (d, e, f). Conventional light (a, d), epifluorescence (b, e) and epifluorescence of Nile Red stained cells (c, f). Scale bars = 5 µm

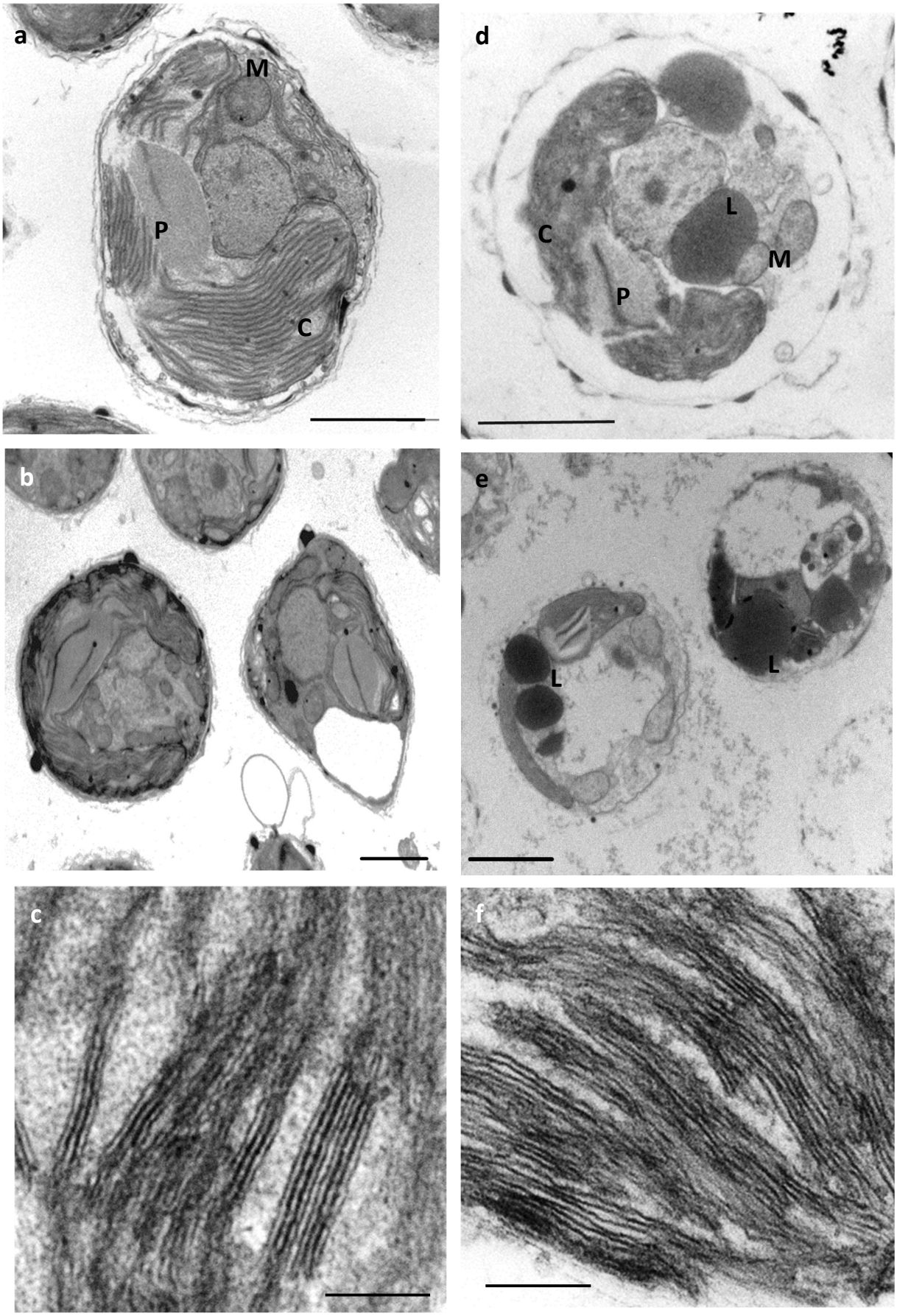

Figure 5 Transmission electron micrographs of *T. lutea* cells at stationary state of batch cultivation in SWES medium (a, b, c) and 80% diluted brine (d, e, f). C chloroplast; P pyrenoid; L lipid globules; M mitochondrion. Scale bars (μm): a, b, d, e = 2; c, = 0.2

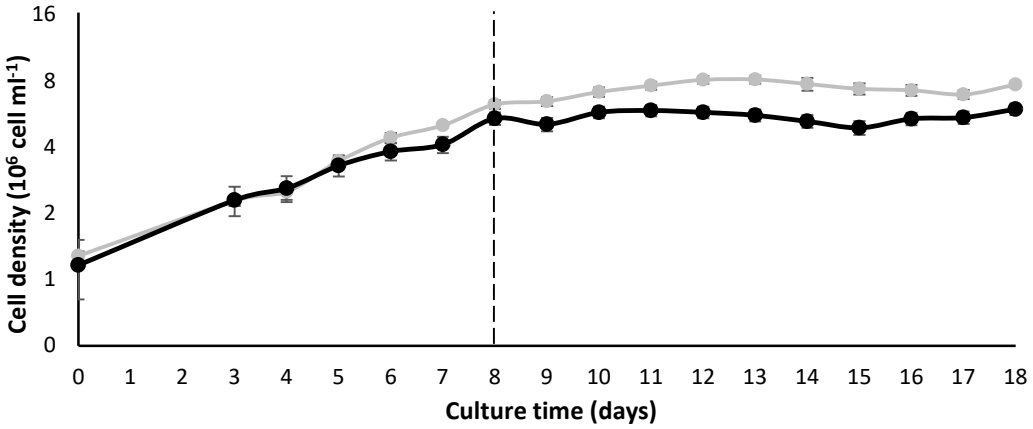

Figure 6 Growth kinetics of *T. lutea* semi-continuous cultures in 80% diluted brine (black - 65‰) and SWES medium (grey - 40‰). Data are plotted on a logarithmic scale. Values are means ± SD. The dushed line indicates the beginning of semi-continuous cultivation: 10% of the culture was daily removed and replaced with fresh SWES medium or diluted brine. To improve the readability of the picture, the two-way ANOVA results are reported in Table 1 in the appendix to this chapter.

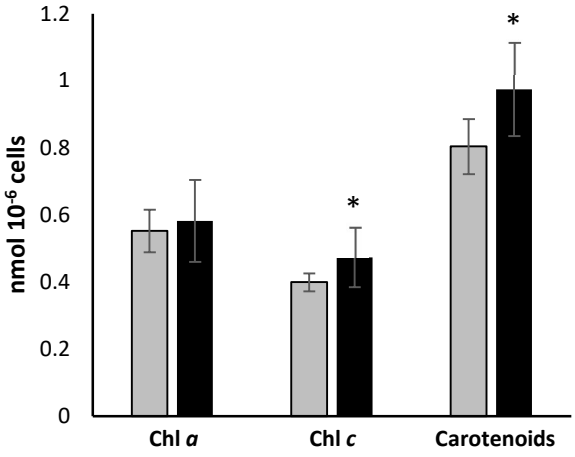

Figure 7 Photosynthetic pigments content (nmon of pigments 10^{-6} cell) in *T. lutea* cells during the stationary state of the semi-continuous cultivation. SWES medium (grey); 80% diluted brine (black). Values are means ± SD. * $p < 0.05$ (Student t-test)

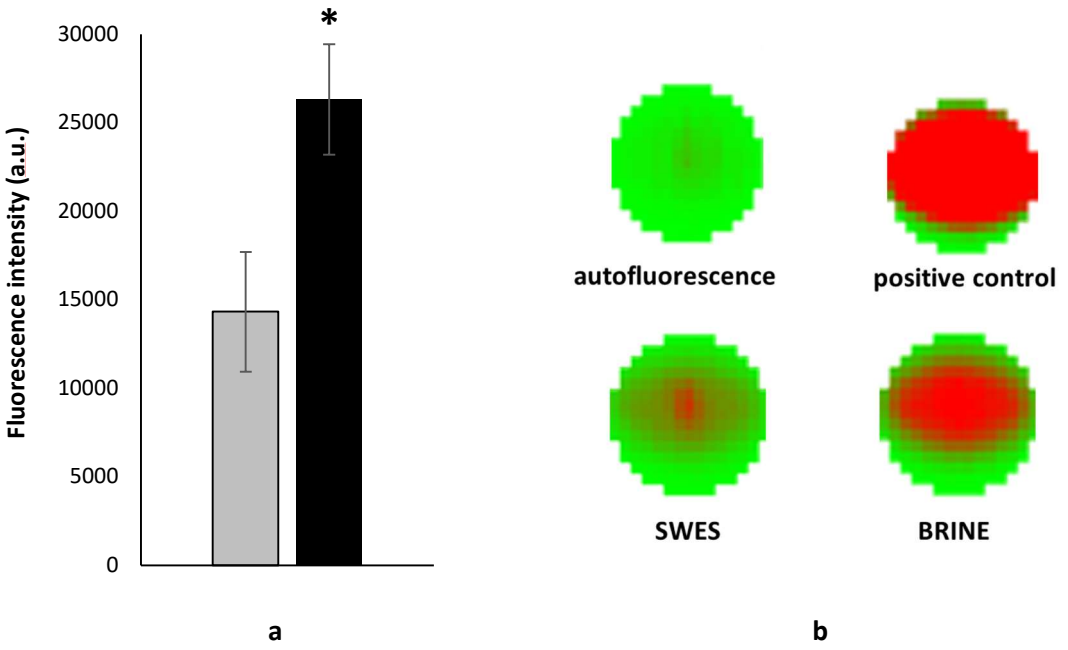

Figure 8 (a) Fluorescence intensity (arbitrary units) of *T. lutea* cells stained with Nile Red (NR) during the stationary state of the semi-continuous cultivation. SWES medium (grey); 80% diluted brine (black). Values are means ± SD. * $p < 0.05$ (Student t-test) (b) Graphical representation of the fluorescence emitted by wells containing *T. lutea* cells without NR staining (autofluorescence); milk diluted in fresh medium (1µl/ml) stained with NR (positive control); *T. lutea* cells stained with NR grown in SWES medium (SWES) or 80% diluted brine (BRINE). (Representative images of replicas)

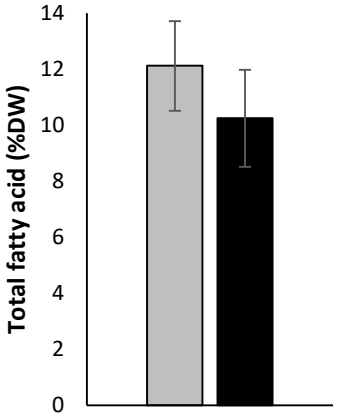

Figure 9 Fatty acid content (% DW) in *T. lutea* cells during the stationary state of the semi-continuous cultures. SWES medium (black); diluted brine (grey). Values are means ± SD

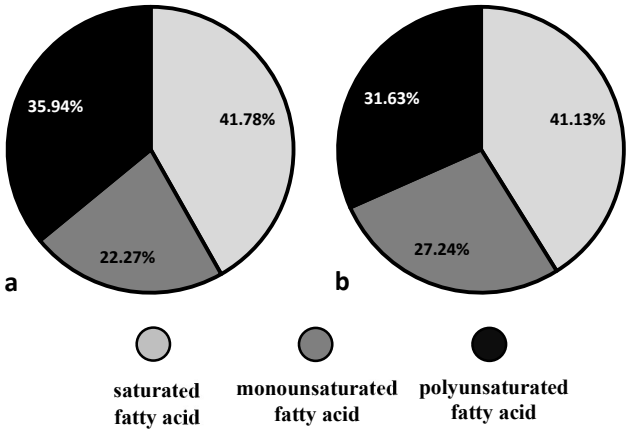

Figure 10 Relative proportions of fatty acids fractions (percentage of total fatty acids, %) in *T. lutea* cells during the stationary state of the semi-continuous cultures. SWES medium (a); diluted brine (b)

Table 2 Fatty acid profile (percentage of total fatty acids) in *T. lutea* cells during the stationary state of the semi-continuous cultures in SWES medium and diluted brine. Values are means ± SD

Fatty acid	SWES medium		diluted brine	
	Mean	SD	Mean	SD
14:0	17.53	0.44	14.47	0.21
16:0	9.72	0.27	13.54	0.38
16:1n7	6.01	0.14	6.39	0.13
16:2n4	1.05	0.05	0.90	0.03
18:0	0.60	0.14	0.46	0.24
18:1n9	7.86	0.22	16.06	0.89
18:1n7	0.47	0.10	0.22	0.15
18:2n6	6.22	0.78	3.08	0.36
18:3n3 (ALA)	12.88	0.39	7.16	0.26
18:4n3 (SDA)	14.40	0.98	19.42	0.69
20:1n9	5.46	0.34	2.47	0.42
20:5n3 (EPA)	0.62	0.18	0.80	0.21
22:6n3 (DHA)	12.74	0.59	12.43	0.64
other	4.46	0.59	2.60	0.17

Appendix

Table 2 Two-way ANOVA followed by Tukey post-hoc test results referred to the growth data of *T. lutea* in SWES medium (controls – SWES in the table) and diluted brine (treatments – Brine in the table) at different culture time (Fig. 6). Means that do not share a letter are significantly different ($p < 0.05$).

Culture medium	Culture time (days)	Mean	Groups													
SWES	13	7.36	a													
SWES	12	7.34	a													
SWES	18	6.98	a	b												
SWES	11	6.9	a	b												
SWES	15	6.68		b	c											
SWES	16	6.58		b	c	d										
SWES	10	6.46		b	c	d										
SWES	14	6.3			c	d	e									
SWES	17	6.3			c	d	e									
SWES	9	6.08				d	e									
SWES	8	5.88					e	f								
Brine	18	5.4						f	g							
Brine	11	5.32							g							
Brine	10	5.22							g	h						
Brine	12	5.22							g	h						
Brine	8	5.08							g	h						
Brine	13	5.06							g	h						
Brine	17	4.94							g	h	i					
Brine	16	4.88							g	h	i					
Brine	9	4.78								h	i					
SWES	7	4.73								h	i					
Brine	15	4.44									i	j				
SWES	6	4.15										j	k			
Brine	7	3.87											k	l		
Brine	14	3.84											k	l		
Brine	6	3.6												l	m	
SWES	5	3.25													m	
Brine	5	3.1													m	
Brine	4	2.45														n
SWES	4	2.355														n
Brine	3	2.16														n
SWES	3	2.15														n
SWES	0	1.205														o
Brine	0	1.095														o

References

Al-Enazi NM (2020) Salinization and wastewater effects on the growth and some cell contents of *Scenedesmus bijugatus*. Saudi Journal of Biological Sciences, Volume 27, Issue 7, Pages 1773-1780. https://doi.org/10.1016/j.sjbs.2020.05.021

Aljohani NS, Al-Farawati RK, Shabbaj II, Al-Mur BA, Kavil YN, Abdel Salam M (2021) Environmental remediation of desalination plant outfall brine discharge from heavy metals and salinity using halloysite Nanoclay. *Water*. 13(7):969. https://doi.org/10.3390/w13070969

Almutairi AW, El-Sayed AEKB, Reda MM (2020) Combined effect of salinity and pH on lipid content and fatty acid composition of *Tisochrysis lutea*. Saudi Journal of Biological Sciences, 27(12), 3553-3558. https://doi.org/10.1016/j.sjbs.2020.07.027

Ambati R.R., Gogisetty D., Aswathanarayana R.G., Ravi S., Bikkina P.N., Bo L., Yuepeng S (2019) Industrial potential of carotenoid pigments from microalgae: Current trends and future prospects. Crit. Rev. Food Sci. Nutr.;59:1880–1902. https://doi.org/10.1080/10408398.2018.1432561

An M, Mou S, Zhang X, Zheng Z, Ye N, Wang D, Zhang W, Miao J (2013) Expression of fatty acid desaturase genes and fatty acid accumulation in *Chlamydomonas* sp. ICE-L under salt stress. Bioresource technology, 149, pp.77-83. https://doi.org/10.1016/j.biortech.2013.09.027

Arif Y, Singh P, Siddiqui H, Bajguz A, Hayat S (2020) Salinity induced physiological and biochemical changes in plants: An omic approach towards salt stress tolerance. Plant Physiology and Biochemistry, 156, 64-77. https://doi.org/10.1016/j.plaphy.2020.08.042

Arora N, Kumari P, Kumar A, Gangwar R, Gulati K, Pruthi PA, Prasad R, Kumar D, Pruthi V, KM Poluri (2019) Delineating the molecular responses of a halotolerant microalga using integrated omics approach to identify genetic engineering targets for enhanced TAG production. Biotechnol Biofuels 12, 2. https://doi.org/10.1186/s13068-018-1343-1

Atikij T, Syaputri Y, Iwahashi H, Praneenararat T, Sirisattha S, Kageyama H, Waditee-Sirisattha R (2019) Enhanced lipid production and molecular dynamics under salinity stress in green microalga *Chlamydomonas reinhardtii* (137C). MarineDrugs.;17(8):484. https://doi.org/10.3390/md17080484

Azachi M, Sadka A, Fisher M, Goldshlag P, Gokhman I, Zamir A (2002) Salt induction of fatty acid elongase and membrane lipid modifications in the extreme halotolerant alga *Dunaliella salina*. Plant physiology, 129(3), pp.1320-1329. https://doi.org/10.1104/pp.001909

Baldisserotto C, Demaria S, Accoto O, Marchesini R, Zanella M, Benetti L, Avolio F, Maglie M, Ferroni L, Pancaldi S (2020) Removal of nitrogen and phosphorus from thickening effluent of an urban wastewater treatment plant by an isolated green microalga. Plants. 9(12):1802. https://doi.org/10.3390/plants9121802

Bendif E M, Probert I, Schroeder DC, de Vargas C (2013) On the description of *Tisochrysis lutea* gen. nov. sp. nov. and *Isochrysis nuda* sp. nov. in the Isochrysidales, and the transfer of *Dicrateria* to the *Prymnesiales* (Haptophyta). Journal of applied phycology, 25(6), 1763-1776. https://doi.org/10.1007/s10811-013-0037-0

BenMoussa-Dahmen I, Chtourou H, Rezgui F, Sayadi S Dhouib A (2016) Salinity stress increases lipid, secondary metabolites and enzyme activity in *Amphora subtropica* and *Dunaliella* sp. for biodiesel production. Bioresource technology, 218, pp.816-825. https://doi.org/10.1016/j.biortech.2016.07.022

Bhola VK, Swalaha FM, Nasr M, Kumari S, Bux F (2016) Physiological responses of carbon-sequestering microalgae to elevated carbon regimes. Eur J Phycol 51:401–412. https://doi.org/10.1080/09670262.2016.1193902

Bogdanov D, Farfan J, Sadovskaia K, Aghahosseini A, Child M, Gulagi A, Oyewo AS, Barbosa L, Breyer C (2019) Radical transformation pathway towards sustainable electricity via evolutionary steps. Nat Commun 10, 1077. https://doi.org/10.1038/s41467-019-08855-1

Cañavate J-P, Fernández-Díaz C (2021a) Salinity induces unique changes in lipid classes and fatty acids of the estuarine haptophyte *Diacronema vlkianum.* European Journal of Phycology. https://doi.org/10.1080/09670262.2021.1970234

Cañavate JP, Hachero-Cruzado I, Pérez-Gavilán C, Fernández-Díaz C (2020) Lipid dynamics and nutritional value of the estuarine strain *Isochrysis galbana* VLP grown from hypo to hyper salinity. Journal of Applied Phycology, 32(6), pp.3749-3766. https://doi.org/10.1007/s10811-020-02258-2

Cañavate J-P, Fernández-Díaz C (2021b) An appraisal of the variable response of microalgal lipids to culture salinity. Rev Aquacult.; 14: 192– 212. https://doi.org/10.1111/raq.12592

Cipolletta G, Lancioni N, Akyol Ç, Eusebi AL, Fatone F (2021) Brine treatment technologies towards minimum/zero liquid discharge and resource recovery: State of the art and techno-economic assessment. Journal of Environmental Management, Volume 300, 113681. https://doi.org/10.1016/j.jenvman.2021.113681

Clark GF, Knott NA, Miller BM, Kelaher BP, Coleman MA, Ushiama S, Johnston EL (2018) First large-scale ecological impact study of desalination outfall reveals trade-offs in effects of hypersalinity and hydrodynamics (2018) Water Research, Volume 145, Pages 757-768, https://doi.org/10.1016/j.watres.2018.08.071

Cosgrove J, Borowitzka MA (2010) Chlorophyll fluorescence terminology: an introduction. In: Suggett DJ, Prášil O, Borowitzka MA (eds) Chlorophyll *a* fluorescence in aquatic sciences: methods and applications. Springer, Dordrecht, pp 1–17. https://doi.org/10.1007/978-90-481-9268-7_1

Damania R, Desbureaux S, Hyland M, Islam A, Rodella AS, Russ J, Zaveri E (2017) Uncharted waters: The new economics of water scarcity and variability. World Bank Publications. (© World Bank. https://openknowledge.worldbank.org/handle/10986/28096 License: CC BY 3.0 IGO)

Ding W, Cui J, Zhao YT, Han BY, Li T, Zhao P, Xu J-W, Yu X (2019). Enhancing *Haematococcus pluvialis* biomass and γ-aminobutyric acid accumulation by two-step cultivation and salt supplementation. Bioresour. Technol.:285. https://doi.org/10.1016/j.biortech.2019.121334

Fernández-Torquemada Y, Carratalá A, Sánchez-Lizaso JL (2019) Impact of brine on the marine environment and how it can be reduced. Desalination and Water Treatment, 167: 27-37. https://doi.org/10.5004/dwt.2019.24615

Gan X, Shen G, Xin B, Li M (2016) Simultaneous biological desalination and lipid production by Scenedesmus obliquus cultured with brackish water. Desalination, 400, pp. 1-6. https://doi.org/10.1016/j.desal.2016.09.012

Gao F, Teles I, Ferrer-Ledo N, Wijffels RH, Barbosa MJ (2020) Production and high throughput quantification of fucoxanthin and lipids in Tisochrysis lutea using single-cell fluorescence. Bioresource Technology, 318, 124104. https://doi.org/10.1016/j.biortech.2020.124104

Gilmour DJ (2019) Chapter One - Microalgae for biofuel production. Gadd GM, Sariaslani S (eds) Advances in Applied Microbiology, Academic Press, Volume 109, Pages 1-30. https://doi.org/10.1016/bs.aambs.2019.10.001

Giovanardi M, Baldisserotto C, Daglia M, Ferroni, L, Sabia A, Pancaldi S (2016) Morpho-physiological aspects of *Scenedesmus acutus* PVUW12 cultivated with a dairy industry waste and after starvation. Plant Biosystems-An International Journal Dealing with all Aspects of Plant Biology, 150(4), 767-775. https://doi.org/10.1080/11263504.2014.991361

Giovanardi M, Ferroni L, Baldisserotto C, Tedeschi P, Maietti A, Pantaleoni, L., & Pancaldi, S. (2013). Morphophysiological analyses of *Neochloris oleoabundans* (Chlorophyta) grown mixotrophically in a carbon-rich waste product. Protoplasma, 250(1), 161-174. https://doi.org/10.1007/s00709-012-0390-x

Hanley R (2018) Desalination concentrate disposal: ecological effects and sustainable solutions. Global Honors Theses. 54. https://digitalcommons.tacoma.uw.edu/gh_theses/54

Hansen K, Breyer C, Lund H (2019) Status and perspectives on 100% renewable energy systems. Energy, 175, pp. 471-480. https://doi.org/10.1016/j.energy.2019.03.092

Hinojosa-Vidal E, Marco F, Martínez-Alberola F, Escaray FJ, García-Breijo FJ, Reig-Armiñana J, Carrasco P, Barreno E (2018) Characterization of the responses to saline stress in the symbiotic green microalga *Trebouxia* sp. TR9. Planta 248, 1473–1486. https://doi.org/10.1007/s00425-018-2993-8

Ishika T, Bahri PA, Laird DW, Moheimani NR (2018) The effect of gradual increase in salinity on the biomass productivity and biochemical composition of several marine, halotolerant, and halophilic microalgae. Journal of applied phycology, 30(3), 1453-1464. https://doi.org/10.1007/s10811-017-1377-y

Ishika T, Moheimani NR, Bahri PA, Laird DW, Blair S, Parlevliet D (2017) Halo-adapted microalgae for fucoxanthin production: Effect of incremental increase in salinity, Algal Research,Volume 28, Pages 66-73. https://doi.org/10.1016/j.algal.2017.10.002

Jones E, Qadir M, van Vliet MTH, Smakhtin V, Kang S (2019) The state of desalination and brine production: A global outlook. Science of the total environment. Volume 657, Pages 1343-1356. https://doi.org/10.1016/j.scitotenv.2018.12.076

Liu C, Liu J, Hu S, Wang X, Wang X, Guan Q (2019) Isolation and identification of a halophilic and alkaliphilic microalgal strain. PeerJ, 7, e7189. https://doi.org/10.7717/peerj.7189

Loganathan P Naidu G Vigneswaran S (2017) Mining valuable minerals from seawater: a critical review. Environ. Sci.: Water Res. Technol., 3, pp. 37-53. https://doi.org/10.1039/C6EW00268D

Maglie M, Baldisserotto C, Guerrini A, Sabia A, Ferroni L, Pancaldi S (2021) A co-cultivation process of *Nannochloropsis oculata* and *Tisochrysis lutea* induces morpho-physiological and biochemical variations potentially useful for biotechnological purposes. J Appl Phycol 33, 2817–2832. https://doi.org/10.1007/s10811-021-02511-2

Matos AP, Moecke EHS, Sant'Anna ES (2017) The use of desalination concentrate as a potential substrate for microalgae cultivation in Brazil. Algal Research, Volume 24, Part B, Pages 505-508. https://doi.org/10.1016/j.algal.2016.08.003

Miranda C, Bettencourt S, Pozdniakova T, Pereira J, Sampaio P, Franco-Duarte R, Pais C (2020) Modified high-throughput Nile red fluorescence assay for the rapid screening of oleaginous yeasts using acetic acid as carbon source. BMC Microbiol **20,** 60. https://doi.org/10.1186/s12866-020-01742-6

Missimer TM, Maliva RG (2018) Environmental issues in seawater reverse osmosis desalination: Intakes and outfalls. Desalination, Volume 434, Pages 198-215. https://doi.org/10.1016/j.desal.2017.07.012

Mohamadnia S, Tavakoli O, Faramarzi MA (2021) Enhancing production of fucoxanthin by the optimization of culture media of the microalga *Tisochrysis lutea*. Aquaculture, 533, 736074. https://doi.org/10.1016/j.aquaculture.2020.736074

Nedbalová L, Střížek A, Sigler K, Řezanka T (2016) Effect of salinity on the fatty acid and triacylglycerol composition of five haptophyte algae from the genera Coccolithophora, Isochrysis and Prymnesium determined by LC-MS/APCI, Phytochemistry, Volume 130, Pages 64-76. https://doi.org/10.1016/j.phytochem.2016.06.001

Novoveská L, Ross ME, Stanley MS, Pradelles R, Wasiolek V, Sassi JF (2019) Microalgal Carotenoids: A Review of Production, Current Markets, Regulations, and Future Direction. Mar Drugs. Nov 13;17(11):640. https://doi.org/10.3390/md17110640

Pal D, Khozin-Goldberg I, Cohen Z, Boussiba S (2011) The effect of light, salinity, and nitrogen availability on lipid production by *Nannochloropsis* sp. Applied microbiology and biotechnology, 90(4), pp.1429-1441. https://doi.org/10.1007/s00253-011-3170-1

Panagopoulos A, Haralambous K-J, Loizidou M (2019) Desalination brine disposal methods and treatment technologies - A review, Science of The Total Environment, Volume 693, 133545. https://doi.org/10.1016/j.scitotenv.2019.07.351

Pancha I, Chokshi K, Maurya R, Trivedi K, Patidar SK, Ghosh A, Mishra S (2015) Salinity induced oxidative stress enhanced biofuel production potential of microalgae *Scenedesmus* sp. CCNM 1077. Bioresource Technology, Volume 189, Pages 341-348. https://doi.org/10.1016/j.biortech.2015.04.017

Papry RI, Fujisawa S, Zai Y, Akhyar O, Mashio AS, Hasegawa H (2021) Freshwater phytoplankton: Salinity stress on arsenic biotransformation. Environmental Pollution, Volume 270, 116090, https://doi.org/10.1016/j.envpol.2020.116090

Patil S, Arvind ML, Gunjan P (2020) An efficient algae cell wall disruption methodology for recovery of intact chloroplasts from microalgae. Journal of Applied Biology & Biotechnology Vol 8.03: 23-28. http://doi.org/10.7324/JABB.2020.80305

Pistocchi A (a), Bleninger T, Dorati C (2020) Screening the hurdles to sea disposal of desalination brine around the Mediterranean. Desalination, Volume 491, 114570. https://doi.org/10.1016/j.desal.2020.114570

Pistocchi A (b), Bleninger T, Breyer C, Caldera U, Dorati C, Ganora D, Millán MM, Paton C, Poullis D, Salas Herrero F, Sapiano M, Semiat R, Sommariva C, Yuece S, Zaragoza G (2020) Can seawater desalination be a win-win fix to our water cycle? Water Research, Volume 182, 115906. https://doi.org/10.1016/j.watres.2020.115906

Premaratne M., Liyanaarachchi VC, Nimarshana PHV, Ariyadasa TU, Malik A, Attalage RA (2021) Co-production of fucoxanthin, docosahexaenoic acid (DHA) and bioethanol from the marine microalga *Tisochrysis lutea.* Biochemical Engineering Journal, 176, 108160. https://doi.org/10.1016/j.bej.2021.108160

Pugkaew W, Meetam M, Yokthongwattana K, Leeratsuwan N, Pokethitiyook P (2019) Effects of salinity changes on growth, photosynthetic activity, biochemical composition, and lipid productivity of marine microalga *Tetraselmis suecica*. J Appl Phycol 31, 969–979 (2019). https://doi.org/10.1007/s10811-018-1619-7

Quist-Jensen CA, Macedonio F, Drioli E (2016) Integrated membrane desalination systems with membrane crystallization units for resource recovery: a new approach for mining from the sea. Crystals, 6, pp. 1-13. https://doi.org/10.3390/cryst6040036

Ren Y, Sun H, Deng J, Huang J, Chen F (2021) Carotenoid Production from microalgae: Biosynthesis, Salinity Responses and Novel Biotechnologies. Marine Drugs, 19(12), 713. https://doi.org/10.3390/md19120713

Rodríguez-Rojas F, López-Marras A, Celis-Plá PSM, Muñoz P, García-Bartolomei E, Valenzuela F, Orrego R, Carratalá A, Sánchez-Lizaso JL, Sáez CA (2020) Ecophysiological and cellular stress responses in the cosmopolitan brown macroalga *Ectocarpus* as biomonitoring tools for assessing desalination brine impacts. Desalination, Volume 489, 114527. https://doi.org/10.1016/j.desal.2020.114527

Sahle-Demessie E, Hassan AA, El Badawy A (2019) Bio-desalination of brackish and seawater using halophytic algae. Desalination, 465, pp. 104-113. https://doi.org/10.1016/j.desal.2019.05.002

Sánchez AS, Nogueira IBR, Kalid RA (2015) Uses of the reject brine from inland desalination for fish farming, *Spirulina* cultivation, and irrigation of forage shrub and crops. Desalination, 364, 96-107. https://doi.org/10.1016/j.desal.2015.01.034

Sedjati S, Santosa GW, Yudiati E, Supriyantini E, Ridlo A, Kimberly FD (2019) Chlorophyll and carotenoid content of *Dunaliella salina* at various salinity stress and harvesting time. In IOP Conference Series: Earth and Environmental Science (Vol. 246, No. 1, p. 012025). IOP Publishing. https://doi.org/10.1088/1755-1315/246/1/012025

Shetty P, Gitau MM, Maróti G (2019) Salinity stress responses and adaptation mechanisms in eukaryotic green microalgae. Cells. 2019; 8(12):1657. https://doi.org/10.3390/cells8121657

Shi TQ, Wang LR, Zhang ZX, Sun XM, Huang H (2020) Stresses as first-line tools for enhancing lipid and carotenoid production in microalgae. Frontiers in bioengineering and biotechnology, 8, 610. https://doi.org/10.3389/fbioe.2020.00610

Shirazi SA, Rastegary J, Aghajani M, Ghassemi A (2018) Simultaneous biomass production and water desalination concentrate treatment by using microalgae. Desalin Water Treat, 135, 101-107. https://doi.org/10.5004/dwt.2018.23163

Sola I, Fernández-Torquemada Y, Forcada A, Valle C, del Pilar-Ruso Y, González-Correa JM, Sánchez-Lizaso JL (2020) Sustainable desalination: Long-term monitoring of brine discharge in the marine environment, Marine Pollution Bulletin, Volume 161, Part B, 111813. https://doi.org/10.1016/j.marpolbul.2020.111813

Sun X-M, Ren L-J, Bi Z-Q, Ji X-J, Zhao Q-Y, Huang H (2018) Adaptive evolution of microalgae *Schizochytrium* sp. under high salinity stress to alleviate oxidative damage and improve lipid biosynthesis. Bioresource Technology, Volume 267, Pages 438-444. https://doi.org/10.1016/j.biortech.2018.07.079

Torres GF, Bermejo-Padilla E, Pittman J, Theodoropoulos C (2021) Microalgae strain catalogue: A strain selection guide for microalgae users: cultivation and chemical characteristics for high added-value products. 3rd ed. Zenodo, 2021. 163 p. https://doi.org/10.5281/zenodo.5034149

Wei J, Gao L, Shen G, Yang X, Li M (2020) The role of adsorption in microalgae biological desalination: Salt removal from brackish water using *Scenedesmus obliquus*. Desalination, Volume 493, 114616. https://doi.org/10.1016/j.desal.2020.114616

Xie Y, Lu K, Zhao X, Ma R, Chen J, Ho SH (2019) Manipulating nutritional conditions and salinity-gradient stress for enhanced lutein production in marine microalga *Chlamydomonas* sp. Biotechnology journal, 14(4), 1800380. https://doi.org/10.1002/biot.201800380

Yadav N, Gupta N, Singh DP (2021) Ameliorating effect of bicarbonate on salinity induced changes in the growth, nutrient status, cell constituents and photosynthetic attributes of microalga *Chlorella vulgaris*. Bull Environ Contam Toxicol. https://doi.org/10.1007/s00128-021-03135-5

Yang Z-Y, Gao F, Liu J-Z, Yang J-S, Liu M, Ge Y-M, Chen D-Z, Chen J-M (2021) Improving sedimentation and lipid production of microalgae in the photobioreactor using saline wastewater. Bioresource Technology, 126392. https://doi.org/10.1016/j.biortech.2021.126392

Yang Z-Y, Gao F, Liu J-Z, Yang J-S, Liu M, Ge Y-M, Chen D-Z, Chen J-M (2021) Improving sedimentation and lipid production of microalgae in the photobioreactor using saline wastewater. Bioresource Technology, 126392. https://doi.org/10.1016/j.biortech.2021.126392

Zhao Y, Wang HP, Han B, Yu X (2019) Coupling of abiotic stresses and phytohormones for the production of lipids and high-value by-products by microalgae: a review. Bioresource technology, 274, 549-556. https://doi.org/10.1016/j.biortech.2018.12.030

Chapter 5

Tisochrysis lutea cultivation under mixotrophic and semi-continuous conditions: morpho- physiological, biochemical variations and antioxidant activity evaluation

1. Introduction

Microalgae have great potential both to produce bioactive molecules and as a source for biofuel (Baldisserotto et al 2016; Maglie et al. 2021; Ma et al. 2022). However, despite continuous research in this field, the cost of microalgal biomass production sometimes is still too high (Legrand et al. 2021; Pereira et al. 2021). The use of mixotrophic cultures is one of the solutions proposed to address this problem (Baldisserotto et al. 2021; Patel et al. 2021; Pereira et al. 2021). Under mixotrophy condition some microalgae can use an organic carbon supplied in the culture medium together with light. This cultivation strategy is considered a promising method to achieve both higher biomass and high-value molecules production than autotrophic or heterotrophic cultivations (Giovanardi et al. 2017; Pang et al. 2019; Penhaul Smith et al. 2020). The most common sources of organic carbon added to culture media are glucose, fructose, acetate and glycerol (Penhaul Smith et al. 2020; Patel et al. 2020; Baldisserotto et. al. 2021). However, the benefits of this cultivation method could be limited by the high cost of carbon sources, which can account for 50-80% of growth medium (Heredia-Arroyo et al. 2010). For this reason, alternative sources of organic carbon, such as by-products of industrial processes, can be used in the cultivation of microalgae (Giovanardi et al. 2013; Giovanardi et al. 2016; Baldisserotto et al. 2021; Pereira et al. 2021). Although *T. lutea* is traditionally considered to be an autotrophic microalga, under alternative culture conditions it is able to exploit organic carbon sources added to the culture medium (Alkhamis and Qin, 2016; Hu et al. 2018). In a recent study Hu and coworkers (2018) tested the growth of *T. lutea* with different carbon sources: glycerol, glucose and acetate. It was found that only glycerol can be used by this microalga. The ability of *T. lutea* to use glycerol, and not the other carbon sources, is related to the fact that the metabolism of organic carbon in microalgae is species-dependent and depends on the presence of specific transporters or permeases (Gupta et al. 2016; Pang et al. 2019; Baldisserotto et al. 2019). Hu et al. (2018) therefore assumed that *T. lutea* has specific transporters for glycerol and not for the other carbon sources tested in their work. They also found that glycerol can only be adequately utilised in the presence of light (mixotrophic conditions) and not in complete heterotrophy. In fact, glycerol is assimilated in parallel with CO_2 fixation. The latter occurs through the Calvin cycle and, thus, contributes to the biomass production (Baldisserotto et al. 2021). This study was aimed at further investigating the ability of *T. lutea* to grow mixotrophically using glycerol as a carbon source. Furthermore, a semi-continuous culture strategy was applied in other to maximise the possibility of growth of this

alga. In fact, in semi-continuous culture, biomass is intermittently harvested by supplementing the fresh culture medium. With proper control of the feeding rates of the culture medium, high biomass productivity can be achieved (Liu et al. 2019; Yin et al. 2020; Solís-Salinas et al. 2021). Furthermore, unlike continuous techniques, semi-continuous cultivation does not necessarily require excessive automation of the system, thus reducing process costs. As mixotrophic culture is known to strongly influence cell metabolism (Baldisserotto et al. 2021), in addition to studying growth, morpho-physiological changes and photosynthetic pigment and lipid accumulation in *T. lute*a, we compared the total antioxidant activity of methanolic and water extracts obtained from the cultures under mixotrophy and autotrophy conditions. In fact, due to the growing demand for natural antioxidants as an alternative to synthetic ones, microalgae are increasingly being considered as a potential source of natural antioxidants by the food industry as well as the cosmetics and nutraceutical industries (Conde et al. 2021). Compared to synthetic antioxidants, natural antioxidants are more biocompatible and eco-friendly (Koyande et al. 2019; Coulombier et al. 2021). In this study the antioxidant activity was evaluated by $ABTS^{\cdot+}$ and DPPH· radical scavenging assays. Indeed, these assays are among the most commonly used tests because they are methodologically simple, inexpensive and the radicals are stable. The ABTS assay evaluates the ability of the extracts to reduce the $ABTS^{\cdot+}$ radical previously produced by the oxidation of ABTS by potassium persulphate, while the DPPH test assesses the ability of the extracts to reduce the DPPH· radical, which is itself stable (Liang and Kitts 2014; Munteanu and Apetrei 2021). Although these two methods are also widely used in the literature to evaluate the antioxidant activity of microalgal extracts *in vitro*, they could present some critical points. Indeed, the results are very heterogeneous and depend on the microalgae species studied, on the protocols used to obtain the extracts and also on the protocols employed to perform the tests that may vary from one study to another (Conde et al. 2021; Coulombier et al. 2021). A further difficulty in comparing results from different studies concerns the way the results are expressed. For example, in the assays used in this study results could be expressed in different ways: as a percentage of inhibition at a given concentration of the substance tested, as Half Maximum Inhibitory Concentration (IC50), or in equivalent moles of a substance with known antioxidant activity, such as Trolox or ascorbic acid using a calibration curve. The latter is the method used in this study and the standard molecule employed for the calibration curve was the α-tocopherol. The DPPH and ABTS tests are applied to evaluate the total antioxidant capacity of the sample. Such measurement is therefore useful for screening/measuring the antioxidant capacity of different samples but does not provide specific information on the antioxidant activity of the different molecules present in the extracts

tested (Lewoyehu and Amare 2019). *T. lutea* is indeed known as an important source of biologically active compounds, which are excellent candidates for antioxidants and anti-inflammatory agents due to their chemical properties (Bigagli et al. 2021). Among these molecules, carotenoids play an important role, first and foremost fucoxanthin, which is produced in large quantities by this microalga (Gao et al. 2020; Mohamadnia et al. 2020, 2021). *Tisochrysis lutea* is also a source of phenolic compounds (Matos et al. 2019) that exhibit a wide range of biological activities, including antioxidant effects (Jerez-Martel et al. 2017; Silva et al. 2021). Chlorophylls also have antioxidant activity, although generally less than that of carotenoids. However, unlike studies on carotenoids, knowledge of their exact oxidation mechanisms is limited (Pérez-Gálvez et al. 2020). Finally, this microalga is one of the main sources of important fatty acids: for example, among the polyunsaturated fatty acids and especially the omega-3, such as eicosapentaenoic acid (EPA) and docosahexaenoic acid (DHA) are known for their beneficial properties, including their antioxidant effects (Kotue et al. 2019; Hu et al. 2019; Maglie et al. 2021; Lafuente et al. 2021). The demand for natural antioxidant molecules is constantly increasing worldwide and this study may open new perspectives for the use of *T. lutea* as a source of such compounds.

2. Material and methods

Algal culture condition and growth

Tisochrysis lutea (Bendif et al. 2013; strain CCAP 927/14) was obtained from the Culture Collection of Algae and Protozoa of Scottish Marine Institute (Scotland, UK; www.ccap.ac.uk). Axenic cultures were grown and maintained in liquid f/2 medium (Guillard and Ryther 1962; Guillard 1975) in artificial seawater ESAW (Berges et al. 2001) in a growth chamber (25 ± 1 °C; 60 $\mu mol_{photons}$ m^{-2} s^{-1} photosynthetically active radiation (PAR); 16:8 h light-dark photoperiod), without shaking, and no additional CO_2. For the experiment, *T. lutea* cells were inoculated at a density of $2 \pm 0.1 \times 10^6$ cells mL^{-1} and grown in the conditions described above. Based on preliminary experiments (data not shown), mixotrophic cultures were prepared by adding glycerol to the cultures at a final concentration of 2.5 g L^{-1}. Before addition to the culture, the glycerol was sterilised by double filtration with Whatman syringe filters with a porosity of 0.22 µm. Cells were cultivated in semi-continuous mode: every 7 days, both autotrophic and mixotrophic cultures were brought back to the initial concentration of 2 x 10^6 cells mL^{-1} adding fresh medium. Three cultivation cycles were carried out in this way, with a total experiment duration of 21 days. Both autotrophic and mixotrophic cultures were inoculated at least in triplicate and grown in 300-mL Erlenmeyer flasks with 150 mL of total

culture volume. Growth was estimated by measuring the optical density at 750 nm and by counting the cells with a Thoma's chamber (HBG, Germany) sampling 1 mL of culture on days 0, 3, 5 and 7 of each cultivation cycle. To make the cell counting easier, 100 µL of Lugol's iodine was added to 1 mL of culture to stop cell movements.

Glycerol concentration determination

According to Kuhn et al. (2015) with minor modification, 2 mL of *T. lutea* mixotrophic cultures were collected on days 0, 3, 5 and 7 of each cultivation cycle and centrifugated. The supernatant (cell-free medium) was transferred into a new tube and stored at -20°C for glycerol determination. Two reagents were needed for the assay. The periodate reagent consisted of 18 mg mL^{-1} sodium periodate (VWR) dissolved in distilled water containing 10% (v/v) acetic acid (VWR). After appropriate mixing, 77 mg mL^{-1} ammonium acetate (VWR) was added. Acetylacetone reagent, consisted of 1% (v/v) acetylacetone (Carlo Erba Reagents Srl) in isopropyl alcohol (VWR). This reagent had to be stored in the dark. The amount of sodium periodate in periodate reagent was calculated for a calibration curve from 0.0 g L^{-1} to 0.2 g L^{-1} glycerol. To ensure that the analysed glycerol concentrations were within this range, each sample was diluted 1:25 with fresh culture medium prior to analysis. An aliquot of 120 µL of sample (cell-free diluted medium) was pipetted into each tube. Then 120 µL of periodate reagent were added and mixed using a vortex. After an incubation time of 10 min, 375 µL of acetylacetone reagent were added and vortexed. The absorption at 410 nm was measured after 25 min of dark incubation at room temperature. The glycerol content in the samples was calculated based on a glycerol calibration curve (Figure 1a). The absorbance measurement was performed using a UV/Visible spectrophotometer (Pharmacia Biotech Ultrospec ®2000).

Light and fluorescence microscopy

Cell samples were observed under a Zeiss Axiophot photomicroscope equipped with conventional or fluorescent attachments. The light source for chlorophyll fluorescence examinations was an HBO 100 W pressure mercury vapour lamp (filter set, BP436/10 FT 460, LP470). To highlight the intracellular lipid accumulation, cells were stained with Nile Red, NR (9-diethylamina-5Hbenzo[α]phenoxazine-5-one; Sigma-Aldrich, Gallarate, Milano, Italy) according to Giovanardi et al. (2013), with some modifications. Aliquots of 10 µL NR (0.5 mg dissolved in 100 mL acetone) were added to 1.9 mL of a cell suspension with 0.5×10^6 cells. After incubation at 37 °C in darkness for 15 min, cells were observed with 485 nm excitation wavelength (filter set BP485, LP520). At the end of each cultivation cycle (7, 14, 21 days),

pictures were taken with a VisiCAM PR0 20C digital camera equipped with a microscope adapter. According to Hillebrand et al. (1999) images were employed to calculate the cell volume using "ImageJ" software (https://imagej.nih.gov/ij/index.html).

Transmission electron microscopy

For transmission electron microscopy (TEM), cells were harvested by centrifugation at the end of each cultivation cycle (7, 14, 21 days) and prepared as reported in Baldisserotto et al. (2020) with minor modifications according to Maglie et al. (2021): the phosphate buffer was substituted with 0.1 M sodium cacodylate buffer (pH 7.2) and 0.25 M sucrose. Ultra-thin sections were observed with a Hitachi H800 electron microscope (Electron Microscopy Centre, University of Ferrara).

Chlorophyll fluorescence measurements

On days 0, 3, 5 and 7 of each cultivation cycle, fluorescence measurements were performed on cell pellets prepared as described by Ferroni et al. (2011). After 15 min of dark incubation, initial fluorescence F_0 and maximum fluorescence F_M were used to calculate the maximum quantum yield of PSII (F_V/F_M ratio). After testing a range between 5 and 40 min of dark adaptation time, 15 min were found to be the optimal adaptation time. For analyses, a pulse amplitude modulation fluorometer (PAM; Junior-PAM, Walz, Germany) was used with the following setting: measuring light (ML) with intensity and frequency at level 1; 0.6 s saturation pulse at level 6.

Photosynthetic pigment extraction and quantification

Both autotrophic and mixotrophic cultures were collected by centrifugation at the end of each cultivation cycle (7, 14, 21 days) to evaluate the photosynthetic pigments content. Cells were treated with 100% methanol for 10 min at 80 °C (Baldisserotto et al. 2012). Absorption of extracts was measured at 665 nm for chlorophyll *a* (Chl *a*), 632 nm for chlorophyll *c* (Chl *c*) and 470 nm for carotenoids (Cars) (Wellburn 1994; Ritchie 2006). Extracts were manipulated under dim light to avoid photo-degradation. Chlorophyll *a* and *c* concentration was evaluated using the equations of Ritchie (2006). Otherwise, the equations of Wellburn (1994) were employed to determine the carotenoid concentration.

Fatty acid determination by gas chromatography

Lipid analysis was performed thanks to the kind collaboration of Prof. A Maietti at the Department of Chemical and Pharmaceutical Sciences of the University of Ferrara. At the end

of each cultivation cycle (7, 14, 21 days), both autotrophic and mixotrophic cultures were collected by centrifugation at 5300×*g* for 15 min. The resulting pellet was frozen and subsequently used for lipid extraction and fatty acid characterisation. To remove residual water, the samples were thawed and centrifuged at 5300×g for 10 min before analysis. The pellet of each sample was resuspended by adding 5 mL chloroform:methanol solution (2:1) and sonicated with an ULTRAsonik NEY 28X Sonicator for 20 min. A centrifugation was performed at 5300×g for 10 min and the supernatant transferred to a 50 mL glass flask. These procedures were repeated twice to optimise lipid extraction. The solvent was evaporated using a Buchi RotavaporR-3 Laboxact and samples were recovered by adding 2 mL of hexane and transferred to a glass tube. The samples were then transesterified by adding 1 mL of standard methanolic sodium hydroxide solution and shaking the tube vigorously. Once the two phases were separated, the supernatant was removed and injected into a GC Variant 3900 SATURN 2100T gas chromatograph. Gas chromatography was performed using a 60 m wax column; helium (He) was used as a carrier gas to pass the sample across the column. Each chromatographic run lasted 12 hours.

Antioxidant activity assay

Both autotrophic and mixotrophic cultures were collected by centrifugation at the end of each cultivation cycle (7, 14, 21 days) to evaluate the antioxidant activity. For this purpose, the DPPH and ABTS tests were used. Two types of extracts, obtained from a cell suspension with a density of $10x10^6$ cell mL^{-1}, were tested. A methanolic extract (ME) was prepared according to Baldisserotto et al. (2012) as described above for the quantification of photosynthetic pigments. In order to obtain an aqueous extract (AE), the blanched pellet obtained by the previous extraction was subjected to a second extraction in distilled water at 80° C for 15 min to extract the hydrophilic substances. All the analysis were performed under dim light to avoid photo-degradation of extracts and reagents.

DPPH assay

The test was performed according to Brand-Williams et al. (1995) with numerous adaptations due to the use of different instruments. A stock solution of 1,1-diphenyl-2-picrylhydrazyl (DPPH; Sigma-Aldrich, Gallarate, Milano, Italy) in 100% methanol at the concentration of 0.6 mM was prepared. Before use, DPPH · solution was diluted with 100% methanol to an absorbance of 0.390 (±0.01) at 517 nm, corresponding at a concentration of 0.03 mM (±0.001). This was the final concentration at which the extracts were tested based on the preliminary

experiments. Aliquots of the extract were added to 1 mL of DPPH˙ diluted solution and mixed with the vortex and allowed to react for 30 min at room temperature in the dark. After 30 min the absorbance at 517 nm was read and the scavenging activities (%) calculated as:

% Inhibition = (1-*Abs net*)/*Abs blanc*

Where:

- *Abs net* is the absorbance of 500 µL of sample added to 1mL of DPPH˙ diluted solution, from which is subtracted the absorbance of 500 µl of sample added to 1 ml of methanol.
- *Abs blanc* is the absorbance of 1 mL of DPPH˙ diluted solution.

The antioxidant activity of the extracts was expressed as µM of α-tocopherol equivalents (α-TE µM) based on a calibration curve (Figure 1b) by measuring the DPPH˙ scavenging activities (%) of 0, 3, 6, 9, 12 µM of α-tocopherol in methanol. The absorbance measurement was performed using a UV/Visible spectrophotometer (Pharmacia Biotech Ultrospec ®2000).

ABTS assay

According to Re et al. (1999) with minor modifications, 2,2′-azino-bis-3-ethylbenzthiazoline-6-sulphonic acid (ABTS; Sigma-Aldrich, Gallarate, Milano, Italy) was dissolved in distilled water at a concentration of 7 mM. The ABTS radical cation ($ABTS^{\cdot+}$) was generated by adding potassium persulphate (final concentration, 2.45 mM) to the aqueous ABTS solution. The mixture reacted in the dark at room temperature for 12-16 hours. Before use, $ABTS^{\cdot+}$ solution was diluted with 100% methanol to an absorbance of 0.70 (±0.02) at 734 nm. Aliquots of 500 µL of extract were added at 1mL of $ABTS^{\cdot+}$ diluted solution. After 5 min the absorbance at 734 nm was read and the scavenging activities (%) calculated as:

% Inhibition = (1- *Abs sample*)/*Abs blanc*

Where:

- *Abs sample* is the absorbance of 500 µL of sample added at 1mL of $ABTS^{\cdot+}$ diluted solution.
- *Abs blanc* is the absorbance of 500 µL of MeOH added at 1mL of $ABTS^{\cdot+}$ diluted solution.

The antioxidant activity of the extracts was expressed as µM of α-tocopherol equivalents (α-TE µM) based on a calibration curve (Figure 1c) by measuring the $ABTS^{\cdot+}$ scavenging activities (%) of 0, 3, 6, 9, 12, 15 µM of α-tocopherol in methanol. The absorbance measurement was performed using a UV/Visible spectrophotometer (Pharmacia Biotech Ultrospec ®2000).

Statistical analysis

Data were processed and analysed using Microsoft® Excel® (version 2111). When necessary, statistical tests such as Student *t*-test, one-, two-way ANOVA were performed using Origin® 2021 analysis software, followed by Tukey post-hoc test ($p < 0.05$). All the experiments were conducted at least in triplicate.

3. Results

Growth kinetics

Figure 2 shows the growth kinetics of *T. lutea* under autotrophic and mixotrophic conditions employing semi-continuous strategy. During all three cycles of semi-continuous cultivation, mixotrophic cultures resulted always more concentrated than the autotrophic ones ($p < 0.05$; two-way ANOVA followed by post-hot Tukey test). Moreover, the mixotrophic cultures showed variations in growth trend from one cultivation cycle to the next. In particular, the cultures reached maximum cell density in a shorter time in each cycle. For example, the cell density in the first cultivation cycle, 3 days after inoculation, was 3.42 x 10^6 cells mL^{-1}. After 3 days from the beginning of the second cycle (10 experimental days), the cell density was significantly higher (4.35 x 10^6 cells mL^{-1}) ($p < 0.05$; two-way ANOVA followed by post-hot Tukey test). An even faster increase was observed on the 3rd day of the last cultivation cycle (17 experimental days), when a value of 5.65 x 10^6 cells mL^{-1} was observed. This value was not significantly different ($p > 0.05$; two-way ANOVA followed by Tukey test) from the maximum cell density values observed at the end of the first and second cultivation cycles (7 and 14 experimental days) (6.02 and 6.28 x 10^6 cells mL^{-1}, respectively). On the contrary, the growth trend of the autotrophic culture was the same during the three cultivation cycles (0-7; 7-14 and 14-21 days of cultivation) without significant differences ($p > 0.05$; Two-way ANOVA followed by post-hoc Tukey test). In each cycle, the average cell density increased from 2 x 10^6 cells mL^{-1} on the day of inoculation or culture dilution to about 3x10^6 cell mL^{-1} after three days of cultivation. Between the 3rd and the 5th day of cultivation of each cycle, growth slowed, but cultures did not enter a stationary phase. In fact, after the 5th day in each cycle, cell density continued to grow until the end of each cycle (7, 14, 21 days). Only at 21 days of cultivation the autotrophic cultures showed a significant lower cell density than that at the end times of the previous two cultivation cycles (7 and 14 days) ($p < 0.05$; Two-way ANOVA followed by post-

hoc Tukey test). On the other hand, the average cell density of the autotrophic culture was significantly different from that of the mixotrophic culture (t-test, $p < 0.05$).

Glycerol consumption in mixotrophic culture

Figure 3 shows the concentration of glycerol in the culture medium and the growth of the cells grown under mixotrophic conditions over the course of the experimental days. With increasing cell density, the concentration of glycerol in the culture medium decreased. During the first culture cycle (0-7 days), cells consumption of glycerol was gradual. The glycerol concentration decreased significantly from 2.54 ± 0.18 g L^{-1} (0 day) to 1.35 ± 0.34 g L^{-1} (7 days) ($p < 0.05$; Two-way ANOVA followed by post-hoc Tukey test). Between day 0 and day 3, glycerol concentration decreased (2.06 ± 0.31 g L^{-1} at day 3), but the difference was not significant ($p > 0.05$; Two-way ANOVA followed by post-hoc Tukey test). In contrast, a more rapid decrease in glycerol concentration was observed during the second semi-continuous culture cycle (7-14 days). In only three days (from day 7 to day 10), the glycerol concentration decreased from 2.53 ± 0.18 g L^{-1} to 1.17 ± 0.09 g L^{-1} ($p < 0.05$; Two-way ANOVA followed by post-hoc Tukey test). The glycerol content in the culture medium then decreased further to 0.66 ± 0.03 g L^{-1} on day 14, the last day of the second cultivation cycle. During the third and last cycle of semi-continuous cultivation (14-21 days), the glycerol consumption of the cells was faster than in the first cycle, but less rapid than in the second. During the first three days (from day 14 to day 17), the glycerol concentration decreased significantly (from 2.58 ± 0.13 g L^{-1} to 1.44 ± 0.26 g L^{-1}) ($p < 0.05$; Two-way ANOVA followed by post-hoc Tukey test). However, the further decreases in glycerol concentration observed in the period from 17 to 21 days were not statistically significant as instead was observed in the second cycle during the same time interval ($p > 0.05$; Two-way ANOVA followed by post-hoc Tukey test).

Cell morphology

Light microscopy observations were performed in both conventional light and fluorescence on *T. lutea* cultures grown under autotrophic and mixotrophic conditions. Figure 4 shows cells in conventional light and the epifluorescence of Nile Red stained cells. Observations under conventional light showed differences between cells in autotrophy and those in mixotrophy. However, both autotrophic and mixotrophic cells showed unchanged morphology during the different cycles of semi-continuous cultivation (0-7; 7-14 and 14-21 days), except for cellular volume. In all phases of the experiment, the autotrophic cells were characterised by a yellow-brown or yellow-golden colour (Fig. 4a, e, i). They showed the typical elongated or ovoid shape,

the flagella were clearly visible (Fig. 4a, i), and the cells were well motile. However, during the different cultivation cycles, there was a progressive and significant decrease in cell volume ($p < 0.05$; two-way ANOVA followed by post-hoc Tukey test). At the end of the first cultivation cycle (7 days), the average volume was about 120 μm^3; after 14 days it had decreased to about 85 μm^3 and at the end of the experiment (21 days) the average volume was 65 μm^3. On the other hand, the cells grown in mixotrophy had lost their typical elongated form and showed a spherical shape. However, the flagella and motility were well preserved throughout the experimental phases (Fig. 4c, g, m). On average, the cells in the mixotrophic conditions were larger than those autotrophic. At the end of the first cultivation cycle (0-7 days), the average cell volume was about 130 μm^3, which was very similar to that of the autotrophic cells during the same period of cultivation ($p > 0.05$; two-way ANOVA followed by post-hoc Tukey test). However, during the second cultivation phase (7-14 days), the average cell volume increased dramatically to 305 μm^3 and then decreased at the end of the third cultivation cycle (21 days), when average values of 117 μm^3 were observed. These values were significantly higher than those observed in autotrophic cultures at the same cultivation phases ($p < 0.05$; two-way ANOVA followed by post-hoc Tukey test). Another difference between autotrophy and mixotrophy was observed in the number and size of lipid globules within the cells. In conventional light, the lipid globules appeared as translucent droplets within the cells. Staining with Nile red and subsequent fluorescence observation revealed and confirmed the lipid nature of the droplets. In general, a large number of lipid globules were observed in mixotrophic cells during all cultivation cycle (5 or even 6 globules per cell) (Fig. 4d, h, n). In contrast, autotrophic cells had a smaller number of lipid globules (2 or 3 per cell) and these were generally smaller than those in mixotrophic cells (Fig. 4b, f, l).

Subcellular TEM observation

The subcellular features were observed by transmission electron microscopy (Fig. 5). Both autotrophic and mixotrophic cultured cell presented the typical organic scales on the outer surface (Fig. 5c, d). The organisation of the autotrophic cells showed no particular changes during the three cultivation cycles (Fig. 5a, c, e). The plastid arranged along the cell walls with its typical cup shape and the pyrenoid immersed in its interior, crossed by some thylakoid membranes, was clearly visible (Fig. 5a, c). The thylakoid membranes appeared unaltered (Fig. 5a). However, in the first two cycles of cultivation (0-7 and 7-14 days), there were few cells with lipid globules. In contrast, in the cell samples at the end of the third cycle of cultivation in autotrophy (21 days), the cells with lipid globules were more abundant than those at the

previously cultivation phases (Fig. 5e). Already during the first cultivation cycle (0-7 days), the thylakoid membranes resulted more appressed in the mixotrophic cells than those in the autotrophic cells (Fig. 5b). Furthermore, the general structures of the cells and of the plastid showed altered morphologies in the subsequent culture phases (Fig. 5d, f). However, the mitochondria were clearly visible, indicating intense metabolic activity (Fig. 5d, f). In contrast to what was observed during autotrophic cultivation, lipid globules were clearly visible from the second cultivation cycle (7-14) onwards, in numbers of 2 or 3 per cell. The lipid globules were dark in colour, large and occupied a large space within the cell (Fig. 5d, f).

PSII maximum quantum yield measurement

Figure 6 shows the effects of autotrophic and mixotrophic culture on the F_V/F_M values allowing an estimation of photosynthetic efficiency. Under autotrophic conditions, *T. lutea* showed constant F_V/F_M values throughout the experiment. The values varied between 0.65 and 0.63 and always remained above the threshold value of 0.6. The only significant decrease in photosynthetic efficiency was observed at the end of the experiment (21 days), when the F_V/F_M value dropped to 0.57 ($p < 0.5$; Two-way ANOVA followed by post-hoc Tukey test). In contrast, the mixotrophic cultures showed a discontinuous trend in F_V/F_M values, but always similar both in each of the three cultivation cycles (0-7, 7-14 and 14-21 days). Indeed, in each of the three cultivation cycles, F_V/F_M values increased in the first three days (3, 10 and 17 days) and reached their maximum value (between 0.69 and 0.68). Thereafter, the values started to decrease, remained above the threshold of 0.6 until the fifth day of each cycle (5, 12, 19 days) and finally dropped to values between 0.54 and 0.52 on the last days of each cycle (7, 14 and 21).

Photosynthetic pigments content

At the end of each cultivation cycle (7, 14, 21 days), the concentrations of chlorophyll *a*, *c* and total carotenoids were measured in the methanolic extracts of both autotrophic and mixotrophic cells. In both cultures, the concentration of Chl a did not vary significantly over time ($p > 0.05$; Two-way ANOVA followed by post-hoc Tukey test). However, autotrophically grown cells showed a significantly higher Chl *a* concentration after 14 and 21 days compared to mixotrophic cells (about 50% higher in both cases) (Fig. 7a) ($p < 0.05$; Two-way ANOVA followed by post-hoc Tukey test). The same trend was observed for Chl *c* concentrations, which were 42.11% and 53.33% higher in the autotrophic cultures than in the mixotrophic cultures on days 14 and 21, respectively (Fig. 7b). Finally, there was no significant difference in the concentration of

carotenoids, which remained stable over time and showed similar concentrations in autotrophic and mixotrophic cultures ($p > 0.05$; Two-way ANOVA followed by post-hoc Tukey test) (Fig. 7c).

Fatty acid determination by gas chromatography

The fatty acids extraction and analysis by gas chromatography were performed on cells collected at the end of each cultivation cycle (7, 14, 21 days). Figure 8 shows the relative proportions of saturated, mono- and polyunsaturated fatty acids in autotrophic and mixotrophic cells at 7, 14 and 21 days of cultivation. In autotrophy, the proportion of saturated fatty acids tended to decrease over time. After 7 days, saturated fatty acids accounted for 61% of the total, after 14 days 53% and after 21 days 48%, with a significative variation between 7 and 21 days ($p < 0.05$; two-way ANOVA followed by post-hoc Tukey test). An opposite trend was observed for polyunsaturated fatty acids, which increased from 17% after 7 days to 26% after 21 days, with a significative variation between 7 and 21 days ($p < 0.05$; two-way ANOVA followed by post-hoc Tukey test). There were no major changes in the monounsaturated fatty acids ($p > 0.05$; two-way ANOVA followed by post-hoc Tukey test). In the mixotrophic cultures, saturated fatty acids ranged from 46% at day 7 to 40% at day 21, a significative decrease compared to the autotrophic cultures ($p < 0.05$; two-way ANOVA followed by post-hoc Tukey test- except between 21 days autotrophic results and 7 days mixotrophic results), but almost constant over time ($p > 0.05$; two-way ANOVA followed by post-hoc Tukey test). Polyunsaturated fatty acids also remained constant between the first and last cultivation cycle, amounting to about 25% of the total fatty acids ($p > 0.05$; two-way ANOVA followed by post-hoc Tukey test). For the monounsaturated fatty acids, a very slight increase from 29 to 35% was observed in the period from 7 to 21 days. These differences not resulted statistically significant ($p > 0.05$; one-way ANOVA followed by post-hoc Tukey test) but at 14 and 21 days the monounsaturated fatty acids in mixotrophic cultures were significatively higher than those in autotrophic cultures ($p < 0.05$; one-way ANOVA followed by post-hoc Tukey test). These differences were accompanied by variations in the lipid profile of the mixotrophic and autotrophic cultures. Indeed, the proportions of specific fatty acids changed between control and treated samples. Table 2 reported the fatty acid profile characterized by GC-MS. In the autotrophic cultures, the most abundant fatty acid was palmitic acid (16:0), followed by tridecylic acid (13:0) and elaidic acid (18:1n9). High levels of 16:0 were also observed in the mixotrophic cultures, but the most abundant fatty acid was 18:1n9. Elaidic acid also increased slightly over time (24%, 27% and 29% after 7, 14 and 21 days, respectively) and its percentage

content was higher than that observed in the autotrophic samples. In terms of ω-3 fatty acid content, in mixotrophic cultures eicosapentaenoic acid (EPA; 20:5n3) accounted for 12.86% after 7 days, compared to 8.61% in the autotrophic cultures. After 14 and 21 days, however, the values of EPA were almost the same in autotrophic and mixotrophic cultures. Finally, the important ω-3 docosahexaenoic acid **(**DHA; 22:6n3), after 7 days, was more abundant in the mixotrophic cultures than in the autotrophic ones (5% and 1.84% respectively). But as already observed at EPA, the mixotrophic cultures have approximately the same percentage content after 14 and 21 days.

Antioxidant activity evaluation

Through DPPH and ABTS assays, the antioxidant activity of methanolic and aqueous extracts of both autotrophic and mixotrophic cultures was evaluated at the end of each cultivation cycle (7, 14, 21 days). Using the DPPH assay, the antioxidant activity of the methanolic extracts from the autotrophic cultures (MEa) showed greater antioxidant activity than that of the mixotrophic cultures (MEm) after 7 and 21 days ($p < 0.05$; two-way ANOVA followed by post-hoc Tukey test) (Fig. 9a). MEa was 26.3% more effective than MEm after 7 days and 125% more effective after 21 days. There was no significant difference between the efficiency of the two extracts at 14 days ($p > 0.05$; two-way ANOVA followed by post-hoc Tukey test). When comparing the efficiency of the extracts in terms of μM of α-tocopherol equivalent (α-TE; μM), the antioxidant activity declined over time both for MEa and Mem ($p < 0.05$; two-way ANOVA followed by post-hoc Tukey test). In fact, MEa showed an antioxidant activity of 5.37 α- TE μM after seven days, and 2.79 α- TE μM after 21 days. The same trend was observed for MEm: 4.25 and 1.24 α- TE μM after 7 and 21 days respectively. The results of the ABTS assay are shown in Figure 9b. The assay confirmed a higher antioxidant activity of MEa compared to MEm after 7 and 21 days (36.6% and 20.64% higher, respectively) ($p < 0.05$ two-way ANOVA followed by post-hoc Tukey test). Again, no significant difference was observed between the efficiency of the two extracts at 14 days ($p > 0.05$; two-way ANOVA followed by post-hoc Tukey test). When the efficacy of the extracts is assessed in terms of α-TE μM, MEa showed approximately the same efficacy at both 7 and 21 days (13.29 and 12.85 α-TE μM, respectively; $p < 0.05$; two-way ANOVA followed by post-hoc Tukey test). The lowest efficacy was observed after 14 days (7.42 α-TE μM). MEm, on the other hand, showed no significant difference between 7 and 14 days (9.72 and 8.78 α-TE μM, respectively; $p < 0.05$; two-way ANOVA followed by post-hoc Tukey test). After 21 days, the highest efficacy was observed at 10.75, slightly but significantly higher than after 7 and 14 days ($p < 0.05$; two-way ANOVA followed by post-hoc Tukey test).

The evaluation of the antioxidant activity of the aqueous extracts (AE) has not yielded results in some cases (Figure 10). The extracts obtained at the end of the first cultivation cycle (7 days) showed inconsistent results between the DPPH assay and the ABTS assay. Indeed, AEm showed much higher antioxidant activity than AEa (218.9% higher) in the DPPH assay. However, the ABTS assay showed no difference between the effects of the two extracts. Moreover, the activity of AEm was not detectable in the DPPH assay at 14 and 21 days. Other controversial results were observed in the ABTS assay between 14 and 21 days. After 14 days, both AEa and AEm showed antioxidant activity (2.82 and 3.14 α-TE μM, respectively). However, after 21 days, only the antioxidant activity of AEm was detectable, while AEa activity was not detectable.

4. Discussion

In this study, *Tisochrysis lutea* has been cultivated under autotrophic and mixotrophic conditions. In the mixotrophic culture, glycerol was added at a concentration of 2.5 g L^{-1}. Cells were grown using a semi-continuous cultivation strategy: every 7 days part of the biomass was collected and both autotrophic and mixotrophic cultures were diluted with fresh medium until the initial concentration of 2 x 10^6 cells mL^{-1} was returned. The whole experiment lasted 21 days for a total of three 3 cultivation cycles. During all the phases of the experiment, the growth of *T. lutea* was stimulated in mixotrophy compared to that of controls in autotrophy. This result was consistent with studies conducted by Hu and colleagues (2018) that tested the growth of *T. lutea* in mixotrophy using glycerol, glucose and acetate as carbon sources at a concentration of 5 g L^{-1}. Furthermore, that *T. lutea* preferred glycerol as carbon source. In fact, the consumption of specific carbon sources such as glucose, glycerol, and acetate under mixotrophic condition is species-specific and is influenced by the presence of specific transporters or permeases (Gupta et al. 2016; Baldisserotto et al. 2021). In the experiments conducted by Hu et al. (2018), the mixotrophic cultures required an 8-day adaptation period, during which there were no differences compared to growth in autotrophy. However, after day 8, the biomass in mixotrophy was higher than that in autotrophy. In our experiment, the cultures showed did not show any adaptation phase. Indeed, already on the 3rd day of the first culture cycle, a higher cell density was observed in the mixotrophic cultures than in the autotrophic ones. Nevertheless, in our experiment, it can be assumed that the utilisation of the carbon source by *T. lutea* cells improved over time. Indeed, with each subsequent cultivation cycle, the mixotrophic cultures reached the maximum cell density in a shorter time. For example, on the 3rd day of the last cultivation cycle, the cultures reached a cell density comparable to that observed at the end of the first cultivation

cycle (7 days). Analyses of the glycerol content in the exhausted culture medium confirmed this hypothesis. Indeed, the glycerol content decreased more and more rapidly over time in the cultivation cycles following the first one. Moreover, the faster decrease in glycerol corresponded to a higher cell density of the cell cultures. These results are consistent with the observations of Hu et al. (2018), who found that the trend of decrease in glycerol corresponded to the increase in biomass in the mixotrophic cultures. Thus, the cultivation protocol used in the present work leads to achieve a higher cell density in a shorter time with each cultivation cycle, which seems to be related to the increasingly better adaptation of the cells to the use of the carbon source in the medium after each cultivation cycle. Regarding the effects of mixotrophic cultivation on photosynthetic pigments, the presence of glycerol in the culture medium negatively affected the chlorophyll *a* and *c* content in the cells, while no changes were observed in the content of carotenoids, which were present in similar concentrations in autotrophic and mixotrophic cultures. This result contrasted with those of Alkhamis and Qin (2016), where both chlorophylls and carotenoid concentrations have increased of about 60% when *T. lutea* was grown mixotrophically by supplementing the culture medium with glycerol (final concentration 50 mM). The analysis of the PSII maximum quantum yield by PAM fluorimetry allows an estimate of the photosynthetic efficiency and can be used as a rapid parameter to evidence the physiological stress in microalgae. F_V/F_M values above 0.6 indicate that the cells are in a good state, while values below 0.6 confirm that the cells are in a condition that does not allow photosynthetic processes to take place efficiently (Cosgrove and Borowitzka 2010; Bhola et al. 2016; Patil et al. 2020). F_V/F_M values in the autotrophic cultures remained more or less constant and above 0.6 throughout the experiment and did not appear to change in response to changes in cultures growth. This was consistent with observations made with TEM. In fact, the chloroplast and thylakoid membranes of the autotrophic cells appeared in good conditions throughout the experiment. In contrast, in mixotrophic cells observed at the end of each cultivation cycle (7, 14 and 21 days), alterations were evident in the chloroplast, which appeared flattened and with more appressed thylakoid membranes. Consistently, at 7, 14 and 21 days, the F_V/F_M values (0.53 ± 0.01) were below 0.6. However, the F_V/F_M values of the mixotrophic cultures were not as constant as those observed in autotrophy. On the contrary, the changes in F_V/F_M values appeared to be correlated with the changes in culture cell density and glycerol consumption. Indeed, in each of the three cultivation cycles, an increase in F_V/F_M values was observed during the exponential phase of mixotrophic growth. In the exponential growth phase, mixotrophic cultures had a significantly higher photosynthetic efficiency than autotrophic ones. Then, F_V/F_M values gradually decreased until they were below 0.6 at the end of each cultivation

cycle. Interestingly, higher F_V/F_M values during the exponential phase of growth in mixotrophic cultures was previously observed in other microalgae. For example, *Thalassiosira pseudonana* grown in the presence of pure or crude glycerol showed an increase in F_V/F_M values during the exponential growth phase (Baldisserotto et al. 2021). The same phenomenon was also observed in the green alga *N. oleoabundans* grown in a mixotrophic medium: in that case, it was found that the decrease in chloro-respiration induced by mixotrophy and better use of light for photosynthesis led to an increase in F_V/F_M values (Baldisserotto et al. 2014; Baldisserotto et. al. 2016; Giovanardi et al. 2017; Ferroni et al. 2018). As observed in other microalgae in mixotrophic culture such as *T. pseudonana* (Baldisserotto et al. 2021) and *P. tricornutum* (Villanova et al. 2017), the accumulation of lipid globules also occurred in *T. lutea* at the same time as the photosynthetic efficiency was reduced. This was highlighted both from the microscope fluorescence observations after Nile Red staining and from the observations at TEM. Analysing the fatty acid profile of *T. lutea*, variations in the proportions of specific fatty acids between autotrophic and mixotrophic cultures were observed. In general, the mixotrophic cultures had a higher content of monounsaturated fatty acids than the autotrophic ones, while the saturated fatty acids were present in lower proportions. The content of polyunsaturated fatty acids, on the other hand, was almost unchanged. However, there were no significant changes in the proportions of the different fatty acid components in the mixotrophic cultures when compared after 7, 14 and 21 days. These results were in contradiction with the findings of Hu et al. (2018) in *T. lutea*, because in that study not only no differences in the content of polyunsaturated fatty acids between autotrophic and mixotrophic cultures were present, but also no differences in the proportions of saturated and monounsaturated fatty acids. In addition, the results of the present study differed from those reported for *T. lutea* from Alkhamis and Qin (2016), where a greater accumulation of saturated and polyunsaturated fatty acids was observed during mixotrophic cultivation, while autotrophic cultures had greater amounts of monounsaturated fatty acids. However, many Authors reported that mixotrophy can lead to changes in the fatty acid composition of microalgae (Alkhamis and Qin, 2016; Baldisserotto et al. 2016; Baldisserotto et al. 2021; Patel et al. 2021). These changes are generally very variable and depend on the microalgal species, on the carbon source used and on the other variables in the cultivation conditions, such as light and nutrients availability (Patelet et al. 2021). When the proportions of specific fatty acids were compared, it was found that two saturated fatty acids (16:0 and 13:0) were actually most strongly represented in autotrophy, while the monounsaturated 18:1n9 fatty acid was among the most present in mixotrophic cultures. Although there were no differences in total polyunsaturated fatty acid

content between cells in mixotrophy and those in autotrophy, interestingly, at the end of the first cultivation cycle (7 days), the levels of two important omega-3 fatty acids, eicosapentaenoic acid (EPA) and docosahexaenoic acid (DHA), were much higher in mixotrophy than in autotrophy. EPA and DHA are two important fatty acids for the entire marine trophic chain and play a role in human physiology (Ramesh Kumar et al. 2019; Zhang et al. 2019). Since microalgae are the main producers of these molecules, the study of new methods to increase their productivity in these microorganisms is interesting for an economic, healthy and environmental perspective (Peltomaa et al. 2018; Maglie et al. 2021). In addition to playing an essential role in nutrition, omega-3 fatty acids are molecules with antioxidant properties (Conde et al. 2021). In this study, besides to comparing the morpho-physiological aspects and the content of photosynthetic pigments and fatty acids in *T. lutea* under mixotrophic and autotrophic conditions, tests to evaluate the antioxidant activity of methanolic and aqueous extracts of microalgal biomass under the two different growth conditions were also performed. The antioxidant activity was evaluated *in vitro* using the DPPH and the ABTS assays, two common and fast colorimetric assays performed through spectrophotometry. Although the two tests may have different sensitivities to the antioxidant molecules tested, both are based on the assessment of the scavenging activity of antioxidant molecules, such as pigments, phenols and fatty acids (Floegel et al. 2011; Conde et al. 2021). Therefore, they were used in parallel in this study to obtain a dual analysis of the extracts tested and to better understand their effects. To date, this is the first time that the antioxidant activity of *T lutea* extracts has been evaluated by comparing the effects of autotrophy and mixotrophy using a semi-continuous cultivation protocol. In the case of the water extracts, the results obtained are not easy to be interpreted due to the high variability of the data obtained. The lack of antioxidant activity of some extracts at certain experimental times not only makes it impossible to assess how the different cultivation cycles may affect the antioxidant activity, but in some cases does not even allow a comparison between the two cultivation methods. On the other hand, with methanolic extracts, both tests gave comparable results. Although the ABTS test was more sensitive and showed higher α-TE values than the DPPH test for all methanolic extracts tested, one test confirmed the data of the other. Thus, greater antioxidant activity was observed in the extracts from autotrophic cultures. This was clearly visible in the extracts after 7 and 21 days in both tests. After 14 days, the extracts showed the same antioxidant activity. We believe that, in this study, the molecules with antioxidant activity are the photosynthetic pigments and the fatty acids. Among the former, carotenoids are the molecules with the highest antioxidant power, while among the latter, polyunsaturated fatty acids have the highest antioxidant activity (Coulombier et al. 2021; Conde

et al. 2021). However, the similar concentrations of carotenoids and polyunsaturated fatty acids found between autotrophic and mixotrophic cultures do not provide an explanation for the increased antioxidant activity found in microalgal extracts at days 7 and 21. However, interestingly both autotrophic and mixotrophic extracts produced by *T. lutea* showed antioxidant activity. The antioxidant activity in microalgae is well known and represents an opportunity from an economic and a biotechnological point of view. Indeed, there is an ongoing search for new molecules with antioxidant activity that can be employed in the food industry (e.g., as preservatives) and in the cosmetic/pharmaceutical sector to prevent damage caused by oxidative stress and, at the same time, the development of various diseases (Nethravathy et al. 2019; Conde et al. 2021). Moreover, antioxidants of microalgal origin have shown higher bioavailability compared to synthetic antioxidants (Koyande et al. 2019). Overall, in this study, it was shown that the ability of *T. lutea* to grow under mixotrophic conditions with glycerol as an organic carbon source resulted in higher growth compared to autotrophic cultures. Furthermore, it was shown that growth under mixotrophic conditions can be further increased by using a semi-continuous cultivation protocol, allowing the mixotrophic cultures to reach their maximum density in a shorter time after each cultivation cycle. Furthermore, the antioxidant activity of extracts, both from autotrophic and mixotrophic cultures, showed that *T. lutea* can be a good source of high-value molecules. However, in this context, it was shown that there were no differences between the content of high value compounds, such as carotenoids and polyunsaturated fatty acids, when autotrophic and mixotrophic cultures were compared. Nevertheless, the cultivation protocol described in this work could be used in the future in order to achieve a higher algal biomass through mixotrophic cultivation and, at the same time, to increase the content of high-value molecules by changing parameters, such as salinity and light quality once the maximum cell density has been reached.

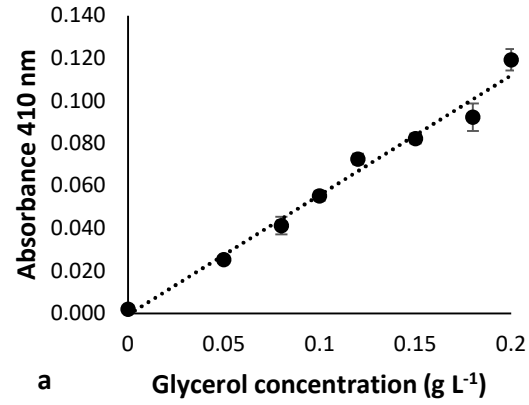

Figure 1 a Calibration curve of glycerol concentration (g L^{-1}). R^2 = 0.982. b Calibration curve of α-Tocopherol DPPH free radical scavenging activity in percentage (%). R^2 = 0.977. c Calibration curve of α-Tocopherol ABTS free radical scavenging activity in percentage (%). R^2 = 0.9991.

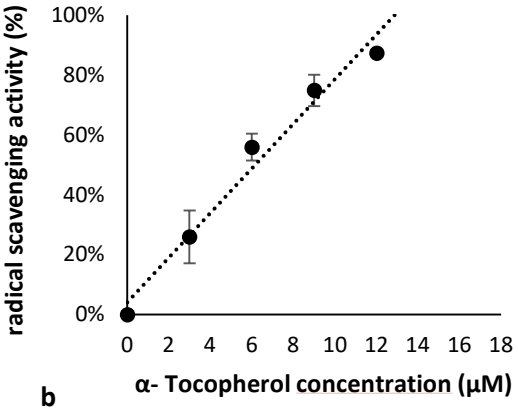

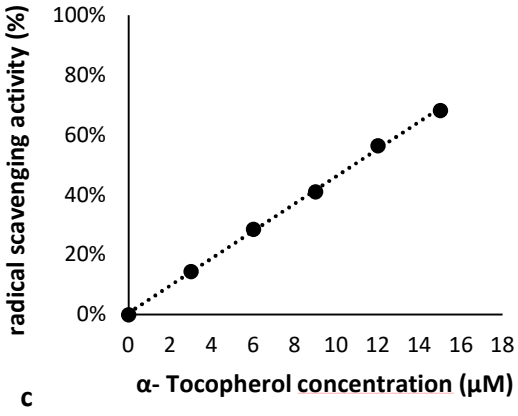

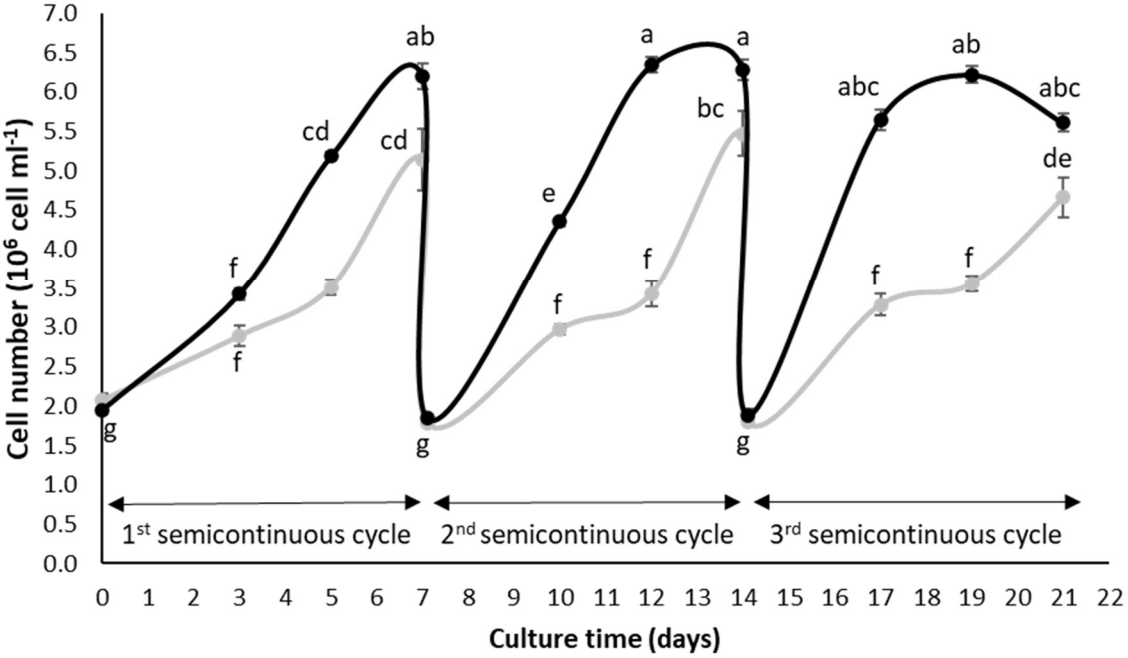

Figure 2 Growth kinetics of *T. lutea* under autotrophic (grey) mixotrophic (black) conditions. Values are means ± SD. Different letters indicate statistically significant differences ($p < 0.05$, three-way ANOVA). Arrows indicate the 3 cultivation cycles. At the end of each cycle, the cultures were diluted with fresh culture medium to the initial concentration of $2x10^6$ cell mL^{-1}.

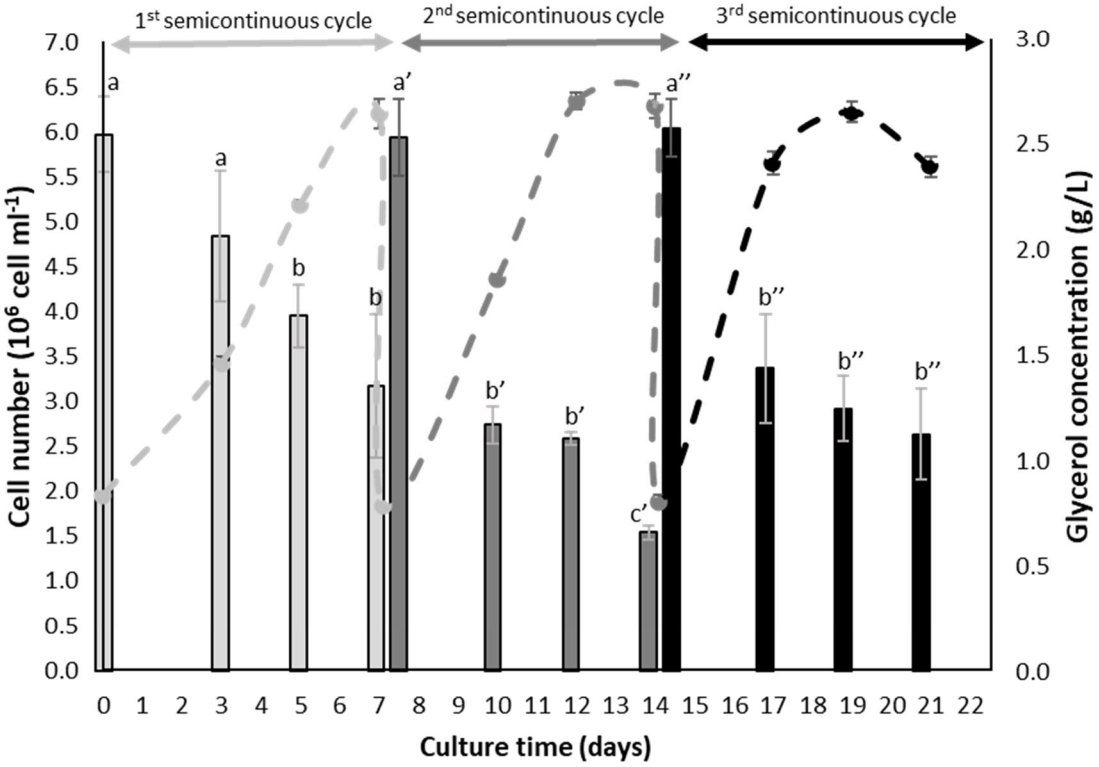

Figure 3 Dotted line indicate the growth kinetics of *T. lutea* under mixotrophic conditions. Bars indicate the concentration of glycerol concentrations (g/L) in the exhausted culture medium during the three cultivation cycles: 1st cycle (light grey), 2nd cycle (dark grey), 3rd cycle (black). Arrows indicate the 3 cultivation cycles. At the end of each cycle, the cultures were diluted with fresh culture medium to the initial concentration of $2x10^6$ cell mL^{-1}.

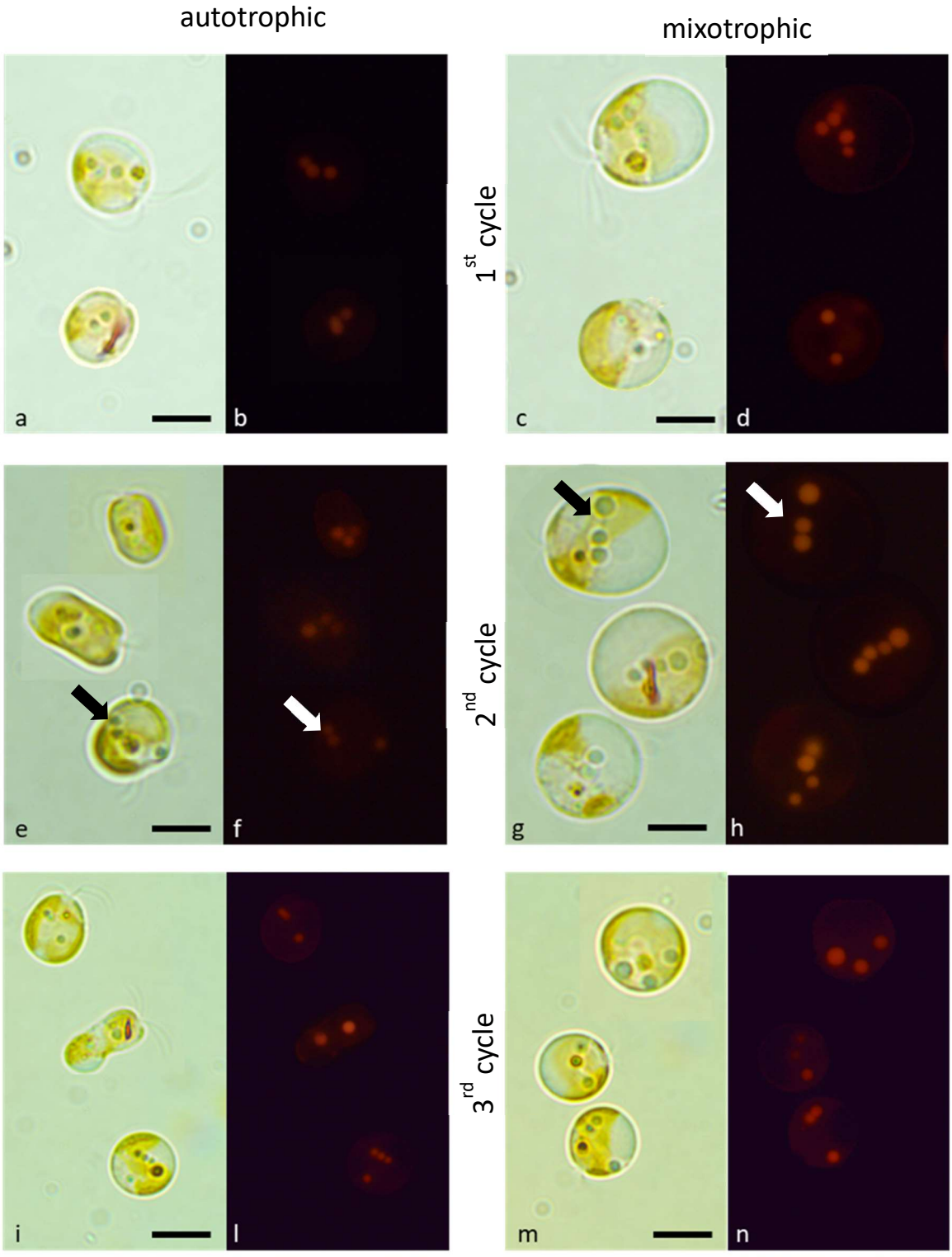

Figure 4 Microscope observations of *T. lutea* cells under autotrophic (a, b, e, f, i, l) and mixotrophic (c, d, g, h, m, n) conditions at the end of each cultivation cycle: 1st cycle, 7 days (a-d); 2nd cycle 14 days (e-h); 3rd cycle, 21 days (i-n). Conventional light (a, e, i, c, g, m) and epifluorescence of Nile Red stained cells (b, f, l, d,, h, n). Arrows show lipid globules in some cells. Scale bars = 5 µm

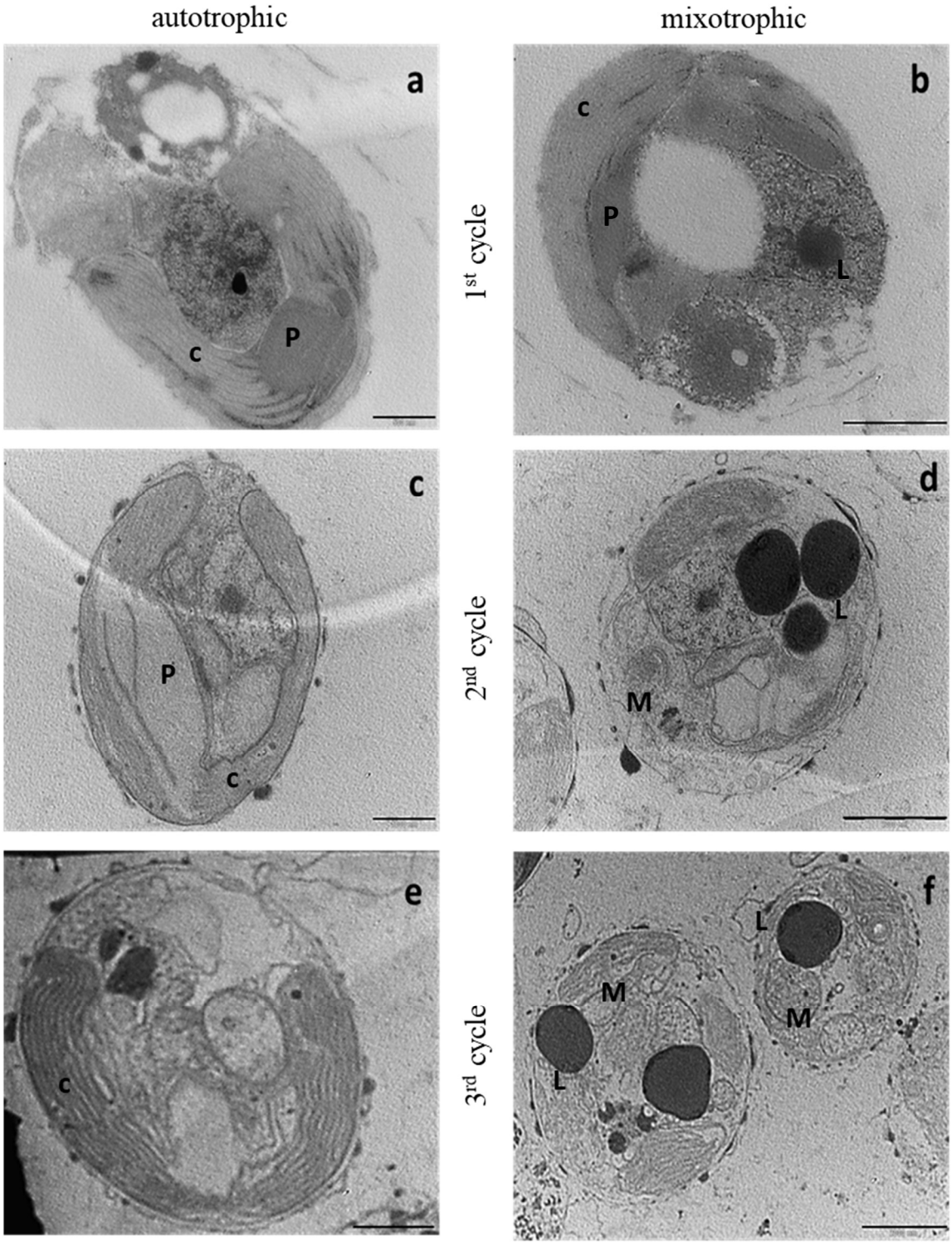

Figure 5 Transmission electron micrographs of *T. lutea* cells under autotrophic (a, c, e) mixotrophic (b, d, f) conditions at the end of each cultivation cycle: 1st cycle, 7 days (a, b); 2nd cycle 14 days (c, d); 3rd cycle, 21 days (e, f). C chloroplast; P pyrenoid; L lipid globules; M mitochondrion. Bars: a = 0.5 μm; b-c-e = 1 μm; d-f = 2 μm

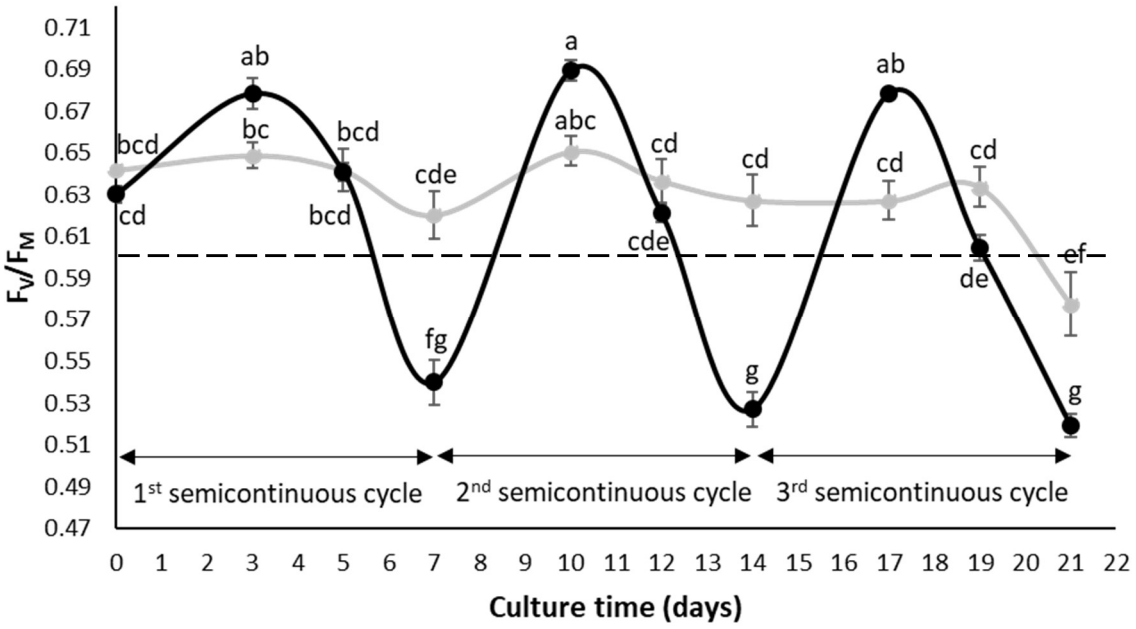

Figure 6 Time-course variations of F_V/F_M ratio in *T. lutea* cells under autotrophic (grey) mixotrophic (black) conditions. Dashed lines indicate the optimal 0.6 value of F_V/F_M. Values are means ± SD. Different letters indicate statistically significant differences ($p < 0.05$, two-way ANOVA)

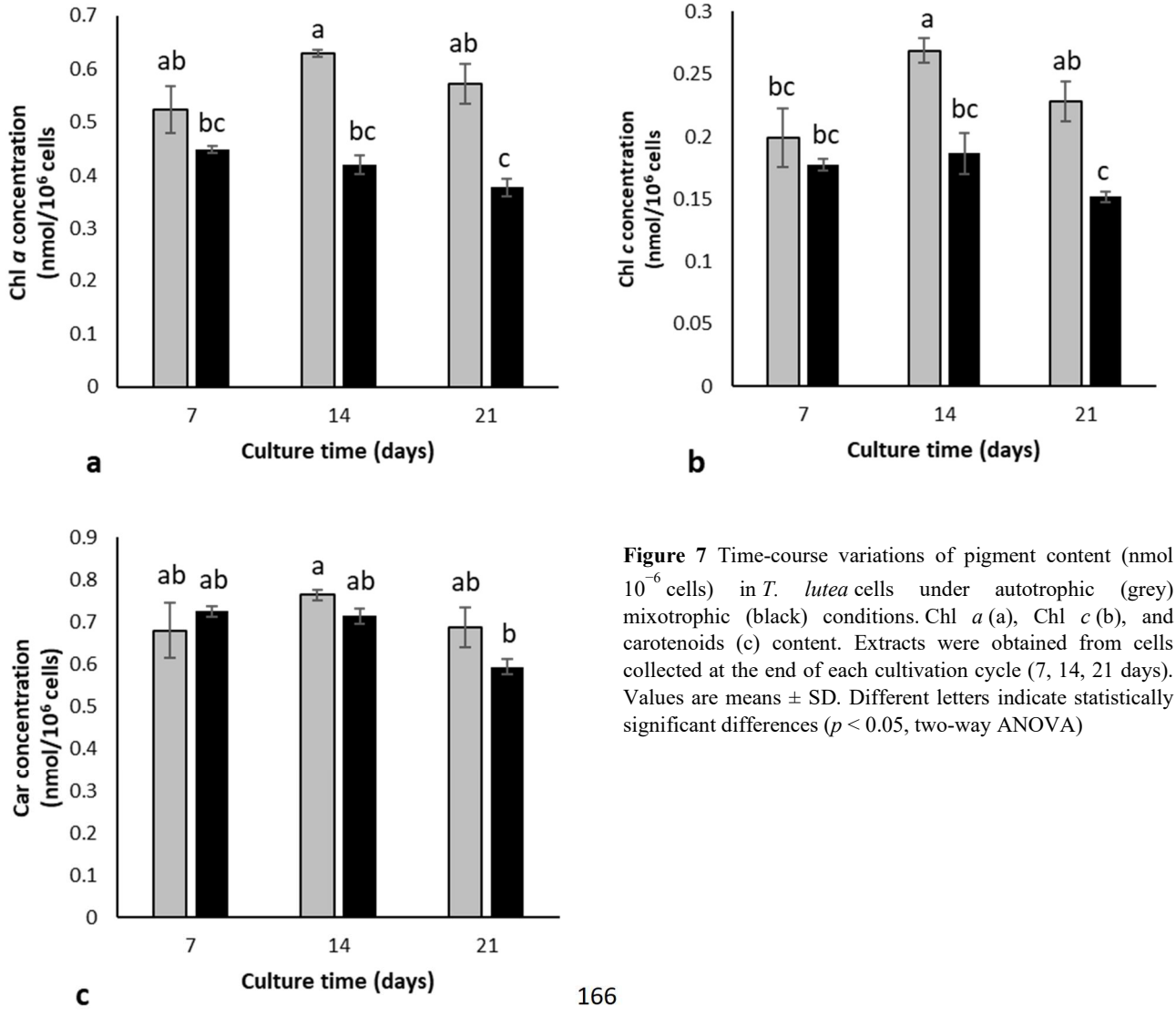

Figure 7 Time-course variations of pigment content (nmol 10^{-6} cells) in *T. lutea* cells under autotrophic (grey) mixotrophic (black) conditions. Chl *a* (a), Chl *c* (b), and carotenoids (c) content. Extracts were obtained from cells collected at the end of each cultivation cycle (7, 14, 21 days). Values are means ± SD. Different letters indicate statistically significant differences ($p < 0.05$, two-way ANOVA)

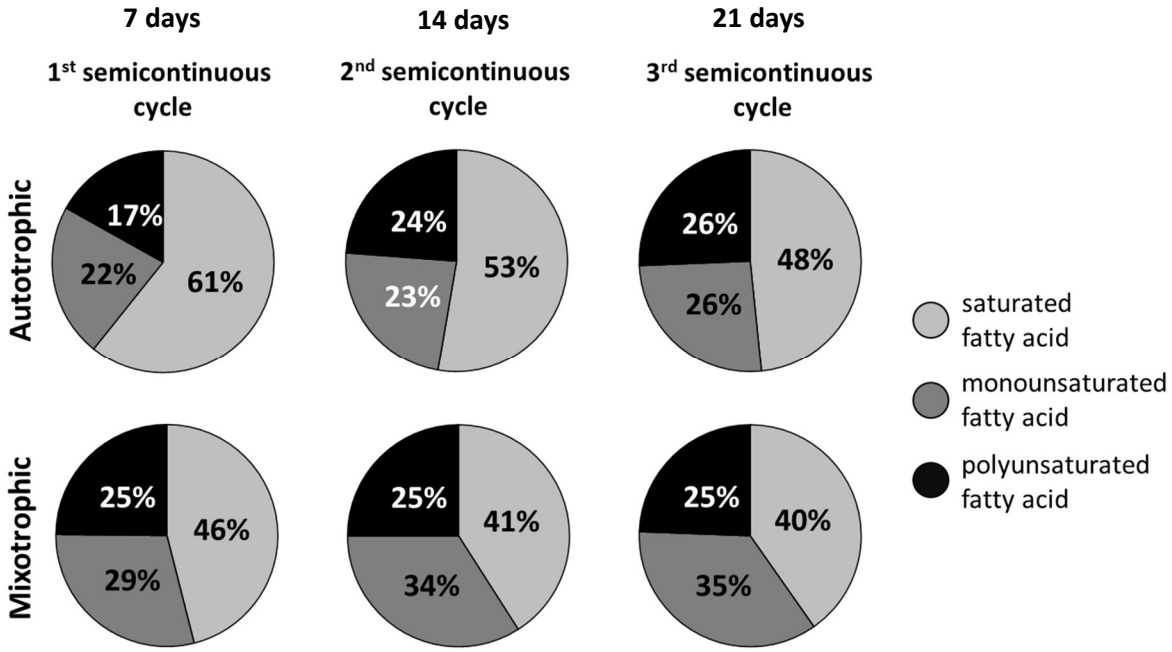

Figure 8 Relative proportions of fatty acids fractions (percentage of total fatty acids, %) in *T. lutea* cells under autotrophic and mixotrophic conditions, at the end of each cultivation cycle (7, 14, 21 days)

Table 1 Fatty acid profile (percentage of total fatty acids) in *T. lutea* cell grown under autotrophic and mixotrophic conditions, at the end of each cultivation cycle (7, 14, 21 days). Values are means ± SD

	7 days				14 days				21 days			
	autotrophy		mixotrophy		autotrophy		mixotrophy		autotrophy		mixotrophy	
Fatty acid	**Mean**	**SD**	**Mean**	**SD**	**Mean**	**SD**	**Mean**	**SD**	**Mean**	**SD**	**Mean**	**SD**
C13:0	19.66	9.42	18.94	0.29	15.03	1.07	15.59	1.75	16.34	2.48	13.29	0.78
C15:0	1.54	0.67	0.80	0.04	0.99	1.41	0.79	0.27	0.96	0.33	0.49	0.03
C16:0	21.48	0.34	18.81	0.81	20.62	1.24	19.24	1.20	18.31	1.67	19.65	0.22
C16:1n7	5.53	0.80	5.08	0.16	6.47	0.61	5.87	0.25	5.98	0.79	5.23	0.08
C16:2n4	2.31	1.20	1.24	0.34	0.60	0.85	1.03	0.34	0.72	0.14	0.93	0.25
C18:0	18.07	12.37	5.91	1.01	15.28	5.19	3.00	0.19	10.13	0.47	3.89	0.13
C18:1n9	16.79	2.27	24.03	0.94	17.01	2.96	27.36	2.78	19.99	1.21	29.15	0.64
C18:2n6	2.08	0.44	2.94	0.26	2.67	0.78	3.71	0.52	2.60	0.62	3.73	0.22
C18:3n3 (ALA)	2.07	0.35	2.82	0.26	3.28	0.05	3.26	0.15	3.37	0.43	3.04	0.22
C20:5n3 (EPA)	8.61	2.66	12.86	0.05	12.95	2.25	11.50	0.01	13.40	0.85	10.84	0.66
C20:0	--	--	0.40	0.57	0.36	0.51	0.66	0.08	1.43	1.14	0.72	0.05
C22:0	--	--	1.18	0.10	0.42	0.59	1.68	0.39	1.20	0.14	2.22	0.27
C22:1n9	--	--	--	--	--	--	0.79	0.05	--	--	0.95	0.18
C22:6n3 (DHA)	1.84	0.24	5.00	0.61	4.32	0.05	5.52	1.03	5.56	0.51	5.86	0.03

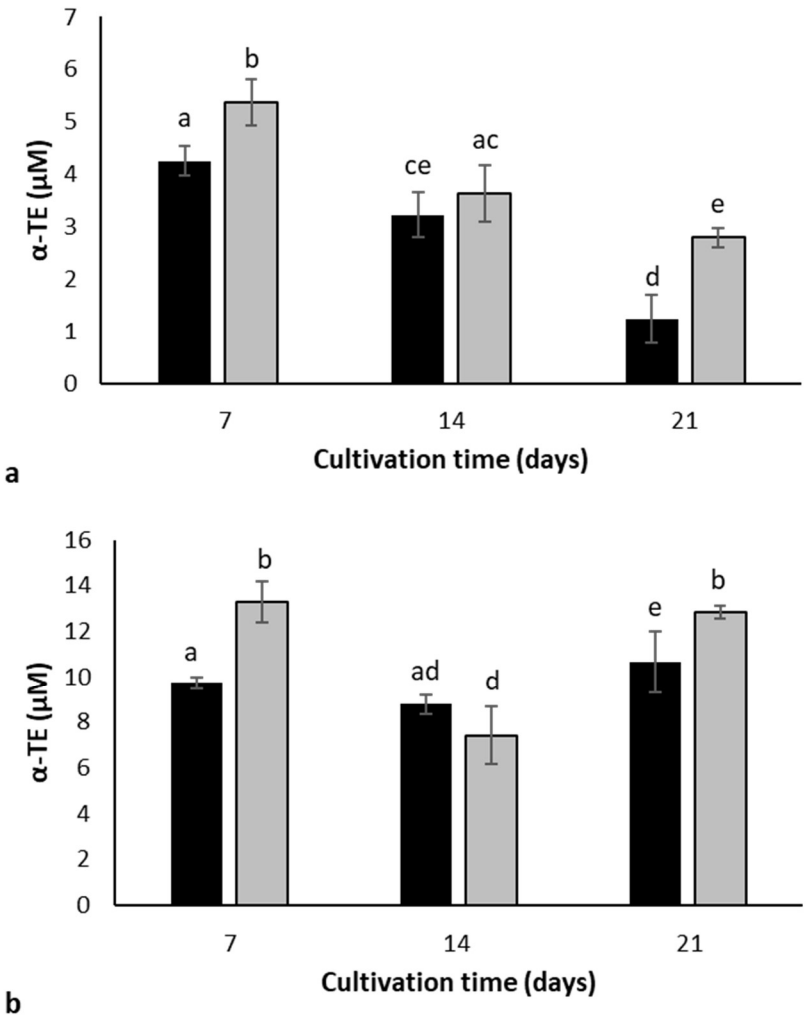

Figure 9 Anti-oxidant activity of methanolic extracts of *T. lutea* grown under autotrophic (grey) and mixotrophic (black) conditions. Extracts were obtained from cells collected at the end of each cultivation cycle (7, 14, 21 days). Results are expressed as micromoles of α-tocopherol equivalents (α-TE μM). a DPPH assay; b ABTS assay. Values are means ± SD. Different letters indicate statistically significant difference ($p<0.05$ two-way ANOVA)

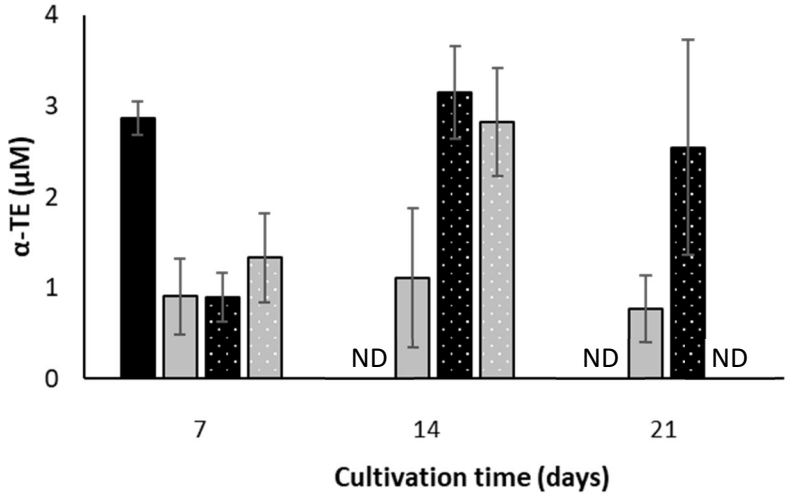

Figure 10 Anti-oxidant activity of aqueous extracts of *T. lutea* grown under autotrophic (grey) and mixotrophic (black) conditions. Extracts were obtained from cells collected at the end of each cultivation cycle (7, 14, 21 days). Results are expressed as micromoles of α-tocopherol equivalents (α-TE μM). Full coloured bars are referred to DPPH assay; dotted bars are referred to ABTS assay. When no bars are present, the tests produced no results. Values are means ± SD. ND, Not detectable.

References

Alkhamis Y, Qin JG (2016) Comparison of pigment and proximate compositions of *Tisochrysis lutea* in phototrophic and mixotrophic cultures. J Appl Phycol 28, 35–42. https://doi.org/10.1007/s10811-015-0599-0

Andruleviciute V, Makareviciene V, Skorupskaite V, Gumbyte M (2014). Biomass and oil content of *Chlorella* sp., *Haematococcus* sp., *Nannochloris* sp. and *Scenedesmus* sp. under mixotrophic growth conditions in the presence of technical glycerol. Journal of applied phycology, 26(1), 83-90. https://doi.org/10.1007/s10811-013-0048-x

Baldisserotto C, Sabia A, Guerrini A, Demaria S, Maglie M, Ferroni L, Pancaldi S (2021) Mixotrophic cultivation of *Thalassiosira pseudonana* with pure and crude glycerol: Impact on lipid profile. Algal Research, Volume 54,102194. https://doi.org/10.1016/j.algal.2021.102194

Baldisserotto C, Giovanardi M, Ferroni L, Pancaldi S (2014) Growth, morphology and photosynthetic responses of *Neochloris oleoabundans* during cultivation in a mixotrophic brackish medium and subsequent starvation. Acta Physiol. Plant., 36, pp. 461-472. https://doi.org/10.1007/s11738-013-1426-3

Baldisserotto C, Popovich C, Giovanardi M, Sabia A, Ferroni L, Constenla D, Leonardi P, Pancaldi S (2016) Photosynthetic aspects and lipid profiles in the mixotrophic alga *Neochloris oleoabundans* as useful parameters for biodiesel production. Algal Res., 16, pp. 255-265. https://doi.org/10.1016/j.algal.2016.03.022

Bendif E M, Probert I, Schroeder DC, de Vargas C (2013) On the description of *Tisochrysis lutea* gen. nov. sp. nov. and *Isochrysis nuda* sp. nov. in the Isochrysidales, and the transfer of *Dicrateria* to the *Prymnesiales* (Haptophyta). Journal of applied phycology, 25(6), 1763-1776. https://doi.org/10.1007/s10811-013-0037-0

Berges JA, Franklin DJ, Harrison PJ (2001) Evolution of an artificial seawater medium: improvements in enriched seawater, artificial water over the last two decades. J Phycol 37:1138–1145. https://doi.org/10.1046/j.1529-8817.2001.01052.x

Bhola VK, Swalaha FM, Nasr M, Kumari S, Bux F (2016) Physiological responses of carbon-sequestering microalgae to elevated carbon regimes. Eur J Phycol 51:401–412. https://doi.org/10.1080/09670262.2016.1193902

Bhola VK, Swalaha FM, Nasr M, Kumari S, Bux F (2016) Physiological responses of carbon-sequestering microalgae to elevated carbon regimes. Eur J Phycol 51:401–412. https://doi.org/10.1080/09670262.2016.1193902

Bigagli E, D'Ambrosio M, Cinci L, Niccolai A, Biondi N, Rodolfi L, Dos Santos Nascimiento LB, Tredici MR, Luceri C (2021) A Comparative In Vitro Evaluation of the Anti-Inflammatory Effects of a *Tisochrysis lutea* Extract and Fucoxanthin. *Marine Drugs*.; 19(6):334. https://doi.org/10.3390/md19060334

Brand-Williams W, Cuvelier ME, Berset C (1995) Use of a free radical method to evaluate antioxidant activity, LWT - Food Science and Technology, Volume 28, Issue 1, Pages 25-30, https://doi.org/10.1016/S0023-6438(95)80008-5

Conde TA, Neves BF, Couto D, Melo T, Neves B, Costa M, Silva J, Domingues P, Domingues MR (2021) Microalgae as Sustainable Bio-Factories of Healthy Lipids: Evaluating Fatty Acid Content and Antioxidant Activity. *Marine Drugs*.; 19(7):357. https://doi.org/10.3390/md19070357

Cosgrove J, Borowitzka MA (2010) Chlorophyll fluorescence terminology: an introduction. In: Suggett DJ, Prášil O, Borowitzka MA (eds) Chlorophyll *a* fluorescence in aquatic sciences: methods and applications. Springer, Dordrecht, pp 1–17. https://doi.org/10.1007/978-90-481-9268-7_1

Coulombier N, Jauffrais T, Lebouvier N. (2021) Antioxidant Compounds from Microalgae: A Review. *Marine Drugs*.; 19(10):549. https://doi.org/10.3390/md19100549

Ferroni L, Baldisserotto C, Giovanardi M, Pantaleoni L, Morosinotto T, Pancaldi S (2011) Revised assignment of room-temperature chlorophyll fluorescence emission bands in single living cells of *Chlamydomonas reinhardtii*. J Bioenerg Biomembr 43:163–173. https://doi.org/10.1007/s10863-011-9343-x

Ferroni L, Giovanardi M, Poggioli MC, Baldisserotto C, Pancaldi S (2018) Enhanced photosynthetic linear electron flow in mixotrophic green microalga *Ettlia oleoabundans* UTEX 1185. Plant Physiol. Biochem., 130 (2018), pp. 215-223. https://doi.org/10.1016/j.plaphy.2018.07.005

Floegel A, Kim D-O, Chung S-J, Koo SI, Chun OK (2011) Comparison of ABTS/DPPH assays to measure antioxidant capacity in popular antioxidant-rich US foods, Journal of Food Composition and Analysis, Volume 24, Issue 7, Pages 1043-1048. https://doi.org/10.1016/j.jfca.2011.01.008

Gao F, Teles I, Ferrer-Ledo N, Wijffels RH, Barbosa MJ (2020) Production and high throughput quantification of fucoxanthin and lipids in *Tisochrysis lutea* using single-cell fluorescence. Bioresource Technology, 318, 124104. https://doi.org/10.1016/j.biortech.2020.124104

Giovanardi M, Ferroni L, Baldisserotto C, Tedeschi P, Maietti A, Pantaleoni L, Pancaldi S (2013). Morphophysiological analyses of *Neochloris oleoabundans* (Chlorophyta) grown mixotrophically in a carbon-rich waste product. Protoplasma, 250(1), 161-174. https://doi.org/10.1007/s00709-012-0390-x

Giovanardi M, Poggioli M, Ferroni L, Lespinasse M, Baldisserotto C, Aro EM, Pancaldi S (2017) Higher packing of thylakoid complexes ensures a preserved photosystem II activity in mixotrophic *Neochloris oleoabundans*. Algal Res., 25 (2017), pp. 322-332. https://doi.org/10.1016/j.algal.2017.05.020

Guillard RRL (1975) Culture of phytoplankton for feeding marine invertebrates. In: Smith WL, Chanley MH (eds) Culture of marine invertebrate animals. Plenum Press, New York, pp 29–60. https://doi.org/10.1007/978-1-4615-8714-9_3

Guillard RRL, Ryther JH (1962) Studies of marine planktonic diatoms. I. *Cyclotella nana* Hustedt and *Detonula confervacea* (Cleve). Can J Microbiol 8:229–239 https://doi.org/10.1139/m62-029

Gupta PL, Choi H-J, Pawar RR, Jung SP, Lee S-M (2016) Enhanced biomass production through optimization of carbon source and utilization of wastewater as a nutrient source. J Environ Manag 184:585–595. https://doi.org/10.1016/j.jenvman.2016.10.018

Gupta PL, Choi H-J, Pawar RR, Jung SP, Lee S-M (2016) Enhanced biomass production through optimization of carbon source and utilization of wastewater as a nutrient source. Journal of Environmental Management, Volume 184, Part 3, Pages 585-595. https://doi.org/10.1016/j.jenvman.2016.10.018

Hillebrand H, Dürselen C-D, Kirschtel D, Pollingher U, Zohary T (1999) Biovolume calculation for pelagic and benthic microalgae. J Phycol 35:403–424. https://doi.org/10.1046/j.1529-8817.1999.3520403.x

Hu H, Li JY, Pan XR, Zhang F, Ma LL, Wang HJ, Zeng RJ (2019). Different DHA or EPA production responses to nutrient stress in the marine microalga Tisochrysis lutea and the freshwater microalga Monodus subterraneus. Science of the Total Environment, 656, 140-149. https://doi.org/10.1016/j.scitotenv.2018.11.346

Hu H, Ma LL, Shen XF, Li J-Y, Wang H-F, Zeng RJ (2018) Effect of cultivation mode on the production of docosahexaenoic acid by *Tisochrysis lutea*. AMB Expr 8, 50. https://doi.org/10.1186/s13568-018-0580-9

Jerez-Martel I, García-Poza S, Rodríguez-Martel G, Rico M, Afonso-Olivares C, Gómez-Pinchetti JL (2017) Phenolic profile and antioxidant activity of crude extracts from microalgae and cyanobacteria strains. Journal of Food Quality, 2017. https://doi.org/10.1155/2017/2924508

Kotue TC, Djote WNB, Marlyne M, Pieme AC, Kansci G, Fokou E. Antisickling and Antioxidant Properties of Omega-3 Fatty Acids EPA/DHA. Nutri Food Sci Int J. 2019. 9(1): 555752. https://doi.org/10.19080/NFSIJ.2019.09.555752

Koyande AK, Chew KW, Rambabu K, Tao Y, Toi CD, Loke SP (2019) Microalgae: A potential alternative to health supplementation for humans. Food Science and Human Wellness, 8, 16–24. https://doi.org/10.1016/j.fshw.2019.03.001

Kuhn J, Müller H, Salzig D, Czermak P (2015) A rapid method for an offline glycerol determination during microbial fermentation. Electronic Journal of Biotechnology, Volume 18, Issue 3, Pages 252-255. https://doi.org/10.1016/j.ejbt.2015.01.005

Lafuente M, Rodríguez González-Herrero ME, Romeo Villadóniga S, Domingo JC (2021) Antioxidant Activity and Neuroprotective Role of Docosahexaenoic Acid (DHA) Supplementation in Eye Diseases That Can Lead to Blindness: A Narrative Review. Antioxidants, 10(3), 386.

Legrand J, Artu A, Pruvost, J (2021) A review on photobioreactor design and modelling for microalgae production. Reaction Chemistry & Engineering. https://doi.org/10.1039/D0RE00450B

Lewoyehu M, Amare M (2019). Comparative evaluation of analytical methods for determining the antioxidant activities of honey: A review. Cogent Food & Agriculture, 5(1), 1685059. https://doi.org/10.1080/23311932.2019.1685059

Liang N, Kitts DD (2014) Antioxidant property of coffee components: assessment of methods that define mechanisms of action. *Molecules*, *19*(11), 19180-19208. https://doi.org/10.3390/molecules191119180

Liu S, Elvira P, Wang Y, Wang W (2019) Growth and nutrient utilization of green algae in batch and semi-continuous autotrophic cultivation under high CO_2 concentration. Appl Biochem Biotechnol 188, 836–853. https://doi.org/10.1007/s12010-018-02940-9

Ma X., Mi Y, Zhao C, Wei Q (2022) A comprehensive review on carbon source effect of microalgae lipid accumulation for biofuel production. Science of The Total Environment, 806, 151387. https://doi.org/10.1016/j.scitotenv.2021.151387

Maglie, M., Baldisserotto, C., Guerrini, A. *et al.* A co-cultivation process of *Nannochloropsis oculata* and *Tisochrysis lutea* induces morpho-physiological and biochemical variations potentially useful for biotechnological purposes. J Appl Phycol 33, 2817–2832 (2021). https://doi.org/10.1007/s10811-021-02511-2

Matos J, Cardoso C, Gomes A, Campos AM, Falé P, Afonso C, Bandarra, N M (2019) Bioprospection of *Isochrysis galbana* and its potential as a nutraceutical. Food & function, 10(11), 7333-7342. https://doi.org/10.1039/C9FO01364D

Mohamadnia S, Tavakoli O, Faramarzi MA (2021). Enhancing production of fucoxanthin by the optimization of culture media of the microalga *Tisochrysis lutea*. *Aquaculture*, *533*, 736074. https://doi.org/10.1016/j.aquaculture.2020.736074

Mohamadnia S, Tavakoli O, Faramarzi MA, Shamsollahi Z (2020) Production of fucoxanthin by the microalga *Tisochrysis lutea*: A review of recent developments. Aquaculture, 516, 734637. https://doi.org/10.1016/j.aquaculture.2019.734637

Munteanu IG, Apetrei C (2021) Analytical Methods Used in Determining Antioxidant Activity: A Review. International Journal of Molecular Sciences, 22(7), 3380. https://doi.org/10.3390/ijms22073380

Nethravathy MU, Mehar JG, Mudliar SN, Shekh AY (2019) Recent Advances in Microalgal Bioactives for Food, Feed, and Healthcare Products: Commercial Potential, Market Space, and Sustainability. Comprehensive Reviews in Food Science and Food Safety, 18: 1882-1897. https://doi.org/10.1111/1541-4337.12500

Pang N, Gu X, Chen S, Kirchhoff H, Lei H, S Roje (2019) Exploiting mixotrophy for improving productivities of biomass and coproducts of microalgae. Renew. Sust. Energ. Rev., 112 (2019), pp. 450-460. https://doi.org/10.1016/j.rser.2019.06.001

Patel AK, Singhania RR, Dong C-D, Obulisami PK, Sim SJ (2021) Mixotrophic biorefinery: A promising algal platform for sustainable biofuels and high value coproducts. Renewable and Sustainable Energy Reviews, Volume 152, 111669. https://doi.org/10.1016/j.rser.2021.111669

Patil S, Arvind ML, Gunjan P (2020) An efficient algae cell wall disruption methodology for recovery of intact chloroplasts from microalgae. Journal of Applied Biology & Biotechnology Vol 8.03: 23-28. http://doi.org/10.7324/JABB.2020.80305

Peltomaa E, Johnson MD, Taipale SJ (2018) Marine cryptophytes are great sources of EPA and DHA. Marine drugs, 16(1), 3. https://doi.org/10.3390/md16010003

Penhaul Smith JK, Hughes AD, McEvoy L, Day JG (2020) Tailoring of the biochemical profiles of microalgae by employing mixotrophic cultivation. Bioresor. Technol. Rep., 9, p. 100321 https://doi.org/10.1016/j.biteb.2019.100321

Pereira I, Rangel A, Chagas B, de Moura B, Urbano S, Sassi R, Castro C (2021). Microalgae Growth under Mixotrophic Condition Using Agro-Industrial Waste: A Review. Biomass. http://doi.org/10.5772/intechopen.93964

Pérez-Gálvez, A, Viera I, Roca M (2020) Carotenoids and chlorophylls as antioxidants. Antioxidants, 9(6), 505. https://doi.org/10.3390/antiox9060505

Ramesh Kumar B, Deviram G, Mathimani T, Duc PA, Pugazhendhi A (2019) Microalgae as rich source of polyunsaturated fatty acids. Biocatal Ag Biotech 17:583–588584 https://doi.org/10.1016/j.bcab.2019.01.017

Re R, Pellegrini N, Proteggente A, Pannala A, Yang M, Rice-Evans C (1999) Antioxidant activity applying an improved ABTS radical cation decolorization assay. Free Radical Biology and Medicine, Volume 26, Issues 9–10 Pages 1231-1237. https://doi.org/10.1016/S0891-5849(98)00315-3

Ritchie RJ (2006) Consistent sets of spectrophotometric chlorophyll equations for acetone, methanol and ethanol solvents. Photosynth Res 89:27–41 https://doi.org/10.1007/s11120-006-9065-9

Silva METD, Martins MA, Leite MDO, Milião GL, Coimbra JSDR (2021) Microalga Scenedesmus obliquus: extraction of bioactive compounds and antioxidant activity. Revista Ciência Agronômica, 52. https://doi.org/10.5935/1806-6690.20210036

Solís-Salinas CE, Patlán-Juárez G, Okoye PU, Guillén-Garcés A, Sebastian PJ, Arias DM (2021) Long-term semi-continuous production of carbohydrate-enriched microalgae biomass cultivated in low-loaded domestic wastewater. Science of The Total Environment, Volume 798, 149227, https://doi.org/10.1016/j.scitotenv.2021.149227

Villanova V, Fortunato AE, Singh D, Dal Bo D, M. Conte M, Obata T, Jouhet J, Fernie AR, Marechal A, Falciatore A, Pagliardini J, Le Monnier A, Poolman M, Curien G, Petroutsos D, Finazzi G (2017) Investigating mixotrophic metabolism in the model diatom *Phaeodactylum tricornutum*. Philos. Trans. R. Soc. B, 372 (2017), p. 20160404. https://doi.org/10.6084/m9.figshare.c.3799462

Wellburn AR (1994) The spectral determination of chlorophylls *a* and *b*, as well as total carotenoids, using various solvents with spectrophotometers of different resolution. J Plant Physiol 144:307–313. https://doi.org/10.1016/S0176-1617(11)81192-2

Yin Z, Zhu L, Li S, Hu T, Chu R, Mo F, Hu D, Liu C, Li B (2020) A comprehensive review on cultivation and harvesting of microalgae for biodiesel production: Environmental pollution control and future directions. Bioresource Technology, Volume 301, 122804. https://doi.org/10.1016/j.biortech.2020.122804

Zhang T-T, Xu J, Wang Y-M, Xue C-H (2019) Health benefits of dietary marine DHA/EPA-enriched glycerophospholipids. Prog Lipid Res 75:1009972. https://doi.org/10.1016/j.plipres.2019.100997